SOVIET PHYSICS

JETP

A translation of the Journal of Experimental and Theoretical Physics of the USSR.

SOVIET PHYSICS—JETP VOL. 4, NO. 5, PP 623-775 JUNE, 1957

Oscillographic Determination of Energy of Electric Explosion of Wires

I. F. KVARTSKHAVA, V. V. BONDARENKO, A. A. PLIUTTO AND A. A. CHERNOV

(Submitted to JETP editor April 16, 1956)
J. Exptl. Theoret. Phys. (U.S.S.R.) **31**, 745-751 (November, 1956)

A procedure is described for oscillographic determination of the energy of the electric explosion of wires; this procedure is free of the errors due to the inductive distortion of the explosion oscillograms. It is shown that in high-voltage electric explosions the wire resistance is not a single-valued function of the amount of energy supplied.

1. INTRODUCTION

ARTICLES devoted to various aspects of the investigation of electric explosion of wires have been appearing recently with increasing frequency[1-10]. The interest in this phenomenon is due principally to the fact that it permits investigation of the properties of a substance to which a large quantity of energy is supplied (behavior of substances at high temperatures, transitions between different aggregate states, emission properties, electric resistance, etc.). It is evident that as accurate a determination as possible of the energy supplied is essential in these investigations. The energy is usually calculated from the current and voltage oscillograms. In view of the short duration of the explosion process, energy losses due to thermal radiation, thermal conduction, convection, etc., are neglected.

Given below are experimental results on the oscillography of electric explosion of wires, performed over a relatively wide range of voltages across the capacitor of the explosion circuit. A "current-measuring resistor," described in Ref. 6, was used to obtain current oscillograms free of any inductive distortion whatever. The energy supplied to the wire is calculated only from current oscillograms and from known values of the initial capacitor voltage and capacitance, and from the inductance of the explosion circuit. The data obtained point to several conclusions concerning the variation of the wire resistance with the energy supplied and with the relative energy balance during the electric explosion.

2. MEASUREMENT PROCEDURE AND EXPERIMENTAL RESULTS

The electric explosion was produced by discharging a high-voltage capacitor through the wire. A diagram of the explosion circuit and a description of the oscillography procedure and of the construction of the "current-measuring resistor" are given in Ref. 6.

This investigation concerns primarily copper wires, for it is in this case that the principal features of electric explosions become most pronounced. The wires were 60 mm long and 0.05, 0.1 and 0.15 mm in diameter. Approximately these dimensions are the most frequently encountered in investigations of this type. Experiments were made with a 2.5 microfarad bank of capacitors at initial voltages U_0 ranging from 5 to 40 kv and at two values of the total inductance of the explosion circuit, 0.4 and 4.2 microhenries. Two corresponding groups of oscillograms are given in Figs. 1 and 2. These oscillograms show that as U_0 increases, or as L decreases, the first current pulse that causes the electric explosion of the wire becomes shorter and taller. At relatively low values of U_0, the first current pulse in the explosion circuit is followed by a discharge "pause," which frequently ends in a more powerful current pulse. There is no discharge pause at high values of U_0 and the current again starts increasing after reaching a certain nonzero minimum. Analogous oscillograms are obtained for other size wires.

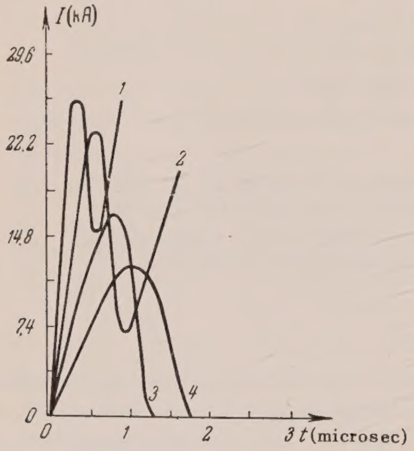

FIG. 1. Current oscillograms, obtained in an explosion of copper wires 60 mm long and 0.15 mm in diameter. Explosion-circuit inductance $L = 0.4 \times 10^{-6}$ henry. Oscillograms *1, 2, 3, 4* correspond to capacitor voltage of 35, 25, 15 and 10 kv. T – time, I – current.

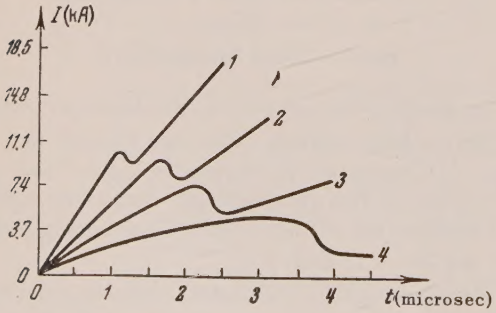

FIG. 2. Current oscillograms for the same wires as in Fig. 1 at $L = 4.2 \times 10^{-6}$ henry. Oscillograms *1, 2, 3, 4* correspond to values of U_0 = 40, 30, 20 and 10 kv.

Figure 3 shows two current oscillograms that illustrate the role of the inductive distortion of the oscillograms in the calculation of the explosion energy. Curve *1* was obtained with the "current-measuring resistor" connected as usual in the oscillograph circuit, while curve *2* was obtained with this resistor connected noninductively*. Curve *3* represents the difference of these two curves and evidently shows the approximate behavior of the inductive voltage drop across the "current-measuring resistor," while curve *2* shows the purely resistive drop, proportional to the explosion circuit. As could be expected, curve *1* of these oscillograms intersects curve *2* at the maximum of the latter where $dI/dt = 0$. It follows from the curves that the inductive voltage drop is comparable with the resistive drop, even exceeding it considerably in the initial portion, and it is therefore evident that the use of the upper oscillogram for energy calculation results in energy values that are much too high.

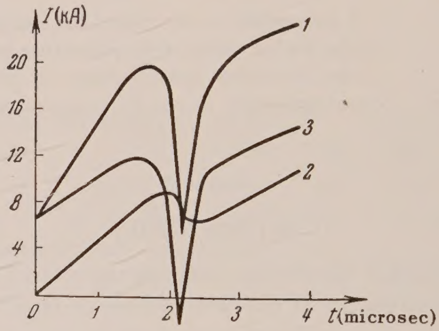

FIG. 3. Oscillograms illustrating the role of inductive distortion.

We start the wire energy calculation with the current oscillogram. Knowing the explosion-circuit parameters and the initial capacitor voltage, we can calculate the energy E_t delivered to the wire within the time t elapsed since the start of the discharge. During this time, the capacitor supplies an amount of energy

$$E(t) = (C/2)\,[U_0^2 - (U_0 - \Delta U)^2] \qquad (1)$$

$$= U_0 \Delta Q - \Delta Q^2/2C,$$

---

* The inductance for curve *1* is somewhat different from that for curve *2*.

where U_0 is the initial capacitor voltage, ΔU is the decrease in this voltage during the time t, and $\Delta Q = C\,\Delta U$ is the discharge from the capacitor during the same time. ΔQ can be calculated from the current oscillogram using the following equation:

$$\Delta Q = \int_0^t I(t)\,dt,$$

where $I(t)$ is the value of the current at the instant t, also determined from the current oscillogram. Knowing U_0, C and ΔQ we obtain $E(t)$ from Eq. (1). However, not all of $E(t)$ is liberated in the wire. Neglecting, in view of the short duration of the process, the energy lost through thermal radiation, electromagnetic radiation of the explosion circuit, etc., we can assume that part of the energy $E(t)$ in the wire is in the form of Joule heat E_t and the remaining part is in the form of the energy of the magnetic field produced by the current*. The latter can be calculated from the well-known equation

$$E_m = LI^2(t)/2,$$

where L is determined from the expression for the period of the damped oscillations of the explosion circuit. Knowing $E(t)$ and E_m, we can calculate E_t as the difference

$$E_t = E(t) - E_m. \qquad (2)$$

The oscillograms obtained make it possible to determine the values of the current with an accuracy to 2-3%. The measurement accuracy of U_0, L and C are of the same order, and E_t can therefore be determined with an accuracy to not less than 4-6%. Figure 4 shows curves of the energy delivered to the wire by the time the current reaches its first maximum relative to the capacitor voltage U_0.

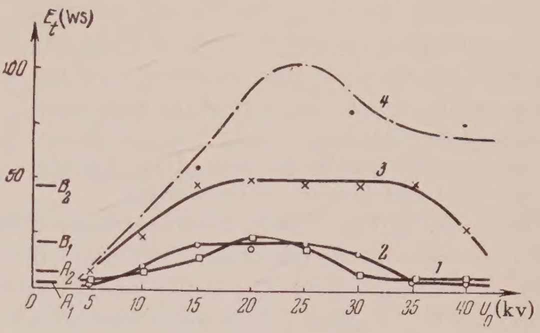

FIG. 4. Curves showing the dependence of E_t on the capacitor voltage. Wire diameter is 0.10 mm in curves *1* and *2* and 0.15 in curves *3* and *4*; L is 0.4×10^{-6} henry for curves 1 and 4 and 4.2×10^{-6} henry for curves *2* and *3*.

Dashes A_1 and A_2 parallel to the abscissa show the values of energy, obtained from tabular data, required to melt wires 0.1 and 0.15 mm in diameter by heating from room temperature. Markers P_1 and P_2 give the energy required for total evaporation of these wires under the same conditions. We restrict ourselves only to the calculation of E_t for the first current maximum, for by the instant the maximum occurs all the remaining capacitor voltage is across the ohmic resistance of the wire making it possible to calculate the value of this resistance with sufficient accuracy without needing to allow for the inductive voltage drop in the explosion circuit. It must be noted that our oscillograms show that the rate at which the current increases, dI/dt, remains constant at relatively large values of U_0 (> 10 kv) from the start of the discharge almost up to the occurrence of the first maximum. It follows from this that in this region the ohmic resistance of the wire is much smaller than the surge resistance of the tuned circuit, and its value cannot readily be computed with any accuracy. It is only near the current maximum that the wire resistance begins to increase rapidly, continuing to increase also beyond the current maximum (see also the curves of Fig. 3 in Ref. 6, obtained for copper wires at relatively low voltages). It follows that near the current maximum the rate at which the energy is liberated begins to increase very rapidly leading eventually to a rapid increase in the wire resistance and to formation of a discharge pause.

The curves of Fig. 4 show that E_t does not increase monotonically with U_0, as expected, but begins to diminish upon reaching a certain maximum that either exceeds or approximates the energy of total evaporation of the wire. If the explosion circuit inductance is high, these curves exhibit a wide plateau, where E_t does not vary with E_0 (curves *2* and *3*). At low values of U_0 (less than 5 kv) E_t approaches the energy needed to melt the corresponding wire, in agreement with our data[6] and in contradiction with the data of Refs. 3-5. One can therefore conclude from examination of the curves in Fig. 4 that the start of the processes leading to the discharge pause does not depend on the energy delivered to the wire alone, but also on the value and duration of the current.

---

* The resistance of the remaining portion of the explosion circuit is assumed negligible compared with that of the wire. Evidently the estimate of the energy supplied to the wire is somewhat exaggerated here. An estimate based on the attenuation decrement of the circuit shows that this exaggeration does not exceed 10-15%, and therefore does not affect the deductions substantially.

The curves of Fig. 5 show the dependence of the wire resistance for the maximum of the first current pulse, $R_m = (U_0 - \Delta U)/I_m$, on the initial capacitor voltage U_0. Curves *1*, *2*, *3* and *4* correspond to curves *1*, *2*, *3* and *4* of Fig. 4. They show that R_m increases with U_0 for identical wires. For the same value of U_0 and for the same wire, R_m increases with the inductance L. This apparently is due to the increased duration of the current at large values of L. It follows from comparison of the curves of Figs. 4 and 5 that the value of R_m is not determined uniquely by the amount of energy as supplied, but is also a function of I_m and τ_m, where τ_m is the time interval from the start of the discharge to the occurrence of the first current maximum; this interval characterizes the time of action of the current. It is evident from examination of the current oscillogram that the wire resistance behaves analogously near the maximum of the first current pulse and to the right of it up to the following current minimum, where if there is no discharge pause, the resistance assumes a maximum value and then drops sharply to a very small value owing to the wire "breakdown;" if a discharge pause occurs, the resistance continues to increase and tends to infinity.

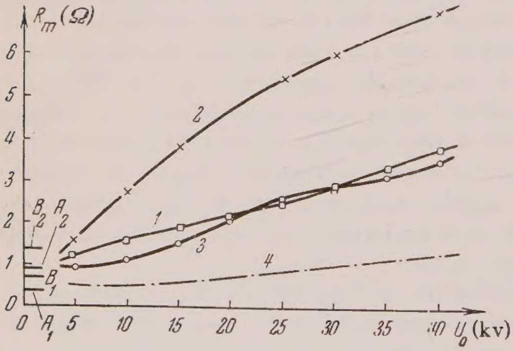

FIG. 5. Dependence of wire resistance R_m at the instant of the maximum of the first current pulse on the capacitor voltage.

Markers A_1, A_2, B_1 and B_2 on Fig. 5 correspond to the tabular values of copper wire resistance: A_1 and A_2 give the resistances of 0.15 and 0.1 mm diameter wires just below their melting point, and B_1 and B_2 give the resistances of the same wire towards the end of their melting. Comparing these resistances with the values R_m obtained from the curves of Fig. 5, we see that at low values of U_0 (approximately 5 kv) R_m assumes values that are comparable with the above data. At higher values of U_0, the value of R_m exceeds considerably the resistance corresponding to the fully melted wire.

Figure 6 gives curves of τ_m vs. U_0. Curves *1*, *2*, *3* and *4* correspond to curves *1*, *2*, *3* and *4* of Fig. 4. They show that as U_0 increases, the value of τ_m diminishes at all times for all wire diameters and for all values of the inductance L. At high values of U_0 the rate at which τ_m decreases is constant, while the rate at which I_m increases tends to zero (see oscillograms and also curves of Fig. 7).

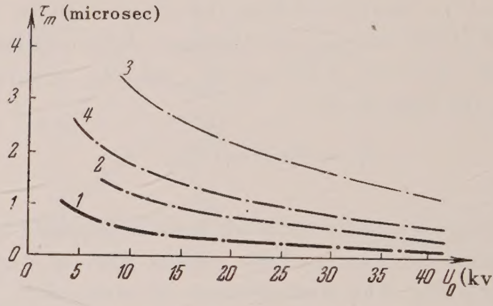

FIG. 6. Curves showing τ_m vs. capacitor voltage.

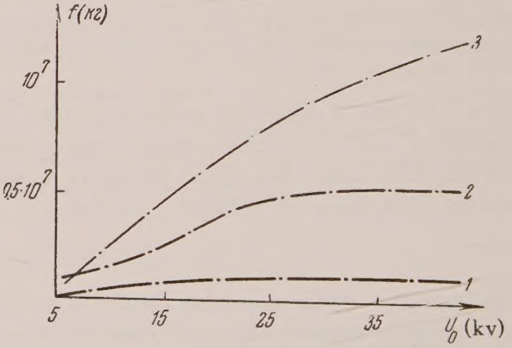

FIG. 7. Dependence of the force compressing the wire on the initial capacitor voltage. Curves *1*, *2* and *3* correspond to wire diameters of 0.05, 0.10 and 0.15 mm.

3. EVALUATION OF RESULTS

It is possible to conclude from the data given that at high capacitor voltages the resistance of a wire in electric explosion is not uniquely determined by the energy supplied to it. It follows from a comparison of the curves of Figs. 4 and 5 that under certain experimental conditions (low inductance in the explosion circuit) the wire absorbs more energy and has less resistance, while under other conditions (greater inductance in explosion circuit) it absorbs less energy and has a higher resistance. The resistances may differ by a factor of several times for the same value of voltage and for identical wires. It appears to us, in agreement with Ref. 11, that such large resistance variations cannot be explained with the aid of any electronic mechanism whatever. It is most sensible, apparently, to admit the existence of energy leakage from the wire during the explosion process itself, this leakage depending on the discharge conditions. The apparent "excess energy" could then be attributed to this leakage. Careful examination of the electric-explosion process makes it possible to ascertain whether such energy leakage exists.

In fact, according to the explanation of the electric explosion given in Ref. 10, the characteristic feature of the explosion is its irregularity, or more accurately, its periodicity in space. Shadow photographs given in that reference show that at a certain stage of development the wire explosion breaks up into a large number of separate "micro-explosions," which are distributed approximately periodically along the wire and which occur simultaneously over the entire length of the wire. Upon further development, the micro-explosions merge into one overall explosion. The total power of the micro-explosions is considerably greater than the average wire-explosion power in view of their short duration and in view of the fact that they liberate a large amount of energy, and therefore, as the same photographs show, the products of the micro-explosions, having a higher velocity, penetrate deeper into the surrounding medium (air) than the main mass of explosion products that follows them. It is evident that the dispersion of the micro-explosion products is associated with consumption of a certain portion of the capacitor energy, which indeed determines, in our opinion, the "excess energy" in the wire.

It is possible to estimate approximately the "excess energy" from the spatial periodicity of the explosion process and from experiments made with wire explosions in vacuum. Shadow photographs[10] illustrating the periodicity and the radial stratification of the explosion show that the mass expelled by the micro-explosions does not exceed approximately one-tenth of the total mass of the wire. The mass of a wire 0.15 mm in diameter and 16 mm long is approximately 10^{-2} gm. Consequently, the "excess energy" should be carried away by a mass approximately 10^{-3} gm. It is impossible to determine the "excess energy" from the curves of Figs. 4 and 5, for the increased resistance of the wire may be due either to the heating and partial evaporation*, or to the dispersion of the still-unevaporated portions of the wire under the influence of the shock waves that propagate from the centers of the micro-explosions[10]. One can estimate, however, the upper limit of the "excess energy" in the case, for example, of curve *4* of Fig. 4, to be approximately several tens of Joules. Let us assume that this limit for the maximum of the curve is 100 J or 10^9 erg. Then, if all this energy is converted into the kinetic energy of the expelled mass, the approximate velocity of this mass should be 10^6 cm/sec. Experiments made in a vacuum chamber with a ballistic pendulum have shown that with 40 kv across the capacitor the average escape velocity of the explosion products from the wire reaches 2×10^5 cm/sec, and when the voltage is decreased to 20 kv the escape velocity decreases to 10^5 cm/sec. Taking into account the statements made earlier about the micro-explosion power, one must assume that the escape velocity of the micro-explosion products should be considerably greater than the escape velocity of all the explosion products. In addition, we know that when a wire explodes in vacuum it is shunted by the arc discharge that is produced in the metal vapor, and this should evidently result in a lower micro-explosion energy in vacuum compared with micro-explosions in air, where no shunting or wire "breakdown" is observed up to the first current maximum. Under the conditions in which a wire explodes in air an escape velocity of approximately 10^6 cm/sec for the micro-explosion products appears quite reasonable, and the energy carried away in this case is quantitatively quite adequate to account for the "anomalous" behavior of the resistance described above. No difficult-to-explain anomalies are thus encountered with respect to the relationship between the wire resistance and the amount of energy supplied even if the current density is approximately 10^8 a/cm^2 (the maximum current density for a wire 0.15 mm diameter at $U_0 = 40$ kv is 1.6×10^8 a/sq.-cm). It would be interesting to determine quantitatively, from the curves of Figs. 4 and 5, the behavior of the "excess energy" as a function of U_0, but we are not in a position to do so, owing to the complexity of the processes leading to the increase in the wire resistance near the current maximum. Not knowing the amount of energy remaining in the wire, we can nevertheless assume that R_m will be proportional to the amount of this energy. It is then clear from the curves of Figs. 4 and 5 that the behavior of the "excess energy" as a function of the behavior of E_t should be qualitatively characterized by the presence of a maximum. In order to understand such a behavior of the "excess energy", let us turn to Figs. 6 and 7. Figure 7 shows curves for the voltage vs. the force that compresses the wire in a radial direction and that is caused by the magnetic field. This force can be expressed by the well-known equation[12]

---

* We have in mind here not the evaporation of the wire at the sites of the micro-explosions, but the evaporation of the remaining parts, for the micro-explosion sections are strongly heated and enveloped by low-resistance arcs, thus not affecting noticeably the overall resistance of the wire.

$$f = \sigma j^2,$$

where f is the force acting on unit volume of wire carrying current on its periphery, σ is the circumference of the wire section, and j is the current density; f is given in dynes if σ is given in centimeters and j in electromagnetic current units. It is evident from these curves that f varies over a wide range and becomes large enough to compress the liquid portions of the wire for a very short time. This compression indeed causes micro-explosions in accordance with the mechanism suggested in Ref. 10 for the electric explosion. Assuming that f is either constant or increases slowly at high capacitor voltages, one can conclude that the micro-explosion energy will be determined by the time of action of this force. Quantitatively, this energy is roughly the square of the momentum $(f\tau_m)^2$. Calculations of this product, based on the data of Figs. 6 and 7, show that the behavior of $(f\tau_m)^2$ as a function of the voltage across the capacitor is analogous to the behavior of the "excess energy" described above. This confirms the assumption made above that energy leakage causes the "anomalous" behavior of the resistance during the electric explosion of the wire.

An assumption was stated in Ref. 10 that the action of the magnetic field on the wire imposes an upper limit on the current density attainable in an electric explosion. The oscillograms obtained show that for small-diameter wires (0.1 mm and below) such a limit indeed exists and equals approximately 10^8 a/cm^2 (see Fig. 7). It follows from the same oscillograms that increasing the wire diameter and using a voltage source of sufficient energy increases the attainable current densities, although slowly. One must evidently seek in this direction a possible path for obtaining higher current densities.

4. CONCLUSIONS

1. The experiments described above have established that at relatively low capacitor voltages the electric explosion produces during the time interval from the start of the discharge to the first current maximum no anomalies in the relationship between the energy supplied and the wire resistance, at least for copper wire.

2. At high capacitor voltages, to the contrary, the resistance of the wire exhibits an absence of a unique relationship between the energy liberated, even within these limits; this is attributed to energy leakage from the wire during the explosion process.

3. The compressing action of the magnetic field of the current in the electric explosion limits attainable values of current density, particularly in the case of thin wires. As the wire diameter increases, the attainable current densities also increase.

---

[1] A. A. Ignat'eva and S. G. Kalashnikov, J. Exptl. Theoret. Phys. (U.S.S.R.) 22, 385 (1952).

[2] E. S. Borovik, Dokl. Akad. Nauk SSSR 91, 771 (1953).

[3] S. V. Lebedev and S. E. Khaikin, J. Exptl. Theoret. Phys. (U.S.S.R.) 26, 629, 723 (1954).

[4] S. V. Lebedev, J. Exptl. Theoret. Phys. (U.S.S.R.) 27, 487, 605 (1954).

[5] L. N. Borodovskaia and S. V. Lebedev, J. Exptl. Theoret. Phys. (U.S.S.R.) 28, 96 (1955); Soviet Phys. JETP 1, 71 (1955).

[6] Bondarenko, Kvartskhava, Pliutto and Chernov, J. Exptl. Theoret. Phys. (U.S.S.R.) 28, 191 (1955); Soviet Phys. JETP 1, 221 (1955).

[7] W. M. Conn, Phys. Rev. 79, 213 (1950); J. Opt. Soc. Am. 41, 445 (1951); Nature (London) 169, 1950 (1952; Phys. Rev. 98, 1551 (1955).

[8] B. Eiselt, Z. Physik 132, 54 (1952).

[9] J. Wrana, Arch. Elektrotech. 33, 656 (1938).

[10] Kvartskhava, Pliutto, Chernov and Bondarenko, J. Exptl. Theoret. Phys. (U.S.S.R.) 30, 42 (1956); Soviet Phys. JETP 3, 40 (1956).

[11] V. L. Ginzburg and V. P. Shabanskii, Dokl. Akad. Nauk SSSR 100, 445 (1955).

[12] E. F. Russ, J. Tech. Phys. 12, 529 (1930).

Translated by J. G. Adashko
166

SOVIET PHYSICS JETP VOLUME 4, NUMBER 5 JUNE, 1957

The Ionization Spectrum of Cosmic Rays 3250 m above Sea Level

A. G. MESHKOVSKII AND L. I. SOKOLOV

(Submitted to JETP editor May 30,1956)
J. Exptl. Theoret. Phys. (U.S.S.R.) 31, 752-755 (November, 1956)

Using a previously described method,[1] we measured the ionization spectra produced by the soft and hard components of cosmic rays of various ranges at 3250 m above sea level. The proton momentum spectrum was obtained in the interval 0.36–1.0 bev/c.

IN an earlier paper,[1] we described in detail a method for measuring the ionization spectrum of cosmic rays. The basic idea of the method is to select the minimum ionization produced by a particle as it passes through several scintillation crystals; experiments at sea level showed that quantitative information about the proton component of cosmic rays with ranges 2 to 15 cm of lead could be obtained.

It was interesting to apply this method to the ionization spectra of cosmic rays at mountain altitudes, especially as the resolving power of our system was considerably better than that available to previous authors.[2,3] With this in mind, the apparatus was transported to the Alagez high altitude (3250 m above sea level) station of the Academy of Sciences of the Armenian SSR.

Two series of measurements were made. In the first series, lasting 407 hours, we measured the ionization spectrum of particles having ranges 2–3, 3–5, 5–9 and 9–15 cm of lead. In the second series, which lasted 270 hours, the lead filters were replaced by carbon ones equivalent to 1–1.5, 1.5–2, and 2–3 cm of lead. During both series, the ionization spectrum of particles with ranges in excess of 15 cm of lead was also measured.

The amount of material above the apparatus was kept to a minimum and consisted of a single layer of iron roofing plus 0.5 cm plywood. During both series of measurements (i.e., for ranges 2 to 15 cm of lead) we counted the number of times two or more particles went through the system together (multiple traversals). In analyzing the data, these multiple traversals were discarded, so that our results for the soft component refer to single particles only. Multiple traversals in the hard component were not registered.

Figure 1 shows the ionization spectrum obtained for the hard component (particles with ranges of more than 15 cm of lead); from it we can obtain the resolving power of our system. Ionization in arbitrary units is plotted along the abscissa, and the relative intensity in some ionization interval along the ordinate. Our method[1] is such that the ionization spectrum shown in Fig. 1, together with all the other spectra presented in this paper, is the product of the differential distribution of ionization and the fourth power of the integral distribution. The curve in the figure is almost symmetric and has one sharp maximum. The relative width at half maximum is 18%.

Seven ionization spectra for particles of various ranges in the soft component were taken. As an example of these, Fig. 2 gives the spectrum corresponding to 1–1.5 cm of lead. The insert shows the right-hand side of the spectrum on an enlarged scale. In this graph ionization is measured in units of the minimal ionization, which is taken to be the ionization at the maximum in the spectrum corresponding to the hard component. The arrows show the most probable ionization Δ_0 for μ-mesons, protons and mesons of masses 550 and 965 electron masses. The other 6 ionization spectra for the

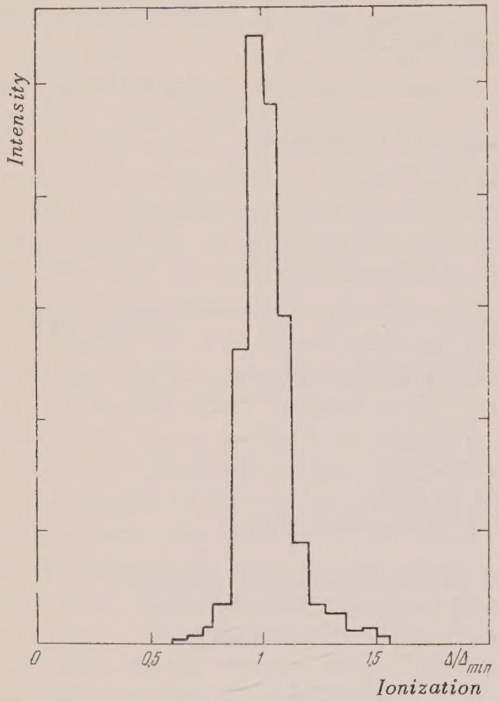

FIG. 1. Ionization spectrum for the hard component

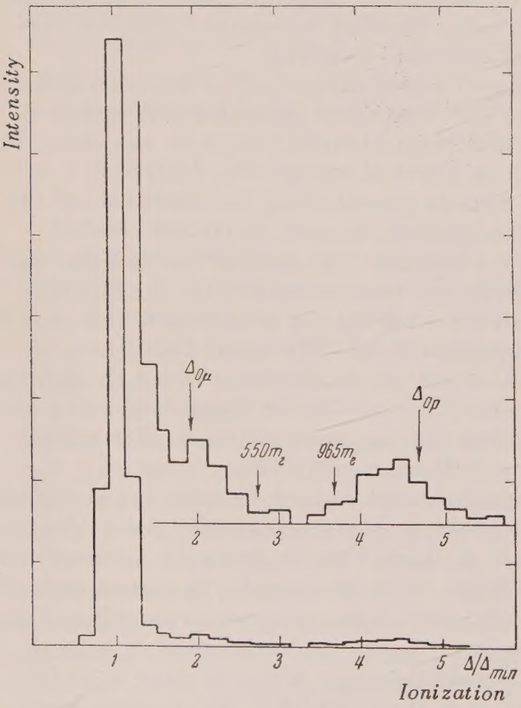

FIG. 2. Ionization spectrum for particles with ranges 1–1.5 cm Pb.

soft component are similar to the one in Fig. 2. Two well separated groups of particles are visible. The right-hand group consists of protons, the left-hand one of μ-mesons and electrons. The total spectrum for ionization by the soft component can be obtained by adding all the data for a given group. For example, Fig. 3 shows the sum of the five spectra corresponding to ranges 0.7–1, 1–1.5, 1.5–2, 2–3 and 3–5 cm of lead. We see that in the total spectrum the large range interval (0.7 to 5 cm of lead) has smeared out the distinction between protons and μ-mesons and electrons, so that we have a smooth ionization curve.

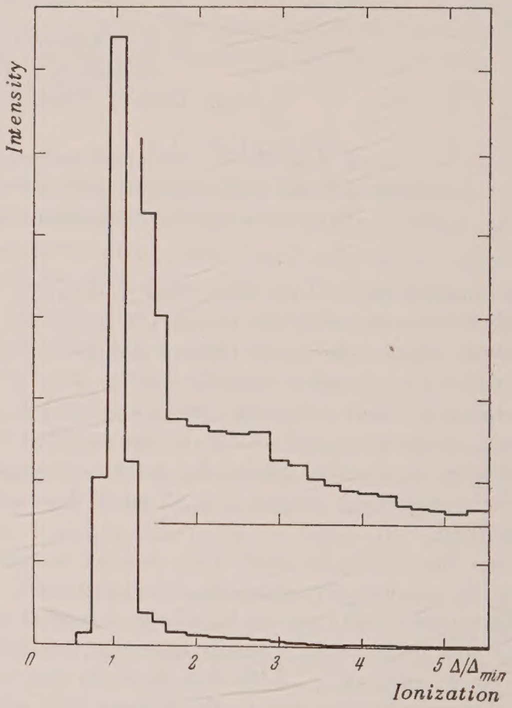

FIG. 3. The total ionization spectrum for particles in the soft component (ranges 0.7 to 5 cm Pb.)

Can our method detect particles with masses intermediate between those of the proton and μ-meson? From Fig. 2 we see that the left-hand edge of the proton spectrum overlaps the calculated most probable ionization due to K-mesons, so that it is hardly likely that our spectra can separate these particles from protons.

Indeed, since there was little matter above our apparatus, one would not expect many K-mesons to appear in our spectra. There are, however, a considerable number of particles in the interval corresponding to the most probable ionization by mesons of mass 550 m_e[4]. The resolution, as obtained from Fig. 1, and the number of μ-mesons with ranges 1–1.5 cm of lead are not large enough to account for these particles as the right-hand side of the μ-meson ionization spectrum. Calculations show that almost all the particles with ionization 2.4 to 3.2 Δ_{min} can be accounted for as non-ionizing protons stopping in the layer corresponding to ranges 1–1.5 cm of lead, and hence nothing definite can be said about the presence in this spectrum of mesons with mass of about 500 m_e.

Our spectra lead to certain conclusions about the proton component of cosmic rays 3250 m above sea level and with ranges 0.7 to 15 cm of lead. The results are shown in the following Table, which also gives the number of multiple traversals of particles through our system.

The proton momentum spectrum shown in Fig. 4 was drawn from the results in the Table. The absolute value of the vertical proton current was obtained from the vertical current of μ-mesons with range more than 15 cm Pb. The latter current was taken to be 1.56 cm^{-2} sec^{-1} $sterad^{-1}$, in agreement with Rossi.[5] The spectrum is corrected for non-ionizing protons.

Range interval cm Pb	Number of protons observed	Number of protons, corrected for those which stop without ionizing	Number of protons in % (corrected for those which stop without ionizing)		Number of multiple traversals
			Relative to the total number of particles in a given range interval	Relative to the number of particles with range more than 15 cm Pb	
0.7—1.0	58	59	3.50±0.46	0.407±0.053	0
1.0—1.5	83	85	3.38±0.37	0.610±0.066	0
1.5—2.0	75	79	5.09±0.57	0.540±0.060	2
2—3	318	346	7.08±0.39	0.863±0.047	10
3—5	338	365	15.15±0.80	1.395±0.072	14
5—9	414	480	18.69±1.87	1.870±0.187	20
9—15	362	500	24.91±4.00	2.110±0.338	42
0.7—5			6.18±0.19	3.820±0.114	
0.7—15			9.71±0.77	7.810±0.610	

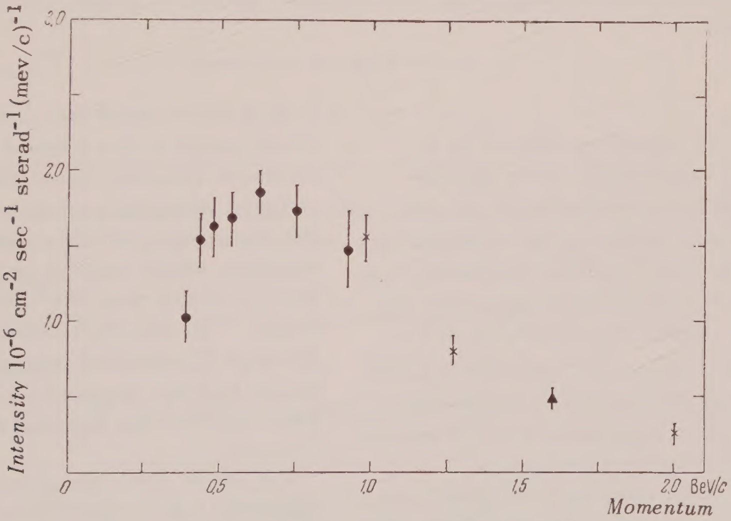

FIG. 4. Momentum spectrum of protons 3250 m above sea level; ×–Ref. 7, ▲–Ref. 6, ●–our data.

In the momentum range 0.36–0.6 bev/c our spectrum agrees well with that obtained by Kocharian[6], who used a magnetic spectrometer. For momenta greater than 0.6 bev/c our curve lies above Kocharian's data, but agrees well with the data of Miller *et al.*,[7] which were obtained by a Wilson cloud chamber in a magnetic field. For momenta larger than 1 bev/c, where we have no data, we show several points obtained by other workers.[6,7]

In conclusion we should like to express our deep gratitude to A. I. Alikhanian, who made the present research possible at Alagez, and to A. D. Maiorov for his help in carrying out the experiments.

---

[1] A. G. Meshkovskii and L. I. Sokolov, J. Exptl. Theoret. Phys. (U.S.S.R.) 30, 840 (1956); Soviet Phys. JETP 3, 683 (1956).

[2] S. Ia. Nikitin, J. Exptl. Theoret. Phys. (U.S.S.R.) 18, 577 (1948).

[3] Dobrotin, Graevskaia, Grigorov, Nikol'skii and Rappoport, Dokl. Akad. Nauk SSSR 77, 599 (1951).

[4] A. I. Alikhanian, Lecture at the Conference on High Energy Physics in Moscow, May, 1956.

[5] B. Rossi, Rev. Mod. Phys. 20, 537 (1948).

[6] N. M. Kocharian, J. Exptl. Theoret. Phys. (U.S.S.R.) 28, 160 (1955); Soviet Phys. JETP 1, 128 (1955).

[7] Miller, Henderson, Garrison, Potter, Sandstrom and Todd, Phys. Rev. 94, 167 (1954).

Translated by R. Krotkov
167

SOVIET PHYSICS JETP VOLUME 4, NUMBER 5 JUNE, 1957

Investigation of σ-Stars Induced by Negative π-Mesons

S. A. AZIMOV, U. G. GULIAMOV, E. A. ZAMCHALOVA,
M. NIZAMETDINOVA, M. I. PODGORETSKII AND A. IULDASHEV
P. N. Lebedev Physical Institute, Academy of Sciences, USSR
Academy of Sciences, Uzbek SSR

(Submitted to JETP editor June 1, 1956)
J. Exptl. Theoret. Phys. (U.S.S.R.) 31, 756-761 (November, 1956)

The properties of σ-stars produced by π^--mesons stopping in an emulsion chamber were investigated. Data obtained from the analysis of 938 σ-stars were used to determine the distribution of the number of prongs as well as the energy distribution of secondary particles. The obtained energy spectrum is compared to the data on σ-stars produced by K^--mesons.

---

1. THE properties of σ-stars, produced by π^--mesons stopping in emulsion, were investigated by Menon, Muirhead and Rochat[1]. In particular, data were given on the energy distribution of the secondary particles formed in the interaction. This information is of considerable interest for the sake of elucidating of the capture process of π^--mesons by nuclei, and for comparison with σ-stars produced by other unstable particles, for instance, the K^--mesons. This is especially true for secondary particles of energy higher than 30 mev.

The experimental data, however, are grossly inaccurate in this energy region. This is due to the fact that the particles under consideration have a very long range, and therefore cannot come to a stop in relatively thin single emulsion layers used by the authors of Ref. 1. The energy could therefore have been determined only by ionization measurement or, in a few cases, by multiple scattering, procedures which are connected with large errors.

In order to avoid this limitation, the σ-stars were investigated in the present work by means of an emulsion chamber, consisting of a large number of stripped emulsion layers. An appreciable part of the secondary particles came to a stop within the chamber, which made it possible to determine their energy simply from the value of their ionization range. The emulsion chamber used consisted of 126 type P emulsion layers, each 450 μ thick. The layers had the shape of a circle 10 cm in diameter. The chamber was exposed in the stratosphere for 7 hours.

For every disk, the central part only, 4 cm in diameter, was scanned at a low magnification. Since the range of the investigated secondary particles is not larger than 3 cm, the particles of even highest energy could leave the chamber through its top or bottom surface only, which permitted a simple calculation of the geometrical corrections. In fact, these corrections were necessary only for the case these corrections were necessary only for the case of protons with energy greater than 60 mev and even in this case were very small. The cases of light negative mesons coming to a stop were noted in scanning and the cases possessing at least one heavy charged secondary were selected. In this way, the cases of π^-- and μ^--mesons were practically separated. Furthermore, the inherent length of each track was determined, the track being followed from one emulsion to another if necessary, up to the end point of the trajectory.

The secondary particles were not positively identified, and therefore the energy of each was determined conditionally from its range under the assumption that the particle was a proton. In the energy region of interest, this assumption does not lead to serious errors, since in this region the secondary particles are, in fact, mainly protons.

Those σ-stars, from the center of which tracks of slow electrons emerged, were especially noted in scanning. Such electrons are connected with the mesic atom stage of the negative pion capture and are as a rule formed in π^--meson capture by the heavy (Ag and Br) emulsion nuclei. Very slow electrons have such a small range that their tracks appear as blobs consisting of several adjoining grains. Such events were ascribed to slow electrons and the corresponding σ-stars were assumed to represent the disintegration of the Ag and Br nuclei.

A minor part of the σ-stars with slow electrons and blobs can, in fact, be due to the random overlapping of grains. Some 103 cases of the π-μ-decay of positive pions were selected to estimate the real contribution of this background effect. In nine of them, slow electrons and blobs, which seemed to be connected with the points of stopping of pions, were observed. Corresponding corrections were introduced in all the succeeding data.

2. The distribution of the prong number, obtained from the analysis of 983 σ-stars, is given in Table I. The results are in good agreement with those of Ref. 1.

Analogous distributions for stars with and without slow electrons and blobs are given in Tables II and III, respectively. The comparison shows that, during the capture of π^--mesons by heavy nuclei, σ-stars with a small number of prongs are more frequently produced. This result is also in accord with the data of Ref. 1.

TABLE I. Prong number distribution of σ-stars. Mean number of prongs 2.06 ±0.03.

Number of prongs	1	2	3	4	5	6	Total
Number of stars. .	395	262	213	95	16	2	983
%	40.1±2.0	26.7±1.6	21.7±1.3	9.7±1.0	1.6±0.4	0.2±0.2	100

TABLE II. σ-Stars without slow electrons and blobs. Mean number of prongs 2.63 ± 0.05.

Number of prongs	1	2	3	4	5	6	Total
Number of stars. .	82	102	137	76	16	2	415
%	19.3±3.8	24.6±4.0	33.0±4.5	18.3±3.7	3.8±1.8	0.5±0.5	100

TABLE III. σ-Stars with slow electrons and blobs. Mean number of prongs 1.65 ±0.03.

Number of prongs	1	2	3	4	5	6	Total
Number of stars. .	313	160	76	19	0	0	568
%	55.1±4.1	28.2±3.7	13.4±2.8	3.3±1.5	0	0	100

We shall now pass on to the discussion of energy relations. Data on the number of secondary particles of various energies, for stars with different number of prongs, are given in Tables IV and V. It should be noted that, since the energy of secondary particles was determined from the range under the assumption that all the particles were protons, the data in the low energy region represent the range spectrum rather than the energy spectrum. Table IV pertains to 356 stars possessing slow electrons and blobs, and Table V to 622 stars not having any. The number of the σ-stars with secondary particles of energies greater than 30 mev amounts to 20.1 ± 1.3%*, which differs appreciably from the value 11.9 ± 1.4% given in Ref. 1. The difference is probably due to the fact that, in the present work, the energy of the secondary particles was determined from their range under the assumption that all of them were protons, while in Ref. 1 the particle energy was determined basically from the ionization.

TABLE IV. Energy spectrum of secondary particles produced in heavy emulsion nuclei disintegrations.

Energy region, mev	Number of prongs in star					
	1	2	3	4	5	6
	Number of secondary particles					
0—5	51	125	141	49	—	—
5—10	84	90	45	10	—	—
10—15	45	25	14	7	—	—
15—20	27	22	6	2	—	—
20—25	20	13	6	2	—	—
25—30	21	7	6	—	—	—
30—35	11	14	5	1	—	—
35—40	12	8	2	2	—	—
40—45	12	4	1	1	—	—
45—50	9	7	—	—	—	—
50—55	9	—	—	—	—	—
55—60	5	—	—	—	—	—
60—65	2	1	—	1	—	—
65—70	2	1	—	—	—	—
70—75	1	—	—	—	—	—
75—80	—	—	—	—	—	—
80—85	1	—	—	—	—	—
85—90	1	—	—	—	—	—
90—95	—	—	—	—	—	—

It is interesting to note that the proportion of stars with secondary particles with $E \geq 30$ mev is almost the same for both heavy and light nuclei. For the σ-stars with slow electrons and blobs, their share amounts to 20.5 ± 1.8%, while for the other stars, it equals 19.5 ± 1.8%. An analogous statement can be made with respect to the energy distribution of secondary particles in the energy region represented in the histograms 1, 2 and 3. Figure 1 pertains to the case of the σ-stars with slow electrons and blobs, Fig. 2 to the σ-stars without them, and Fig. 3 to all σ-stars. The histograms all have a similar shape. The mean energy values, calculated for particles with $E \geq 30$ mev are, correspondingly, almost identical.

It is interesting to compare the obtained energy spectrum with the data on the σ-stars produced by K^--mesons. It is thought at present[2,3] that, during the nuclear capture of a stopping K^--meson, a fast pion and a hyperon are created. The latter remains mostly within the nucleus in a bound state and finally transforms into a Λ^0-particle. The possibility that the Λ^0-particle is created in the primary reaction is also not excluded. The relatively slow pion, produced in the decay of the Λ^0-particle, is kept in the nucleus and creates a star similar to the σ-stars produced by pions. If the fast pion produced in the first stage of the process transfers its energy to the nucleus, then the star will be of considerably higher energy than a pion produced σ-star. In this way, σ-stars produced by K^--mesons will, on the average, possess secondary particles of higher energy, and also with

---

* We recall that only σ-stars with at least one charged secondary were considered.

TABLE V. Energy spectrum of secondary particles produced in light emulsion nuclei disintegrations.

Energy region, mev	Number of prongs in star					
	1	2	3	4	5	6
	Number of secondary particles					
0— 5	16	98	255	195	51	7
5—10	27	39	87	49	12	2
10—15	5	19	21	21	6	1
15—20	9	12	16	11	4	—
20—25	4	6	9	7	2	—
25—30	6	7	7	6	—	1
30—35	5	8	5	10	2	—
35—40	3	4	4	1	—	1
40—45	2	1	5	1	—	—
45—50	1	3	2	2	—	—
50—55	2	3	2	—	—	—
55—60	—	—	—	1	1	—
60—65	—	2	2	—	—	—
65—70	—	1	2	—	—	—
70—75	1	—	—	—	—	—
75—80	—	—	1	—	—	—
80—85	—	1	—	—	—	—
85—90	1	—	—	—	—	—
90—95	—	—	1	—	—	—

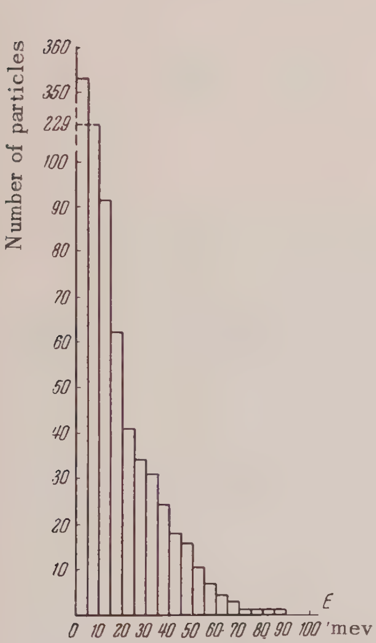

FIG. 1. $\overline{\overline{E}} = (43.3 \pm 0.9)$ mev.

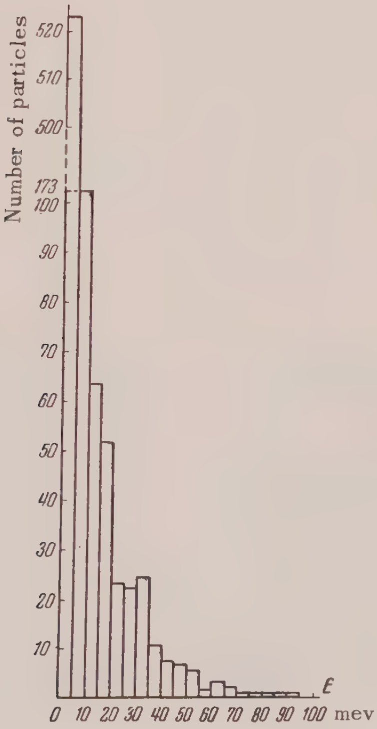

FIG. 2. $\overline{E} = (44.3 \pm 1.2)$ mev.

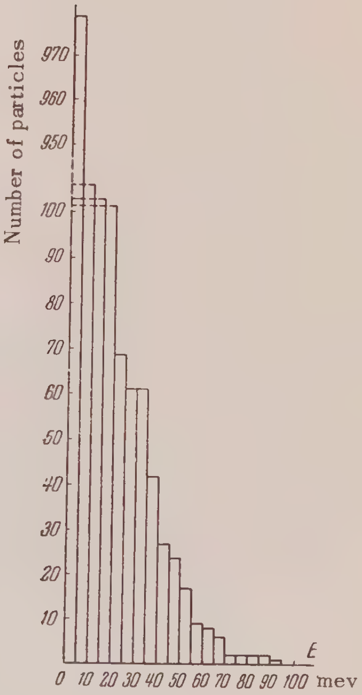

FIG. 3. $\overline{E} = (42.7 \pm 0.6)$ mev.

a greater frequency, than will the π^--meson produced σ-stars. This deduction is in good agreement with experimental data[4-7].

We shall now consider only those σ-stars produced by K^--mesons which do not contain π-meson tracks. Among such stars, 65.4 ± 10.0% possess secondary particles of energy $E \geq 30$ mev, which is considerably more than the corresponding value for the π^--meson produced σ-stars. The mean value of the energy, calculated for secondary particles with $E \geq 30$ mev, equals 79.2 ± 8.5 mev, i.e., is also much higher than for the secondary particles in the π^--meson produced σ-stars.

The energy distribution of secondary particles in K^--meson produced σ-stars is shown in Fig. 4 . Comparison with Fig. 3 reveals a slower decrease of the histogram with increasing E and the presence of secondary particles of considerably higher energy than is the case for the π^--meson produced σ-stars.

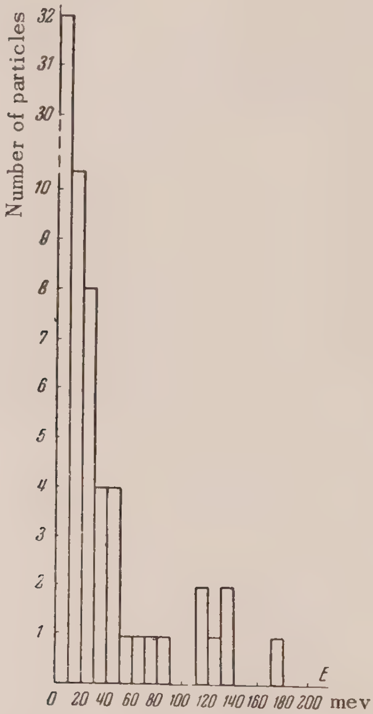

FIG. 4. $\bar{E} = (79.2 \pm 8.5)$ mev.

The authors wish to express their thanks to A.T. Barfolomeev and I. M. Gramenitskii for their participation in the discussion.

---

[1] Menon, Muirhead and Rochat, Phil. Mag. 41, 583 (1950).

[2] Gramenitskii, Zamchalova, Podgoretskii, Tret'iakova and Shcherbakova, J. Exptl. Theoret. Phys. (U.S.S.R.) 28, 616 (1955); Soviet Phys. JETP 1, 562 (1955).

[3] A. O. Vaisenberg, Usp. Fiz. Nauk 57, 631 (1955).

[4] C. F. Powell, Nuovo Cimento 11, Suppl. 2, 165 (1954).

[5] Lal, Yash, Pal and Peters, Phys. Rev. 92, 438 (1953).

[6] Padua Meeting, Nuovo Cimento 12, Suppl. 2, 257 (1954).

[7] Chupp, Goldhaber, Goldhaber and Webb, Conferenza Internazionale Particelle Elementari Pisa, 185 (1955).

Translated by H. Kasha
168

SOVIET PHYSICS JETP VOLUME 4, NUMBER 5 JUNE, 1957

Electrical Explosion of Wires in Vacuum

I. F. KVARTSKHAVA, V. V. BONDARENKO, R. D. MELADZE
AND K. V. SULADZE

(Submitted to JETP editor April 10,1956)
J. Exptl. Theoret. Phys. (U.S.S.R.) 31, 737-744 (November, 1956)

Results of an investigation of electric explosion of wires in vacuum are described. It is shown that regardless of the initial shape of the wire the explosion products propagate as in an ordinary explosion, in a direction normal to the surface of the wire. If the voltage across the capacitor of the explosion circuit is relatively low, the vapor streams, as in the case of an explosion in air, from layers that range themselves perpendicular to the wire. It has been established that at high capacitor voltages the motion of the vapor streams affects the distribution of the discharge current in the space around the wire. A qualitative explanation is given for the observed effects.

1. INTRODUCTION

MANY investigations [1-5] have been devoted to electric explosion of wires in air and in various condensed media, but explosion of wires in vacuum still receives little attention. It would be interesting to investigate this phenomenon because the absence of the perturbing effects of the surrounding medium and the ready condensibility of the metal vapors could make it possible to obtain much additional information concerning the mechanism of the wire explosion to investigate the streams of the explosion products, to study the effect of the motion of these products on the spatial distribution of the discharge about the wire, etc.

We give below the results of experiments on the explosion of wires in a vacuum of approximately 10^{-5} mm Hg in a relatively large chamber.

There is no need for a higher vacuum, for further reduction in pressure does not affect the observed phenomena.

2. PROCEDURE AND EXPERIMENTAL RESULTS

Reference 3 gives the electric diagram of the set-up used in the experiments described below. A cross section through the explosion chamber is shown in Fig. 1, where *1* is the body of the chamber, *2* the high-voltage electrode, and *3* the wire under investigation; the linkage *4* serves to connect the chamber to the vacuum pump. The inside walls of the chamber were covered with a thick layer of lampblack to prevent reflection of light. Both flanges *5* are equipped with symmetrically-located windows of thick plane-parallel glass through which the explosion is photographed. The experiments were performed principally with copper wires. The explosion circuit comprised a 1.2-microhenry inductance and a four-microfarad capacitor.

In the investigation of the explosion-product condensation the wire was enclosed in a coaxial aluminum screen. A time exposure of the explosion was made in the natural light of the discharge in a direction perpendicular to the axis of the wire. The explosion picture was scanned with a mirror through a slit placed transversely through the wire near its center. The corresponding photographs are shown in Figs. 2–10.

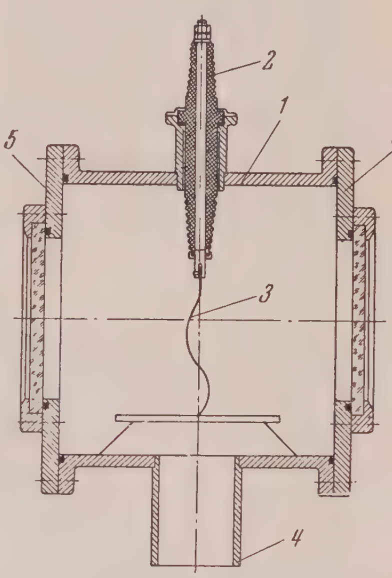

FIG. 1. Diagram of a vacuum chamber.

Figures 2–9 show the photographs of the condensates and of the time-exposures for copper wires in vacuum. Figure 2 shows a part of the aluminum screen coated with the explosion-product condensate from a straight copper wire. It is seen that the condensate forms stripes of constant height over the entire length of the screen. The stripes are perpendicular to the wire, and the height of the condensate is almost equal to the length of the wire. This indicates a radial distribution of the vapor streams from the wire. Figure 3 shows the developed screen with the condensate from an exploded wire bent in an arc; the ends of this arc lie on the axis of the screen. As can be seen, the height of the condensate goes in this case through two unequal maxima and two minima over the length of the screen. The two maxima are located where the plane of the bent wire intersects the screen, the greater maximum being on the convex side of the wire arc, and the smaller on the concave one. The two minima are closer to the smaller maximum and are symmetrical about it. It follows from simple geometric considerations that the geometric locus of the normal projections of the surface points of the wire on the screen reproduces the form and dimensions of the condensate with sufficient accuracy. This leads to a general conclusion that the products of the electric explosion of the wire propagate in directions normal to each point of its surface, regardless of the initial shape of the wire. It should be noted that this propagation of explosion products is similar to the usual explosion caused by strongly stretched charges.

It is evident that under these experimental conditions only the leading front of the vapor stream moves in a high vacuum, and the remaining portions of the stream move in a lower vacuum. Nevertheless, as can be seen from the photographs enclosed, boundaries of the condensate remain distinct and reproduce well the stratified structure of the vapor streams. This is possible only if the vapor streams move at very high radial velocities. Experiments with a ballistic pendulum have shown that the average vapor-stream velocities in our conditions reach approximately 2×10^5 cm/sec.

It must be noted that the stratification of the explosion in vacuum, as in air, is characterized by a certain periodicity, which is well noticeable in the structure of the condensate in Figs. 2 and 3. Fig. 4, obtained with six kv on the capacitor, shows clearly the stratified scattering of the explosion products. The same photographs exhibit also a certain stringing of the charge around the wire (the diameter of the string is approximately 4 millimeters). Fig. 5, obtained with 4 kv on the capacitor, shows that the wire did not have a chance to scatter during the discharge time of the capacitor and assumed a clearly pronounced wavy form owing to the shock compression caused by the rapid heating. No. stringing of the discharge is noted

FIG. 2. Part of aluminum shield on which the wire-explosion product condensed. Wire diameter 0.2 mm, length 60 mm. Capacitator voltage $U_0 = 40$ kv.

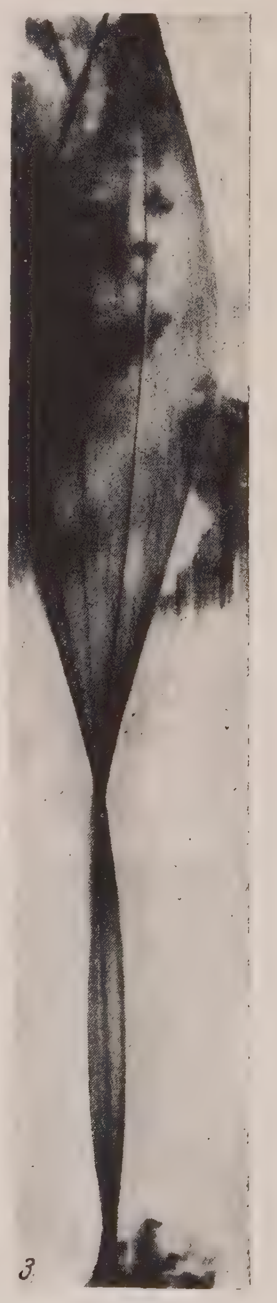

FIG. 3. Developed view of screen with condensed wire-explosion products. Wire 0.3 mm in diameter and 45 mm long, bent in an arc of 50 mm radius. $U_0 = 40$ kv.

here. The attached pictures are good illustrations that the mechanism described in Ref. 4 for the electric explosion of wire in air is correct.

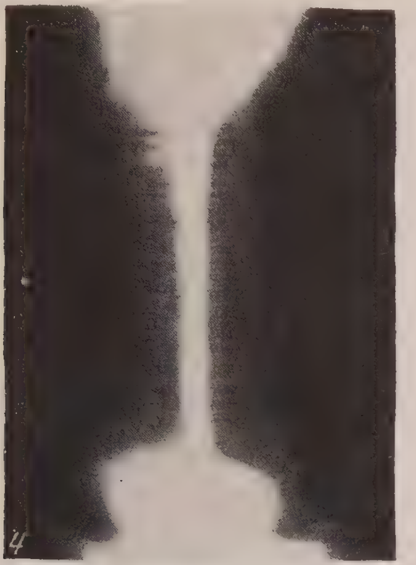

FIG. 4. Wire 45 mm long, 0.15 mm dia. $U_0 = 6$ kv.

Figures 6 and 7 show examples of integral photographs of explosion of straight wires. The signs + and – indicate the positions of the high-voltage and grounded discharge electrodes. What is striking about these photographs is that although they represent a violent explosion process, they exhibit clearly certain discharge states that are, so to speak, stabilized. The physical interpretation and the time sequence of the appearance of these states can be represented as follows. The center of each photograph shows the image of the still unexploded wire, related evidently to the initial stage of the discharge. As can be seen, the wire is surrounded in this stage by a thin layer of discharge, which glows more brightly than the wire itself. It is indeed its small thickness that causes the glowing layer to produce a brighter image at the edges of the wire, and the greatest thickness of the layer is consequently projected on the photographic plate. The fact that the discharge is concentrated in a thin cylindrical layer about the wire can be attributed to compression of the discharge around the wire by the strong magnetic field produced by the current reaching hundreds of thousands of oersteds (see below) at the surface of the wire. In view of the high discharge power the wire is almost instantaneously transformed, toward the end of this stage, into a high-pressure gas of high heat content and of almost the density as the wire. Under these conditions, as is known from the theory of explosive processes [6], the wire vapors scatter radially into the vacuum at high velocities. As the discharge develops further, each photograph shows the image of a thin-wall glowing cylinder, which flares out towards the electrodes, always more towards the high-voltage electrode than toward the grounded one, regardless of the polarity.

FIG. 5. Wire 150 mm long, 0.15 mm dia. $U_0 = 4$ kv. Capacitator 10 microfarad.

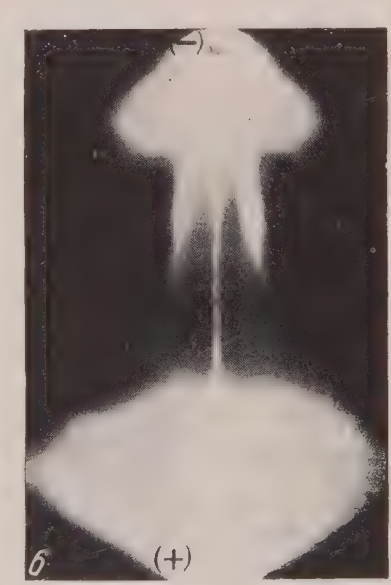

FIG. 6. Wire 45 mm long, 0.15 dia. $U_0 = 20$ kv.

Assuming that the glow of the discharge must under these experimental conditions be due to the flow of current through the gas, it is possible to deduce from the distribution of the brightness in the second glowing layer, (from the sharp increase in the brightness towards its edges) that in this discharge stage the total current is concentrated principally in the thin glowing layer (second layer), bounded on the outside and on the inside by two coaxial surfaces of revolutions.

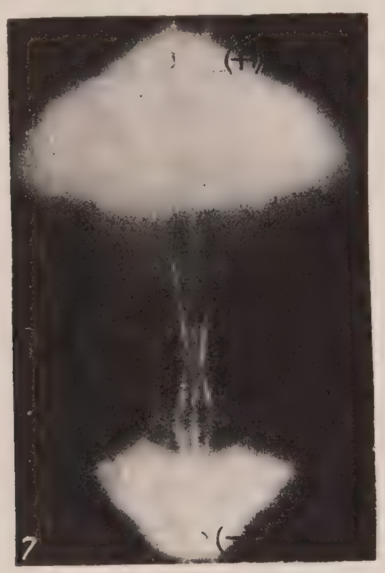

FIG. 7. Wire 45 mm long, 0.15 mm dia, $U_0 = 30$ kv.

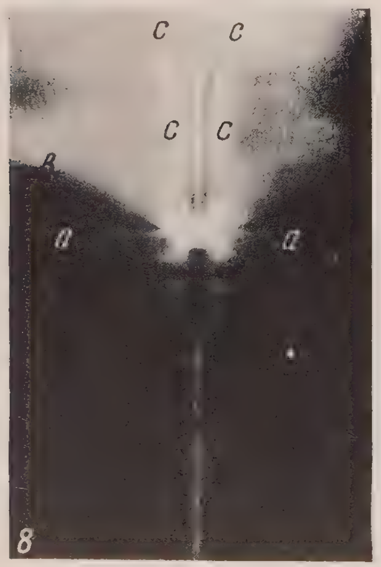

FIG. 8. Wire 90 mm long, 0.15 mm dia, $U_0 = 35$ kv. A plexiglass plate measuring 1 × 100 × 100 mm was placed transverse to the wire.

Figures 6–10 are time-exposure and mirror-scanned photographs of wires exploded in vacuum.

Figure 7 shows that increasing the capacitor voltage not only increases the radial dimensions of the second glowing layer, but produces also a third layer coaxial with the second. In the case of longer wires, several third layers are produced in sequence along the wire. The third layers are sometimes internal branches of the second layer.

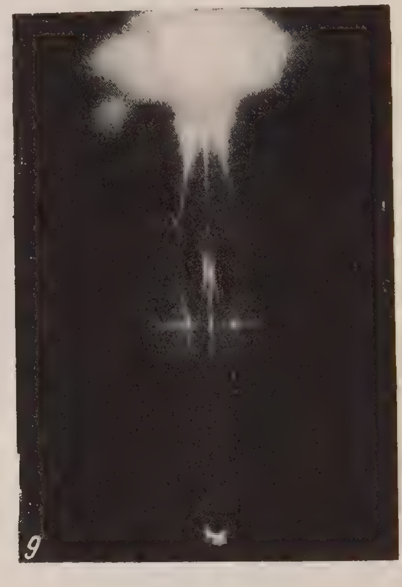

FIG. 9. Photograph analogous to that of Fig. 8, but with 20 mm hole in the plate and $U_0 = 30$ kv.

FIG. 10. Mirror scan of explosion of wire 90 mm long, 0.15 mm dia, at $U_0 = 30$ kv (full size).

Decreasing the wire diameter reduces the radial dimensions of the glowing channels as shown in the corresponding photographs. If the exploded wires are bent in an arc, the generatrices of the glowing channels are similarly bent. An axial time-exposed photograph of an exploding wire with right angle bends on the ends shows an almost-uniform glowing circle around the wire.

All the time-exposed photographs obtained by us indicate the presence of brightly glowing vapor streams originating at both discharge electrodes. Assuming the duration of the glow not to exceed the discharge time of the capacitor (40 microseconds) the average velocity of these streams parallel to the wire amounts to 10^4 cm/sec. Interaction with the radial streams apparently causes these longitudinal streams to slow down in an axial direction and to accelerate in a radial direction.

We proposed that the main cause of the formation of the glowing channels described above is the radial motion of the wire vapors in the strong magnetic field of the current. To check this premise, we set up experiments to determine how disturbances of the vapor streams and forced redistribution of the current around the wire would influence the effect under investigation. Figure 8 illustrates the explosion of a wire across which an insulating plate of organic glass is placed. The wire passes through the center of a 3 mm hole in the middle of this plate. In the photograph, the projection of the plate coincides with the illuminated line *aa*. As can be seen, introducing the insulating plate results in a strong disturbance to the radial vapor streams and in addition to changing the integral picture, it also causes a considerable redistribution of the discharge current. The increased current density causes the maximum brightness of the glow to occur in the region of the hole. From the structure of this region it can be seen that the current density is not uniformly distributed over the cross section of the hole: it increases towards the edges of the glowing cones that lead upwards and downwards from the plane of the hole. In the upper portion of the discharge, the current first flows over the conical channels *bb* (outside cones) and *cc* (inside cone), which result from the reflection of the radial vapor stream from the edges of the hole. Both these cones merge in the upper base (where the radial streams are still undisturbed) with current channels analagous to the second and third channels of Fig. 7. The second channel, owing to its considerable spreading, is not very pronounced on this photograph, but it can be easily distinguished on the corresponding negative.

Located over the bases of the cones is a region of sufficiently bright diffused discharge glow due apparently to the fact that the presence of the insulating plate in this region diverts a portion of the current to the nearest walls of the grounded chamber causing it to flow over the radial streams of the vapor. Here one must expect the current flowing through the radial vapor streams to scatter some of the vapor atoms in an axial direction. After the wire explodes, the upper portion of the plate actually becomes covered by noticeable deposit of copper, while below, where there is no noticeable discharge glow, and where consequently the radial streams are hardly disturbed by the current, the plate remains quite clean. The deposit above has a sharp boundary which is a circle of equal diameter as the upper base of the cone *bb*, and which is concentric with the hole in the plate. The deposit is much thinner inside the circular boundary than outside. On the circle itself the thickness of the deposit has a very sharp and relatively high maximum, this being apparently due to the additional material carried away by the copper ions from the section of the second glowing channel. The photometry curve for the copper deposit, taken with transmitted light along one of the diameter of the boundary circle (Fig. 11), illustrates well the deposit structure described below. The presence of a round deposit boundary of an increased thickness confirms the above hypothesis that the current is concentrated in thin-layered cylindrical channels.

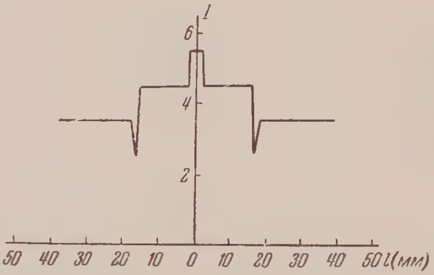

FIG. 11. Photometry curve of copper deposited on insulating plate. *I*—intensity of light in relative units, *l*—distance from center of hole in plate.

In the region between the plate and the grounded electrode one can also see a very weakly glowing channel (approximately cylindrical in shape), which is a continuation of the second upper channel (it is more distinguishable on the corresponding negative). The weak glow of this channel and its smaller radial dimensions (compared with the second upper channel) must be attributed to the smaller current flowing in the region under consideration owing to the presence of the insulating barrier, since the explosion conditions for the wire, and consequently the velocities of the radial vapor streams, are identical on both sides of the insulating plate.

Figure 9 shows an explosion with a 20 mm round hole in the insulating plates. Here the channels are seen more clearly. They pass freely through the large hole, experiencing thereby a certain deformation. The radius of the second channel becomes somewhat smaller in the vicinity of the hole, and the third channel is discontinuous as it passes through the plane of the hole. The deformation of the second channel is apparently due to the lower velocity of the radial streams due to their collision with the edges of the hole.

If the non-conducting plate transverse to the wire in Fig. 8 is replaced by a conducting plate, insulated from the chamber walls of equal size and with the same size hole, the channels remain the same as in the absence of the plate, as can be seen from the corresponding photograph. Only in the direct vicinity of the conducting plate do the channels become discontinuous, probably owing to a reflection of the vapor streams from the edges of the hole. Here, too, a copper deposit of noticeable thickness is formed only on the side of the positive electrode, with hardly any deposit on the negative-electrode side.

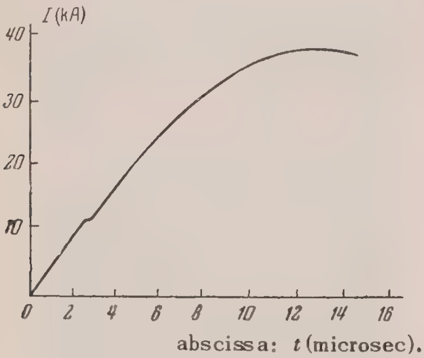

FIG. 12. Oscillogram of current for wire explosion in vacuum. Wire 45 mm long, 0.15 mm dia, $U_0 = 25$ kv.

Figure 10 shows the wire explosion in vacuum, scanned from left to right with a mirror through a transverse slit. The speed of the image along the photograph film is 2.2×10^5 cm/sec. Starting at the bottom, the photograph shows the glowing wire in its state prior to the start of the explosion. Towards the end of the explosion, the glowing region starts moving rapidly upwards in a radial direction (speed of displacement greater than 5×10^5 cm/sec). The displacement is then slowed down and the glowing section settles at a certain distance from the wire image. This evidently corresponds to the position of the second current channel (the lower half of this channel is outside the photographed area). The glow from the stabilized channel lasts approximately 10 microseconds. The half period of the discharge in the explosion circuit is 12 microseconds in this case.

The photograph therefore confirms the assumed sequence with which the current channels are formed, and shows at the same time that these channels are formed and exist only in the first half period of the current.

3. ANALYSIS OF RESULTS

The experimental results given above shows that when electric explosion occurs in vacuum the wire vapors escape at high velocities in directions perpendicular to the wire surfaces. It is known that the explosion of ordinary explosive substances has analogous properties. The physical features of processes that develop in ordinary explosions have been sufficiently well studied at the present time. In view of the common basic properties that electric explosions have with ordinary explosions, the qualitative results given above can be understood from the existing theory of ordinary explosive processes, particularly if the explosion has cylindrical symmetry (see, for example, Ref. 6).

Unlike ordinary explosions, electric explosions are characterized by forces that result from a strong magnetic field due to the current. These forces, as was already noted in Ref. 4, cause certain anomalies of the electric explosion, such as periodic stratification of the escaping wire vapors and others, occurring as the joint result of the axial compression of the wire by thermal shock and a radial compression of the wire by the magnetic field of the current. Figures 2–5 confirm the ideas presented in that work concerning the mechanism of the electric explosion of the wire.

Let us analyze in greater detail the possible causes of the thin-layered cylindrical current channels formed by electric explosion of wires in a vacuum. Starting from the interpretation of the time exposures of the explosion as given above, and also of the mirror scanning of the explosion, one must assume that the main cause the current is concentrated in thin-layered channels is the radial motion of the wire vapors at high velocities in a strong magnetic field of the current.

The time exposures shows that prior to the explosion, the wire is surrounded by a thin layer of a strongly stringing and brightly glowing discharge. Let us assume that the radial thickness of this layer is zero and that the current is distributed uniformly over the cross section of the wire (i.e., we neglect the skin effect, a valid assumption for the dimensions of our wire). In this case the leading front of the vapor stream launched by the explosion must break through the magnetic field H of the current. Inside the wire we have

$$H = 2Ir/r_0^2, \tag{1}$$

where I is the total current in the wire, r_0 the wire radius and r the distance from the point of observation to the wire axis. Outside the wire we have

$$H = 2I/r. \tag{2}$$

In our experiments the current is of the order of 10^4 amperes and r of the order of 10^{-2} cm, making H approximately 10^5 oersteds on the surface of the wire.

A ballistic determination of the average escape velocity of the escape of the wire vapor yields approximately 10^5 cm/sec. Considering that in explosive evaporation in vacuum the velocity of the leading stream of particles is generally considerably higher than the average escape velocity of the explosion products,[6] we can assume the escape velocity of the vapor to be even higher at the beginning of the explosion.

The stream moving through the magnetic field must produce electric field (see Ref. 7, for example) determined from the vector product

$$\mathbf{E} = (1/c)\,[\mathbf{vH}], \tag{3}$$

where c is the velocity of light, $\mathbf{v}$ the velocity of the vapor stream, and H the magnetic field intensity. When the vapors scatter radically this field has the same as the external field E_k. We thus have an effective total field $E_k + E$ outside the wire, while inside the wire, where $\mathbf{v} = 0$ and consequently $E = 0$, the field intensity is only E_k. For the order of magnitude of v and H in our experiments, we have from (3) a field E of 1,000 v/cm on the surface of the wire. An additional field E formed where the vapor streams move should accelerate the ignition of the arc discharge along the wire and correspondingly decrease the discharge resistance. To illustrate this process, Fig. 12 shows the oscillogram of the current produced during an explosion of a wire in vacuum. It is evident from this oscillogram that the current in the wire first increases smoothly until it reaches a "plateau" of 1.2×10^4 a (in the explosion circuit) approximately two microseconds after the start of the discharge. The width of the "plateau" is approximately 0.3 microseconds. Within the "plateau" region the discharge resistance becomes sufficient to carry the remaining capacitor voltage and the current stops increasing. The firing of the arc and the sharp reduction in the resistance at the end of the discharge "plateau" causes the current to resume its increase.

According to Eq. (2), the magnetic field on the surface of the wire reaches a value of approximately 3×10^5 oersteds in the "plateau" region. The formation of such a large magnetic field leads to a strong stringing of the discharge.[7] This gives rise to the first current channel, described above in the discussion of the wire-explosion time exposures. At this stage of the discharge, the total current flow should divide between the wire and the first channel according to the ratio of their resistances.

The first current channel can remain stable at the surface of the wire as long as the pressure from the side of the radial vapor stream against the strung discharge layer does not exceed the counter-pressure due to the magnetic field of the total current. In view of the high discharge power, particularly in the "plateau" stage, a pressure excess is bound to occur and initiate a rapid radial broadening of the channel.

The broadening of the channel forms first of all an arc discharge along the wire and reduces correspondingly the applied field E_k from several thousands v/cm in the "plateau" stage to several v/cm in the arc. This should result in a certain redistribution of the current in the discharge gap, owing to the effect of the radial motion of the wire vapor and of the magnetic field on the distribution of the field E. The current is guided along the channel axis only by the weak field E_k, for H and v are equal to zero here and hence $E = 0$ from (3). Towards the outer boundary of the channel we have [from Eq. (1)] that H increases in proportion to the radius (it is assumed that in this stage the current is distributed approximately uniformly over the cross section of the channel), reaches a very sharp maximum on the outer boundary of the channel, and then starts diminishing in inverse proportion to the radius, in accordance with Eq. (2). The dependence of the stream velocity v on the radius can be given here only qualitatively. At the start of the explosion the velocity on the surface of the wire increases almost in a jump to a certain critical value, beyond which it does not experience any considerable variation.[6] In view of the fact that the metal vapor shows good condensation properties, the same distribution should be maintained from there on.

Based on the above-mentioned distributions of v and H, Eq. (3) shows that the distribution of the field E will be characterized by a sharp maximum at the outer boundary of the current channel. From the values of H and v given above it follows that the value of this maximum is considerably greater than the value of E_k in the arc, and almost the entire discharge current should therefore be concentrated in the narrow region around the maximum of the field E.

As the current channel expands the current density in its conducting layer diminishes to agree with the accompanying decrease in H and E. The concentration of the particles in the radial streams which penetrate the thin walls of the channel also decreases. The walls of the channel therefore become continuously more "transparent" to these streams, and at a certain distance from the wire axis a new equilibrium is established between the forces accelerating the channel and the pressure of the magnetic field which retards its radial expansion. This makes possible the stabilized state corresponding to the second current channel. In view of the cylindrical symmetry of the magnetic field and of the radial vapor streams, these channels should be coaxial with the wire.

The duration of the stabilized channel should depend on the time interval during which E remains sufficiently high in the thin conducting layer of the channel. From Eq. (3), this should be determined in turn by the character of the time dependence of H and v. We do not know tht time dependence of v, but it follows from the current oscillogram on Fig. 12 that H can stay sufficiently high for a considerable fraction of the first half cycle of the current. Assuming that v also remains sufficiently high during the same time, one can say that the duration of the stabilized state of the second channel cannot exceed the first half cycle of current.

Once the discharge current passes through zero at the end of the first half cycle, the second current channel cannot form again since the conditions necessary for its formation no longer exist (no stringing of the current and no high-velocity radial vapor stream). This is in good agreement with the mirror-scanned picture of the wire explosion in vacuum given above.

It follows also from the above qualitative mechanism for the formation of current channel that the greater the initial voltage on the capacitor, i.e., the greater the radial velocities and the concentration of particles in the vapor stream, and also the greater the current density in the corresponding channels, the greater the diameter of the stable channel should be. It is also easier to understand the variation in channel diameter and of its glow intensity with the disturbances produced by the radial vapor streams and of the re-distribution of the current in the discharge gap (Figs. 8 and 9). These changes are related to the corresponding changes in the radial velocity of the vapor streams and of the magnetic field. The broadening of the second current channel near the discharge electrodes (Fig. 6 and 7) is due to the fact that the electrode streamsers, by compressing the radial flow axially, cause it to become radially accelerated to some extent.

The above discussion makes it possible to understand the principal features of the processes that lead to the formation of the first and second current channels in electric explosion of wires in a vacuum. It is evident, however, that the picture given above is merely a rough approximation of actuality and cannot pretend to offer any complete description of the phenomena observed. For example, it is still not understood why third current channels are produced at high capacitor voltages, etc. A more complete analysis of the observed phenomena should evidently be based on a quantitative theory of magnetic-hydrodynamic discharges in a moving gas stream.

The authors express their gratitude to A. T. Kapin for aid in the experimental work.

---

[1] S. V. Lebedev and S. E. Khaikin, J. Exptl. Theoret. Phys. (U.S.S.R.) **26**, 629(1954); **26**, 723 (1954).

[2] S. V. Lebedev, J. Exptl. Theoret. Phys. (U.S.S.R.) **27**, 487, 605 (1954).

[3] Bondarenko, Kvartskhava, Pliutto and Chernov, J. Exptl. Theoret. Phys. (U.S.S.R.) **28**, 191 (1955); Soviet Phys. JETP **1**, 221 (1955).

[4] Kvartskhava, Pliutto, Chernov and Bondareno, J. Exptl. Theoret. Phys. (U.S.S.R.) **30**, 46 (1956).

[5] W. M. Cohn, Phys. Rev. **79**, 213(1950); J. Opt. Soc. Am. **41**, 445 (1951); Nature **169**, 1950 (1952); Phys. Rev. **98**, 1951 (1955); Z. Angew. Phys. **7**, 539 (1955).

[6] N. K. N. Staniukovich, *Unsteady Motion of a Continuous Medium*, GITTL, 1955.

[7] H. Alfven, *Cosmic Electrodynamics*, 1952.

Translated by J. G. Adashko
165

SOVIET PHYSICS JETP VOLUME 4, NUMBER 5 JUNE, 1957

Alpha Decay of Pu^{240}

L. N. KONDRAT'EV, G. I. NOVIKOV, IU. P. SOBOLEV AND L. L. GOL'DIN

(Submitted to JETP editor July 23, 1956)
J. Exptl. Theoret. Phys. (U.S.S.R.) 31, 771-774 (November, 1956)

In this work results are given of investigations on the α-spectrum of Pu^{240} carried out with the help of an α-spectrometer. The α-spectra obtained are presented along with a level scheme for the U^{236} nucleus. The parameters of the 4^+ level are given with precision; the first α-line corresponding to the transition to a 6^+ level is observed and the parameters of this level measured; two weak lines are found which can be assigned to the α-decay of Pu^{240}. A comparison of the experimental data with the theoretical formula of Landau is made for the intensities of the 0^+, 2^+, 4^+ and 6^+ levels.

As is now well known, the low-lying levels of heavy nuclei have a rotational character if the number of neutrons and protons in these nuclei are sufficiently distant from the magic numbers. The low-lying levels of nuclei are particularly clearly exhibited in α-decay; for this reason the investigation of the fine structure of α-spectra appears to be an important method for studying rotational levels. Particularly interesting is the investigation of the α-decay of even-even nuclei for which the theoretical formulas have a simple form and the comparisons with experiment take place in the most direct way.

For rotational levels of even nuclei the excitation energies are described by the known formula[1]

$$E_I = (\hbar^2/2J)\, I\,(I+1), \tag{1}$$

where J is the effective moment of inertia of the nucleus, and I is the angular momentum of the nucleus in the excited state having an energy E_I.

For the calculation of the intensities of the α-decay to levels belonging to the same rotational band, there is an approximate formula by Landau[2]

$$\lambda = (2I+1)\, e^{-\alpha I\,(I+1)}, \tag{2}$$

where λ is the probability of the α-decay to a level with momentum I and α is a constant which can be determined experimentally. Formula (2) is in good agreement with the intensities of the decay to the 2^+ and 4^+ levels of even nuclei. Until now it was not possible to check this formula for 6^+ levels because of the lack of experimental data.

We carried out investigations of the α-spectra in the energy region 4.800 to 5.050 mev for two plutonium sources. The isotopic composition of these two sources is shown in Table I.

The measurements were carried out with the α-spectrometer of the Academy of Sciences of the USSR[3]. The results of two exposures, each of which lasted two weeks, are shown in Fig. 1.

TABLE I

Source	Isotopic Composition			
	Pu^{239} in %	Pu^{240} in %	Pu^{241} in %	Pu^{242} in %
A	12	88	<0.2	<0.2
B	80	17	3	0.5

Line A_1, clearly displayed in Fig. 1A, is known from the literature[4,5] as the line due to the α-decay of Pu^{240} to the 4^+ level of the daughter nucleus. This level was measured by us in this work with substantially better resolution than in a previous experiment[5] and therefore we were able to determine more precisely the parameters obtained earlier for this level (see Table III).

In the spectrum of source A, besides line A_1, several other lines are also observed: A_2, A_3, A_4 and A_5. In the spectrum of source B, besides line B_1 which corresponds to A_1, lines B_4 and B_5 are observed. These last two lines are explained by the admixture of Pu^{241} and Pu^{242} in source B. The energy of line B_4 is in good agreement with the energies of the main levels in the α-spectra of Pu^{241} and Pu^{242}, while line B_5 is due to their unresolved first satellites.

As illustration the energies and relative intensities of α-particles from Pu^{241} and Pu^{242}, taken from Ref. 4, and lines B_4 and B_5 are displayed in Table II.

Line A_5 is known not to belong to either Pu^{241} or Pu^{242}, since its intensity is larger, rather than

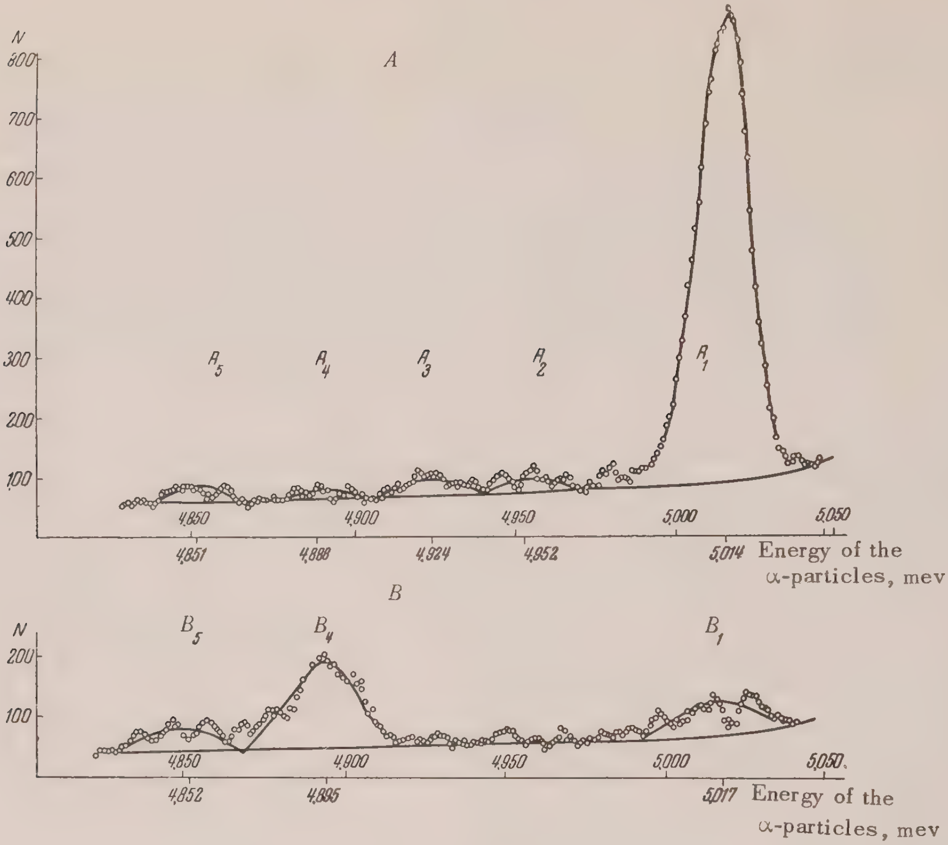

FIG. 1. The α-spectrum of two samples of Pu with different isotopic compositions. (N is the average number of particles in a 0.2 mm strip.)

TABLE II. The energies and intensities of the α-lines from Pu^{241} and Pu^{242} and lines B_4 and B_5.

	Energy of the α-particles	Intensity in %
Pu^{241}	4.893 4.848	75 25
Pu^{242}	4.898 4.854	80 20
Line B_4	4.895	80
Line B_5	4.852	20

3 times smaller, than the intensity of line A_4. By comparison with the intensities of the main Pu^{239} α-lines of sources A and B (not shown in Fig. 1) it is not difficult to calculate that any line belonging to Pu^{239} must be 3.5 times more intense on Fig. 1B than on Fig. 1A. Therefore, one can state that none of the lines on Fig. 1, including also line A_5, belong to Pu^{239}.

There remains the assumption that line A_5 belongs to Pu^{240}. This assumption is particularly natural because the excitation corresponds to a level at 313 kev, which is the energy calculated from Eq. (1) for a 6^+ state. According to Ref. 6, the excitation energy of the first level of Pu^{240} is 44.9 kev. The excitation energy of the 4^+ level calculated from the spectrum presented in Fig. 1*A* is 147 kev. The ratios of the energies of the 2^+, 4^+ and 6^+ levels go as 1:3.28:7.0, while Eq. (1) predicts 1:3.33:7.0 in excellent agreement with experiment.

At this time it is difficult to say anything about the weak lines A_2 and A_3. They cannot belong to Pu^{239}, or Pu^{241} or Pu^{242}. Evidently they are also connected with the α-decay of Pu^{240}. In such a case, it is natural to assume that they belong to an odd rotational structure and that they have angular moments and parities of 1^- and 3^-. The experimental results of the work are presented in Table III. The energies of the α-lines in Table III were computed relative to the main Pu^{240} line, the energy of which was taken to be 5158.9 kev[6].

The α-decay scheme of Pu^{240} and the levels of the daughter nucleus U^{236} are shown in Fig. 2.

TABLE III. New lines in the α-spectrum of Pu^{240}.

Line	Energy of the α-particles, in mev	Energy of the level, in kev	Intensity	Spin and parity
α_{147}	5.014 ± 0.002	147 ± 2	$(9.1 \pm 0.6) \cdot 10^{-4}$	4+
α_{210}?	4.952 ± 0.008	210 ± 8	$(2.7 \pm 2) \cdot 10^{-5}$	1—?
α_{239}?	4.924 ± 0.008	239 ± 8	$(3.1 \pm 1) \cdot 10^{-5}$	3—?
α_{313}	4.851 ± 0.005	313 ± 5	$(3.2 \pm 1) \cdot 10^{-5}$	6+

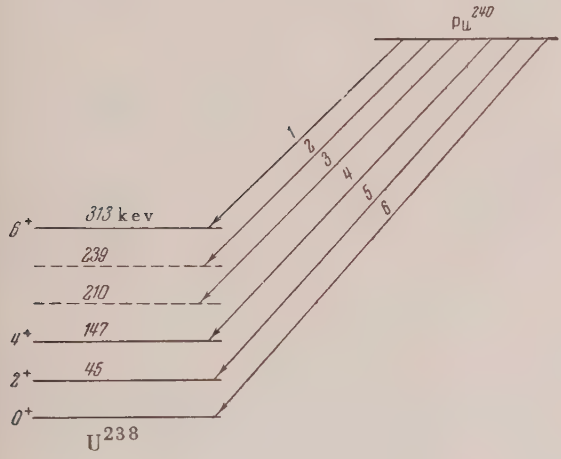

FIG. 2. The α-decay of Pu^{240} and the level scheme of U^{236}. Transitions: *1* – 4.851 mev (3.2×10^{-3} percent); *2* – 4.924 mev (3.1×10^{-3} percent); *3* – 4.952 mev (2.7×10^{-3} percent); *4* – 5.014 mev (0.091 percent); *5* – 5.115 mev (24.4 percent); *6* – 5.159 mev (75.5 percent).

Let us compare the intensity of the α-lines of Pu^{240} with Eq. (2). Choosing constant $\alpha = 0.46$, so that the formula describes correctly the intensities of the first levels, we will find the theoretical ratios $1:0.32:1.2 \times 10^{-3}:5 \times 10^{-8}$ for the intensities of the transitions to the 2^+, 4^+ and 6^+ levels. The observed intensity of the transition to the 6^+ level then turns out to be 800 times larger than the calculated value. Let us note that the fact that the experimental intensities are greater than the calculated ones was already noted in the work of Gol'din, Novikov and Tret'iakov[5] for U^{233}.

We take this occasion to express our gratitude to G. M. Kukavadze for his mass-spectroscopic investigation of the plutonium samples and E. F. Tret'iakov, I. I. Agapkin and G. I. Grishuk for their help in the work.

---

[1] A. Bohr and B. A. Mottelson, Kgl. Danske Mat. Fys. Medd **27**, No. 16 (1953).

[2] L. D. Landau, Paper at the VI th Conference on Nuclear Structure, Moscow, 1956.

[3] L. L. Gol'din and E. F. Tret'iakov, Paper at the VI th Conference on Nuclear Structure, Moscow, 1956; Izv. Akad. Nauk USSR, Ser. Fiz. **20**, No. 8, 859 (1956).

[4] I. Perlman and F. Asaro, Ann. Rev. Nuclear Science, 159 (1954).

[5] Gol'din, Novikov and Tret'iakov, Paper at the VI th Conference on Nuclear Structure, Moscow, 1956; Phys. Rev. **103**, 1004 (1956).

[6] Gol'din, Tret'iakov and Novikov, Session of the Academy of Sciences of the USSR on the peaceful uses of atomic energy, meeting of the division of Physical-Mathematical Sciences, Moscow, 1955.

Translated by F. Ajzenberg-Selove
170

SOVIET PHYSICS JETP VOLUME 4, NUMBER 5 JUNE, 1957

Three Body Problem for Short Range Forces. I. Scattering of Low Energy Neutrons by Deuterons

G. V. SKORNIAKOV AND K. A. TER-MARTIROSIAN

(Submitted to JETP editor July 23, 1955)
J. Exptl. Theoret. Phys. (U.S.S.R.) 31, 775-790 (November, 1956)

An exact solution is obtained for the three body problem in the limiting case of a vanishingly small radius of action of the forces. In this case, the Schrödinger equation for the system of three particles reduces, for motion with a definite momentum, to an integral equation for a function of a single variable. The solution is used for the calculation of the neutron-deuteron scattering cross section. In the limiting case of zero energy of the neutrons, the theory gives the values $a_{3/2} = 0.51 \times 10^{-12}$ cm, $a_{1/2} = 0.30 \times 10^{-12}$cm for the scattering amplitudes.

THE problem of the motion of two nucleons at low energy E has a solution in the form of a series in powers of the small parameters r_0/λ and αr_0, where r_0 is the radius of action of the nuclear forces, $\lambda = \hbar/\sqrt{ME}$ is the wavelength, and $1/\alpha$ is the radius of the bound state or scattering length.

In the zeroth approximation, which corresponds to $r_0 \to 0$, the wave function of the two-nucleon system can be constructed beyond the range of action of the forces if we put upon it the boundary condition

$$\left\{\frac{d}{d\rho}\ln(\rho\Psi)\right\}_{\rho=0} = -\alpha \tag{1}$$

and consider that the potential in the Schrödinger equation has the form:

$$U^{(0)}(\rho) = -(4\pi\hbar^2/M)\rho\delta(\rho), \tag{2}$$

i.e., that it vanishes everywhere for $\rho \neq 0$. In this approximation, which corresponds to the Bethe-Peierls theory of the deuteron[1], the properties of the system do not depend upon the details of the path of the actual potential function $U(\rho)$ and are determined by the value of only a single parameter α.

In the next approximation the wave function can be determined in an expansion in powers of r_0 (outside the range of action of the forces) if the potential in the Schrödinger equation remains in the form (2) as before, but the boundary condition is made more precise:

$$\left[\frac{d}{d\rho}\ln(\rho\Psi)\right]_{\rho=0} = -\alpha + {}^1/_2(\alpha^2 + \bar{\lambda}^{-2})r_0 + Tr_0^3\bar{\lambda}^{-4} + \dots, \tag{1a}$$

where α, r_0 and T are parameters which characterize the actual potential $U(\rho)$.

A similar expansion in powers of r_0 can be carried out for the problem of the motion of three nucleons at small values of the energy E, when the characteristic dimensions of the system, which are defined by the length $\bar{\lambda} = \hbar/\sqrt{ME}$, greatly exceed the radius of force action, r_0. We consider below the zeroth approximation of this expansion, which corresponds to $r_0 \to 0$ (i.e., the Bethe-Peierls theory in the case of two nucleons), in application to the problem of the scattering of neutrons at low energy $E_n < 20$ mev by deuterons.

The problem of the bound state of three nucleons (the nuclei H^3 and He^3) is not considered here, since, in the approximation $r_0 \to 0$, it has no solution; for $r_0 \to 0$, the binding energy becomes infinite[2]. In this case, a more accurate analysis is required, with account being taken of terms of higher order in the expansion in r_0.

In the approximation $r_0 \to 0$ (where the effective depth $U_0 \sim \hbar^2/Mr_0^2$ of the potential well is infinite) the wave function $\Psi(\mathbf{r}_1, \mathbf{r}_2, \mathbf{r}_3)$ of the system of three nucleons satisfies the boundary condition (1), just as in the case of two nucleons, for $\rho_{ik} = |\mathbf{r}_i - \mathbf{r}_k| \to 0$ $(i, k = 1, 2, 3)$. Here the boundary condition can be constructed approximately (with accuracy up to terms of order $r_0/\bar{\lambda}$ and αr_0) outside the range of force action for a potential of the form (2) in the Schrödinger equation. As is shown below, the problem here reduces to the solution of an integral equation for a function which depends on the three variables, or, if we are dealing with a state of definite momentum, on a single variable.

For simplicity, the analysis is first carried out without consideration of the isotopic spin of the nucleons for the three particle system.

1. CASE OF THREE IDENTICAL PARTICLES. THE INTEGRAL EQUATION.

We shall describe the position of the particles in the center-of-mass system:

$$\rho_{23} = \mathbf{r}_2 - \mathbf{r}_3; \quad \rho_1 = \mathbf{r}_1 - {}^1\!/_2 (\mathbf{r}_2 + \mathbf{r}_3),$$

where, in analogy to ρ_{23}, ρ_1, we can also introduce two pairs of vectors ρ_{12}, ρ_3 and ρ_{31}, ρ_2, the furnishing of which (along with the first pair) determines the position of the particles. Between these three systems of vectors we have the following relations

$$\begin{aligned} \rho_{23} &= -{}^1\!/_2\, \rho_{12} - \rho_3 = -{}^1\!/_2\, \rho_{31} + \rho_2, \\ \rho_1 &= {}^3\!/_4 \rho_{12} - {}^1\!/_2\, \rho_3 = -{}^3\!/_4\, \rho_{31} - {}^1\!/_2 \rho_2. \end{aligned} \qquad (3)$$

The wave function of the system is symmetric relative to a permutation of particles; in particular,

$$\Psi(\rho_{23}, \rho_1) = \Psi(\rho_{12}, \rho_3) = \Psi(\rho_{13}, \rho_2); \qquad (3a)$$

$$\Psi(\rho_{23}, \rho_1) = \Psi(-\rho_{23}, \rho_1)$$

etc., and satisfies the Schrödinger equation

$$\begin{aligned} \{-(\hbar^2/M)(\nabla^2_{\rho 23} + {}^3\!/_4 \nabla^2_{\rho 1}) - E\}\, \Psi(\rho_{23}, \rho_1) \quad (4) \\ = -\{U(\rho_{23}) + U(\rho_{12}) + U(\rho_{31})\}\, \Psi(\rho_{23}, \rho_1). \end{aligned}$$

For what follows, it is useful to transform this equation into integral form. For this purpose, we introduce the Green's function

$$G_E(\rho_{23}, \rho_1) = \int e^{i\mathbf{k}\rho_1} (e^{-\gamma_k \rho_{23}} / \rho_{23})\, d\mathbf{k} / (2\pi)^3, \qquad (5)$$

where $\gamma_k = \sqrt{3k^2/4 - ME/\hbar^2}$ if $3k^2/4 - ME/\hbar^2 > 0$ and $\gamma_k = -i\sqrt{ME/\hbar^2 - 3k^2/4}$ in the opposite case*; it satisfies the condition

$$\left(\nabla^2_{\rho_{23}} + \frac{3}{4}\nabla^2_{\rho_1} + \frac{ME}{\hbar^2}\right) G_E(\rho_{23}, \rho_1) \\ = -4\pi\delta(\rho_{23})\,\delta(\rho_1).$$

In spite of the external asymmetry of the description, the function G_E is symmetric relative to a permutation of coordinates $\mathbf{r}_1$, $\mathbf{r}_2$ and $\mathbf{r}_3$; actually, it is not difficult to prove that Eq. (5) for G_E represents an expansion in the Fourier integral of a function that is symmetric in the coordinates of the nucleons:

$$G_E(\rho_{23}, \rho_1) = \frac{2i}{3\sqrt{3}\pi} \frac{ME}{\hbar^2 R^2} H_2^{(1)}\left(\sqrt{\frac{ME}{\hbar^2}}\, R\right)$$

$$= -\frac{8}{3\sqrt{3}\pi^2}\left(\frac{ME}{\hbar^2}\right) \int_0^{2\infty} \exp = \left\{ i\tau \frac{ME}{\hbar^2} R^2 + \frac{i}{4\tau} \right\} \tau\, d\tau,$$

where $H_2^{(1)}$ is an Hankel function and $R^2 = \rho_{23}^2 + 4/3\, \rho_1^2 = 4/3(r_1^2 + r_2^2 + r_3^2 - \mathbf{r}_1 \cdot \mathbf{r}_2 - \mathbf{r}_1 \cdot \mathbf{r}_3 - \mathbf{r}_2 \cdot \mathbf{r}_3)$, and where it must be kept in mind that $\sqrt{ME/\hbar^2} = +i\sqrt{M(-E)/\hbar^2}$, if E is negative (in order that G_E decrease and not increase as $R \to \infty$; this corresponds to the definition of γ_k given above).

By means of the function G_E, the Schrödinger equation (4) can be written in the form*

$$\Psi(\rho_{23}, \rho_1) = \int G_E(\rho_{23} - \rho'_{23},; \rho_1 - \rho'_1)\{u(\rho'_{23}) \qquad (6) \\ + u(\rho'_{12}) + u(\rho'_{31})\} \\ \times \Psi(\rho'_{23}, \rho'_1)\, d\rho'_{23}\, d\rho'_1.$$

Here we have introduced the notation $u(\rho) = -(M/4\pi\hbar^2)U(\rho)$ where, for $r_0 \to 0$, $u(\rho) \to \delta\rho(\rho)$.

Substituting the function (5) in (6), and transforming to the Fourier representation of the wave function,

$$F(\rho_{23}, \mathbf{k}) = \int e^{-i\mathbf{k}\cdot\rho_1} \Psi(\rho_{23}, \rho_1)\, d\rho_1,$$

we get [taking into account the symmetry of Ψ relative to r_1, r_2, r_3 and making use of Eq. (3)], after

---

* In order that G_E have the form of a diverging wave at large ρ_{23}.

* It would be necessary to add the plane wave

$$\Psi_0 = \exp(i\mathbf{k}_0\rho_1 + i\mathbf{f}_0\rho_{23}), \quad f_0^2 + 3k_0^2/4 = ME/\hbar^2,$$

to the right-hand side of Eq. (6) if we were interested in the state $\Psi(\rho_{23}, \rho_1)$, which corresponds to the motion of all three nucleons to infinity with definite momenta (such a state can arise, for example, in the photoeffect on H^3 or He^3). In the problem of the scattering of a particle on the bound state of two others (or in the problem of the bound state of all three particles) the right side of (6) ought not to contain the term Ψ_0.

some transformations*,

$$F(\rho, \mathbf{k}) = \int \frac{\exp\{-\gamma_k |\rho - \rho'|\}}{|\rho - \rho'|} u(\rho') F(\rho', \mathbf{k})\, d\rho' + 8\pi \int \frac{d\mathbf{k}'}{(2\pi)^3} \times \frac{\cos(\mathbf{k}' + \mathbf{k}/2, \rho) \int \cos(\mathbf{k} + \mathbf{k}'/2, \rho')\, u(\rho') F(\rho', \mathbf{k}')\, d\rho'}{k^2 + k'^2 + \mathbf{k}\mathbf{k}' - ME/\hbar^2 - i\tau} \tag{7}$$

or

$$\{\nabla_\rho^2 - 4\pi u(\rho) + ME_k/\hbar^2\} F(\rho, \mathbf{k}) = -8\pi \int \frac{d\mathbf{k}'}{(2\pi)^3} \cos(\mathbf{k}' + \mathbf{k}/2,\ \rho) \times \int \cos(\mathbf{k} + \mathbf{k}'/2,\ \rho')\, u(\rho') F(\rho', \mathbf{k}')\, d\rho'. \tag{8}$$

Here $E_k = E - 3\hbar^2 k^2/4M$; for brevity, the indices on ρ_{23} are omitted everywhere; the quantity $\tau > 0$, $\tau \to 0$ furnishes the rule in (7) for detouring the poles; (8) is obtained from (7) by application of the operator $\nabla_\rho^2 - \gamma_k^2 = \nabla_\rho^2 + ME_k/\hbar^2$. The form of Eqs. (7) and (8) of the Schrödinger equation is suitable for consideration of the case in which $u(\rho)$ is the short range potential. It follows from Eq. (7) that the function $F(\rho, \mathbf{k})$ is defined for arbitrary ρ if its values are known in the region of action of the forces, $\rho \le r_0$. In this region, we can limit consideration, with accuracy up to terms of order $(r_0/\bar{\lambda})^3$, to the spherically symmetric part of F:

$$F_0(\rho, \mathbf{k}) = \int F(\rho, \mathbf{k})\, d\Omega_\rho / 4\pi$$

[in order to establish this, we can substitute in Eq. (7)

$$F(\rho_1, \mathbf{k}) = \sum_{l=0}^{\infty} (2l + 1) F_l(\rho, \mathbf{k}) P_l(\rho\mathbf{k}/\rho k)$$

and estimate the contribution from terms with $l \neq 0$].

But in the region $\rho \le r_0$, we can neglect the right-hand side of Eq. (8). Actually, substituting unity for the cosines in Eq. (8), we get for it the estimate

$$\sim \int (2\pi)^{-3} d\mathbf{k} \int u(\rho') F_0(\rho', \mathbf{k}')\, d\rho' \sim r_0 \int (2\pi)^{-3} d\mathbf{k}' F_0(r_0, \mathbf{k}') \sim \sim r_0^{-2} (r_0/\bar{\lambda})^3 F_0(r_0, \mathbf{k}).$$

[In obtaining this estimate, it has been taken into account that $\int u(\rho') d\rho' \sim r^0$ and also that k and k' are everywhere of order α (or $1/\bar{\lambda}$, if $\bar{\lambda}^{-1} > \alpha$); for large values of k, the function $F_0(\rho, \mathbf{k})$ vanishes or oscillates.]

Comparing this estimate with any of the terms on the left-hand side of Eq. (8),

$$\nabla_\rho^2 F \sim u(\rho) F \sim r_0^{-2} F \quad (\rho \lesssim r_0),$$

$$(ME_k/\hbar^2) F \sim r_0^{-2} (r_0/\bar{\lambda})^2 F,$$

we note that the right-hand side of Eq. (8) differs by the factor $(r_0/\bar{\lambda}) < 1$ from the smallest term $(ME_k/\hbar^2) F$ on the left-hand side.

Thus, in the zeroth approximation, we do not have to take the right-hand side of Eq. (8) into consideration. But this means that the function $F_0(\rho, \mathbf{k})$, which is regular for $\rho = 0$, satisfies the same equation

$$[d^2/d\rho^2 - 4\pi u(\rho) + ME_k/\hbar^2][\rho F_0(\rho, \mathbf{k})] = 0 \tag{9}$$

in the region $\rho \lesssim r_0$ as the function of the system of two particles, i.e., for $\rho = r_0$, it has the same value (1) of the logarithmic derivative as the wave function for the two-particle system. Physically, neglect of the right-hand side of Eq. (8) [i.e., use of Eq. (1)] corresponds to neglect of random penetrations of the third particle into the region of interaction of the other two.

Therefore, in accord with Eq. (1), we have, in

---

* The first term in Eq. (7) follows trivially from the term in (6) which contains the factor $u(\rho'_{23})$; the Fourier component of the following term in (6), which contains $u(\rho'_{12})$ is transformed, by means of (3) and (3a), into the form

$$\int \exp\left[i\mathbf{k}\left(\frac{3}{4}\rho'_{12} - \frac{1}{2}\rho'_3\right)\right] \frac{\exp[-\gamma_k |\rho_{23} + {}^1\!/_2\rho'_{12} + \rho'_3|]}{|\rho_{23} + {}^1\!/_2\rho'_{12} + \rho'_3|} \times u(\rho'_{12}) \Psi(\rho'_{12}, \rho'_3)\, d\rho'_{12}\, d\rho'_3 \equiv$$

$$\equiv \int \frac{d\mathbf{k}\, 4\pi \exp[-i(\mathbf{k}' + \mathbf{k}/2, \rho_{23})]}{(2\pi)^3 (k^2 + k'^2 + \mathbf{k}\mathbf{k}' - ME/\hbar^2 - i\tau)} \times \int \exp[-i(\mathbf{k} + \frac{1}{2}\mathbf{k}', \rho'_{12})]\, u(\rho'_{12}) F(\rho'_{12}, \mathbf{k}')\, d\rho'_{12}.$$

Along with the Fourier component of the third term in Eq. (6), this expression gives the second component in Eq. (7).

the approximation $r_0 \to 0$,

$$\left\{\frac{d}{d\rho}[\rho F_0(\rho, \mathbf{k})]\right\}_{\rho=0} = -\alpha[\rho F_0(\rho, \mathbf{k})]_{\rho=0}. \qquad (10)$$

In this approximation, we have, by Eqs. (2) and (7),

$$F(\rho, \mathbf{k}) = \frac{\exp(-\gamma_k \rho)}{\rho}\chi(\mathbf{k}) \qquad (11)$$

$$+ 8\pi \int \frac{d\mathbf{k}'}{(2\pi)^3} \frac{\chi(\mathbf{k}')\cos(\mathbf{k}' + \mathbf{k}/2, \rho)}{k^2 + k'^2 + \mathbf{k}\mathbf{k}' - (ME/\hbar^2) - i\tau},$$

$$\chi(\mathbf{k}) = \lim_{\rho \to 0}\{\rho F(\rho, \mathbf{k})\} = \lim_{\rho \to 0}\{\rho F_0(\rho, \mathbf{k})\}.$$

Substituting Eq. (11) in Eq. (10), we get an integral equation for $\chi(\mathbf{k})$:

$$(\alpha - \gamma_k)\chi(\mathbf{k}) \qquad (12)$$

$$+ 8\pi \int \frac{d\mathbf{k}'}{(2\pi)^3} \frac{\chi(\mathbf{k}')}{k^2 + k'^2 + \mathbf{k}\mathbf{k}' - (ME/\hbar^2) - i\tau} = 0.$$

The solution of this equation determines the wave function of the system, in accord with Eq. (11). For states with a definite quantity of momentum, Eq. (12) reduces to an equation for a function which depends on one independent variable, which can be solved numerically.

The idea for this consideration of the three body problem was supplied by L. D. Landau.

2. CASE OF THREE IDENTICAL PARTICLES. THE SCATTERING OF A PARTICLE BY THE BOUND STATE OF THE OTHER TWO.

If $\alpha > 0$, then there exists a bound state of two particles with binding energy $\epsilon = \hbar^2\alpha^2/M$. This state is described, beyond the region of action of the forces, by the wave function

$$\varphi_0(\rho) = \sqrt{\alpha/2\pi}\exp(-\alpha\rho)/\rho.$$

Let us consider the problem of the scattering of a third particle by such a system.

Let $\hbar\mathbf{k}_0$ be the momentum relative to the motion of the incident particle. Then

$$E = \hbar^2 k_0^2/2\mu - \hbar^2\alpha^2/M; \quad \mu = {}^2/_3 M,$$

$$\text{i.e., } ME/\hbar^2 = -[\alpha^2 - 3k_0^2/4].$$

The wave function of the system of three particles Ψ, for large ρ_1 (or ρ_2 or ρ_3), ought to undergo transition to the product of the function φ_0 and the sum of a plane and a diverging wave. This requirement will be satisfied if Eq. (11) has a solution of the form

$$\chi(\mathbf{k}) = \sqrt{\frac{\alpha}{2\pi}}\left\{(2\pi)^3\delta(\mathbf{k} - \mathbf{k}_0) + \frac{4\pi a(\mathbf{k}, \mathbf{k}_0)}{k^2 - k_0^2 - i\tau}\right\}, \qquad (13)$$

where the amplitude of elastic scattering is

$$a(\vartheta) = \lim_{k^2 \to k_0^2}\frac{k^2 - k_0^2}{4\pi}\int \varphi_0^*(\rho) F(\rho, \mathbf{k})\, d\rho;$$

for such a choice, $\chi(\mathbf{k})$ is seen equal to

$$a(\vartheta) = [a(\mathbf{k}, \mathbf{k}_0)]_{k=k_0};$$

ϑ is the angle between $\mathbf{k}$ and $\mathbf{k}_0$ [the second term in Eq. (11) vanishes after multiplication by $k^2 - k_0^2$, if $k^2 \to k_0^2$].

In a similar way, the inelastic scattering amplitude is determined by the equation

$$a(\mathbf{k}_f, \mathbf{f}; \mathbf{k}_0 d) = \left\{\frac{k^2 - k_f^2}{4\pi}\int \varphi_{\mathbf{f}}^*(\rho) F(\rho, \mathbf{k})\, d\rho\right\}_{k \to k_f}$$

Here, in the approximation $r_0 \to 0$,

$$\varphi_{\mathbf{f}} = e^{i\mathbf{f}\rho} + a_f e^{if\rho}/\rho, \quad a_f = -1/(\alpha + if)$$

is the wave function of the final state of two particles with relative momentum $\mathbf{f}$:

$${}^3/_4 k_f^2 + f^2 = {}^3/_4 k_0^2 - \alpha^2;$$

$$k_f = \sqrt{k_0^2 - {}^4/_3(\alpha^2 + f^2)},$$

k_f is the momentum of the particle after inelastic scattering. This amplitude can also be expressed by $a(\mathbf{k}, \mathbf{k}_0)$, with the aid of Eqs. (11) and (12):

$$a(\mathbf{k}_f, \mathbf{f}, \mathbf{k}_0 d) = \sqrt{8\pi a}\left\{\frac{a(\mathbf{k}_f, \mathbf{k}_0)}{(f + i\alpha)^2} + \frac{a(\mathbf{f} - {}^1/_2\mathbf{k}_f, \mathbf{k}_0)}{{}^3/_4[(\mathbf{f} - {}^1/_2\mathbf{k}_f)^2 - \mathbf{k}_0^2]} + \frac{a(-\mathbf{f} - {}^1/_2\mathbf{k}_f, \mathbf{k}_0)}{{}^3/_4[(\mathbf{f} + {}^1/_2\mathbf{k}_f)^2 - k_0^2]}\right\}.$$

Substituting (13) in (12), we get the inhomogeneous equation

$$\frac{{}^3/_8\, a(\mathbf{k}, \mathbf{k}_0)}{\alpha + \sqrt{3k^2/4 - ME/\hbar^2}} \qquad (14)$$

$$= \frac{1}{k^2 + k_0^2 + \mathbf{k}\mathbf{k}_0 - (ME/\hbar^2) - i\tau}$$

$$+ 4\pi \int \frac{a(\mathbf{k}', \mathbf{k}_0)}{(k^2 + k'^2 + \mathbf{k}\mathbf{k}' - (ME/\hbar^2) - i\tau)(k'^2 - k_0^2 - i\tau)} \times \frac{d\mathbf{k}'}{(2\pi)^3},$$

whose solution, in accord with Eqs. (13) and (11), determines (in zeroth approximation in r_0) the wave function of the system and all the scattering amplitudes. This equation has a much simpler form for $k_0 \to 0$, $ME/\hbar^2 \to -\alpha^2$, when the scattering is spherically symmetric.

If we introduce the dimensionless quantity

$$a(\mathbf{k}, 0) = a(k, \vartheta) = \alpha^{-1}\tilde{a}(x), \quad x = k/\alpha,$$

we get

$$\frac{{}^3/_8\,\tilde{a}(x)}{\sqrt{3x^2/4+1}+1} = \frac{1}{1+x^2} \tag{15}$$

$$+\frac{2}{\pi}\int_0^\infty \frac{1}{2xx'} \ln\frac{1+x^2+x'^2+xx'}{1+x^2+x'^2-xx'}\,\tilde{a}(x')\,dx',$$

where the scattering amplitude of particles with zero energy is determined by the value $\tilde{a}$ (0):

$$a_0 = a(0, 0) = \alpha^{-1}\tilde{a}(0).$$

The function $\tilde{a}(x)$ is plotted in Fig. 1. This function was obtained by numerical integration of Eq. (15). According to Fig. 1,

$$\tilde{a}(0) = \left(\frac{8}{3}\right)\left[1 + \frac{4}{\pi}\int_0^\infty \frac{\tilde{a}(x')\,dx'}{1+x'^2}\right] \approx 2.5.$$

For $k_0 \neq 0$, we can expand the function $a(\mathbf{k}, \mathbf{k}_0)$ in a series of Legendre polynomials:

$$a(\mathbf{k}, \mathbf{k}_0) = \sum_{l=0}^{\infty}(2l+1)\,a_l(k, k_0)\,P_l(\cos\vartheta). \tag{16}$$

The equations for $a_l(k, k_0)$ follow from (14), in analogy to Eq. (15). These can be solved numerically (this is done in the Appendix at the end of this paper). In contrast to Eq. (15), the kernel of these equations is complex*, so that the quantities $a_l(k, k_0)$ are complex for $k_0 \neq 0$.

It should be noted that Eq. (12) formally has the form of a three-dimensional Schrödinger equation. Actually, introducing the function

$$\psi(\rho_1) \tag{17}$$

$$= \int\left[\frac{4\pi}{\alpha+\sqrt{3k^2/4 - ME/\hbar^2}}\right]^{1/2}\chi(\mathbf{k})\,e^{i\mathbf{k}\rho_1}\,d\mathbf{k}/(2\pi)^3,$$

which, for $\rho_1 \to \infty$ has the form [in accord with Eq. (13)]:

$$\psi(\rho_1) \sim e^{i\mathbf{k}_0\rho_1} + a(\mathbf{k}_0', \mathbf{k}_0)\,e^{ik_0\rho_1}/\rho_1,$$

$\mathbf{k}' = k_0\rho_1/\rho_1$, i.e., it describes the elastic scattering of a particle on the bound state of the other two; we note that Eq. (12) is equivalent to the Schrödinger equation for $\psi(\rho_1)$ in the usual form:

$$[-(\hbar^2/2\mu)\nabla^2_{\rho 1} + \hat{V}]\,\psi(\rho_1) = (\hbar^2k_0^2/2\mu)\,\psi(\rho_1),$$

where $\mu = 2M/3$ is the reduced mass. Here $\hat{V}$ is the interaction operator (of one particle with the bound state of the two others), defined by the matrix elements

$$\int e^{i\mathbf{k}\rho_1}\hat{V}e^{-i\mathbf{k}\rho_1}\,d\rho_1 \tag{18}$$

$$= -\frac{8\pi\hbar^2}{M}\,\frac{[(\alpha+\gamma_k)(\alpha+\gamma_{k'})]^{1/2}}{(K^2/4)+3q^2-(ME/\hbar^2)-i\tau} = V(\mathbf{K}, \mathbf{q}),$$

$$\mathbf{k} = \mathbf{q} + \mathbf{K}/2,\ \ \mathbf{k}' = \mathbf{q} - \mathbf{K}/2,\ \ \hat{V}\,\psi(\rho_1)$$

$$= \int V(\rho_1, \rho_1')\,\psi(\rho_1')\,d\rho_1',$$

$$V(\rho_1, \rho_1') = \iint \exp\{i\mathbf{K}(\rho_1 + \rho_1')/2$$

$$+ i\mathbf{q}(\rho_1 - \rho_1')\}\,V(\mathbf{K}, \mathbf{q})(2\pi)^{-6}\,d\mathbf{K}\,d\mathbf{q}.$$

The operator $\hat{V}$ is Hermitian only when the energy $\hbar^2k_0^2/2\mu$ of the particle is less than the energy ϵ binding the other two, i.e., under the condition

$$E = \hbar^2k_0^2/2\mu - \varepsilon < 0;$$

in the converse case (when inelastic scattering is impossible) the potential (18) is complex*.

---

* For $k_0 \neq 0$, the quantity

$$k'^2[k'^2 - k_0^2 - i\tau]^{-1} \equiv P\,\frac{k'^2}{k'^2 - k_0^2} + i\pi k'^2\delta(k'^2 - k_0^2)$$

in Eq. (14) is complex (for $k_0 = 0$, it reduces to unity).

* For its crude estimate, we set $V(\mathbf{K}, \mathbf{q}) \approx V(\mathbf{K}, 0)$. This gives $V(\rho_1) \approx V(\rho_1)\psi(\rho_1)$ where, for $V(\rho_1)$, we get the estimate $V(\rho_1) \approx -(16\epsilon/\alpha\rho_1)\,e^{-2\alpha\rho_1}$ for $k_0 = 0$ and $V(\rho_1) \sim \exp(i\rho_1/\lambda\!\!\!^{-})$ for $3k_0^2/4 \gg \alpha^2$. For $k_0 = 0$, the potential falls off with increase in ρ_1 as the density of the bound state $|\varphi_0|^2$.

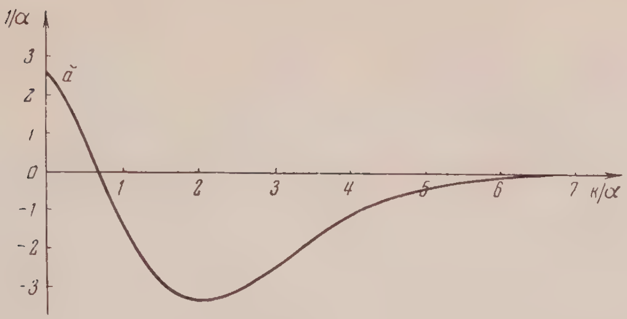

FIG. 1.

3. CONSIDERATION OF SPIN AND ISOTOPIC SPIN

The previous analysis can be generalized to the case of the motion of three nucleons, in which spin and isotopic spin are taken into account. We assume that central forces (we do not consider non-pair forces, triple forces and also tensor forces) act between each pair of nucleons. The potential for such forces,

$$\hat{U}(\rho) = U_1(\rho) + (\sigma_1\sigma_2)\,U_2(\rho) \tag{19}$$

$$+ (\tau_1\tau_2)\,U_3(\rho) + (\sigma_1\sigma_2)(\tau_1\tau_2)\,U_4(\rho)$$

corresponds to the hypothesis of isotopic invariance of nuclear forces; here U_1, U_2, U_3 and U_4 are certain functions of ρ which vanish for $\rho > r_0$, and σ and τ are the operators of spin and isotopic spin, respectively. In this case, the total spin S, the isotopic spin T, and their projections on the OZ axis---S_z and T_z---will be constants of the motion.

Let $\alpha_i = \alpha(\xi_i)$ and $\beta_i = \beta(\xi_i)$ be the spin wave functions of the ith nucleon (ξ_i is the spin variable) corresponding to the spin projections $S_z = 1/2$ and $S_z = -1/2$. The wave functions of the system of three nucleons can be constructed from α_i and β_i by making use of the well-known values of the coefficients of the Clebsch-Gordan series; for $S_z = 1/2$, we get two functions in the case $S = 1/2$:

$$\chi_1 = \frac{1}{\sqrt{2}}(\alpha_2\beta_3 - \beta_2\alpha_3)\,\alpha_1,$$

$$\chi_2 = \frac{1}{\sqrt{3}}\alpha_1\frac{1}{\sqrt{2}}(\alpha_2\beta_3 + \beta_2\alpha_3) - \sqrt{\frac{2}{3}}\,\beta_1\alpha_2\alpha_3,$$

and one in the case $S = 3/2$:

$$\chi_3 = \sqrt{\frac{2}{3}}\,\alpha_1\frac{1}{\sqrt{2}}(\alpha_2\beta_3 + \beta_2\alpha_3) + \frac{1}{\sqrt{3}}\,\beta_1\alpha_2\alpha_3.$$

Of these, χ_3 is symmetric relative to a permutation $\hat{P}^{(\sigma)}_{ik}$ of the spin variables of an arbitrary pair of nucleons: $\hat{P}^{(\sigma)}_{ik}\chi_3 \equiv \chi_3$, while χ_1 and χ_2 transform lineraly into each other upon permutations: χ_1 is antisymmetric and χ_2 is symmetric relative to the permutation $\hat{P}^{(\sigma)}_{23}$ so that the permutation $\hat{P}^{(\sigma)}_{23}$ corresponds to the matrix $M_{23} = \begin{pmatrix} -1 & 0 \\ 0 & 1 \end{pmatrix}$ of a linear transformation of the functions χ_1 and χ_2; similarly, it is not difficult to prove that the matrices

$$M_{13} = \begin{pmatrix} 1/2 & -\sqrt{3}/2 \\ -\sqrt{3}/2 & -1/2 \end{pmatrix} \text{ and } M_{12} = \begin{pmatrix} 1/2 & \sqrt{3}/2 \\ \sqrt{3}/2 & -1/2 \end{pmatrix}.$$

correspond to the permutations $\hat{P}^{(\sigma)}_{13}$ and $\hat{P}^{(\sigma)}_{12}$. We note that the functions χ_1 and χ_2 and χ_3 can be obtained as a result of application of the operators

$$\hat{P}^{(\sigma)}_1 = \frac{1}{\sqrt{2}}(\hat{P}^{(\sigma)}_{13} - \hat{P}^{(\sigma)}_{12}), \tag{20}$$

$$\hat{P}^{(\sigma)}_2 = \frac{1}{\sqrt{6}}(\hat{P}^{(\sigma)}_{13} + \hat{P}^{(\sigma)}_{12}) - \sqrt{\frac{2}{3}}\,\hat{P}^{(\sigma)}_{23},$$

and the symmetrization operator

$$\hat{P}^{(\sigma)}_3 = \frac{1}{\sqrt{3}}(\hat{P}^{(\sigma)}_{13} + \hat{P}^{(\sigma)}_{12} + \hat{P}^{(\sigma)}_{23})$$

to the function $\beta_1\alpha_2\alpha_3$, which is symmetric in the spins of the 2nd and 3rd nucleons. Similar functions of isotopic spin for $T_z = 1/2$ (this value of T_z corresponds to a system of two neutrons and one proton) are denoted by ϑ_1 and ϑ_2 for $T = 1/2$ and ϑ_3 for $T = 3/2$.

The spin and isotopic spin wave functions Φ are obtained by multiplication of the functions χ and ϑ;

we have, evidently,

for $T = 3/2$, $S = 3/2$, the function $\widetilde{\Phi}_c = \chi_3\ \vartheta_3$;
for $T = 3/2$, $S = 1/2$, two functions $\widetilde{\Phi}_1' = \chi_1\ \vartheta_3$
and $\widetilde{\Phi}_2' = \chi_2\ \vartheta_3$;
for $T = 1/2$, $S = 3/2$, two functions $\Phi_1' = \chi_3\ \vartheta_1$
and $\Phi_2' = \chi_3\ \vartheta_2$;
for $T = 1/2$, $S = 1/2$, four functions $\chi_1\vartheta_1$, $\chi_2\vartheta_2$,
$\chi_2\ \vartheta_1$ and $\chi_1\ \vartheta_2$.

In the latter case, instead of the four functions listed, it is appropriate to choose (as the basic system) linear combinations of them, which possess definite properties relative to permutations. Such combinations are[4]:

$$\Phi_a = \frac{1}{\sqrt{2}}(\chi_1\vartheta_2 - \chi_2\vartheta_1);\quad \Phi_1 = \frac{1}{\sqrt{2}}(\chi_1\vartheta_2 + \chi_2\vartheta_1);$$
$$\Phi_c = \frac{1}{\sqrt{2}}(\chi_1\vartheta_1 + \chi_2\vartheta_2);\quad \Phi_2 = \frac{1}{\sqrt{2}}(\chi_1\vartheta_1 - \chi_2\vartheta_2)$$

[the factor $1/\sqrt{2}$ is introduced for normalization: $(\Phi^+, \Phi) = 1$]. As is not difficult to show, Φ_a is antisymmetric relative to simultaneous permutation of the spin and isotopic spin of an arbitrary pair of nucleons, Φ_c is completely symmetric, while the pair of functions Φ_1 and Φ_2 transform into each other in the same fashion as the functions χ_1 and χ_2 (i.e., with the help of the matrices M_{23}, M_{13} and M_{12}). Evidently, the pairs Φ_1', Φ_2' and $\widetilde{\Phi}_1'$, $\widetilde{\Phi}_2'$ possess this same property of transformation.

It should be noted that if Ψ_1 and Ψ_2 (functions of the coordinates of the nucleons), which transform into one another upon a permutation $\hat{P}_{ik}^{(r)}$ of the coordinates $\mathbf{r}_i$ and $\mathbf{r}_k$ ($i, k = 1, 2, 3$; $i \neq k$), in the same way as χ_1 and χ_2 transform under a permutation of the corresponding spins, then we can construct (in analogy to Φ_a, constructed from χ and ϑ) the function

$$\Psi_1\Phi_2 - \Psi_2\Phi_1,$$

which will be antisymmetric relative to the permutation $\hat{P}_{ik}^{(\sigma)}\hat{P}_{ik}^{(\tau)}\hat{P}_{ik}^{(r)}$ of all coordinates of any pair of nucleons. Taking this into account, we write the antisymmetric function of a system of three nucleons in the form:

$$\begin{aligned} T = {}^3/_2,\quad S = {}^3/_2{:}\quad & \Psi_{^3/_2,\,^3/_2} = \widetilde{\Psi}_a\widetilde{\Phi}_c, \\ T = {}^3/_2,\quad S = {}^1/_2{:}\quad & \Psi_{^3/_2,\,^1/_2} = \widetilde{\Psi}_1'\widetilde{\Phi}_1' - \widetilde{\Psi}_2'\widetilde{\Phi}_1', \\ T = {}^1/_2,\quad S = {}^3/_2{:}\quad & \Psi_{^1/_2,\,^3/_2} = \Psi_1'\Phi_2' - \Psi_2'\Phi_1' \\ T = {}^1/_2,\quad S = {}^1/_2{:}\ \sqrt{2}\, & \Psi_{^1/_2,\,^1/_2} = \Psi_a\Phi_c - \Psi_c\Phi_a \\ & + \Psi_1\Phi_2 - \Psi_2\Phi_1. \end{aligned} \tag{21}$$

All the functions $\Psi_{T,S}$ will be antisymmetric relative to a permutation $\hat{P}_{ik}^{(\sigma)}\hat{P}_{ik}^{(\tau)}\hat{P}_{ik}^{(r)}$ of all coordinates of any pair of nucleons if, upon permutation $\hat{P}_{ik}^{(r)}$ of the coordinates $\mathbf{r}_i$, $\mathbf{r}_k$, the functions $\widetilde{\Psi}_a$ and Ψ_a will be antisymmetric, Ψ_c will be symmetric and the pairs Ψ_1 and Ψ_2; Ψ_1' and Ψ_2'; $\widetilde{\Psi}_1'$ and $\widetilde{\Psi}_2'$ will transform linearly one into the other, just as χ_1 and χ_2 transform upon the corresponding permutation of spins (the factor $\sqrt{2}$ for $\Psi_{½,½}$ is written for normalization purposes).

The isotopic spin of the deuteron is equal to zero, and that of the neutron is one-half. Therefore, keeping in mind the problem of deuteron-neutron scattering, it suffices to limit ourselves to a consideration of the latter two of the states described above, i.e., the states with $T = 1/2$. We find the coordinate part of Ψ_c, Ψ_a, Ψ_1, Ψ_2 and Ψ_1', Ψ_2' corresponding to the wave functions.

The wave function is a solution of the Schrödinger equation which can be written in the form (6) if by $U(\rho)$ is understood the potential (19).

In the approximation $r_0 \to 0$, in the first term on the right-hand side of (6),

$$\int (G_E(\rho_{23} - \rho_{23}';\ \rho_1 - \rho_1') \times \frac{\{-MU(\rho_{23}')\}}{4\pi\hbar^2}\Psi(\rho_{23}', \rho_1')\, d\rho_{23}'\, d\rho_1',$$

only the region $\rho_{23}' \leq r_0 \to 0$ will be essential for the integration; therefore, the dependence of this term on the coordinates ρ_{23} and ρ_1 is determined by the relation

$$f_{23} = f(\rho_{23}, \rho_1) = \int G_E(\rho_{23}, \rho_1 - \rho) f(\rho)\, d\rho, \tag{22}$$

where

$$f(\rho) = \lim_{\rho_{23}\to 0}\{\rho_{23}\Psi(\rho_{23}, \rho)\}$$

is some unknown function. Similarly, the dependence of the coordinates of the following two terms in (6) is determined by the functions

$$f_{13}=f(\rho_{13},\rho_2) \text{ and } f_{12}=f(\rho_{12},\rho_3).$$

In other words, according to Eq. (6), the coordinate part of the wave function is represented by some linear combination of terms of the form f_{23}, f_{13} and f_{12}. In principle, we could, by substituting the potential (19) in Eq. (6) and multiplying successively both parts of (6) by different functions Ψ of the spin and the isotopic spin, obtain integral equations for the coordinate parts of Ψ only, which would also define the form of the linear combination described above. However, this could also be done, not by writing out the equation for the coordinate part, but by making use only of the symmetry properties of the function Ψ. Since the function Ψ, being symmetric relative to $\mathbf{r}_1$, $\mathbf{r}_2$ and $\mathbf{r}_3$, ought to be equal to the sum $f_{23}+f_{12}+f_{13}$ of the functions f_{ik} which are determined by a single function $f(\rho)$, since only this sum remains unchanged upon the permutation $\hat{P}^{(r)}_{ik}$ of the coordinates of an arbitrary pair of nucleons:

$$\Psi_c=f_{23}+f_{13}+f_{12}. \tag{23}$$

The antisymmetric Ψ_a in the coordinates of the nucleons is a function identically equal to zero, since, in accord with (5) a function of the type (22) is symmetric in $\mathbf{r}_2$ and $\mathbf{r}_3$: $f(\rho_{23},\rho_1)=f(-\rho_{23},\rho_1)$ and as a result of its antisymmetrization in $\mathbf{r}_2$ and $\mathbf{r}_3$, we obtain zero. With the help of integral equations for the coordinate parts of Ψ of the wave function we can show that this result is valid with accuracy up to terms of order $(r_0/\lambda\!\!\!^-)^3$ in comparison with unity.

The functions Ψ_1 and Ψ_2, which transform upon permutation like χ_1 and χ_2, are represented in the form of a linear combination of functions of the type (22), φ_{23}, φ_{13} and φ_{12} [i.e., $\varphi_{23} = \int G_E(\rho_{23},\rho_1-\rho)\,\varphi(\rho)\,d\rho$, where $\varphi(\rho)$ is an unknown function]. Introducing the operators $\hat{P}^{(r)}_1$ and $\hat{P}^{(r)}_2$ which are analogous to (20) but which permute the coordinates of the nucleons, we evidently get $\Psi_1=\sqrt{3/2}\,\hat{P}^{(r)}_1\varphi_{23}$; $\Psi_2=\sqrt{3/2}\,\hat{P}^{(r)}_2\varphi_{23}$ [just the same as χ_1 and χ_2 could be obtained as a result of the action of $\hat{P}^{(\sigma)}_1$ and $\hat{P}^{(\sigma)}_2$ on the function $\beta_1\alpha_2\alpha_3$, which is symmetric in the spins of nucleons 2 and 3; the factor $\sqrt{3/2}$ was chosen for normalizing the functions $\varphi(\rho)$]. Thus,

$$\Psi_1=(\sqrt{3}/2)(\varphi_{12}-\varphi_{13}), \tag{24}$$

$$\Psi_2={}^1\!/_2(\varphi_{12}+\varphi_{13})-\varphi_{23}.$$

In similar fashion, Ψ_1' and Ψ' are expressed by the functions φ_{ik}', where

$$\varphi_{23}'=\int G_E(\rho_{23},\rho_1-\rho)\,\varphi'(\rho)\,d\rho;$$

$\varphi'(\rho)$ is a third unknown function.

Just as in the case of three identical particles, it is appropriate to consider the Fourier component

$$F(\rho_{23},\mathbf{k})=\int e^{-i\mathbf{k}\rho_1}\Psi(\rho_{23},\rho_1)\,d\rho_1$$

of the wave functions in the coordinate ρ_1 of any one of the three nucleons (in view of the symmetry, all are equally suitable); by Eqs. (22), (23) and (24), and using the value (5) of the Green's function G_E, we get [just as was done above for the Fourier components F obtained from the values of (7), (8)]:

$$F_a=0,\qquad F_c=\frac{e^{-\gamma_k\rho_{23}}}{\rho_{23}}\chi(\mathbf{k}) \tag{25}$$

$$+\,8\pi\int\frac{\chi(\mathbf{k}')\cos(\mathbf{k}'+\mathbf{k}/2,\ \rho_{23})}{k^2+k'^2+\mathbf{k}\mathbf{k}'-(ME/\hbar^2)-i\tau}\,\frac{d\mathbf{k}'}{(2\pi)^3},$$

$$F_1=4\pi i\sqrt{3}\int\frac{\xi(\mathbf{k}')\sin(\mathbf{k}'+\mathbf{k}/2,\ \rho_{23})}{k^2+k'^2+\mathbf{k}\mathbf{k}'-(ME/h^2)-i\tau}\,\frac{d\mathbf{k}'}{(2\pi)^3},$$

$$F_2=4\pi\int\frac{\xi(k')\cos(\mathbf{k}'+\mathbf{k}/2,\ \rho_{23})}{k^2+k'^2+\mathbf{k}\mathbf{k}'-(ME/\hbar^2)-i\tau}\,\frac{d\mathbf{k}'}{(2\pi)^3}$$

$$-\,\frac{e^{-\gamma_k\rho_{23}}}{\rho_{23}}\xi(\mathbf{k}).$$

and F_1' and F_2' (the Fourier components of Ψ_1' and Ψ_2') have values similar to F_1 and F_2 upon replacement of $\xi(\mathbf{k})$ by $\xi'(\mathbf{k})$; here $\chi(\mathbf{k})$, $\xi(\mathbf{k})$ and $\xi'(\mathbf{k})$ are functions analogous to $\chi(\mathbf{k})$ in the case of identical particles; these are Fourier components, correspondingly, of $f(\rho)$, $\varphi(\rho)$ and $\varphi'(\rho)$.

Substituting the value of the function $F_{T,S}$ in Eq. (21), we write down the Fourier component of the wave function $F_{T,S}$ of a system of three nucleons for the case $T=1/2$. For $S=1/2$;

$$F_{1/2,\,1/2}={}^1\!/_2F_1(\chi_1\vartheta_1-\chi_2\vartheta_2) \tag{26}$$

$$-\,{}^1\!/_2(F_c+F_2)\chi_1\vartheta_2+{}^1\!/_2(F_c-F_2)\chi_2\vartheta_1;$$

for $S = 3/2$:

$$F_{1/2,\, 3/2} = F'_1\chi_3\vartheta_2 - F'_2\chi_3\vartheta_1. \tag{26'}$$

We can find the functions $\chi(\mathbf{k})$, $\xi(\mathbf{k})$ and $\xi'(\mathbf{k})$ by imposing on the wave function the boundary condition similar to (1) or, more precisely, (1a). In order to obtain this, we note that, similar to the way in which Eq. (9) follows from the integral equation (6), there follow from (6), upon substitution of a potential in the form (19), equations for the coefficients

$$F_t = {}^1/_2(F_c - F_2) \text{ and } F_s = -{}^1/_2(F_c + F_2)$$

for the case of $\chi_2\, \vartheta_1$ and $\chi_1\, \vartheta_2$ in Eq. (26):

$$[(d^2/d\rho^2) - (M/\hbar^2)\, U_t(\rho) \tag{27}$$

$$+ (ME_k/\hbar^2)]\, \{\rho F_t(\rho, \mathbf{k})\} \approx 0,$$

$$[(d^2/d\rho^2) - (M/\hbar^2)\, U_s(\rho)$$

$$+ (ME_k/\hbar^2)]\, \{\rho F_s(\rho, \mathbf{k})\} \approx 0.$$

Here U_t and U_s are potentials acting between the neutron and the proton in the triplet and singlet states:

$$U_t(\rho_{23}) = (\overset{*}{\chi}_2\overset{*}{\vartheta}_1\hat{U}_{23}\chi_2\vartheta_1),$$

$$= U_1 + U_2 - 3U_3 - 3U_4,$$

$$U_s(\rho_{23}) = (\overset{*}{\chi}_1\overset{*}{\vartheta}_2\hat{U}_{23}\chi_1\vartheta_2)$$

$$= U_1 - 3U_2 + U_3 - 3U_4.$$

Equations (27) are approximate, valid with accuracy up to terms of order $(r_0/\bar{\lambda})^3$ in the region of force action [since, on the right-hand side, there are actually small terms in the exact equations similar to the term on the right side of Eq. (8)]. We can also obtain an equation for the function F'_2 in the coefficient for $\chi_3\, \vartheta_1$ in Eq. (26′). This equation is identical with the first of Eq. (27). The validity of Eq. (27), analogous to Eq. (9), is almost self-evident; its precise demonstration is connected with several rough calculations and is not carried out here.

It follows from Eq. (27) that the functions F_t and F_s satisfy boundary conditions of the type (10) at the point $\rho = r_0 \to 0$:

$$\left\{\frac{d}{d\rho_{23}}[\rho_{23}F_t(\rho_{23}, \mathbf{k})]\right\}_{\rho_{23}\to 0} \tag{28}$$

$$= -\alpha_t\{\rho_{23}F_t(\rho_{23}, \mathbf{k})\}_{\rho_{23}\to 0},$$

$$\left\{\frac{d}{d\rho_{23}}[\rho_{23}F_s(\rho_{23}, \mathbf{k})]\right\}_{\rho_{23}\to 0}$$

$$= -\alpha_s\{\rho_{23}F_s(\rho_{23}, \mathbf{k})\}_{\rho_{23}\to 0},$$

where α_t and α_s are reciprocals of the scattering length (in the approximation $r_0 \to 0$, the difference between the scattering length and the radius of the bound state disappears), and are constants which characterize the potentials U_s and U_t. The function $F'_t = -F'_2$ satisfies the boundary condition identical to the condition (28) for F_t.

Substituting (25) in (28), we get, for $S = 1/2$:

$$\left(\sqrt{\frac{3k^2}{4} - \frac{ME}{\hbar^2}} - \alpha_t\right)\{\chi(\mathbf{k}) + \xi(\mathbf{k})\} \tag{29}$$

$$= \int \frac{4\pi\, \{2\chi(\mathbf{k}') - \xi(\mathbf{k}')\}}{k^2 + k'^2 + \mathbf{k}\mathbf{k}' - (ME/\hbar^2) - i\tau}\, \frac{d\mathbf{k}'}{(2\pi)^3},$$

$$\left(\sqrt{\frac{3k^2}{4} - \frac{ME}{\hbar^2}} - \alpha_s\right)\{\chi(\mathbf{k}) - \xi(\mathbf{k})\}$$

$$= \int \frac{4\pi\, \{2\chi(\mathbf{k}') + \xi(\mathbf{k}')\}}{k^2 + k'^2 + \mathbf{k}\mathbf{k}' - (ME/\hbar^2) - i\tau}\, \frac{d\mathbf{k}'}{(2\pi)^3},$$

and for $S = 3/2$,

$$\left(\sqrt{\frac{3k^2}{4} - \frac{ME}{\hbar^2}} - \alpha_t\right)\xi'(\mathbf{k})$$

$$+ \int \frac{4\pi\xi'(\mathbf{k}')}{k^2 + k'^2 + \mathbf{k}\mathbf{k}' - (ME/\hbar^2) - i\tau}\, \frac{d\mathbf{k}'}{(2\pi)^3} = 0.$$

The solutions of these equations determine the wave function of the system in accord with Eqs. (25) and (26). In the case $S = 1/2$, the equations can be written in a more appropriate form if we denote:

$$\chi_t(\mathbf{k}) = {}^1/_2\{\chi(\mathbf{k}) + \xi(\mathbf{k})\},$$

$$\chi_s(\mathbf{k}) = {}^1/_2\{\chi(\mathbf{k}) - \xi(\mathbf{k})\};$$

then we obtain

$$\left(\sqrt{\frac{3k^2}{4} - \frac{ME}{\hbar^2}} - \alpha_t\right)\chi_t(\mathbf{k}) \tag{30}$$

$$= \int \frac{4\pi\, \{{}^1/_2\chi_t(\mathbf{k}') + {}^3/_2\chi_s(\mathbf{k}')\}}{k^2 + k'^2 + \mathbf{k}\mathbf{k}' - (ME/\hbar^2) - i\tau}\, \frac{d\mathbf{k}'}{(2\pi)^3};$$

$$\left(\sqrt{\frac{3k^2}{4} - \frac{ME}{\hbar^2}} - \alpha_s\right)\chi_s(\mathbf{k})$$

$$= \int \frac{4\pi\, \{{}^3/_2\chi_t(\mathbf{k}') + {}^1/_2\chi_s(\mathbf{k}')\}}{k^2 + k'^2 + \mathbf{k}\mathbf{k}' - (ME/\hbar^2) - i\tau}\, \frac{d\mathbf{k}'}{(2\pi)^3}.$$

Here, we have everywhere

$$\sqrt{\frac{3k^2}{4}-\frac{ME}{\hbar^2}} \to -i\sqrt{\frac{ME}{\hbar^2}-\frac{3k^2}{4}},$$

$$\text{if}\quad \frac{ME}{\hbar^2}-\frac{3k^2}{4}>0.$$

Let us consider the problem of the scattering of neutrons by deuterons. For large ρ_1 the wave function of the system must contain the incident wave (which is proportional to $\chi_2\ \vartheta_1$ if $S = 1/2$, and to $\chi_3\ \vartheta_1$ if $S = 3/2$) and various diverging waves. In accord with (25) and (26), this will occur if (29) and (30) have solutions of the form

$$\xi'(\mathbf{k})=\sqrt{\frac{\alpha_t}{2\pi}}\left\{(2\pi)^3\delta(\mathbf{k}-\mathbf{k}_0)+\frac{4\pi a_{3/2}(\mathbf{k},\mathbf{k}_0)}{k^2-k_0^2-i\tau}\right\};$$

$$\chi_t(\mathbf{k})=\sqrt{\frac{\alpha_t}{2\pi}}\left\{(2\pi)^3\delta(\mathbf{k}-\mathbf{k}_0)+\frac{4\pi a_{1/2}(\mathbf{k},\mathbf{k}_0)}{k^2-k_0^2-i\tau}\right\};$$

$$\chi_s(\mathbf{k})=\sqrt{\frac{\alpha_t}{2\pi}}\,\frac{4\pi b_{1/2}(\mathbf{k},\mathbf{k}_0)}{k^2-k_0^2-i\tau} \tag{31}$$

(the function $\chi_s(\mathbf{k})$ actually (as is evident from Eq. (30), where $ME/\hbar^2 = 3k_0^2/4 - \alpha_t^2$), has no pole for $k = k_0$, i.e., $\{b_{1/2}(\mathbf{k},\mathbf{k}_0)\}_{k=k_0} = 0$ is described in the form written above for one-dimensional notation]. Here the amplitudes of elastic scattering of neutrons are:

$$f_{3/2}(\vartheta)=\lim_{k\to k_0}\left\{\frac{k^2-k_0^2}{4\pi}(\overset{*}{\chi}_3\overset{*}{\vartheta}_1\int\overset{*}{\varphi}_0(\rho_{23})\,F_{1/2,\,3/2}(\rho_{23},\mathbf{k})\,d\rho_{23})\right\},$$

$$f_{1/2}(\vartheta)=\lim_{k\to k_0}\left\{\frac{k^2-k_0^2}{4\pi}(\overset{*}{\chi}_2\overset{*}{\vartheta}_1\int\overset{*}{\varphi}_0(\rho_{23})\,F_{1/2,\,1/2}(\rho_{23},\mathbf{k})\,d\rho_{23})\right\},$$

where $\varphi_0(\rho_{23}) = \sqrt{\alpha_t/2\pi}e^{-\alpha_t\rho_{23}}/\rho_{23}$ is the wave function of the deuteron, and, by Eqs. (25), (26) and (31), are equal to

$$f_{3/2}(\vartheta)=\{a_{3/2}(\mathbf{k},\mathbf{k}_0)\}_{k=k_0},$$

$$f_{1/2}(\vartheta)=\{a_{1/2}(\mathbf{k},\mathbf{k}_0)\}_{k=k_0}.$$

Substituting (31) in (29), (30), we get inhomogeneous equations which permit us to find the wave functions of the complicated spectrum:

$$S={}^3/_2:\ \frac{(\sqrt{3k^2/4-(ME/\hbar^2)}-\alpha_t)}{k^2-k_0^2}\,a_{3/2}(\mathbf{k},\mathbf{k}_0)=\frac{-1}{k_0^2+k^2+\mathbf{k}\mathbf{k}_0-(ME/\hbar^2)-i\tau} \tag{32}$$

$$-\int\frac{4\pi a_{3/2}(\mathbf{k}',\mathbf{k}_0)}{(k^2+k'^2+\mathbf{k}\mathbf{k}'-(ME/\hbar^2)-i\tau)\,(k'^2-k_0^2-i\tau)}\,\frac{d\mathbf{k}'}{(2\pi)^3};$$

$$S={}^1/_2\begin{cases}\dfrac{(\sqrt{3k^2/4-(ME/\hbar^2)}-\alpha_t)}{k^2-k_0^2}\,a_{1/2}(\mathbf{k},\mathbf{k}_0)=\dfrac{{}^1/_2}{k_0^2+k^2+\mathbf{k}\mathbf{k}_0-(ME/\hbar^2)-i\tau}\\ \qquad+\displaystyle\int\frac{4\pi\{{}^1/_2a_{1/2}(\mathbf{k}',\mathbf{k}_0)+{}^3/_2b_{1/2}(\mathbf{k}',\mathbf{k}_0)\}}{(k^2+k'^2+\mathbf{k}\mathbf{k}'-(ME/\hbar^2)-i\tau)\,(k'^2-k_0^2-i\tau)}\,\frac{d\mathbf{k}'}{(2\pi)^3},\\ \dfrac{(\sqrt{3k^2/4-(ME/\hbar^2)}-\alpha_s)}{k^2-k_0^2}\,b_{1/2}(\mathbf{k},\mathbf{k}_0)=\dfrac{{}^3/_2}{k_0^2+k^2+\mathbf{k}\mathbf{k}_0-(ME/\hbar^2)-i\tau}\\ \qquad+\displaystyle\int\frac{4\pi\{{}^3/_2a_{1/2}(\mathbf{k}',\mathbf{k}_0)+{}^1/_2b_{1/2}(\mathbf{k}',\mathbf{k}_0)\}}{(k^2+k'^2+\mathbf{k}\mathbf{k}'-(ME/\hbar^2)-i\tau)\,(k'^2-k_0-i\tau)}\,\frac{d\mathbf{k}'}{(2\pi)^3}.\end{cases}$$

For $k_0 \to 0$, similar to the case of three identical particles, we can introduce the dimensionless quantities

$$\tilde{a}_{3/2}(x)=\alpha_t a_{3/2}(k,0),$$

$$\tilde{a}_{1/2}(x)=\alpha_t a_{1/2}(k,0),$$

$$\tilde{b}_{1/2}(x)=\alpha_t b_{1/2}(k,0);\qquad x=k/\alpha_t,$$

for which it follows that

$$S = {}^3/_3:\ \frac{\sqrt{3x^2/4+1}-1}{x^2}\,\tilde{a}_{3/2}(x) = \frac{-1}{x^2+1} - \frac{1}{\pi}\int_0^\infty \tilde{a}_{3/2}(x)\ln\frac{1+x^2+x'^2+xx'}{1+x^2+x'^2-xx'}\,\frac{dx'}{xx'};$$

$$S = {}^1/_2\ \left|\ \begin{array}{l} \dfrac{\sqrt{3x^2/4+1}-1}{x^2}\,\tilde{a}_{1/2}(x) = \dfrac{{}^1/_2}{x^2+1} + \\ + \dfrac{1}{\pi}\displaystyle\int_0^\infty \{{}^1/_2\tilde{a}_{1/2}(x') + {}^3/_2\tilde{b}_{1/2}(x')\}\ln\frac{1+x^2+x'^2+xx'}{1+x^2+x'^2-xx'}\,\frac{dx'}{xx'}; \\ \dfrac{\sqrt{3x^2/4+1}-\dfrac{\alpha_s}{\alpha_t}}{x^2}\,\tilde{b}_{1/2}(x) = \dfrac{{}^3/_2}{x^2+1} + \\ + \dfrac{1}{\pi}\displaystyle\int_0^\infty \{{}^3/_2\tilde{a}_{1/2}(x') + {}^1/_2\tilde{b}_{1/2}(x')\}\ln\frac{1+x^2+x'^2+xx'}{1+x^2+x'^2-xx'}\,\frac{dx'}{xx'}. \end{array}\right.$$

These equations are integrated numerically. The functions $a_{3/2}(k, 0)$, $a_{1/2}(k, 0)$ and $b_{1/2}(k, 0)$ are plotted in Fig. 2; the scattering amplitudes $a_{3/2}(0, 0)$ and $a_{1/2}(0, 0)$ of neutrons with $k_0 = 0$ by deuterons are seen to be equal to

$$a_{3/2}(0,\ 0) = 0.51\cdot 10^{-12}\ \text{cm};$$

$$a_{1/2}(0,\ 0) = 0.30\cdot 10^{-12}\ \text{cm}.$$

Here, for α_t and α_s, we have taken the following values: $1/\alpha_t = 4.32\times 10^{-13}$ cm; $1/\alpha_s = -25\times 10^{-13}$ cm. The results of the calculation depend weakly on the value of α_s, since this quantity enters in the form of a small parameter $-\alpha_s/\alpha_t = 0.173 < 1$ in the sum, with $\sqrt{3x^2/4+1} \gtrsim 1$.

For $k_0 \neq 0$, the functions $a_{3/2}$, $a_{1/2}$, $b_{1/2}$ can be expanded in a series of Legendre polynomials:

$$a_{3/2}(\mathrm{k},\ \mathrm{k}_0) \tag{34}$$

$$= \sum_{l=0}^{\infty}(2l+1)\{C_l^{(1)}(k) + iC_l^{(2)}(k)\}P_l(\cos\vartheta);$$

$$a_{1/2}(\mathrm{k},\ \mathrm{k}_0)$$

$$= \sum_{l=0}^{\infty}(2l+1)\{A_l^{(1)}(k) + iA_l^{(2)}(k)\}P_l(\cos\vartheta);$$

$$b_{1/2}(\mathrm{k},\ \mathrm{k}_0)$$

$$= \sum_{l=0}^{\infty}(2l+1)\{B_l^{(1)}(k) + iB_l^{(2)}(k)\}P_l(\cos\vartheta).$$

The equations which determine the functions $C_l^{(1)}$, $C_l^{(2)}$; $A_l^{(1)}$, $A_l^{(2)}$; $B_l^{(1)}$, $B_l^{(2)}$ are developed in the Appendix.

For the case $k_0 \to 0$, the zeroth approximation in r_0 of the theory corresponds to neglect of terms of the order $\alpha_t r_0 \sim (1.7/4.34) \sim 0.4$, in comparison with unity; therefore, the theoretical values of $a_{3/2}$ and $\alpha_{1/2}$ are valid with accuracy up to terms of the order

$$(\alpha_t r_0)/\alpha_t \sim r_0 = 0.17\cdot 10^{-12}\ \text{cm}.$$

In agreement with the experimental data of Hurst and Alcock[5], $a_{3/2} = (0.64 + 0.01)\times 10^{-12}$ cm; $a_{1/2} = (0.07 \pm 0.03)\times 10^{-12}$ cm; thus, for spin 3/2, the correspondence with experiment is excellent; but the small amplitude of $\alpha_{1/2}$ as determined by the zeroth approximation of the theory is imprecise. Consequently, the first approximation of the theory in an expansion in r_0 will be considered later.

The authors express their gratitude to Acad. L.D. Landau, O. B. Firsov and I. M. Shmushkevich for discussions of the work.

APPENDIX

INTEGRAL EQUATIONS FOR THE CASE $k_0 \neq 0$

Below we obtain equations which determine the wave function of the three-particle system with $k_0 \neq 0$ and with arbitrary momentum.

First, let us consider the case of three identical particles. Making use of the expansion (16) and representing the kernel of the integral equation (14) in the form .

$$[k^2+k'^2+\mathbf{kk}'-(ME/\hbar^2)-i\tau]^{-1} \tag{a}$$

$$=[kk'(Q+\cos\gamma-i\tau)]^{-1}=$$

$$=\sum_{l=0}^{\infty}(2l+1)P_l(\cos\gamma)\frac{G_l(k,k')}{2kk'},$$

$$G_l(k,k')=\int_{-1}^{1}\frac{P_l(x)\,dx}{Q+x-i\tau}$$

$(\tau\to 0)$, where we have introduced the notation $Q(k,k')=(k^2+k'^2-ME/\hbar^2)/kk'$, $x=\cos\gamma = \mathbf{kk}'/kk'$, we obtain, after multiplication of (14) by $P_l(\cos\vartheta)$ and integration over the directions of the vector **k**:

$$\frac{{}^3/{}_8 a_l(k,k_0)}{\alpha+\sqrt{3k^2/4-(ME/\hbar)^2}}=\frac{G_l(k,k_0)}{2kk_0} \tag{b}$$

$$+\frac{2}{\pi}\int_0^{\infty}\frac{G_l(k,k')}{k'^2-k_0^2-i\tau}\,\frac{a_l(k',k_0)}{2kk'}\,k'^2dk'.$$

Taking it into account that

$$\frac{1}{Q+x-i\tau}=\mathrm{P}\frac{1}{Q+x}+i\pi\delta(Q+x)$$

(P denotes the "principal part"), we obtain

$$G_l(k,k')=G_l^{(1)}(k,k')+i\pi\theta(Q)P_l(-Q), \tag{c}$$

where $G_l^{(1)}$ is substantially:

$$G_l^{(1)}(k,k')=\int_{-1}^{1}\mathrm{P}\frac{P_l(x)\,dx}{Q+x}$$

$$=\begin{cases}\ln\left|\dfrac{Q+1}{Q-1}\right|, & l=0;\\ 2-Q\ln\left|\dfrac{Q+1}{Q-1}\right|, & l=1;\\ (3Q^2-1)\ln\left|\dfrac{Q+1}{Q-1}\right|+6Q, & l=2,\ \text{etc.}\end{cases}$$

and by θ is meant the equation $\theta(Q)=1$, for $|Q|<1$ and $\theta(Q)=0$, if $|Q|>1$.

The kernel of the integral equation (b) is complex not only because, in view of (c), $Q_l(k,k')$ has an imaginary part (it differs from zero if $3k_0^2/4>\alpha^2$; otherwise, $Q>1$), but also because of the fact that the factor

$$\frac{k'^2}{k'^2-k_0^2-i\tau}=\mathrm{P}\frac{k'^2}{k'^2-k_0^2}+i\pi k'^2\delta(k'^2-k_0^2)$$

is complex. Therefore, the functions $a_l(k,k_0)$ are complex [except for the case $k_0\to 0$, where they are real, by Eq. (15)]. Writing $a_l(k,k_0)=\xi_l(k)+i\eta_l(k)$, we get the following equations for ξ_l and η_l from (b) and (c):

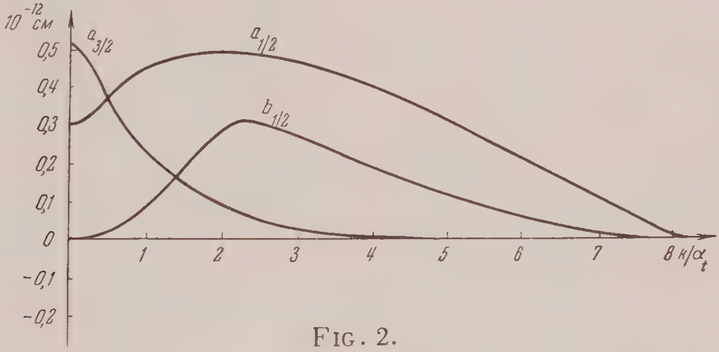

FIG. 2.

$$\frac{(R_k-\alpha)\xi_l(k)+J_k\eta_l(k)}{2(k^2-k_0^2)}$$

$$=\frac{1}{2kk_0}G_l^{(1)}(k,k_0)+\frac{2}{\pi}\int_0^{\infty}\frac{G_l^{(1)}(k,k')}{2kk'}\,\frac{k'^2\xi_l(k')}{(k'^2-k_0^2)}\,dk'$$

$$-\frac{1}{2k}G_l^{(1)}(k,k_0)\,\eta_l(k_0)$$

$$-\int_{|J_k-k/2|}^{J_k+k/2}\frac{k'}{k}\,\frac{P_l\;-Q)}{k'^2-k_0}\,\eta_l(k')\,dk';$$

all the integrals are taken in the sense of the principal value (the integral with the limits from $|J_k-k/2|$ to $J_k+k/2$ arises from the imaginary part of (c): $|Q|<1$ only if k' changes in these limits).

We treat the case of three nucleons in a similar fashion. Taking into account the expansion of Eq. (34) and denoting $C_l=C_l^{(1)}+iC_l^{(2)}$, $A_l=A_l^{(1)}+iA_l^{(2)}$, $B_l=B_l^{(1)}+iB_l^{(2)}$, we get a system of two coupled equations for $S=3/2$:

$$\frac{(R_k-\alpha_t)\,C_l^{(1)}(k)+J_k C_l^{(2)}(k)}{k^2-k_0^2}$$

$$=-\frac{G_l^{(1)}(k,k_0)}{2kk_0}-\frac{1}{\pi}\int\limits_0^\infty \frac{G_l^{(1)}(k,k')}{kk'}\,\frac{k'^2C_l^{(1)}(k')}{k'^2-k_0^2}\,dk'+\frac{G_l^{(1)}(k,k_0)}{2k}\,C_l^{(2)}(k_0)$$

$$+\int\limits_{|J_k-k/2|}^{J_k+k/2}\frac{C_l^{(2)}(k')\,P_l(-Q)}{k'^2-k_0^2}\,\frac{k'}{k}\,dk'\,;$$

$$\frac{(R_k-\alpha_t)\,C_l^{(2)}(k)-J_k\,C_l^{(1)}(k)}{k^2-k_0^2}=-\frac{1}{\pi}\int\limits_0^\infty\frac{G_l^{(1)}(k,k')}{kk'}\,\frac{k'^2C_l^{(2)}(k')}{k'^2-k_0^2}\,dk'$$

$$-\frac{G_l^{(1)}(k,k_0)}{2k}\,C_l^{(1)}(k_0)-\frac{1}{\pi}\int\limits_{|J_k-k/2|}^{|J_k+k/2|}\frac{C_l^{(1)}(k')\,P_l(-Q)}{k'^2-k_0^2}\,\frac{k'}{k}\,dk'\,,$$

and for $S=1/2$, a system of four coupled equations:

$$\frac{(R_k-\alpha_t)\,A_l^{(1)}(k)+J_kA_l^{(2)}(k)}{k^2-k_0^2}=\frac{G_l^{(1)}(k,k_0)}{4kk_0}$$

$$+\frac{1}{\pi}\int\limits_0^\infty\frac{G_l^{(1)}(k,k')\,k'^2\,\{{}^1\!/_2A_l^{(1)}(k')+{}^3\!/_2B_l^{(1)}(k')\}}{kk'\,(k'^2-k_0^2)}\,dk'-\frac{G_l^{(1)}(k,k_0)}{4k}\,A_l^{(2)}(k_0)\cdot$$

$$-\int\limits_{|J_k-k/2|}^{J_k+k/2}\frac{P_l(-Q)\,\{{}^1\!/_2A_l^{(2)}(k')+{}^3\!/_2B_l^{(2)}(k')\}}{k'^2-k_0^2}\,\frac{k'}{k}\,dk';$$

$$\frac{(R_k-\alpha_t)\,A_l^{(2)}(k)-J_kA_l^{(1)}(k)}{k^2-k_0^2}=\frac{1}{\pi}\int\limits_0^\infty\frac{G_l^{(1)}(k,k')\,k'^2\,\{{}^1\!/_2A_l^{(2)}(k')+{}^3\!/_2B_l^{(2)}(k')\}}{kk'\,(k'^2-k_0^2)}\,dk'$$

$$+\frac{G_l^{(1)}(k,k_0)}{4k}\,A_l^{(1)}(k_0)+\int\limits_{|J_k-k/2|}^{J_k+k/2}\frac{P_l(-Q)\,\{{}^1\!/_2A_l^{(1)}(k')+{}^3\!/_2B_l^{(1)}(k')\}}{k'^2-k_0^2}\,\frac{k'}{k}\,dk'\,;$$

$$\frac{(R_k-\alpha_s)B_l^{(1)}(k)+J_kB_l^{(2)}(k)}{k^2-k_0^2}=\frac{3G_l^{(1)}(k,k_0)}{4kk_0}$$

$$+\frac{}{\pi}\int\limits_0^\infty\frac{G_l^{(1)}(k,k')\,k'^2\{{}^3\!/_2A_l^{(1)}(k')+{}^1\!/_2B_l^{(1)}(k')\}}{kk'\,(k'^2-k_0^2)}\,dk'-\frac{3G_l^{(1)}(k,k_0)}{4k}\,A_l^{(2)}(k_0)$$

$$-\int\limits_{|J_k-k/2|}^{J_k+k/2}\frac{P_l(-Q)\,\{{}^3\!/_2A_l^{(2)}(k')+{}^1\!/_2B_l^{(2)}(k')\}}{k'^2-k_0^2}\,\frac{k'}{k}\,dk'\,;$$

$$\frac{(R_k-\alpha_s)\,B_l^{(2)}(k)-J_kB_l^{(1)}(k)}{k^2-k_0^2}=\frac{1}{\pi}\int\limits_0^\infty\frac{G_l^{(1)}(k,k')\,k'^2\,\{{}^3\!/_2A_l^{(2)}(k')+{}^1\!/_2B_l^{(2)}(k')\}}{kk'\,(k'^2-k_0^2)}\,dk'$$

$$+\frac{3G_l^{(1)}(k,k_0)}{4k}\,A_l^{(1)}(k_0)+\int\limits_{|J_k-k/2|}^{J_k+k/2}\frac{P_l(-Q)\,\{{}^3\!/_2A_l^{(1)}(k')+{}^1\!/_2B_l^{(1)}(k')\}}{k'^2-k_0^2}\,\frac{k'}{k}\,dk'\,.$$

---

[1] H. Bethe and R. Peierls, Proc. Roy. Soc. (London) **148A**, 146 (1935).

[2] L. Thomas, Phys. Rev. 47, 903 (1935).

[3] G. V. Skorniakov, J. Exptl. Theoret. Phys. (U.S.S.R.) (in press).

[4] M. Verde, Helv. Phys. Acta 22, 339 (1949).

[5] D. G. Hurst and N. Z. Alcock, Canad. J. Phys. 29, 36 (1951).

Translated by R. T. Beyer
171

SOVIET PHYSICS JETP VOLUME 4, NUMBER 5 JUNE, 1957

Measurement of the Ionizing Power of Particles in a Bubble Chamber

G. A. BLINOV, IU. S. KRESTNIKOV AND M. F. LOMANOV

(Submitted to JETP editor June 6,1956)
(J. Exptl. Theoret. Phys. (U.S.S.R.) **31**, 762-770 (November, 1956)

The possibility of the measurement of the ionizing power of particles in a propane bubble chamber is demonstrated. The chamber was operating in conjunction with an accelerator. The use of the method of the reduction of pressure to a controllable constant level ensured the stability of chamber operation necessary for ionization measurements. The period of sensitivity was 40 m sec. Measurements of the ionizing power of particles were carried out in the range up to eighty times minimum ionization. It was found that the track density changes with the velocity of the particle as $1/\beta^2$ for $\beta < 0.6$. For velocities close to that of light, relativistic increase in the track density is observed. The used methods on the track evaluation are described.

1. INTRODUCTION

IT was shown by Glaser[1] in 1953 that ionizing particles cause an overheated liquid to boil, leaving tracks in the form of vapor bubble chains. It is possible to describe the expected dependence of the number of bubbles along the track on the charge and the velocity of the particle not entering into the detailed formation mechanism of the nuclei of vaporization under the influence of ionization. It is well known that an overheated liquid starts boiling on the vaporization nuclei, the radius of which is greater than a critical value r_{cr}.

$$r_{cr} = 2\sigma/(P_\infty - P_0), \tag{1}$$

where σ is the surface tension coefficient of the liquid-vapor boundary, P_∞ is the pressure of the saturated vapor and P_0 is the hydrostatic pressure of the liquid. The energy losses of a particle due to the ionization of the medium can entail conditions favoring the formation of vaporization nuclei. Bubble chambers usually operate at values of σ in the range from 1–10 dyne/cm and of $(P_\infty - P_0)$ in the range from 5 to 20 atm, which correspond to $r_{cr} = 10^{-5} - 10^{6}$ cm.

It is evident that the nuclei of vaporization are formed in the region where the ionization density, over distances of the order of r_{cr} is considerably larger than the average ionization density along the particle trajectory. This condition is fulfilled by the end points of the tracks of the δ-electrons produced by the particles. Indeed, electrons of about 200 ev lose all their energy on a path shorter than 10^{-5} cm in a liquid, producing some 20 ion pairs*, while for the case of a relativistic particle, the number of ion pairs along the trajectory is not greater than 0.5 per 10^{-5} cm, and the probability of many acts of primary ionization over such a length is vanishingly small. It can be therefore assumed that the number of bubbles along the path of the particle is proportional to the number of δ-electrons of energy greater than 100–200 ev. Neglecting the binding energy of electrons in the atom, we shall obtain the following expression for the number of bubbles per unit length of track (track density):

$$g = g_0 Z^2/\beta^2, \tag{2}$$

where g is the track density, Z is the charge of the particle, β is the particle velocity in terms of the velocity of light, and g_0 is a coefficient depending on the stopping power of the medium, on the temperature and on the "overheating" $P_\infty - P_0$.

---

*The given values of range and of the number of ion pairs are calculated for the case of liquid propane from data concerning the air.[2]

For $\beta \approx 1$, relativistic corrections taking into account the polarization of medium should be introduced into Eq. (2).

Authors of various experimental investigations$^{3-7}$ have not noted that a difference is observed in the density of tracks belonging to different particles; the correlation, however, of the track density with the velocity of the particle has not been found, due to a number of difficulties. In contrast with other authors, who used a constant chamber expansion, we applied the method of pressure reduction to a certain level, which ensured the high stability of the chamber operation necessary for such correlation.

The experimental work was carried out with the synchrocyclotron of the Institute for Nuclear Problems of the Academy of Sciences USSR.

2. CHAMBER CONSTRUCTION AND CHOICE OF OPERATING CONDITIONS

The working volume of the chamber (*A*, Fig. 1) consists of a cylindrical vessel of stainless steel of 92 mm internal diameter and 70 mm high, the ends of which are covered by glass plates 30 mm thick. The joint is made tight by a 1 mm thick fluoroplast gasket. The liquid used is singly distilled technical grade propane, with the vapor pressure equal to 30 atm at 64° C. Water for heating the chamber flows from a thermostat through the pipes 1 and 2 to the chamber and circulates in channels between the chamber's body and its covers. The chamber temperature was usually equal to 64° C with stability better than 0.1° C.

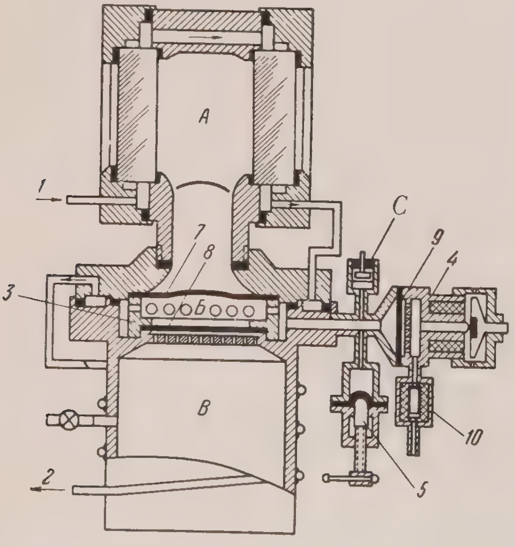

FIG. 1. Chamber construction (schematic).

The volume *B*, filled with water, is connected through openings in the gasket ring 3 with the electromagnetic exhaust valve 4, the vapor phase volume control 5 and the capacitance pressure gauge 6. The working volume of the chamber is separated from the volume *C* by a fluoroplast diaphragm 7. As long as the external pressure is not supplied (the valve 4 is open), the diaphragm 7 remains in the intermediate position, and the rubber diaphragms 8 and 9 are pressed against the respective grids. The vapor phase then has a volume equal to 16 cm.^{3} Since the total volume occupied by the propane equalled 660 cm^3, the maximum volume expansion coefficient amounted to 16/660 = 0.024. The expansion coefficient could be varied by means of the control 5, consisting of a piston with a rubber diaphragm.

The peculiarity of the operation of the chamber lies in the reducing of the pressure to a constant controllable level. The level is set by the pressure of the carbon dioxide gas, which fills the volume *B*.

The operation of the chamber is as follows: carbon dioxide at 38 atm is supplied to the rubber diaphragm 9 through a pressure stabilizer (not shown in the drawing) and the electromagnetic inlet valve 10. This pressure is transmitted by the water to diaphragms 7 and 8, the diaphragm 8 moving against the grid, while the diaphragm 7 compresses the propane. The vapor phase in the chamber condenses completely, and the chamber is ready for expansion.

The moment of expansion is chosen by means of a radio frequency control, the antenna of which is placed near the synchrocyclotron chamber. The antenna is sharply tuned to a frequency close to that of particle ejection. Out of a train of amplified and shaped pulses one is selected, which, after a controllable delay, causes the exhaust valve 4 to open. Within 12 m sec the chamber pressure falls to the value equal to the pressure in the volume *B*. The delay between the synchronizing signal and the beginning of the pressure reduction is chosen so that particles of one of the consecutive intensity pulses traverse the chamber at the stationary pressure P_0. The schematic time diagram of chamber operation, obtained by means of the capacitance gauge and an oscilloscope, is shown in Fig. 2.

Two pulsed illumination lamps of the type ISS 250 were switched on after the passage of the particles. The chamber is flooded by light aimed towards the camera at an angle of 30° to the camera aiis in order to prevent the incident beam from striking the lenses. Dark background is used for the photography. A stereocamera with 75 mm lenses at an aperture of $f/60$ and a reduction of 3.5 diameters is used. The light flash duration is 1 to 4 m sec. the exact time within these limits being chosen to produce the best images of the smallest bubbles. About ten seconds are needed for preparing the chamber for the next expansion.

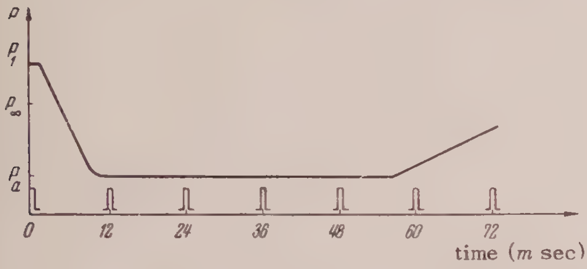

FIG. 2. Change of the pressure in chamber during expansion. $P_1 = 38$ atm, $p_\infty = 30$ atm— pressure of the saturated vapor of the working liquid at 64° C; P_0 — level of the pressure reduction (22–25 atm). Times of the passage of particles from the accelerator are shown. Duration of pulse about 300 μ sec.

In the first variant of the chamber, the working volume was connected with the volume C by a pipe of 12 mm internal diameter. A fast reduction of pressure caused a turbulent ebullition in this pipe which considerably shortened the sensitivity period of the chamber. The pipe diameter was therefore enlarged to 50 mm. This resulted in a period of sensitivity in excess of 40 m sec, which was tested by photographing particle tracks from three intensity pulses of the accelerator. The measurements of the track density of fast electrons have shown that the chamber sensitivity varies by a factor of about 1.5 from one intensity pulse to the next, arriving 12 m sec later. Synchronization of the beginning of the pressure reduction with the accelerator pulses made it possible, however, to obtain consistently reproducible results. Measurements have shown that the sensitivity is uniform over the whole volume of the chamber, and is constant for hundreds of pictures taken under the same operational conditions.

The sensitivity of the chamber could easily and quickly be controlled by the gas pressure in the volume B. This method was used for the selection of the sensitivity at which ionization measurements in the given region were most accurate. The resulting dependence of the sensitivity of the chamber on the "overheating" $P_\infty - P_0$ at the temperature of 64° C is given in Fig. 3. It can be seen that it is necessary to keep the pressure P_0 constant within a few hundredths of an atmosphere in order to ensure the stability of the operation of the chamber. In our case, this was effected by hermetic sealing of the volume B (Fig. 1) containing the gas, and the thermostating of it together with the body of the chamber.

In the course of the work with the accelerator, the chamber was placed either into the emerging collimated neutron beam with a mean energy of 590 mev, or into the beam of γ-rays from the π^0-meson decay, or into the beam of particles emitted from the targets and the walls of the collimator in the direction of the proton beam. The control system governing the necessary synchronization and delay was placed at a considerable distance from the chamber behind a concrete shield. This system also permitted remote measurement of the temperature and pressure in the chamber, and the remote control of the motor, the thermostat heaters, the light flashes, and the pressure. At a dangerously high pressure the thermostat was automatically switched off and the exhaust valve opened, preventing the chamber from exploding.

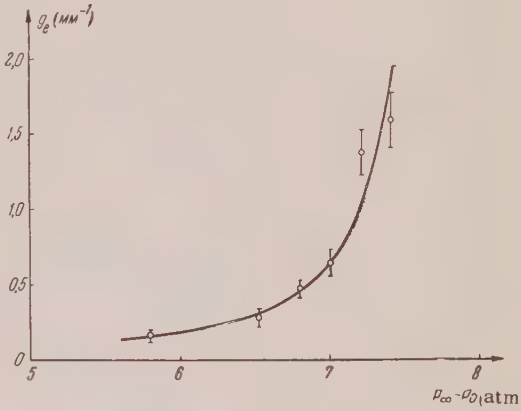

FIG. 3. Dependence of the track density of minimum ionization electrons ($E = 1$–5 mev) on the "overheating" ($P_\infty - P_0$) for $P = 30$ atm.

3. METHODS OF TRACK DENSITY MEASUREMENTS

The observed number of bubbles usually differs from the number of primarily produced bubbles. There are several causes of this: overlapping of the bubble images, interaction of closely spaced growing bubbles and subjective errors on the part of the observer connected with the difficulty of discerning single bubbles in clusters. At present, the methods of the measurement of the mean gap length and of the number of gaps are used for the determination of the track density in nuclear emulsions; these exclude the sources of the above errors. Analogous methods were used by us. Formulas correlating the measured value with the track density depend on the statistical distributions of bubbles along the track. In accordance with our ideas about the bubble creation mechanism mentioned in the introduction, the bubbles, similarly to δ-electrons, should be produced with equal probability at any point of the path of the particle, provided its velocity is constant. In this case the probability of finding n bubbles on the length x is given by the Poisson distribution:

$$w(n, gx) = (gx)^n e^{-gx}/n!, \tag{3}$$

where g is the track density.

Comparison with experiment revealed marked deviation from the Poisson distribution for tracks consisting of bubbles of a relatively large diameter (< 0.2 mm) and an observed density of more than two bubbles per mm (Fig. 4*b*). Such tracks appear sometimes as uniform chains of bubbles, the number of bubbles being largely independent of the velocity of the particle. This effect is caused by the interaction of the neighboring bubbles during their increase. Further measurements were therefore made only for the case of tracks consisting of sufficiently small bubbles, so that their optical images were essentially smaller than the developed images on the film. The effects connected with bubble interaction are then negligible. The preponderant majority of the pictures obtained conformed with this condition. The average diameter of the bubble image on the film was 0.035 mm, which, taking into account the camera reduction, gives 0.1 mm, while the real bubble was approximately half this size. The distribution obtained for such tracks is shown in Fig. 4*a*. The slight narrowing of this distribution, as compared to Poisson distribution, is explained by the overlapping of bubble images.[8]

Tracks of various densities were treated by different methods depending on the measure of the overlapping of the images gD, where D is the mean diameter of the bubble image, the camera reduction factor being accounted for. The three methods of track density measurement described below were chosen as the most sensitive.

1. The method of the straightforward bubble counting, or, more exactly, of the measurement of the length of the blackened part of the track, was used for $gD < 0.4$. It can be shown that, in this case, the track density is given by the following expression:

$$g = \frac{1}{D} \ln \frac{1}{1 - (L'/L)}, \tag{4}$$

where L' is the length of the blackened part of the track, and L is the total track length.

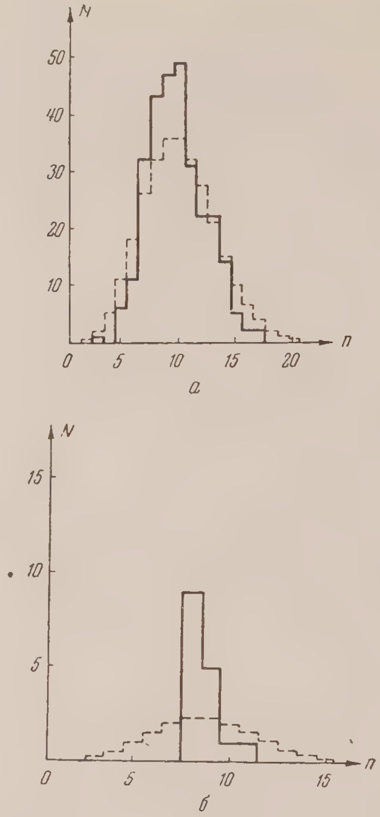

FIG. 4. Distribution of the cases of the production of n bubbles on a length x of the tracks for monoenergetic particles. *a*— "good" tracks; interaction of neighboring bubbles not visible in photographs. Bubble diameter less than 0.05 mm, diameter of the bubble image (camera reduction accounted for) $D = 0.1$ mm, $g = 3$ mm^{-1}, $x = 3.5$ mm. *b*—"bad" tracks, diameter of bubbles equal to image diameter, D—0.5 mm; observed track density $g_{obs} = 2$ mm^{-1}, $x = 4$ mm, broken line represents the Poisson distribution.

In practice, the length of the blackened part was determined by counting the number of bubbles under the assumption that the number of bubbles in a cluster equals the length of the cluster divided by the diameter of a single bubble. The length of a cluster was estimated visually, which entailed subjective errors. For small values of overlapping ($gD < 0.4$), however, the subjective error is small and the method was widely used because of its simplicity. In this case, Eq. (4) has the following form, obtained by Williams[9]:

$$g = \frac{1}{D} \ln \frac{1}{1 - kD}, \tag{5}$$

where $k = N/L$ and N is the observed number of bubbles. The statistical error is given by the formula:

$$\Delta g/g = N^{-1/2}. \tag{6}$$

2. The mean gap length method is the most objective one, since its results do not depend on the average bubble diameter. It is more difficult than the first method.

It is known[10] that the gap length distribution is exponential:

$$W(l)\,dl = ge^{-gl}dl, \tag{7}$$

where $W(l)\,dl$ is the probability of the gap length to fall between 1 and 1 $\neq$ dl. This fact is confirmed by direct measurements of fast electron tracks (Fig. 5). It can be seen from the histogram, however, that the experimental distribution differs from the theoretical only for gap lengths smaller than $D/2$. This is connected with the fact that the outlines of the bubble images are blurred. The method of the measurement of the mean length of gaps larger than a certain value ϵ was therefore used. ϵ was usually taken to be equal to $D/2$.

The track density can be found from the measured mean gap length larger than ϵ according to the following formula:[10]

$$g = 1/(l_\varepsilon - \varepsilon) \tag{8}$$

with a statistical error

$$\Delta g/g = N_\varepsilon^{-1/2}, \tag{9}$$

where N_ϵ is the number of such gaps, and 1_ϵ their mean length.

3. For dense tracks ($gD > 1$), the method of counting of the number of gaps larger than ϵ is more accurate. According to reference 10, the number of tracks is connected with the track density by the following relation:

$$N_\varepsilon = gLe^{-g(D+\varepsilon)}. \tag{10}$$

The dispersion of the gap number distribution in an analogous problem was calculated by Domb[11]: Making use of his results, the statistical error of the track density is easily found to be:

$$\frac{\Delta g}{g} = \frac{(1 - 2j_\varepsilon e^{-j_\varepsilon})^{1/2}}{\sqrt{N_\varepsilon}\,|1 - j_\varepsilon|}, \tag{11}$$

where

$$j_\varepsilon = g(D + \varepsilon).$$

The validity of the formulas for the statistical error estimate was checked by us experimentally. Some 23 fast electron tracks were used for this purpose. The tracks were divided into intervals of equal length, and the dispersion of the distribution of the values of N, N_ϵ and 1_ϵ was measured. The result of the measurements can be represented in the following form:

$$\Delta g/g = C/\sqrt{N_m}. \tag{12}$$

where N_m is the number of counts of bubbles or gaps larger than ϵ. The coefficient C depends on the method used and on the value of $j_\epsilon = g(D + \epsilon)$.

The theoretical dependence of C on j_ϵ for the different methods and the experimental points are shown in Fig. 6. The satisfactory agreement between the experimental points and the theoretical curve indicates the correctness of the application of the formulas (6), (9) and (11) for the calculation of statistical errors.

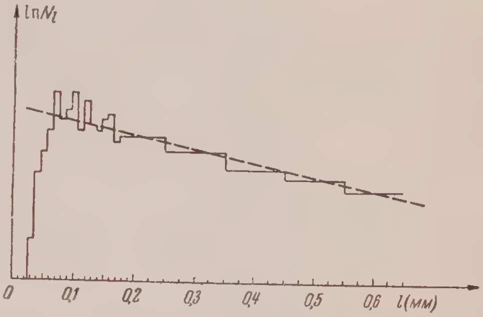

FIG. 5. Gap length distribution. N_1 –number of gaps with length between 1 and 1 + dl.

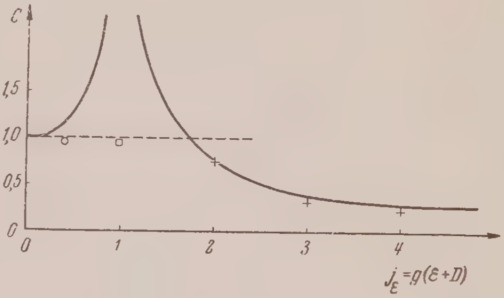

FIG. 6. Dependence of coefficient C in Eq. (12) on $j_\epsilon = g(D + \epsilon)$ +–gap number method (solid curve); □–mean gap length method (broken line); O–straightforward bubble counting.

It was assumed in the calculations that all the bubble images are of the same diameter. In reality, the values are distributed. with an average value equal to D (taking the camera reduction into account) and a dispersion σ^2. In our case, the ratio σ/D equalled 0.1, and the distribution width was negligible. It is desirable to have a smaller D for better accuracy. The ratio σ/D is then larger. It was found from cloud chamber pictures, taken by 3. V. Chirokov, that $\sigma/D = 0.4$ for $D = 0.05$ mm. The results of measurements of the statistical error for tracks 5 cm in length, depending on the measure of overlapping, are given in the Table for two values of the ratio σ/D. The errors are given for the most accurate method of measurement in each case.

It can be seen from the Table that, for tracks 5 cm in length, the variation of the density by a factor of 20 with an error of 6–10% is possible without any change of the chamber sensitivity setting.

	Method of Measurement	number of bubbles		mean gap length $\epsilon = D/2$		number of gaps $\epsilon = D$		number of gaps $\epsilon = D/2$			
	gD	0,2	0,3	0,4	0,8	0,9	1,2	1,4	2,0	3,0	4,0
$\Delta g/g(\%)$	$D = 0{,}1$ мм $\sigma/D \leqslant 0{,}1$	10,5	8,8	9,5	9,0	9,2	7,3	6,7	6,3	6,7	9,0
	$D = 0{,}05$ мм $\sigma/D = 0{,}4$	8,8	7,7	8,1	7,5	7,5	6,1	5,9	5,7	7,0	10

By controlling the chamber sensitivity and using various methods of track density measurements we measured ionization, varying from minimum ionization up to a value greater by a factor of eighty.

4. IDENTIFICATION OF PARTICLES AND DEPENDENCE OF THE TRACK DENSITY ON PARTICLE VELOCITY

Since the particle beams used by us were not monoenergetic, correct identification of the particles from their tracks constituted a most important problem.

The stopping power of the liquid used was determined from the range of monoenergetic muons from the $\pi-\mu$ decay (Fig. 7) obtained by means of the proton beam. The measured mean range of four muons equalled 3.05 ± 0.12 mm, which agrees with the value calculated for propane at muon energy of 4.17 mev. The photographs obtained with the neutron beam contained a large number of tracks of different particles. The horizontal tracks of stopping ionizing particles and tracks of electrons of various energies were selected for evaluation.

The identification of the particle tracks was done in the following way: particles having minimum ionization tracks with strong multiple scattering were classified as electrons (Fig. 8), which were in turn divided into two energy groups. Tracks with strong multiple scattering, terminating in the chamber, correspond to electrons of energy between 1 and 5 mev, and tracks with weaker scattering, extending beyond the chamber, to electrons of 10–100 mev. Protons, deuterons and pions stopping in the chamber were identified on the basis of a number of criteria: 1) the total number of bubbles in a chosen residual range 2) the dependence of track density on range 3) the value of the multiple scattering and 4) the nuclear interaction at the end of the pion track (Fig. 9).

The distribution of the total number of bubbles over the residual range equal to 36 mm for 20 stopping particles is shown in Fig. 10. The corresponding photographs were obtained at low sensitivity conditions, where the tracks of fast electrons had a density of 0.24 bubbles per mm and were almost invisible (operation conditions No. 1, $P_0 = 24.2$ atm). As it can be seen from the histogram, the tracks are divided into three groups with the mean values of 51, 100 and 131 bubbles in the residual range of 36 mm. According to the criteria given above, the particles of the first group were identified as pions, of the second as protons, and of the third as deuterons. These particles leave the steel walls of the chamber, and also are formed within the chamber during the disintegrations of nuclei by neutrons. On the basis of conservation law considerations and the initial energy of the neutrons it was shown that α-particles cannot be found among particles having a residual range of 36 mm in propane, and the proportion of tritium nuclei cannot be significant because of their low frequency in stars.[12]

The width of each group is well explained by the statistical spread of the number of bubbles. It is also easily shown that the probability of the fluctuation by which a particle from the second group can be found in the third group is smaller than 1%.

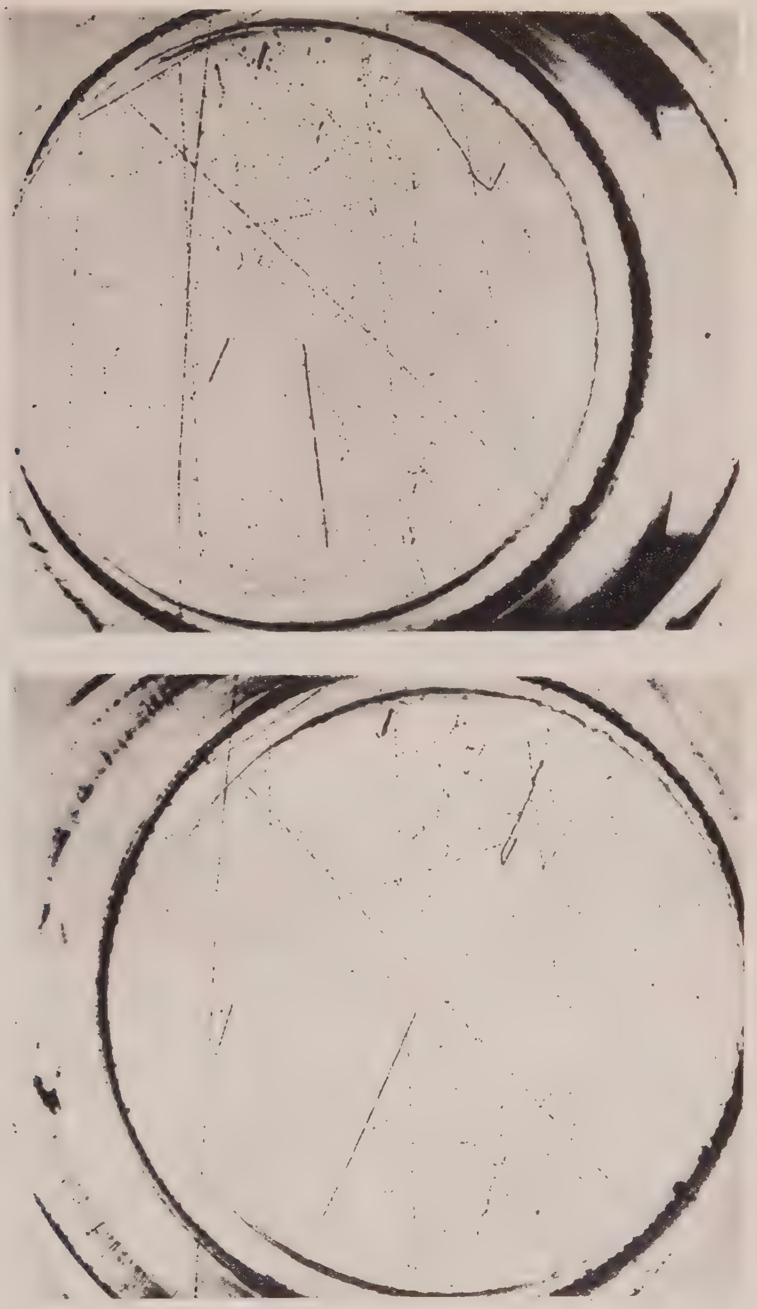

FIG. 7. Photograph of π–μ–e decay. The pion emerges from the rear window of the chamber.

The measurements showed that the track density varied approximately as $1/\beta^2$, β being determined from the range and the assumed mass of the particle. The measured ratios of the numbers of bubbles

$$N_p / N_\pi = 1.96 \pm 0.25 \text{ and } N_d / N_p = 1.31 \pm 0{,}08$$

are in good agreement with the ratios calculated under the assumption of a $1/\beta^2$ dependence:

$$(N_p/N_\pi)_{\text{calc}} = 2.2; \qquad (N_d/N_p)_{\text{calc}} = 1.35.$$

For more accurate results, the tracks were divided into intervals of 3 mm each, and the mean track density was determined in intervals with a given distance to the end of the track for every particle group. Tne velocity was determined from the range and the mass of the particle. The dependence of the track density on the velocity of particle was sought in the form

$$g = g_0/\beta^n. \tag{13}$$

The values of g_0 and n, found with the help of the least squares method for operation conditions *I*, are: $n = 2.07 \pm 0.17$; $g_0 = 0.155\ \mathrm{mm}^{-1}$.

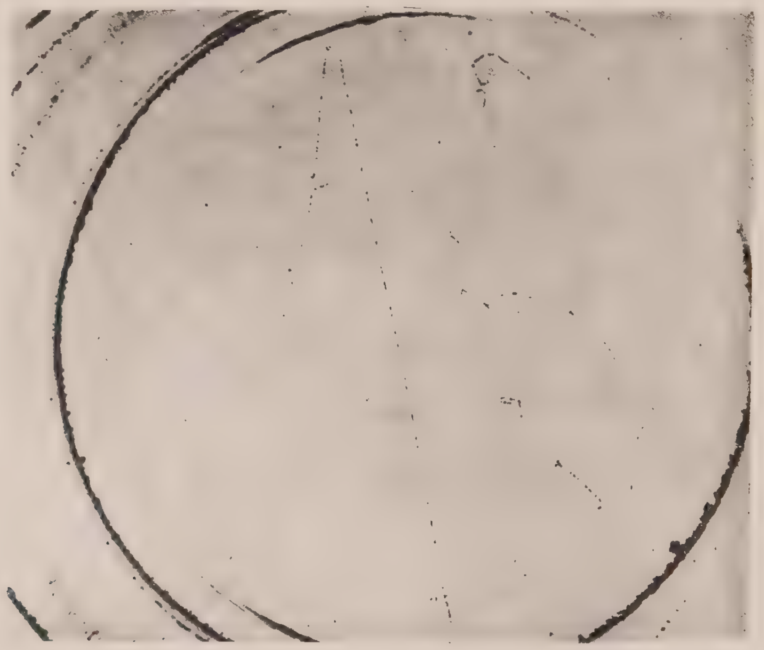

FIG. 8. Tracks of electrons of various energies. The electrons are produced in the walls of the chamber, placed in a beam of γ-rays.

For higher sensitivity of the chamber (operation conditions *II* $P_0 = 23.5$ atm) the analysis of 7 cases of protons, 2 deuterons and 7 electrons yielded the following values: $n = 2.02 \pm 0.34$; $g_0 = 0.200\ \mathrm{mm}^{-1}$.

For operation conditions *III* ($P_0 = 22.8$ atm, $g_0 = 0.28$), tracks of four pions and 29 electrons were analyzed, one of the pions, which left the chamber, being identified by multiple scattering. The value of n was not determined since the number of particles coming to a stop was small, while g_0 was obtained from the comparison of the electron track densities with those of operation conditions *II*.

The experimental data on the dependence of the track density on the particle velocity for all three operation conditions are shown in Fig. 11. It was assumed that $n = 2$ and new values of g_0 were calculated. The straight line in Fig. 11 corresponds to the equation

$$g/g_0 = 1/\beta^2. \tag{14}$$

Satisfactory agreement of the experimental points for all three operation conditions with Eq. (14) permits us to conclude that the value of g/g_0 is directly related to the velocity of the particle or, more accurately, to the ratio Z^2/β^2. An increase in the track density, deviating from Eq. (14), is observed for electrons of velocities close to the velocity of light. Measurements of 148 cases have shown that tracks of electrons of 10–100 mev have a density 12 5% higher than the tracks of 1–5 mev electrons.

It is possible to state, therefore, that a relativistic increase of the track density exists in the bubble chamber.

The authors wish to express their gratitude to A. I. Alikhanov, A. G. Meshkovskii and 3. V. Chirikov for discussion of results and to M. G. Meshcheriakov for making it possible to use the synchrocyclotron of the Institute of Nuclear Problems.

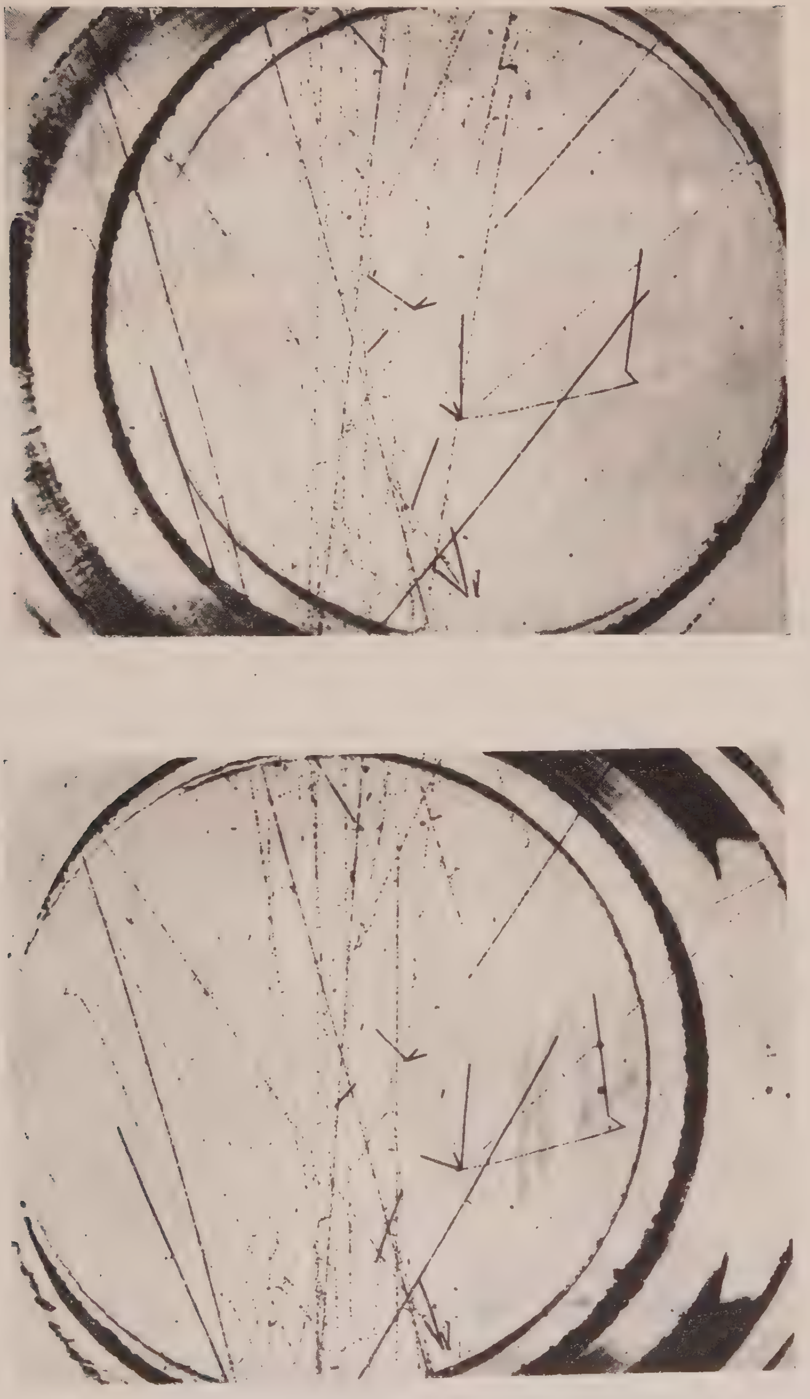

FIG. 9. Pion stopping in the chamber produce a two-prong star. The pion was created in disintegration of a *C* nucleus by a neutron (six-prong star). Tracks of protons and electrons produced by the neutron beam which traverses the chamber (mean energy 590 mev) are also visible in the photograph.

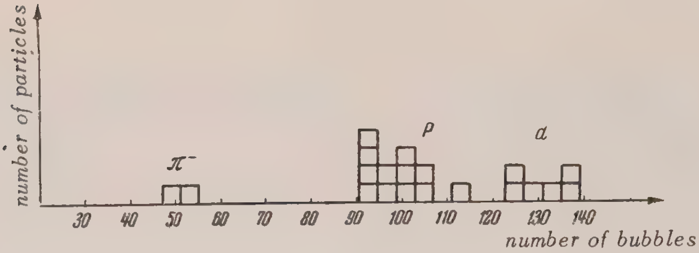

FIG. 10. Distribution of the number of bubbles in the residual range of 36 mm in tracks of stopping ionizing Particles.

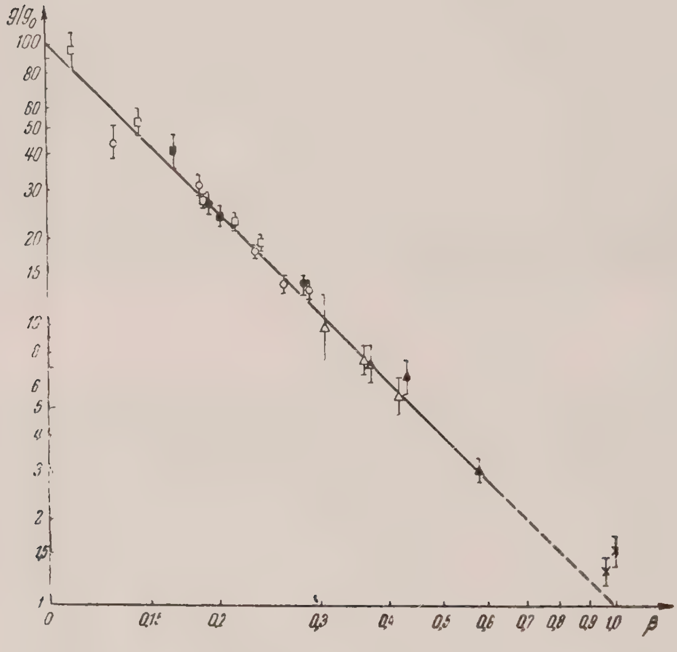

FIG. 11. Dependence of g/g_0 on β. Log–Log coordinates. O–protons, □ –deuterons and Δ–pions for operation conditions *I*; ●–protons, □–deuterons and X–electrons for conditions *II*; ▲–pions and X–electrons for conditions *III*.

---

[1] D. A. Glaser, Phys. Rev. **91**, 762 (1953).

[2] Landolt-Bornstein, Zahlenwerte und Funktionen, 6 Auflage, 1952, I Band, 5 Teil, S. 343.

[3] D. A. Glaser and D. C. Rohm, Phys. Rev. **97**, 474 (1955).

[4] Blinov, Krestnikov and Pershin, Dokl. Akad. Nauk SSSR **99**, 929 (1954).

[5] Blinov, Krestnikov and Pershin, Izv. Akad. Nauk SSSR, Ser. Fiz. **19**, 758 (1955).

[6] C. Dodd, Nature **176**, 142 (1955).

[7] D. Parmentier and A. J. Schwemin, Rev. Scient. Instr. **26**, 954 (1955).

[8] Happ, Hull and Morris, Canad. J. Phys. **30**, 699 (1952).

[9] E. J. Williams, Proc. Roy. Soc. (London) **A172**, 207 (1939).

[10] M. G. K. Menon and C. O.'Callaigh, Proc. Roy. Soc. **A221**, 292 (1954).

[11] C. Domb, Proc. Camb. Phil. Soc. **43**, 329 (1947).

[12] Bernardini, Booth and Lindenbaum, Phys. Rev. **85**, 826 (1952).

Translated by H. Kasha
169

SOVIET PHYSICS JETP VOLUME 4, NUMBER 5 JUNE, 1957

On the Construction of the Scattering Matrix. I. Integral Causality Condition in Bogoliubov's Method

B. V. MEDVEDEV
Mathematical Institute, Academy of Sciences, USSR

(Submitted to JETP editor June 28,1955)
J. Exptl. Theoret. Phys. (U.S.S.R.) 31, 791-802 (November, 1956)

An integral causality condition is formulated in Bogoliubov's method for the construction of the scattering matrix. Starting from this method, the compatibility of the conditions imposed on the scattering matrix and the existence theorem for the matrix are demonstrated; the scattering matrix is obtained in explicit form for the local theory.

IN most works on quantum field theory, the scattering matrix is constructed by starting either from Schrödinger's equation in the interaction representation[1-3] or from the equations of motion for the field operator in the Heisenberg representation[4,5]. In other words, the S–matrix is obtained as the solution of certain equations within the framework of the Hamiltonian method. However it was shown[6] some time ago that an analysis of the scattering matrix opens the way for the construction of a wider class of theories than the Hamiltonian. There is therefore considerable interest in a method recently proposed by Bogoliubov[7,8] (developing an idea of Stueckelberg[9]) for constructing the scattering matrix without reference to the equations of motion. We would especially like to emphasize that this method offers new possibilities for non-local theories which are apparently irreconcilable with the Hamiltonian scheme.

In order to preserve the possibility of a space-time description, one introduces in Bogoliubov's* method a function $g(x)$ ranging over the interval $[0, 1]$ which describes inclusion or exclusion of an interaction; the effective interaction $L(x)\,dx$ is changed to $L(x)\,g(x)\,dx$, and one seeks the scattering matrix for such an interaction, considering it as a function of g, through a formal decomposition in "powers" of $g(x)$:

$$S(g) = 1 + \sum_{n=1}^{\infty} \frac{1}{n!} \times \int S_n(x_1, \ldots, x_n)\, g(x_1) \ldots g(x_n)\, dx_1 \ldots dx_n. \qquad (1)$$

Instead of using the equation of motion, one applies obvious physical requirements to the scattering matrix: A–correspondence with the classical theory, B–relativistic invariance, C–unitarity $S(g)\,S^+(g) = S^+(g)\,S(g) = 1$, D–causality. The last, which shall be called the differential causality condition, may be written in the form

$$\frac{\delta}{\delta g(x)}\left(\frac{\delta S(g)}{\delta g(y)} S^+(g)\right) = 0 \quad \text{for} \quad x \lesssim y, \qquad (2)$$

where the sign $\gtrsim$ signifies "later or space-like."

The purpose of the present article is to investigate (within the framework of Bogoliubov's method) the causality condition in a form which differs from (2) and which, it is believed, permits construction of the scattering matrix in a simpler and more natural fashion. Furthermore, the new causality condition which will be introduced here has the substantial advantage that it may be relatively easyly generalized to a non-local theory whose analysis by non-Hamiltonian methods proves of the greatest interest.

2. THE INTEGRAL CAUSALITY CONDITION

In order to formulate the causality condition, it is necessary to make use of the concepts "later" and "earlier." Considering two events in classical (non-relativistic) theory, the meaning of these concepts is graphically specified by the sign of the time interval between these events. It is well known that such a specification is not invariant in relativistic theory, and in order to specify invariantly the time order of two events, it is necessary to introduce three concepts: "later," "earlier," and "space-like." Since we are seeking here the scattering matrix in the form of a functional obtained by integrating over certain space-time regions, it is natural to start with certain concepts regarding the possible forms of 4-dimensional time order.

Consider two space-time regions G_1 and G_2. Let us construct at each point of G_1 a half-light cone, directed into the future, which we shall call the extended G_1 region, and let us denote by $\overline{G}_1$ the set of points which lie inside or at the boundary of at least one of these cones (Fig. 1). The region $\overline{G}_2$ is constructed in a similar fashion.

Now if the regions G_1 and $\overline{G}_2$ have no common point $G_1 \cap \overline{G}_2 = 0$, we shall say that the region $\overline{G}_1$

---

*Reported by N. N. Bogoliubov at the meeting of the physico-mathematical division of the Jubilee meeting of the Academy of Sciences of the USSR in April 1954.

is situated *not later* than G_2, and write $G_1 \lesssim G_2$. In the opposite case, if $G_1 \cap G_2 \neq 0$, we shall write $G_1 \not\lesssim G_2$. Similar statements will hold for G_2 and G_1.

The relative positions of G_1 and G_2 can now be described by the following four logical possibilities.

1. The region G_1 is situated not later than the region G_2, the region G_2 is not situated not later than the region G_1: $G_1 \lesssim G_2$, $G_2 \not\lesssim G_1$. In this case we shall say that the region G_2 is situated *later* than the region G_1 and write (Fig. 2) $G_1 < G_2$.

2. The region G_2 is situated not later than G_1, G_1 is not situated not later than G_2: $G_2 \lesssim G_1$, $G_1 \not\lesssim G_2$. We shall say that G_1 is situated later than G_2 and write (Fig. 3) $G_2 < G_1$.

3. The region G_1 is situated not later than G_2, the region G_2 is situated not later than G_1 We shall say that G_1 and G_2 are space-like with respect to each other and write (Fig. 4) $G_1 \sim G_2$.

If at least one of these possibilities is present, we shall say that the regions G_1 and G_2 are separable.

4. The region G_1 is not situated not later than G_2, the region G_2 is not situated not later than G_1: $G_1 \not\lesssim G_2$, $G_2 \not\lesssim G_1$. We shall say that the region G_1 and G_2 are unseparable and write (Fig. 5) $G_1 \gtrless G_2$.

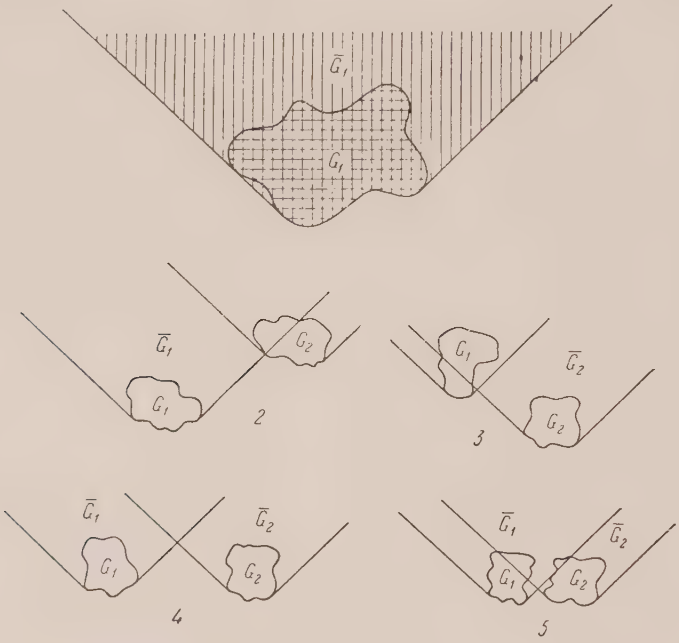

FIGS. 1, 2, 3, 4, 5

It is clear that $G_2 \not\lesssim G_1$ implies that G_1 is situated later than or is space-like with respect to G_2 as reflected by the chosen notation.

In addition to the concepts of chronological order which we have just defined in 4-dimensions, we shall need later a representation of chronological order for two sets of space-time points $\{x_1, \ldots, x_l\}$ and $\{y_1, \ldots, y_m\}$. In order to do this we shall place each set of points $\{x_1, \ldots, x_m\}$ in a suitable 4-dimensional region G, a disconnected region consisting only of the points of the set; now we shall say that the set $\{x_1, \ldots, x_l\}$ is situated later than the set $\{y_1, \ldots, y_m\}$, etc., if the regions G_1, and G_2 are so situated with respect to each other.

Consider now two regions G_1 and G_2 such that G_1 is situated later than or is space-like with respect to G_2, $G_1 \gtrsim G_2$, and define a class of functions $g_1(x)$ and $g_2(x)$ such that

$$g_1(x) \neq 0, \qquad \text{only if} \qquad x \in G_1 \text{ and } g_2(x) \neq 0,$$

$$\text{only if } x \in G_2. \tag{3}$$

It is evident that the principle of causality as it is understood in the usual sense requires that no event in G_1 can have any influence on events in G_2.

It follows that the interaction localized in G_2 [i. e. described in terms of an arbitrary function belonging to the class $g_2(x)$] must act as if there was no interaction at all in the region G_1, i. e. [see Ref. 8, Eq. (3.13)], it must transfer the system from the state described by the constant initial state amplitude Φ_0, to a state of amplitude

$$\Phi_{g_2} = S(g_2)\,\Phi_0.$$

As for the effect on the system of the interaction localized in G_1, it must be independent of the explicit form of the interaction arising in G_2 but must be solely dependent on the final state described by the amplitude Φ_{g_2}, arising as a result of the interaction, i.e., the system must be transferred from the state Φ_{g_2} to the state

$$\Phi_{g_1 g_2} = S(g_1)\,\Phi_{g_2} = S(g_1)\,S(g_2)\,\Phi_0. \qquad (4)$$

But on the other hand it is possible to reach the same final state by considering at once the sum of the effects of the interactions localized in the two regions G_1 and G_2. Application of the general rule [see Ref. (8)] must then yield a state with amplitude

$$\Phi_{g_1+g_2} = S(g_1+g_2)\,\Phi_0. \qquad (5)$$

But amplitudes (4) and (5) describe the same state of the system; therefore, $\Phi_{g_1 g_2} = \Phi_{g_1+g_2}$, i.e.,

$$S(g_1+g_2) = S(g_1)\,S(g_2), \qquad \text{if } G_1 \gtrsim G_2. \qquad (6)$$

Equation (6) may be considered as the mathematical formulation of the causality condition. We shall call it the *integral causality condition.*

Let us restate the integral causality condition in the formalism of the operator functions S_n appearing in Eq. (1) (see Ref. 8, Sec. 1). We substitute expansion (1) for $S(g_1)$, $S(g_2)$, and $S(g_1+g_2)$ in Eq. (6), equate coefficients of equal powers in $g_1(x)$ and $g_2(x)$, and make use of the arbitrariness of the functions $g_1(x)$ and $g_2(x)$ within the boundary conditions imposed on them by Eq. (3) and the condition $G_1 \gtrsim G_2$; the integral causality condition for the operator function $S_n \times (x_1, \ldots, x_n)$, equivalent to the one imposed on the functionals in the total integrity causality condition (6), then becomes*

$$S_n(x_1, \ldots, x_n) \qquad (7a)$$
$$= S_l(x_1, \ldots, x_l)\,S_{n-l}(x_{l+1}, \ldots, x_n),$$
$$\text{if} \quad \{x_1, \ldots, x_l\} \gtrsim \{x_{l+1}, \ldots, x_n\}. \qquad (7b)$$

Comparing Eq. (7) with the analytical form [Ref. 8, Eqs. (4.11) and (4.12)] of the differential causality condition (2), we see that the former is considerably simpler. This reflects the fact that the integral condition (6) is imposed on the *matrix* $S(g)$ *itself*, while the differential condition (2) is imposed on its *variational derivative*.** Thus the integral causality condition seems more natural if the direct construction of the scattering matrix forms the basis of the theory.

We shall now establish the relationship between (6) and the differential condition (2), and show that they are equivalent. Consider a system with an interaction of intensity

$$g(x) = g_1(x) + g_2(x), \qquad (8)$$

where $g_1(x)$ and $g_2(x)$ belong to the class (3), and assume that $G_1 \gtrsim G_2$. Then, applying (6)

$$S(g_1+g_2)$$
$$= S(g_1)\,S(g_2) \text{ and } S^+(g_1+g_2) = S^+(g_2)\,S^+(g_1).$$

Now give the function $g(x)$ an infinitesimal increment $\delta_y g$ in the infinitesimal neighborhood of the

---

* Because of the symmetry of the function S_n in all its arguments, the order of enumeration of the variables in (7) is unessential, and it may be written in the more general form

$$S_n(x_1, \ldots, x_n) \qquad (7'a)$$
$$= S_l(x_{\lambda_1}, \ldots, x_{\lambda_l})\,S_{n-l}(x_{\lambda_{l+1}}, \ldots, x_{\lambda_n}),$$
$$\text{if} \quad \{x_{\lambda_1}, \ldots, x_{\lambda_l}\} \gtrsim \{x_{\lambda_{l+1}}, \ldots, x_{\lambda_n}\}. \qquad (7'b)$$

Later on we shall sometimes write formulas in nonsymmetrical form without mentioning the particular possibility of so doing in analogy with (7′).

**Condition (2) takes on a simpler form if it is imposed on the Hamiltonian $H(x;\, g)$ [Ref. 8, Eq. (4.10)]; it therefore seems more natural if one starts to construct the theory not from the scattering matrix but from the analogue of an equation of the Tomonaga-Schwinger form. Making use of the latter method for constructing the theory it was shown by Bogoliubov that condition (2) physically describes the need for a local Hamiltonian in the interaction representation.

point $y \epsilon G_1$. The operator $1 + \delta_y S(g)\, S^+(g)$ which transforms $\Phi(g)$ into $\Phi(g) + \delta_y \Phi(g)$, then equals

$$1 + \delta_y S(g_1)\cdot S(g_2)\, S^+(g_2)\, S^+(g_1) = 1 + \delta_y S(g_1)\cdot S^+(g_1)$$

and is of course independent of the behavior of $g_2(x)$, i.e., of the behavior of the function $g(x)$ for points $z \epsilon G_2$. The function $g(x)$ having the particular form (8) will then satisfy the equation

$$\frac{\delta}{\delta g(z)}\left(\frac{\delta S(g)}{\delta g(y)}\cdot S^+(g)\right) \tag{9}$$

$$= 0 \quad \text{for} \quad y \in G_1;\ z \in G_2, G_1 \gtrsim G_2,$$

which is the same as the differential condition (2).

Consider now some arbitrary function $g(x)$ and two points $z \lesssim y$. Then it is always possible to construct a space-like hypersurface σ, such that $z < \sigma < y$. Let us construct a family of functions $g_\epsilon(x)$ equal to $g(x)$ if $|x^4 - \sigma| > \epsilon$, equal to zero if $x \epsilon \sigma$, and increasing smoothly on both sides of σ into strips of width ϵ. For any value of ϵ, the functions $g_\epsilon(x)$ obviously belong to the class (8) for which Eq. (9) holds. The original function $g(x)$ may therefore be considered as the limit of the functions $g_\epsilon(x)$ as $\epsilon \to 0$. Accordingly, Eq. (9) applies to any $g(x)$ and $z \lesssim y$.

Thus the differential causality condition (2) follows from the integral causality condition (6).* The reverse statement follows from the fact that equation (2) leads to an expression for $S(g)$ which obviously satisfies Eq. (6) [see Ref. 8, Eq. (4.34)].

3. COMPATIBILITY OF THE CONDITIONS IMPOSED ON THE SCATTERING MATRIX

We shall show that the conditions A–D imposed on the scattering matrix are compatible. Returning to the representation (7) obtained from the causality condition, we note first of all that if the operator functions S_l and S_{n-l} appearing on the right-hand side are correctly transformed [see Ref. 8, Eq. (4.4)], then the same thing will automatically happen to S_n. Now if the variables $x_1, \ldots, x_n$ can be divided into two sets $\{x_1, \ldots, x_l\}$ and $\{x_{l+1}, \ldots, x_n\}$ which are space-like with respect to each other, then it follows from (7) that there are two simultaneous representations for S_n:

$$\begin{aligned} S_n(x_1, \ldots, x_n) &= S_l(x_1, \ldots, x_l) S_{n-l}(x_{l+1}, \ldots, x_n) \\ &= S_{n-l}(x_{l+1}, \ldots, x_n)\, S_l(x_1, \ldots, x_l), \\ &\text{if} \quad \{x_1, \ldots, x_l\} \sim \{x_{l+1}, \ldots, x_n\}. \end{aligned} \tag{10}$$

Therefore, in order to preserve the relativistic invariance of the theory, it is necessary that the operator functions for two sets space-like with respect to each other commute. It is easily seen that this condition is fulfilled if and only if the elementary commutators of the field operators vanish for space-like intervals, as in the case for the ordinary invariant functions D and S. The compatibility of conditions B and D will then be guaranteed.

If the set of arguments $\{x_1, \ldots, x_n\}$ of the operator functions can be divided in more than one way into two subsets satisfying (7b) [or (7′b)], then the causality condition leads to several expressions for the same S_n through operator functions of lower order. We shall show that these expressions are essentially identical, i.e., that the several conditions imposed in such a case on a single S_n are compatible.

Assume that the set of arguments of the function $S_n(x_1, \ldots, x_n)$ can be divided in two ways into two sets satisfying (7b):

$$A \equiv \{x_{\lambda_1}, \ldots, x_{\lambda_l}\} \gtrsim \{x_{\lambda_{l+1}}, \ldots, x_{\lambda_n}\} \equiv \mathbf{A}, \tag{11.1}$$

$$B \equiv \{x_{\mu_1}, \ldots, x_{\mu_m}\} \gtrsim \{x_{\mu_{m+1}}, \ldots, x_{\mu_n}\} \equiv \mathbf{B}. \tag{11.2}$$

According to (7′) these divisions lead to the following expressions for S_n:

$$S_n(x_1, \ldots, x_n) = S(A)\, S(\mathbf{A}), \tag{12.1}$$

$$S_n(x_1, \ldots, x_n) = S(B)\, S(\mathbf{B}). \tag{12.2}$$

In order to show their equivalence, consider the intersection $A \cap B$ of the sets A and B. Since $A \cap B \subset A$, then from (11.1):

$$A \cap B \gtrsim \mathbf{A}. \tag{13.1}$$

On the other hand, $A \cap B \subset B$; therefore, it follows similarly that:

---

*The fact that the differential causality condition imposed on the operator functions S_n follows from (7) may be shown, without recourse to limiting processes, by means of a direct though rather cumbersome combinatorial transformation.

$$A \cap B \gtrsim \mathbf{B}. \qquad (13.2)$$

The set of arguments $A - A\cap B$ contained in A but not in B must be contained in B

$$A - A \cap B \subset \mathbf{B}. \qquad (14.1)$$

Similarly,

$$B - A \cap B \subset \mathbf{A}. \qquad (14.2)$$

But it follows from (14.1) and (13.2) that $A\cap B \gtrsim A - A\cap B$, and from (14.2) and (13.1) that $A\cap B \gtrsim B - A\cap B$. Therefore, it is possible to carry out a further division of the factors $S(A)$ and $S(B)$ and write

in (12.1): $S(A) = S(A\cap B)\, S(A - A\cap B)$

and in (12.2): $S(B) = S(A\cap B)\, S(B - A\cap B)$.

Repeating the same procedure for the sets A and B, we are led to two series of ordered relations*:

$$A \cap B \gtrsim A - A \cap B \gtrsim \mathbf{A} - \mathbf{A} \cap \mathbf{B} \gtrsim \mathbf{A} \cap \mathbf{B}, \qquad (15.1)$$

$$A \cap B \gtrsim B - A \cap B \gtrsim \mathbf{B} - \mathbf{A} \cap \mathbf{B} \gtrsim \mathbf{A} \cap \mathbf{B}, \qquad (15.2)$$

from which are obtained the following representations for S_n:

$$S_n = S(A \cap B)\, S(A - A \cap B)\, S \times (\mathbf{A} - \mathbf{A} \cap \mathbf{B})\, S(\mathbf{A} \cap \mathbf{B}), \qquad (16.1)$$

$$S_n = S(A \cap B)\, S(B - A \cap B)\, S \times (\mathbf{B} - \mathbf{A} \cap \mathbf{B})\, S(\mathbf{A} \cap \mathbf{B}), \qquad (16.2)$$

which only differ in the two inside factors. But it is easily seen that $A - A\cap B = \mathbf{B} - \mathbf{A}\cap\mathbf{B}$ and $B - A\cap B = \mathbf{A} - \mathbf{A}\cap\mathbf{B}$. Calling the first of these sets C, and the second D, it appears that (16.2) is obtained from (16.1) by the exchange $S(C)\,S(D) \to S(D)\,S(C)$. But it follows in particular from (15.1) that $C \gtrsim D$, and from (15.2) that $D \gtrsim C$. Therefore $C \sim D$ and according to (10), $S(C)$ and $S(D)$ commute. The compatibility of various expressions of the causality condition is then demonstrated if this condition can be repeatedly applied to a single S_n.

We shall consider now how expression (7), which follows from the integral causality condition, is related to the condition of unitarity [Ref. 8, Eq. (4.9)]. We shall first examine the simple case wherein one of the points $x_1, \ldots, x_n$ (for instance, x_n) is situated earlier (later) than or is space-like with respect to all the others; we shall then show that the operator functions appearing in Eq. (7) automatically satisfy the unitarity condition for $n > 1$ if it is satisfied for $n = 1$.

Let us rewrite the left-hand side of the unitarity condition [Ref. 8, Eq. (4.9)], separating it into summations over k and over the permutations of terms in which x_n appears in S_k and S^+_{n-k}, and let us apply (7). We obtain

$$S_1^+(x_n)\, S_{n-1}^+(x_1, \ldots, x_{n-1}) + \sum_{k=1}^{n-1} P\left(\frac{x_1, \ldots, x_{k-1}}{x_k, \ldots, x_{n-1}}\right)$$

$$\times\, S_{k-1}(x_1, \ldots, x_{k-1})\, S_1(x_n)\, S_{n-k}^+(x_k, \ldots, x_{n-1}) + \sum_{k=1}^{n-1} P\left(\frac{x_1, \ldots, x_k}{x_{k+1}, \ldots, x_{n-1}}\right)$$

$$\times\, S_k(x_1, \ldots, x_k)\, S_1^+(x_n)\, S_{n-k-1}^+(x_{k+1}, \ldots, x_{n-1}) + S_{n-1}(x_1, \ldots, x_{n-1})\, S_1(x_n).$$

Now carrying out in the first sum the transformation $k \to k + 1$, removing from it the term $k = 0$, and from the second one the term $k = n - 1$, it is found that all the terms occur in pairs whose only difference is the exchange of $S_1(x_n)$ into $S_1^+(x_n)$; the whole expression can then be written in the compact form

$$\sum_{k=0}^{n-1} P\left(\frac{x_1, \ldots, x_k}{x_{k+1}, \ldots, x_{n-1}}\right) S_k(x_1, \ldots, x_k)\, (S_1(x_n) + S_1^+(x_n))\, S_{n-k+1}^+(x_{k+1}, \ldots, x_{n-1}),$$

where it is assumed that $S_0 = S_0^+ = 1$. The last expression has a common factor $S_1(x_n) + S_1^+(x_n)$ which is equal to zero due to the unitarity condition for $n = 1$, and thus the whole expression vanishes.

Our assertion has therefore been proven. We note that the correspondence principle requires that[8] $S_1(x) = iL(x)$ and therefore the unitarity condition for $n = 1$ requires a Hermitian Lagrangian $L(x)$. If $L(x)$ is a Hermitian, the conditions A and C are compatible.

---

*Whenever we write a series of the form

$$A_1 \gtrsim A_2 \gtrsim \cdots \gtrsim A_k,$$

it implies not only the relations $A_1 \gtrsim A_2$, $A_2 \gtrsim A_3$, but also all the relations $A_i \gtrsim A_j$, if $i < j$. This proviso must be added since the relation $\gtrsim$ is not transitive, Consider now the general case wherein the arguments $x_1, \ldots, x_n$ can be divided into two groups

$$\{x_1, \ldots, x_{n-m}\} \gtrsim \{x_{n-m+1}, \ldots, x_n\}. \tag{17}$$

Again we transform the sums over the permutations

$$P\left(\frac{x_1, \ldots, x_k}{x_{k+1}, \ldots, x_n}\right) S_k(x_1, \ldots, x_k)\, S^{+}_{n-k}(x_{k+1}, \ldots, x_n) \tag{18}$$

occuring in Eq. (4.9) of Ref. (8) so as to distinguish permutations within each set $\{x_1, \ldots, x_{n-m}\}$ and $\{x_{n-m+1}, \ldots, x_n\}$, from permutation between sets; we single out in a sum over λ the arguments of the first sets whose subscripts appear in the arguments of S_k. The remaining sum over the permutations $P\left(\frac{x_1, \ldots, x_k}{x_{k+1}, \ldots, x_n}\right)$ is then reduced to a sum over permutations within the first group of arguments $P\left(\frac{x_1, \ldots, x_\lambda}{x_{\lambda+1}, \ldots, x_{n-m}}\right)$ and within the second group

$$P\left(\frac{x_{n-m+1}, \ldots, x_{n-m+k-\lambda}}{x_{n-m+k-\lambda+1}, \ldots, x_n}\right).$$

Expression (18) then becomes

$$\begin{aligned}&\sum_{(\lambda)} P\left(\frac{x_1, \ldots, x_\lambda}{x_{\lambda+1}, \ldots, x_{n-m}}\right) \\ &\quad\times P\left(\frac{x_{n-m+1}, \ldots, x_{n-m+k-\lambda}}{x_{n-m+k-\lambda+1}, \ldots, x_n}\right) \\ &\quad\times S_k(x_1, \ldots, x_\lambda, x_{n-m+1}, \ldots, x_{n-m+k-\lambda}) \\ &\quad\times S^{+}_{n-k}(x_{\lambda+1}, \ldots, x_{n-m}, x_{n-m+k-\lambda+1}, \ldots, x_n),\end{aligned} \tag{19}$$

where the summation limits over λ are given by the inequalities

$$\lambda \geqslant 0;\ \lambda \geqslant k-m;\ \lambda \leqslant k;\ \lambda \leqslant n-m.$$

Now we use the causality condition (7) in order to split each of the operator functions entering in (19) into the product of two factors, and we substitute expression (18), thus transformed, into the equation stating the unitarity condition [Ref. 8, Eq. (4.9)]. We obtain

$$\begin{aligned}&\sum_{k=0}^{n}\sum_{(\lambda)} P\left(\frac{x_1, \ldots, x_\lambda}{x_{\lambda+1}, \ldots, x_{n-m}}\right) \\ &\quad\times P\left(\frac{x_{n-m+1}, \ldots, x_{n-m+k-\lambda}}{x_{n-m+k-\lambda+1}, \ldots, x_n}\right) S_\lambda(x_1, \ldots, x_\lambda) \\ &\quad\times S_{k-\lambda}(x_{n-m+1}, \ldots, x_{n-m+k-\lambda}) \\ &\quad\times S^{+}_{m-k+\lambda}(x_{n-m+k-\lambda+1}, \ldots, x_n) \\ &\quad\times S^{+}_{n-m-\lambda}(x_{\lambda+1}, \ldots, x_{n-m}).\end{aligned} \tag{20}$$

Exchanging the summation variables k and λ for the variables $\mu = k - \lambda$ and λ, the summation region is transformed within the plane μ, λ into a rectangle bounded by the lines $\lambda = 0$, $\lambda = n-m$, $\mu = 0$, and $\mu = m$, i.e., the sums over μ and λ can be carried out independently. Thus we can carry out in (20) an internal sum over μ

$$\sum_{\mu=0}^{m} P\left(\frac{x_{n-m+1}, \ldots, x_{n-m+\mu}}{x_{n-m+\mu+1}, \ldots, x_n}\right)$$

$$S_\mu(x_{n-m+1}, \ldots, x_{n-m+\mu})\, S^{+}_{m-\mu}(x_{n-m+\mu+1}, \ldots, x_n),$$

which will enter in the factor of each term of the sum over λ. But it is obvious that this sum equals the left-hand side of the unitarity condition equation for $n = m$; if we therefore assume that the unitarity condition is satisfied for $m = 1, \ldots, n-1$ and for arbitrary values of the arguments, then (2) automatically vanishes for $0 < m < n$.

Thus if the unitarity condition is satisfied for $m = 1, \ldots, n-1$ and arbitrary values of the arguments, then it is atomatically satisfied for $m=n$ by virtue of the integral causality condition, as long as there exists at least one way to partition the arguments $x_1, \ldots, x_n$ into two non-empty sets satisfying (17). If on the other hand such a partition does not exist, the causality condition generally does not impose any limitations on S_n and the unitarity condition can always be satisfied. Thus the compatibility of the unitarity and causality conditions is demonstrated.

Let us finally note that the compatibility of conditions *A* and *B* is guaranteed if $L(x)$ is a scalar; the compatibility of *A* and *D* is guaranteed by a local Lagrangian; and the compatibility of *B* and *C* follows from the fact that Eq. (4.4) of Ref. 8 requires that S_n transforms identically with all the products $S_n S^{+}_{n-k}$ appearing in the unitary condition [Ref. 8, Eq. (4.9)]. The compatibility of the conditions A–D is thus demonstrated.

The relative simplicity of this demonstration must be ascribed to the use of the integral form (6) of the causality condition. The use of the differential form [Ref. 8, Eqs. (4.11) and (4.12)] considerably complicates the demonstration and it was found easier in Ref. 8 to obtain first an explicit form for $S(g)$ and then demonstrate that it satisfies the conditions A–D.

The existence theorem for the scattering matrix $S(g)$ follows immediately from the proof of the compatibility of conditions A–D. Assume that the quantities $S_1, \ldots, S_n$ constructed above satisfy conditions A–D. Now construct S_{n+1}. If the values of the arguments $x_1, \ldots, x_n$ are such that it is possible to carry out at least one partition of the form (7′b), then the value of S_{n+1} is determined from the causality condition without violating (as demonstrated) any of the other conditions. If the values of the arguments negate the existence of even one such partition, then the value of S_{n+1} may be obtained (even though non-uniquely) by starting from the unitarity condition again without conflicting with the remaining conditions. Thus the existence theorem for the scattering matrix $S(g)$ satisfying conditions A–D, is demonstrated.*

4. THE FORM OF THE SCATTERING MATRIX

We shall show that the method chosen for constructing the scattering matrix leads in a natural fashion to explicit expressions for the coefficients of the functions S_n and thereby to a simple closed form expression for $S(g)$. First we introduce some definitions.

If a set $\{g_1, \ldots, g_n\}$ of space-time regions (in particular the arguments $x_1, \ldots, x_n$ of the operator functions may be such regions) is divided into two non-empty sets $\{g_{\lambda_1}, \ldots, g_{\lambda_l}\}$ and $\{g_{\lambda_{l+1}}, \ldots, g_{\lambda_n}\}$ satisfying a condition of the type (7′b)

$$\{g_{\lambda_1}, \ldots, g_{\lambda_l}\} \gtrsim \{g_{\lambda_{l+1}}, \ldots, g_{\lambda_n}\}, \qquad (21)$$

then we shall say that a *section* has been carried out which has separated the original set into the sum of two sets $\{g_{\lambda_1}, \ldots, g_{\lambda_l}\}$ and $\{g_{\lambda_{l+1}}, \ldots, g_{\lambda_n}\}$.

It is clear that every section is realized by means of some space-like hypersurface σ, such that every region of the first set is situated later than the hypersurface and every region of the second is situated earlier.

If it is impossible to carry out any sections in the set of regions $\{g_1, \ldots, g_n\}$, we shall say that the regions ("points") $g_1, \ldots, g_n$ are *completely unseparable* or the set of these regions is *indecomposable*. In the opposite case we shall say that the set of regions $\{g_1, \ldots, g_n\}$ is *decomposable*.

If a set of regions $\{g_1, \ldots, g_n\}$ can be divided into m groups $\{g_{\lambda_1}, \ldots, g_{\lambda_{\nu_1}}\}, \ldots,$

$$\{g_{\lambda_{\nu_1+\ldots+\nu_{m-1}+1}}, \ldots, g_{\lambda_n}\},$$

such that: a) any two groups

$$\{g^{\lambda}{}_{\nu_1+\ldots+\nu_{j-1}+1}, \ldots, g_{\lambda_{\nu_1+\ldots+\nu_j}}\}$$

$$\text{and}\{g_{\lambda_{\nu_1+\ldots+\nu_{i-1}+1}}, \ldots, g_{\lambda_{\nu_1+\ldots+\nu_i}}\}$$

are separate with respect to each other and b) the regions contained within each group are completely unseparable (i.e., every group of regions is indecomposable), then we shall say that the set of regions $\{g_1, \ldots, g_n\}$ is *completely decomposable*.

Let us consider a decomposable set of regions G. We can by definition perform a section in that set. Let us assume that such a section divides G into the sum of G_1 and G_2 such that $G_1 \gtrsim G_2$. Consider now the set G_1. It may be either indecomposable or decomposable. In the first case we shall consider the set G_2, in the second case there exists a section which divides G_1 into the sum of two sets G_{11} and G_{12}, $G_{11} \gtrsim G_{12}$. Since $G_1 \gtrsim G_2$, such a relationship is also satisfied for each part G_{11} and G_{12} of the set G_1: $G_{11} \gtrsim G_{12}$ and $G_{12} \gtrsim G_2$. We can therefore write (see footnote on page 677):

$$G_{11} \gtrsim G_{12} \gtrsim G_2, \qquad (22)$$

i.e., G is divided into three sets, G_{11}, G_{12} and G_2 satisfying a series of relations (21). (If we have to contend with the first case mentioned above, and G_2 is decomposable, then $G_1 \gtrsim G_{21} \gtrsim G_{22}$; if G_2 is indecomposable, then the problem of representing a decomposable set into a sum of indecomposable sets is immediately solved.) Each of these sets may be either indecomposable—then we no longer consider it—or decomposable. In the latter case there exists a section which decomposes the set G_α into two sets $G_{\alpha 1} \gtrsim G_{\alpha 2}$. By the same arguments which were used to deduce (22), $G_{\alpha 1}$ and $G_{\alpha 2}$ will form another term in the series just like G_α; thus the performance of a section reduces simply to the exchange

---

*The demonstration is of course a formal one inasmuch as we do not concern ourselves with questions of convergence.

$$G_\alpha \to G_{\alpha 1} \gtrsim G_{\alpha 2}$$

in expression (22). Such a process can obviously be continued until the remaining sets are all indecomposable and one obtains the series of relations

$$G_{\nu_1} \gtrsim G_{\nu_2} \gtrsim \ldots \gtrsim G_{\nu_m}; \quad (\Sigma \nu_i = n) \tag{23}$$

($m \leq n$, where n is the number of regions in G wherein one only considers indecomposable sets of regions).

It has therefore been shown that every decomposable set may be decomposed into a sum of indecomposable sets, i.e., *every decomposable set is completely decomposable*,

It has further been shown that every decomposable set can be represented in the form of an *ordered* succession of indecomposable sets satisfying (23).

It is easily seen that every decomposition is unique. Indeed, let us assume that there exists another decomposition of G into indecomposable sets some of which at least do not coincide with the sets appearing in (23). Let G_β be such a set. There are two logical possibilities: either it consists of regions contained in various sets of (23), but such a set cannot be indecomposable since the regions it contains can be divided by one of the sections utilized in (23); or else it consists of regions which are all contained in one of the indeccomposable sets of (23), although they do not exhaust it; but this implies decomposition of an indecomposable set, which is impossible by definition.

On the other hand the representation of a decomposable set in the form of an *ordered* succession of indecomposable sets is not unique. This may be seen, for example, by considering a set $\{g_1, g_2\}$ of two regions space-like with respect to each other $g_1 \sim g_2$. It is obvious that the decomposable set $\{g_1, g_2\}$ may be represented in the form of two non-identically ordered series

$$g_1 \gtrsim g_2 \text{ and } g_2 \gtrsim g_1.$$

In the above example, non-uniqueness follows from the possibility of exhanging in (23) two regions which are space-like with respect to each other. We shall show that this is the case in general. It is obvious from the way in which the ordered series (23) was constructed that there are indeed several series of sections which may be chosen from those avaliable in the original set G, and the non-uniqueness of the ordered series of sets follows from the available non-unique choices of such series of sections. Therefore a transition from one ordering (23) to another is accomplished by a transition from one series of sections to another. But the latter transition can always be carried by successive exchange of one section for another. We have already examined such exchanges when we deduced the compatibility of the various forms of the causality conditions, and we have found that they always reduce to permutations in series of sets of regions of the type (23), which proves our contention.

We shall now stop our geometrical digression and we shall concern ourselves with applying the results which we have obtained to the explicit construction of the coefficients of the functions of the scattering matrix.

In order to do this we shall consider a set of regions G which turn out to be the arguments $x_1, \ldots, x_n$ of the operator functions S_n (the regions consist of one point each). According to the theorem we have just demonstrated, this set may be uniquely decomposed into a sum of m ($1 \leq m \leq n$). indecomposable sets

$$\{x_{\lambda_1}, \ldots, x_{\lambda_{\nu_1}}\}; \ \{x_{\lambda_{\nu_1+1}}, \ldots, x_{\lambda_{\nu_1+\nu_2}}\}, \ldots,$$
$$\{x_{\lambda_{\nu_1+\ldots+\nu_{n-1}+1}}, \ldots, x_{\lambda_n}\},$$

which may be (non-uniquely) ordered into a chronological series

$$\{x_{\lambda_1}, \ldots, x_{\lambda_{\nu_1}}\} \gtrsim \{x_{\lambda_{\nu_1+1}}, \ldots, x_{\lambda_{\nu_1+\nu_2}}\} \tag{24}$$
$$\gtrsim \ldots \gtrsim \{x_{\lambda_{\nu_1+\ldots+\nu_{m-1}+1}}, \ldots, x_{\lambda_n}\}.$$

Applying now the integral causality condition (7′a) to each section figuring in (24), we obtain the following representation for S_n

$$S_n(x_1, \ldots, x_n)$$
$$= S_{\nu_1}(x_{\lambda_1}, \ldots, x_{\lambda_{\nu_1}})\, S_{\nu_2}(x_{\lambda_{\nu_1+1}}, \ldots, x_{\lambda_{\nu_1+\nu_2}})$$
$$\times \ldots S_{\nu_m}(x_{\lambda_{\nu_1+\ldots+\nu_{m-1}+1}}, \ldots, x_{\lambda_n});$$
$$\nu_1 + \ldots + \nu_m = n. \tag{25}$$

Considering now the symmetry of S_n in all its arguments,[8] it is easily seen that (25) can be written in the form of the T-product

$$S_n(x_1, \ldots, x_n) \tag{26}$$
$$= T\,[S_{\nu_1}(x_{\lambda_1}, \ldots, x_{\lambda_{\nu_1}})\, S_{\nu_2}(x_{\lambda_{\nu_1+1}}, \ldots, x_{\lambda_{\nu_1+\nu_2}})$$
$$\times \ldots S_{\nu_m}(x_{\lambda_{\nu_1+\ldots+\nu_{m+1}+1}}, \ldots, x_{\lambda_n})],$$

where it should be kept in mind that chronological ordering is only carried out among distinct indecomposable groups of points. Representation (26) is valid if the set of arguments $\{x_1, \ldots, x_n\}$ may be decomposed into a sum of indecomposable sets $\{x_{\lambda_1}, \ldots, x_{\lambda_{\nu_1}}\}, \ldots, \{x_{\lambda_{\nu_1+\ldots+\nu m-1}+1},$ $\ldots, x_{\lambda_n}\}$. It is not necessary to discuss here orderings of the type appearing in (24) inasmuch as it will be considered in the evaluation of the T-product [the proof of the theorem on the ordering of sums of decomposable sets guarantees that the T-product (26), carries a well-defined meaning].

If in particular all the arguments $x_1, \ldots, x_n$ are pairwise unseparable, then (26) becomes

$$S_n = T\,[S_1(x_1) \ldots S_1(x_n)].$$

Furthermore if the principle of correspondence [Ref. 8, Eq. (4,23) is taken into account, then it is found that

$$S_n = i^n T\,[L(x_1) \ldots L(x_n)], \tag{27}$$

coinciding exactly with the particular solution given in Eq. (4.23) of Ref. 8, which thus appears as a general solution of S_n for pairwise unseparable arguments.

We have therefore expressed all the operator functions S_n in the form of chronological products of operator functions of indecomposable sets of points and a knowledge of these is now sufficient to completely determine the scattering matrix. But in local theory a set of points can only be nondecomposable if all these points coincide. Accordingly, the signfiicance of the operator function of indecomposable point sets appears to be that of quasi-local operators in the sense defined in Ref. 8, Sec. 2.

The causality condition no longer imposes any limitations on these quasi-local operators [apart from the commutation requirement on two such operators for space-like indecomposable sets of points, cf. Eq. (10)], we need therefore only concern ourselves with fulfilling the unitarity condition. It is easily seen that it [Ref. 8, Eq. (4.9)] defines uniquely their Hermitian parts, while their anti-Hermitian parts remain arbitrary. They must be specified during the formulation of a theory. Denoting them by $i\,\tilde{\mathrm{L}}_\nu(x_1, \ldots, x_\nu)$, where $\tilde{\mathrm{L}}_\nu$ is Hermitian (we depart here from the notation of Ref. 8, where quasi-local operators are denoted by Λ_ν), it may be said that (26) uniquely determines all the operator functions S_n by means of the following series of Hermitian quasi-local operators

$$\tilde{\mathrm{L}}_1(x) = L(x), \tag{28}$$

$$\tilde{\mathrm{L}}_2(x_1, x_2), \ldots, \tilde{\mathrm{L}}_n(x_1, \ldots, x_n), \ldots,$$

which must be supplied by a particular theory.

Such a formulation, however, suffers from the disadvantage that it does not assign unique expressions to the functions S_n over the whole range of the arguments. In order to avoid this, it is necessary to represent the value of S_n for an indecomposable group of arguments in the form of a sum of expressions, extending its value in a continuous fashion over a decomposable group of arguments, and certain new quasi-local operators.

In other words we must generalize the definition of the T-product to include the case of coinciding arguments whereby an intuitive chronological order loses significance. This may be done by starting from Wick's theorem; however, in order to give meaning to the products of singular functions with coinciding singularities arising in this case, it is necessary to have recourse to some limiting process (regularization). The result will depend of course on the form of the limiting process. The usual methods of regularization possess the advantage that when they are used to determine the value of the T-product for coinciding arguments, the operator functions S_n automatically satisfy the condition of unitarity (in local theory this is a natural consequence of continuity). The new quasi-local operators will then be anti-Hermitian and we shall denote them by $i\,\mathrm{L}_\nu(x_1, \ldots, x_\nu)$.

Expression (26) may then be written in the form

$$S_n(x_1, \ldots, x_n) \tag{29}$$
$$= \sum T\,[i\,\mathrm{L}_{\nu_1}(x_{\lambda_1}, \ldots, x_{\lambda_{\nu_1}}) \cdot \ldots \cdot i\,\mathrm{L}_{\nu_m}(\ldots, x_{\lambda_n})],$$

where the summation is to be carried out over all possible divisions of the set $\{x_1, \ldots, x_n\}$ into subsets

$$\{x_{\lambda_1}, \ldots, x_{\lambda_{\nu_1}}\}, \ldots, \{x_{\lambda_{\nu_1+\ldots+\nu_{m-1}+1}}, \ldots, x_{\lambda_n}\},$$

wherein the order of the factors appearing within the T-product is unimportant. Writing out the sum appearing in (29) in explicit form yields the expression

$$S_n(x_1, \ldots, x_n) = i^n T(L(x_1) \ldots L(x_n)) \quad (30)$$

$$+ \sum_{\substack{2 \leqslant m \leqslant n-1 \\ \Sigma\nu_i = n}} \frac{i^m}{m!} P(x_1, \ldots, x_{\nu_1}\ x_{\nu_1+1}, \ldots,$$

$$x_{\nu_1+\nu_2} | \ldots | x_{\nu_1+\ldots+\nu_{m-1}+1}, \ldots, x_n)$$

$$\times T(\mathrm{L}_{\nu_1}(x_1, \ldots, x_{\nu_1}) \ldots \mathrm{L}_{\nu_m}$$

$$\times (x_{\nu_1+\ldots+\nu_{m-1}+1}, \ldots, x_n)] + i\mathrm{L}_n(x_1, \ldots, x_n),$$

which coincides with the expression obtained in Ref. 8, Eq. (4.32). Thus the integral causality condition leads automatically (and without the need for any artificial considerations or conjectures) to the general expression (30) obtained by Bogoliubov, for the operator functions S_n.

Combining the whole series of quasi-local operators

$$\mathrm{L}_1(x) = L(x), \mathrm{L}_2(x_1, x_2), \ldots, \mathrm{L}_n(x_1, \ldots, x_n), \ldots, \quad (31)$$

which must be specified in order to determine (30), in the form of a single functional

$$L(x; g) = L(x) \quad (32)$$

$$+ \sum_{\nu=2}^{\infty} \frac{1}{\nu!} \int \mathrm{L}_\nu(x, x_1, \ldots, x_{\nu-1})$$

$$\times g(x_1) \ldots g(x_{\nu-1})\, dx_1 \ldots dx_{\nu-1},$$

we obtain [see Ref. 8, Eqs. (4.30) and (4.34)] the final closed-form expression

$$S(g) = T \exp\left\{i \int L(x; g)\, g(x)\, dx\right\} \quad (33)$$

for the matrix $S(g)$ as a function of the "generalized Lagrangian" $L(x;g)$, and coinciding with the expression obtained in Eq. (4.34), Ref. 8.

The author wishes to take this opportunity to express his deep gratitude to N. N. Bogoliubov for his constant interest in this work and for many valuable suggestions and demonstrations, and also to D. V. Shirkov and V. L. Bonch-Bruevich for fruitful discussions.

---

[1] S. Tomonaga, Progr. Theoret. Phys. **1**, 27 (1946); Koba, Tati, and Tomonaga, Progr. Theoret. Phys. **2**, 101 (1947).

[2] J. Schwinger, Phys. Rev. **74**, 1439 (1948); **76**, 790 (1949).

[3] F. J. Dyson, Phys. Rev. **75**, 486, 1736 (1949).

[4] G. Källen, Ark. for Fys. **2**, 187 (1950); 371 (1951).

[5] C. N. Yang and D. Feldman, Phys. Rev. **79**, 972 (1950).

[6] W. Heisenberg, Zeis. f. Phys. **120**, 513, 673 (1943).

[7] N. N. Bogoliubov, Dokl. Akad. Nauk (SSSR) **81**, 757, 1015 (1951); **82**, 217 (1952); Izv. Akad. Nauk (SSSR), seria fizhika (in press).

[8] N. N. Bogoliubov and D. V. Shirkov, Usp. Fiz. Nauk **55**, 151; **57**, 3 (1955).

[9] E. C. G. Stueckelberg, Phys. Rev. **81**, 130 (1951); Stueckelberg *et al.*, Helv. Phys. Acta **22**, 215 (1949); **24**, 317 (1951); **26**, 499 (1953).

Translated by M. A. Melkanoff
172

SOVIET PHYSICS JETP VOLUME 4, NUMBER 5 JUNE, 1957

Synchrotron Oscillations in Strong Focusing Accelerators. I. Linear Theory

L. L. GOL'DIN AND D. G. KOSHKAREV

(Submitted to JETP editor August 1, 1955)
J. Exptl. Theoret. Phys. (U.S.S.R.) 31, 803-814 (November, 1956)

The equations which describe synchrotron oscillations in strong focusing accelerators are examined, taking into account the relations between the field and the frequency. A general solution is found which describes the oscillations both in the adiabatic and in the critical region and the corresponding integrals of motion are obtained. It is shown that the motion in the critical region can be simply described by means of the "effective frequency" of the oscillations. The effect of fluctuations of the radio frequency, of the accelerating voltage and of the magnetic field is considered, along with the question of the influence of noises on the synchrotron oscillations. The transition through the critical point is studied. The computations are carried to the point of the derived formulas which determine the tolerances for the corresponding fluctuations.

1. EQUATIONS OF SYNCHROTRON OSCILLATIONS

ACCELERATED particles acquire energy under the action of a high-frequency electric field, the frequency of which is equal to, or exceeds by an integral number of times q, the frequency of circulation of the particles in the annular chamber of the accelerator. We shall call the quantity q the multiplicity of the radio frequency.

Let us examine the acceleration of particles which have a charge e. Let the maximum energy acquired per revolution of the particles be eu.

We designate as equilibrium particles those which maintain a constant phase shift relative to the accelerating electric field. Denoting the length of the trajectory of the particles by L and noting that the average field intensity (along the chamber) is equal to u/L, we find for the change in momentum of an equilibrium particle

$$dp/dt = eu \sin\phi/L, \tag{1}$$

where ϕ is the phase of acceleration of the equilibrium particle.

We characterize nonequilibrium particles by the deviation of their momentum and phase from the momentum and phase of equilibrium particles, and introduce the notation Π and φ for these deviations. Then, for small deviations,

$$d\Pi/dt = (eu\cos\phi/L)\,\varphi + (e\sin\phi/L)\,\Delta u/u, \tag{2}$$

where the term containing Δu takes into account the deviation of the amplitude of the accelerating voltage from the ideal value.

For the deviations in phase we have the obvious equality

$$d\varphi/dt = \Delta\omega_p - q\Delta\omega, \tag{3}$$

where $\Delta\omega_p$ is the radiofrequency deviation and $\Delta\omega$ is the deviation of the frequency of revolution of the particles from the ideal value.

We introduce the coefficient α which takes into account the lengthening of the trajectory which is related to the deviation of the momentum,

$$\Delta L/L = \alpha\Pi/p. \tag{4}$$

It is not difficult to convince oneself that

$$\Delta\omega/\omega = [(E_0/E)^2 - \alpha]\,(\Pi/p) + \alpha\Delta H/H, \tag{5}$$

where E is the total relativistic energy of the particles, E_0 is the rest energy, H is the magnetic field intensity and

$$\omega = (2\pi c/L)\ pc/E. \tag{6}$$

From Eqs. (2), (3), (5) and (6) we find

$$\begin{aligned} \frac{d}{dt}\left[\frac{E}{(E_0/E)^2-\alpha}\frac{d\varphi}{dt}\right] + \frac{2\pi q c^2 eu\cos\phi}{L^2}\varphi &= \frac{d}{dt}\left[\frac{E}{(E_0/E)^2-\alpha}\Delta\omega_p\right] \\ &- \frac{2\pi}{L^2} q c^2 eu \sin\phi\,\frac{\Delta u}{u} \\ &- \frac{2\pi q\alpha c}{L}\frac{d}{dt}\left[\frac{(E^2-E_0^2)^{1/2}}{(E_0/E)^2-\alpha}\frac{\Delta H}{H}\right]. \end{aligned} \tag{7}$$

In studying Eq. (7) one should keep in mind that $\Delta\omega_p$ and ΔH, generally speaking, are not independent quantities. If the frequency of the accelerating field follows behind the magnetic field, the deviations $\Delta\omega_p$ are partially related to inaccuracies in the electronics and partially caused by oscillations of the magnetic field. It is natural to examine these latter together with the term which depends on $\Delta H/H$. Let the system of coupling the frequency with the field be characterized by the delay τ, so that instead of the ideal rule

$$\omega_p = (2\pi cq/L)\, eRH\,(E_0^2 + e^2R^2H^2)^{-1/2}, \tag{8}$$

the rule:

$$\Delta\omega_p + \tau d\Delta\omega_p/dt = (2\pi c^2 q/L)(pE_0^2/E^3)\,\Delta H/H \tag{9}$$

occurs. The letter R denotes the radius of curvature of an equilibriun particle in the field H.

We will be interested chiefly in harmonic oscillations of the type $\Delta H = H_w \sin wt$. From Eq. (9) we find

$$\Delta\omega_p = \frac{2\pi c^2 qpE_0^2}{LE^3}\,\frac{H_w}{H}\,\frac{\sin wt - w\tau\cos wt}{1 + w^2\tau^2}. \tag{10}$$

Let us substitute this expression in Eq. (7) and combine it with the term which depends on $\Delta H/H$, keeping the notation $\Delta\omega_p$ for deviations which are associated only with the electronics. We further note that oscillations of the magnetic field are excited by oscillations of the voltage V which supplies the magnet. Disregarding the effective resistance of the magnet windings in comparison with their inductive reactance, we find

$$H_w/H = (\dot{H}/wH)\,V_w/V \tag{11}$$

$$= (eu\sin\phi/Lwp)\,V_w/V.$$

Then Eq. (7) assumes the form:

$$\frac{1}{E}\left[\frac{E_0^2}{E^2} - \alpha\right]\frac{d}{dt}\left[\frac{E}{(E_0/E)^2 - \alpha}\,\frac{d\varphi}{dt}\right] + \Omega_t^2\varphi \tag{12}$$

$$= \frac{1}{E}\left[\frac{E_0^2}{E^2} - \alpha\right]\frac{d}{dt}\left[\frac{E}{(E_0/E)^2 - \alpha}\,\Delta\omega_p\right]$$

$$+ \frac{\Omega_t^2\operatorname{tg}\phi}{w\,(1 + w^2\tau^2)}\,\frac{d}{dt}\Big[\sin wt$$

$$- \frac{w\tau}{(E_0/E)^2 - \alpha}\,\frac{E_0^2}{E^2}\left(\cos wt + \alpha w\tau\,\frac{E^2}{E_0^2}\sin wt\right)\Big]\frac{V_w}{V}$$

$$- \Omega_t^2\operatorname{tg}\phi\,\frac{\Delta u}{u},$$

where

$$\Omega_t^2 = (2\pi qc^2 eu\cos\phi/L^2E)\,[(E_0/E)^2 - \alpha]. \tag{13}$$

Let us introduce in place of the time the independent variable x, defined by the equation

$$x = pc/E_0. \tag{14}$$

We assume that the momentum (and the magnetic field) increases linearly with time, so that the right-hand side of Eq. (1) is constant. From Eq. (1) we have

$$dx/dt = ceu\sin\phi/E_0L. \tag{15}$$

We also introduce the quantity

$$a^2 = (1 - \alpha)/\alpha \approx 1/\alpha \tag{16}$$

and the function

$$f(x) = [1 - (x/a)^2]\,(1 + x^2)^{-3/2}a^2\alpha \tag{17}$$

$$\approx [1 - (x/a)^2]\,(1 + x^2)^{-3/2}.$$

(In strong focusing accelerators $\alpha \ll 1$.) In the new variables, Eq. (12) has the form:

$$f(x)\,\frac{d}{dx}\left[\frac{1}{f(x)}\,\frac{d\varphi}{dx}\right] + \Omega_x^2\varphi \tag{18}$$

$$= \Omega_x^2\operatorname{tg}\phi\,\frac{d}{dx}\left[\frac{x}{(1 + x^2)^{1/2}f(x)}\,\frac{\Delta\omega_p}{\omega_p}\right]$$

$$- \Omega_x^2\operatorname{tg}\phi\,\frac{\Delta u}{u} + \frac{\Omega_x^2\operatorname{tg}\phi}{w_x\,(1 + w^2\tau^2)}\,\frac{d}{dx}\Big[\sin wx$$

$$- \frac{w\tau\cos wx}{(1 + x^2)^{3/2}f(x)}\Big]\frac{V_w}{V}.$$

In writing Eq. (18) it was taken into account that in practically-important cases $\alpha\Omega_0^2\tau^2 \ll 1$. If this is not so, then to $\cos wx$ the term $(E/E_0)^2 \times \alpha w\tau\sin wx$ must be added. The following notation is introduced in Eq. (18):

$$\Omega_x = \Omega_t\,dt/dx = \Omega_0\,|f(x)|^{1/2}, \tag{19}$$

$$\Omega_0^2 = 2\pi qE_0\operatorname{ctg}\phi/eu\sin\phi.$$

Ω_0 is a dimensionless quantity numerically equal to the frequency in x, for $x = 0$.

The equation for free oscillations is obtained from Eq. (18) if the right side is equated to zero:

$$f(x)\,\frac{d}{dx}\left[\frac{1}{f(x)}\,\frac{d\varphi}{dx}\right] + \Omega_x^2\varphi = 0. \tag{20}$$

Equation (18) has a regular singular point for

$x = a$, when $f(x)$ becomes zero. After the singular point $f(x)$ changes sign and the motion remains stable only in the case that Ω_x^2, proportional to $f(x)$, does not change sign; for this it is necessary to change the phase of acceleration from ϕ to $\pi - \phi$.

In the transition through the critical point it is possible to define positive deviation of φ in different ways. It is natural to define it so that during this transition φ be continuous. The momentum Π in the critical point likewise remains continuous. These two conditions determine the transition through the critical point, where $d\varphi/dx$ changes sign.

2. FREE SYNCHROTRON OSCILLATIONS

We introduce new variables

$$v = \varphi\Omega_x^{-1/2}, \quad \psi = \int_a^x \Omega_x dx \quad ; \qquad (21)$$

ψ has the obvious sense of the phase of oscillation. In these variables Eq. (20) acquires the form:

$$(d^2v/d\psi^2) + v\,[1 + f''_x/4f^2\Omega_0^2 \qquad (22)$$

$$- 7\,(f'_x)^2/16\,|\,f\,|^3\Omega_0^2] = 0.$$

In cases of practical interest, Ω_0 is a very large quantity; $\Omega_0 \gg 1$, so that the terms which are added to unity in Eq. (22) are essential only in the vicinity of the point $x = a$, where $f(x)$ becomes zero. In this region they can be expanded in a series, from which we retain only the principal term. Although such a representation becomes inadequate even for $|x - a| \approx 0.4\,a$, the entire correction to unity becomes so small here that it does not play any role. In the vicinity of the point a

$$f(x) \approx 2a^{-3}\,|\,1 - x/a\,|. \qquad (23)$$

Eq. (22) assumes the form

$$(d^2v/d\psi^2) + [1 - 7/36\psi^2]\,v = 0. \qquad (24)$$

The solution of Eq. (24) is:

$$v(\psi) = \psi^{1/2}\,[A_2 J_{2/3}(\psi) + A_1 J_{-2/3}(\psi)], \qquad (25)$$

where $J_{2/3}$ and $J_{-2/3}$ are Bessel functions. Reverting to the variable φ we find:

$$\varphi = (\Omega_x/\Omega_0)^{1/2}\psi^{1/2}\,[C_1 J_{-2/3}(\psi) + C_2 J_{2/3}(\psi)]. \qquad (26)$$

The signs in front of C_1 and C_2 do not depend on which side of the critical point we are on. This follows from the continuity of phase and momentum in the critical point. We note that Bodenstedt[2], who was studying the transition through the critical point on a mechanical model, arrived at an incorrect conclusion concerning a change in sign of C_2 (see Fig. 10 in Ref. 2), which is explained by the properties of his model. For large arguments (the adiabatic region) one can use the asymptotic representation of the Bessel functions:

$$\varphi = (2/\pi)^{1/2}\,(\Omega_x/\Omega_0)^{1/2}\,[C_1 \cos(\psi + \pi/12) \qquad (27)$$

$$+ C_2 \sin(\psi - \pi/12)].$$

For a sufficiently small argument ($|x - a| \ll 0.4a$), one can express ψ by means of Eqs. (19), (21) and (23) through the deviation from the critical point $\xi = |x - a|$:

$$\varphi = 2^{1/4}a^{-1}\,\Omega_{\text{eff}}^{3/4}\,\xi\,[C_1 J_{-2/3}(\Omega_{\text{eff}}^{3/2}\,\xi^{3/2}) \qquad (28)$$

$$+ C_2 J_{2/3}(\Omega_{\text{eff}}^{3/2}\,\xi^{3/2})],$$

$$\Omega_{\text{eff}} = 2\cdot 3^{-2/3}\Omega_0^{2/3}a^{-4/3} \approx \Omega_0^{2/3}a^{-4/3}. \qquad (29)$$

Equations of the type of Eq. (28) we obtained by Kolomenskii and Sabsovich[4] and by Johnson[5].

To facilitate the transition from one region to the other, the constants in Eqs. (26)-(28) were chosen so that C_1 and C_2 agree in these equations and thus are integrals of motion.

Let us examine in greater detail Eq. (27) which describes the phase oscillations in the adiabatic region. The instantaneous frequency of the synchrotron oscillations in x is equal to $d\psi/dx = \Omega_x$. The amplitude of the oscillations decreases on approach to the critical point and increases on going away from it, varying as $(\Omega/\Omega_0)^{1/2} = f^{1/4}$. It reaches a maximum of $0.6\,a^{-3/4}(C_1^2 + C_2^2 - C_1C_2)$ when $x = (3a^2 + 2)^{1/2}$.

Equations (12) and (18) are obtained from Eqs. (2), (3) and (5) through elimination of the momentum Π. With the same success it would be possible to eliminate the phase from them and to obtain the equation for oscillations in momentum. Instead of this we indicate the conversion to momentum directly in the solution. Converting to the variable x in Eq. (2) we obtain

$$\Pi = \frac{E_0}{c}\,\text{ctg}\,\phi \int_{x_0}^{x} \varphi\,dx + \frac{E_0}{c}\int_{x_0}^{x} \frac{\Delta u}{u}\,dx. \qquad (30)$$

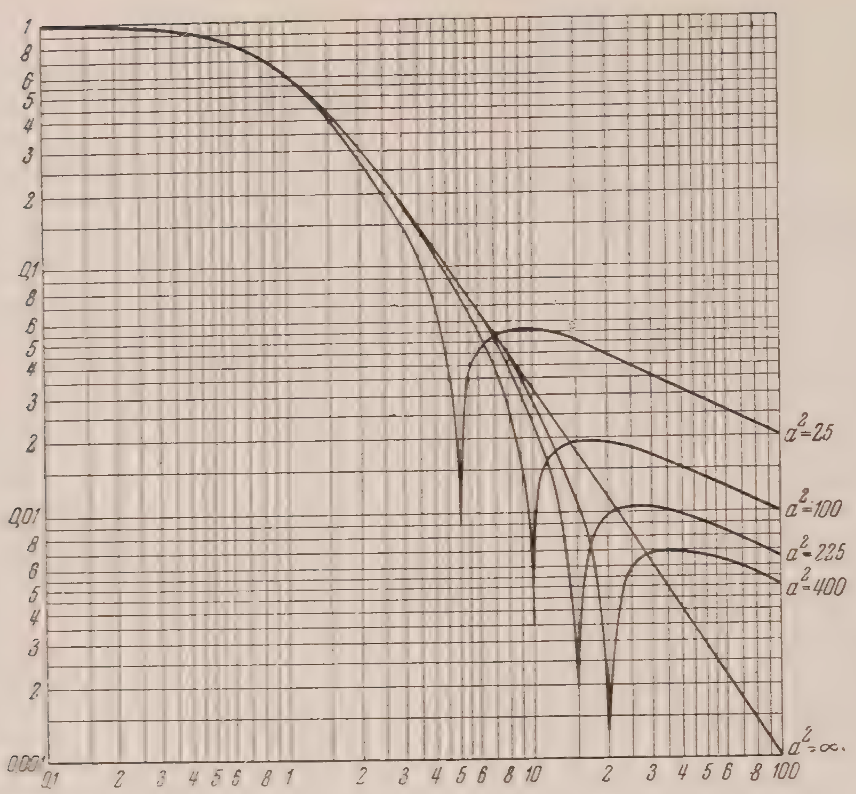

FIG. 1. Graph of the function $\sqrt{f(x)}$.

It follows from Eqs. (27) and (30) that the amplitudes of the oscillations in momentum and phase in the adiabatic region are connected by the relation

$$A_\Pi / A_\varphi = E_0 \operatorname{ctg} \phi / c\Omega_x, \tag{31}$$

such that in this region

$$\Pi(x) = \left(\frac{2}{\pi}\right)^{1/2} \frac{E_0 \operatorname{ctg} \phi}{c\Omega_0} \left(\frac{\Omega_0}{\Omega_x}\right)^{1/2} \left[C_1 \sin\left(\psi + \frac{\pi}{12}\right) - C_2 \cos\left(\psi - \frac{\pi}{12}\right)\right]. \tag{32}$$

The function Ω_x/Ω_0, which enters in Eqs. (27) and (32) is depicted in Fig. 1. For the critical region we obtain:

$$\Pi(\xi) = \left(\frac{2}{3}\right)^{1/2} \frac{E_0 \operatorname{ctg} \phi}{c\Omega_0^{1/2}} \xi^{1/2} \left[C_1 J_{1/3}(\Omega_{\mathrm{eff}}^{3/2} \xi^{3/2}) - C_2 J_{-1/3}(\Omega_{\mathrm{eff}}^{3/2} \xi^{3/2})\right]. \tag{33}$$

From Eq. (32) it is seen that the amplitude of the oscillations in momentum increases on approaching the critical region. Further on, close to $x = (3a^2 + 2)^{1/4}$, the amplitude falls, then rises again roughly speaking as $x^{1/4}$. We note that for the point $x = a$, there follows from Eq. (33):

$$\Pi(a) \approx 0.8 E_0 C_2 \operatorname{ctg} \phi / c\, (\Omega_0 \Omega_{\mathrm{eff}})^{1/2}. \tag{34}$$

Comparison of Eqs. (32) and (34) shows that the oscillations in the critical region have the "effective frequency" Ω_{eff}, specified by Eq. (29). Comparison of Eqs. (27) and (28) leads to practically the same value for Ω_{eff}. This effective frequency enters in almost all tolerances in the critical region.

Here, the calculations lead to the following results, which are unexpected at first glance. In the calculation of tolerances connected with forced oscillations in the critical region, one can assume that, in the region indicated, regular harmonic oscillations occur with constant amplitude and constant frequency numerically equal to the "effective frequency." Although the real picture is essentially more complicated, such a calculation leads to correct answers (within an accuracy of the order of 20%).

Of interest for a beam of particles is the value of the mean square deviation in phase and momentum which is especially essential for an examination of noise modulations (see Sec. 6).

We write Eq. (27) in the form

$$\varphi = a_1 \cos\psi + b_1 \sin\psi, \tag{35}$$

$$a_1 = \left(\frac{2}{\pi}\right)^{1/2}\left(\frac{\Omega}{\Omega_0}\right)^{1/2}\left[C_1 \cos\frac{\pi}{12} - C_2 \sin\frac{\pi}{12}\right], \tag{36}$$
$$b_1 = \left(\frac{2}{\pi}\right)^{1/2}\left(\frac{\Omega}{\Omega_0}\right)^{1/2}\left[C_2 \cos\frac{\pi}{12} - C_1 \sin\frac{\pi}{12}\right].$$

For a beam of particles one can write

$$a_1 = A\cos\chi; \quad b_1 = A\sin\chi, \tag{37}$$

where A and χ are an arbitrary amplitude and phase. Averaging over A and χ we find:

$$\overline{\varphi^2} = {}^1/_2\overline{A^2} = {}^1/_2\,(\overline{a_1^2} + \overline{b_1^2}) \tag{38}$$
$$= (\Omega/\pi\Omega_0)\,(\overline{C_1^2} + \overline{C_2^2} - \overline{C_1C_2}).$$

From Eq. (36) it is easy to obtain $\overline{C_1^2} = \overline{C_2^2} = \overline{2C_1C_2}$, such that

$$\overline{\varphi^2} = (3\Omega_x/2\pi\Omega_0)\,\overline{C_2^2}. \tag{39}$$

Comparing the mean square deviations of the momentum in the critical point and in the adiabatic region, we find

$$\overline{\Pi^2_{\mathrm{cr}}}/\overline{\Pi^2_{\mathrm{ad}}} \approx 1.2\,(\Omega_x/\Omega_{\mathrm{eff}}). \tag{40}$$

3. ELECTROTECHNICAL AND RADIOTECHNICAL TOLERANCES. (NONRESONANCE CASE)

In estimating tolerances, oscillations of the parameters which occur with a frequency close to the instantaneous frequency of the synchrotron oscillations are especially effective. It is natural to examine such perturbations separately. Faster oscillations present no danger, since they are rapidly averaged out. Let us consider abrupt changes in ω_p (a step function) and slow variations (in comparison with the frequency of the free oscillations) in $\Delta\omega_p$, Δu and ΔV.

a) *Tolerances associated with jumps in* ω_p.

In order to find the swing of the oscillations associated with jumps in ω_p, we integrate Eq. (18) over the period of a jump. Considering that before the jump $\varphi = \varphi' = 0$, we get

$$\varphi' = \Omega_0^2 x\,(1 + x^2)^{-1/2}\Delta\omega_p \operatorname{tg}\phi/\omega_p. \tag{41}$$

Thus, a jump in ω_p gives rise (in the adiabatic region) to the appearance of oscillations with amplitude

$$A_\varphi = (\Omega_0^2/\Omega_x)\,x\,(1 + x^2)^{-1/2}\operatorname{tg}\phi\cdot\Delta\omega_p/\omega_p. \tag{42}$$

In Eq. (42) the variable x pertains to the moment of the jump. Furthermore, this amplitude will vary according to the general formula, i.e., as $f^{1/4}$ The effect of the jumps in ω_p becomes all the stronger on approaching the critical region. It is not difficult to find an estimate in the immediate vicinity of the critical point, where the Bessel functions are approximated closely by the first term of a series expansion. It is just as easy in this case to convince onself that

$$\Delta C_2 \approx 0{,}6\cdot a^2 \operatorname{tg}\phi\,\Omega_0^{3/2}\Omega_{\mathrm{eff}}^{-1}\,\xi^{-1}\Delta\omega_p/\omega_p, \tag{43}$$

so that the tolerance in the magnitude of the jump becomes very inflexible. One should have in mind, however, that in this case changes in ω_p, which are rapid in comparison with changes in $1/\xi$, should qualify as jumps, so that the rigid restrictions apply only to extremely sharp changes in ω_p, which are not very substantial in practice. By means of Eq. (31), we obtain the amplitudeof the oscillations in momentum excited by a jump in ω_p:

$$A_\Pi = (E_0/c)\,(\Omega_0/\Omega_x)^2\,x\,(1 + x^2)^{-1/2}\Delta\omega_p/\omega_p. \tag{44}$$

b) *Tolerances associated with slow variation of* $\Delta\omega_p$, Δu, ΔV.

The effect of smooth (in comparison with the free oscillations) changes in $\Delta\omega_p$, $\Delta u/u$, $\Delta V/V$ is easy to take into account, considering the right-hand side of Eq. (18) constant and finding the shift of the equilibrium point of the oscillations.

$$\varphi = \operatorname{tg}\phi\,\frac{d}{dx}\left[\frac{x}{(1 + x^2)^{1/2}}\,\frac{\Omega_0^2}{\Omega_x^2}\,\frac{\Delta\omega_p}{\omega_p}\right] - \operatorname{tg}\phi\,\frac{\Delta u}{u} \tag{45}$$
$$+ \operatorname{tg}\phi\,\frac{1}{w\,(1 + w^2\tau^2)}\,\frac{d}{dx}\left[\sin wx - \frac{w\tau\cos wx}{(1 + x^2)^{3/2}}\,\frac{\Omega_0^2}{\Omega_x^2}\right]\frac{V_w}{V}.$$

For the maximum deviation of the momentum we find:

$$\Pi = \frac{E_0}{c}\cdot\frac{x}{(1 + x^2)^{1/2}}\,\frac{\Omega_0^2}{\Omega_x^2}\,\frac{\Delta\omega_p}{\omega_p} - \frac{E_0}{c}\,\frac{w}{\Omega_x^2}\,\frac{u_w}{u} \tag{46}$$
$$+ \frac{E_0}{c}\,\frac{1}{w\,(1 + w^2\tau^2)}\left[\sin wx - \frac{w\tau\cos wx}{(1 + x^2)^{3/2}}\,\frac{\Omega_0^2}{\Omega_x^2}\right]\frac{V_w}{V}.$$

Strictly speaking, Eqs. (45) and (46) are applied only for the adiabatic region. As was pointed out above, however, in the critical region one can simply replace Ω_x by Ω_{eff}, which is corroborated by accurate calculations. Then, denoting the allowable deviation in phase and in momentum by $\Delta\varphi$ and $\Delta\Pi$, we find for the critical region:

$$\Delta\omega_p / \omega_p \tag{47}$$

$$= (\Delta\Pi / p)\,[eu \sin\phi / 2\pi q E_0 \operatorname{ctg}\phi]^{1/3}\,[E_0 / E_{\text{cr}}]^{5/3},$$

$$\Delta\omega_p / \omega_p \tag{48}$$

$$= (\Delta\varphi / \operatorname{tg}\phi)\,[eu \sin\phi / 2\pi q E_0 \operatorname{ctg}\phi]^{2/3}\,[E_0 / E_{\text{cr}}]^{4/3}.$$

4. THE TRANSITION THROUGH THE CRITICAL POINT

As was pointed out above, the transition through the critical point requires a change in the phase of the acceleration from ϕ to $\pi - \phi$. This switchover cannot be realized precisely at the moment when an equilibrium particle reaches the critical point; there must always be some discrepancies, which we shall characterize by an error τ_1 in the switchover time. During this time Ω_x^2 in Eq. (20) is negative, which corresponds to defocusing of the particles. We shall assume, for definiteness, that the phase of the acceleration is switched over later than it ordinarily should be. (By virtue of the symmetry of the equations about the critical point, the answer does not depend on this assumption.) Then the equation of the phase oscillations in this region takes the form:

$$\varphi = (2^{1/4} / a)\,\Omega_{\text{eff}}^{3/4}\,\xi\,[C_1 i^{2/3} J_{-2/3}(i\Omega_{\text{eff}}^{3/2}\,\xi^{3/2}) \tag{49}$$

$$+ C_2 i^{-2/3} J_{2/3}(i\Omega_{\text{eff}}^{3/2}\,\xi^{3/2})],$$

where C_1 and C_2 have those values which they had up to the critical point. In the moment $\Delta\xi$ the solution Eq. (49) goes over to the solution Eq. (28) with different constants. Having denoted the corrections to the corresponding coefficients by ΔC_1 and ΔC_2, we find for small values of $\Delta\xi$:

$$\Delta C_2 / C_1 \approx 2\Omega_{\text{eff}}\,\Delta\xi, \tag{50}$$

$$\Delta C_1 / C_1 \approx -0.8 \cdot \Omega_{\text{eff}}^3\,(\Delta\xi)^3.$$

It is natural to require that $\Delta C_2 / C_1$ and $\Delta C_1 / C_1$ be small, let us say about 0.1. Then

$$\Delta x = 5 \cdot 10^{-2} \cdot \Omega_{\text{eff}}^{-1} \tag{51}$$

and for the error in time (in seconds)

$$\tau_1 = 5 \cdot 10^{-2}\,[eu \sin\phi / 2\pi q E_0 \operatorname{ctg}\phi]^{1/3} \tag{52}$$

$$\times (E_{\text{cr}} / E_0)^{4/3} E_0 L / ceu \sin\phi.$$

Let us now estimate the disturbances which originate from the phase of the accelerating voltage not switching over instantaneously. We assume that the accelerating voltage is at first switched off and is switched on after the time τ_2, already in the second phase. During the time τ_2, the particles travel by inertia, not being accelerated. It would appear natural to assume, in this case, that the coordinate x does not vary. The calculations turn out simpler, however, if we assume x to vary according to the old rule. Hereupon, the continuous increase of the magnetic field and the change of frequency of the accelerating voltage will be properly taken into account. We assume for definiteness that the switching off of the accelerating voltage occurred after the transition through the critical point. The equation of motion can be obtained by Eq. (18) if we take $\Delta u/u = -1$ and cancel the term $\Omega_x^2 \varphi$.

Then

$$\frac{d}{dx}\left[\frac{1}{f(x)}\frac{d\varphi}{dx}\right] = \Omega_0^2 \operatorname{tg}\phi. \tag{53}$$

Integrating Eq. (53), having used the representation of Eq. (23) for $f(x)$, we find:

$$\varphi = \varphi_0 + {}^1/_2\varphi_0'\,(\xi^2 - \xi_0^2)\,\xi_0^{-1} \tag{54}$$

$$+ 2 \operatorname{tg}\phi\,\Omega_0^2 a^{-4}\,[({}^1/_3\xi - {}^1/_2\xi_0)\,\xi^2 + {}^1/_6\xi_0^3],$$

$$\varphi' = \xi\xi_0^{-1}\varphi_0' + 2 \operatorname{tg}\phi\,\Omega_0^2 a^{-4}\,[\xi - \xi_0]\,\xi,$$

where ξ_0 is the moment of switching off the accelerating voltage and ξ is the moment of switching it on. At the point ξ this solution must be connected with the solution Eq. (28), which also determines the changes in the constants C_1 and C_2. For small values of $\Delta\xi = \Delta x$, neglecting cubic terms in comparison with linear terms, we obtain:

$$\Delta C_1 \approx 0, \quad \Delta C_2 \approx \Omega_{\text{eff}}\,C_1 \Delta x \tag{55}$$

$$+ 1\;3 \cdot \Omega_0^{5/6} a^{-2/3} \operatorname{tg}\phi\,\Delta x.$$

Knowing ΔC_1 and ΔC_2, it is easy to determine the increase in amplitude of the oscillations at the most dangerous point $x = (3a^2 + 2)^{1/2}$.

Inasmuch as a deviation of the momentum is effective precisely in the critical region, where the natural oscillations reach a maximum, it is useful to calculate, by means of Eq. (55), the shift in the momentum common for all particles: $\Delta\Pi/_p = \Delta x/a$, which gives

$$\tau_2 = (\Delta\Pi/p)(E_{\text{cr}}/E_0)E_0L/ceu\sin\phi. \qquad (56)$$

Kolomenskii and Sabsovich[4] and apparently, Johnson[5], also dealt with questions related to the transition through the critcial point.

5. RESONANCE

The frequency of the generator, the magnitude of the accelerating voltage and the voltage on the magnet can oscillate with a frequency equal to the instantaneous frequency of the phase oscillations. In this case a resonance arises, which leads to a strong wave of oscillations.

Accordingly, we shall examine resonance harmonics of the right-hand part. By virtue of the incoherence of the perturbations, one can examine the terms which enter into the right-hand part separately. In the adiabatic approximation we write Eq. (18) in the form

$$(d^2\varphi/dx^2) + \Omega_x^2\varphi = d\cos(wx + \alpha), \qquad (57)$$

where α is the phase of the perturbation. The solution of Eq. (57) without the right-hand part can be represented in the form

$$\varphi = \varphi_1 e^{i\psi} + \overset{*}{\varphi}_1 e^{-i\psi}. \qquad (58)$$

We impose on φ_1 and φ_1^* the supplementary condition:

$$\varphi_1' e^{i\psi} + \overset{*}{\varphi}{}_1' e^{-i\psi} = 0. \qquad (59)$$

Having used Eqs. (58) and (59), we obtain for the principal part of φ_1

$$\varphi_1 = \frac{d}{4i\Omega_x}\int_{x_0}^{x} e^{i(wx-\psi+\alpha)}dx. \qquad (60)$$

Expanding the frequency Ω_x in a series at the resonance point, we obtain

$$\Omega_x = w + \Omega'_{\text{res}}(x - x_{\text{res}}) + \ldots \qquad (61)$$

Then

$$\varphi_1 = \frac{de^{i\beta}}{4\Omega_x}\int_{x_0-x_{\text{pe3}}}^{x-x_{\text{pe3}}} \exp\{-i\Omega'_{\text{pe3}}z^2/2\}\,dz. \qquad (62)$$

Taking $x - x_{\text{res}} = \infty$, $x_0 - x_{\text{res}} = -\infty$ and integrating Eq. (62) we obtain for φ:

$$\varphi = 2\,\text{Re}\,\varphi_1 e^{i\psi} = (d/\Omega_x)[2\pi/\Omega'_{\text{pe3}}]^{1/2}\cos(\psi + \gamma). \qquad (63)$$

Averaging over the arbitrary phase γ, we find for the square of the phase amplitude

$$\overline{\varphi^2} = \pi d^2/2\Omega_{\text{res}}^2\Omega'_{\text{res}} = \pi d^2/\Omega_{\text{res}}\Omega_0^2 f'_{\text{res}}. \qquad (64)$$

Comparing Eqs. (57) and (18) and taking into account the change in the amplitude of the oscillations with frequency, we find finally:

$$\overline{\Delta\varphi^2} = \pi\,\text{tg}^2\phi\,\frac{\Omega_x}{|f'_{\text{res}}|}\left[\frac{\Omega_0^2x^2}{1+x^2}\right]_{\text{res}}\left(\frac{\omega_\Omega}{\omega_{\text{res}}}\right)^2, \qquad (65)$$

$$\overline{\Delta\varphi^2} = \pi\,\text{tg}^2\phi\,\frac{\Omega_x}{|f'_{\text{res}}|}\,\frac{\Omega_{\text{res}}^2}{\Omega_0^2}\left(\frac{u_\Omega}{u}\right)^2,$$

$$\overline{\Delta\varphi^2} = \pi\,\text{tg}^2\phi\,\frac{\Omega_x}{|f'_{\text{res}}|}\,\frac{\Omega_{\text{res}}^2}{\Omega_0^2(1+\Omega_{\text{res}}^2\tau^2)^2} \times \left[1 + \frac{\Omega_0^4\tau^2}{(1+x^2)_{\text{res}}^3\Omega_{\text{res}}^2}\right]\left(\frac{V_\Omega}{V}\right)^2$$

Here, ω_Ω, u_Ω, V_Ω are the amplitudes of the perturbations with frequency Ω;

$$\Delta\omega = \sum_0^\infty \omega_\Omega\cos(\Omega x + \alpha).$$

This result is found to be in agreement with the result of Blachman[1]. Eqs. (65) give the increase of the mean square amplitude of the phase oscillations at any moment, if by Ω_x we understand the instantaneous frequency of the oscillations and by Ω_{res} the resonance frequency, whose effect we are studying. Equations (65) do not have any singularities in the neighborhood of the critical point, which is natural, since on approaching the critical point the resonance is passed all the more rapidly and does not have time to set synchrotron oscillations going to any appreciable extent. Therefore, the critical region does not require special consideration. One must have in mind that the resonance frequencies are included between Ω_0 and Ω_{eff}. At the point where the rate of change of frequency becomes zero $[x = (3a^2 + 2)^{1/2}]$, the next term in the expansion must be taken into account. In this case:

$$\overline{\Delta\varphi^2} = 4{,}4\,\text{tg}^2\phi\,\Omega_0^{10/3}a^{7/3}(\omega_\Omega/\omega)^2, \qquad (66)$$

$$\overline{\Delta\varphi^2} = 1{,}7\,\text{tg}^2\phi\,\Omega_0^{4/3}a^{-2/3}(u_\Omega/u)^2,$$

$$\overline{\Delta\varphi^2} = 1{,}7\,\text{tg}^2\phi\,\Omega_0^{4/3}a^{-2/3}(V_\Omega/V)^2.$$

The oscillations in momentum which reach a maximum in the critical point merit special examination. Variation of the momentum is expressed by Eq. (34), taking into account Eqs. (39) and (65).

6. NOISE EXCITATION OF SYNCHROTRON OSCILLATIONS

The problem of noise excitation of ocsillations without account of adiabatic damping was solved by Blachman, who examined Eq. (12) in the adiabàtic approximation, i.e., in the form

$$(d\varphi^2 / dt^2) + \Omega_t^2\varphi = F(t), \tag{67}$$

where $F(t)$ is an arbitrary noise perturbation with spectral intensity Φ (calculated for a band-width of 1 cycle). According To Ref. 1, the mean square deviation of the phase amplitude is equal to

$$\overline{\varphi^2} = {}^1/_2 \int_{t_0}^{t} (\Phi / \Omega_t^2)\, dt. \tag{68}$$

Comparing Eq. (12) with Eq. (67) and transforming to the variable x, we obtainfor the noise modulation of the frequency with spectral intensity ν (cycles^2/cycle)

$$\overline{\varphi^2} = (2\pi^2 E_0 L / ceu \sin\phi) \int_{x_0}^{x} \nu dx. \tag{69}$$

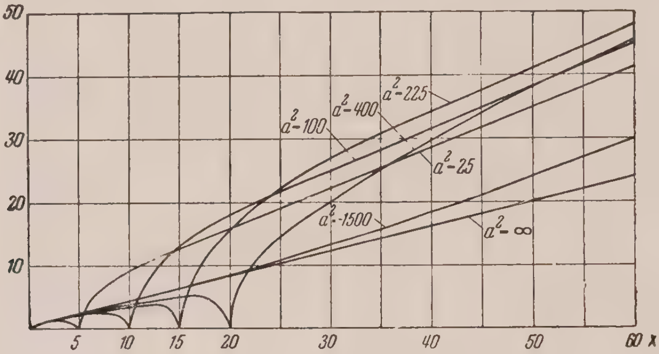

FIG. 2. Graph of the function $f^{1/2}(x)\int_0^x f^{-1/2}(x)\,dx$.

For the noise modulation of the amplitude of the accelerating voltage $\Delta u/u$ with spectral intensity η (cycle^{-1})

$$\overline{\varphi^2} = {}^1/_2 \operatorname{tg}^2\phi\, (ceu \sin\phi / E_0 L) \int_{x_0}^{x} \eta \Omega_x^2 dx \tag{70}$$

and for the noise modulation of the voltage on the magnet $\Delta V/V$ with spectral intensity μ (cycle^{-1})

$$\overline{\varphi^2} = {}^1/_2 \operatorname{tg}^2\phi \frac{ceu \sin\phi}{E_0 L} \times \int_{x_0}^{x} \left[\Omega_x^2 + \frac{\Omega_0^4 \tau^2}{(1+x^2)^3}\right] \frac{\mu dx}{(1+\Omega^2\tau^2)^2}. \tag{71}$$

We now find the expression for $\overline{\varphi^2}$ accounting for the adiabatic change of amplitude of the oscillations. From the relation Eq. (27) for the mean square amplitude we obtain the equation

$$d\overline{\varphi^2} / dx = \overline{\varphi^2} f' / 2f. \tag{72}$$

On the other hand, differentiating Eq. (69), we obtain for the increase in amplitude on account of the noise modulation of the frequency

$$d\overline{\varphi^2} / dx = 2\pi^2 (E_0 L / ceu \sin\phi)\, \nu. \tag{73}$$

On account of the independence of the processes of adiabatic contraction and of noise excitation, there follows from Eqs. (72) and (73):

$$f^{1/2}(x) \frac{d}{dx} [f^{-1/2}(x)\, \overline{\varphi^2}] = 2\pi^2 \frac{E_0 L}{ceu \sin\phi} \nu. \tag{74}$$

Integrating Eq. (74), we obtain:

$$\overline{\varphi_\nu^2} = 2\pi^2 \nu \frac{E_0 L}{ceu \sin\phi} f^{1/2}(x) \int_{x_0}^{x} f^{-1/2}(x)\, dx. \tag{75}$$

Analogously, for the noise modulation of the amplitude of the accelerating voltage

$$\overline{\varphi_\eta^2} = \frac{1}{2} \operatorname{tg}^2\phi\, \eta \frac{ceu \sin\phi}{E_0 L} \Omega_0^2 f^{1/2}(x) \int_{x_0}^{x} f^{1/2}(x)\, dx \tag{76}$$

and for the noise modulation of the voltage on the magnet

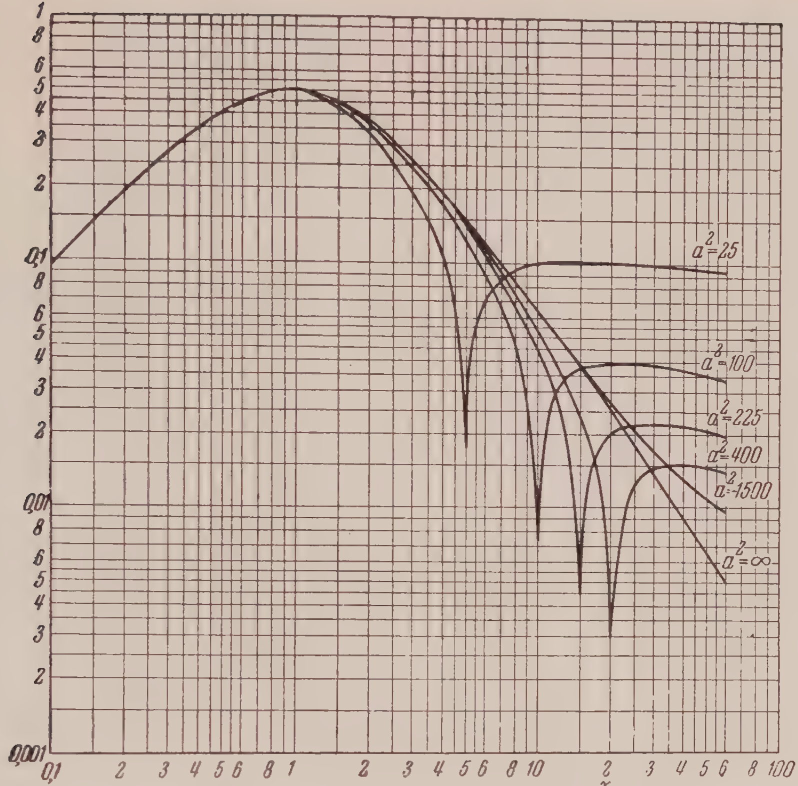

FIG. 3. Graph of the function $f^{1/2}(x)\int_0^x f^{1/2}(x)\,dx$.

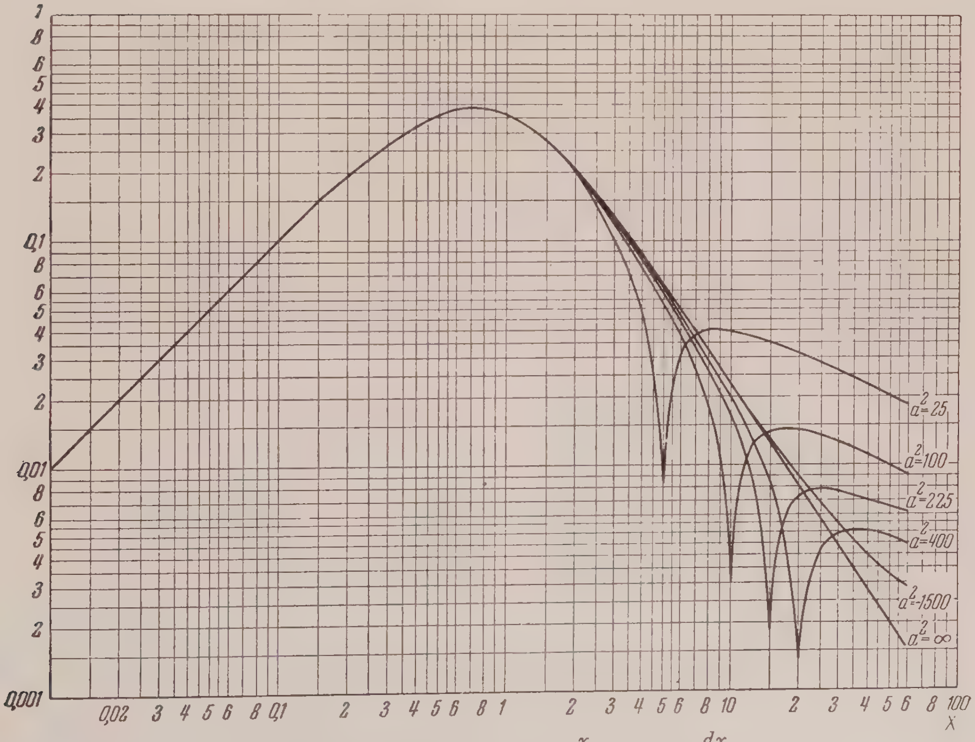

FIG. 4. Graph of the function $f^{1/2}\int_0^x f^{-1/2}(x)\frac{dx}{(1+x^2)^3}$.

$$\overline{\varphi_{\mu}^{2}} = {}^{1}/_{2}\,\mathrm{tg}^{2}\phi\mu\,\frac{ceu\sin\phi}{E_0L}\,\Omega_0^2 f^{1/2}(x)\int\limits_{x_0}^{x}\left[f^{1/2}(x) + \frac{\Omega_0^2\tau^2}{(1+x^2)^3}f^{-1/2}(x)\right]\frac{dx}{(1+\Omega^2\tau^2)^2}. \tag{77}$$

In Eqs. (75) through (77), it is assumed that the values of the spectral intensities ν, η and μ do not depend on the frequency. These formulas determine $\overline{\varphi^2}$ in the adiabatic region. Inasmuch as the effect of noises decreases on approaching the critical region, they can be used during the entire cycle of acceleration.

The mean square deviation of the momentum in the critical region is of interest. It can be calculated by Eqs. (34) and (39) on substituting for $\overline{\varphi^2}$ from Eqs. (75) through (77).

In conclusion, we present graphs of the functions which enter in Eqs. (75) through (77). These functions are evaluated for several positive- and for one negative-value of a^2. Negative values of a^2, characteristic for strong focusing accelerators without a critical energy, were proposed by Vladimirskii and Tarasov[3].

---

[1] N. M. Blachman, Rev. Sci. Instr. 21, 908 (1950).

[2] E. Bodenstedt, Ann. der Phys. 15, 35 (1954).

[3] V. V. Vladimirskii and E. K. Tarasov, *On the Possibility of Eliminating the Critical Energy in Strong-Focusing Accelerators*, Report presented at the International Conference on Peaceful Use of Atomic Energy, 1955.

[4] A. A. Kolomenskii and L. L. Sabsovich, *On the Passage Through the Critical Energy in a Strong-Focusing Accelerator*, Unpublished Report, 1953.

[5] K. Johnsen, Lecture before the Conference on Strong-Focusing Accelerators, Geneva, 1953.

Translated by R. L. Eisner
173

SOVIET PHYSICS JETP VOLUME 4, NUMBER 5 JUNE, 1957

A Comparison of the Fermi-Landau Theory with Some Experimental Data on Cosmic Rays

O. A. GUZHAVINA, V. V. GIZHAVIN AND G. T. ZATSEPIN
P. N. Lebedev Physical Institute, Academy of Sciences, USSR

(Submitted to JETP editor August 20, 1955)
J. Exptl. Theoret. Phys. (U.S.S.R.) 31, 819-830 (November, 1956)

The energy spectra of the secondary particles originating in nuclear collisions of high-energy particles ($10^{12} - 10^{18}$ ev) have been calculated on the basis of the theory of L. D. Landau. A calculation of the altitude dependence of the radioactive particles in the atmosphere, as well as of the number of high-energy μ-mesons at sea level, has been carried out on the basis of the spectra obtained. The results of the calculations are compared with experimental data.

UP to the present time there have been few direct experimental data concerning collisions of super-high energy nucleons ($> 10^{12}$ ev) with nucleons or light nuclei. There exists practically no knowledge of the distribution of energy between the secondary particles of various types formed as a result of such collisions. Hence, in spite of the considerable time since the publication of the Landau theory[1], there have been, up to the present, almost no papers devoted to a comparison of the results of this theory with experimental data. However, although direct experimental data relative to the energy distribution of secondary particles in the energy region $E > 10^{12}$ ev are lacking, we nevertheless have indirect experimental data relative to the formation of secondary particles of super-high energy. For example, in the works of Ryzhkova and Sarycheva[2], and also Kaplon *et al.*[3], the coefficient of absorption is measured in the atmosphere of radioactive particles with energy $\gtrsim 10^{12}$ ev. Moreover, there exist data relative to the number of μ-mesons[4] penetrating a depth of the earth of as much as 3 km of water equivalent, i.e., possessing energies of the order of 3×10^{12} ev. As the calculations show, these data are very sensitive to the mechanism of the elementary act of collision, especially to the form of the energy spectrum of the particles produced in nuclear collisions. Hence, the calculation of the absorption curve of radioactive particles of high energy and the number pf μ-mesons produced in the atmosphere on the basis of any given theory of the elementary act of nuclear collision, allows the verification of the correctness of the results of that theory.

The basic initial data on which the carrying out of the calculations just mentioned is dependent are: 1) the primary particles of the cosmic rays, mainly protons (and we assume below that they are all protons); 2) secondary particles arising as a result of collisions of a nucleon of given energy with a nucleus of an atom of the air. The energy spectrum of the primary cosmic rays has been determined as a result of many experimental investigations, and we have taken it to be in accordance with Ref. 4. The energy spectra of the secondary particles were calculated on the basis of the Landau theory, the results of which may be satisfactorily reconciled with a number of experimental results obtained by the method of photoemulsions[5] and which, in the case of an elementary analysis of the properties of wide atmospheric showers[5,6], do not display the sharp contradictions with these properties which are shown, for example, by the Fermi theory[5,7].

ENERGY SPECTRUM OF THE PARTICLES ARISING IN NUCLEAR COLLISIONS ACCORDING TO THE LANDAU THEORY

In a nucleon-nucleon collision the total number of secondary particles $N(E_0)$ is equal to

$$N(E_0) = K\,(E_0/2M_{H}c^2)^{1/4}, \tag{1}$$

where M_H is the mass of the nucleon, E_0 is the energy of the generating particle, and $K \approx 2$ (Ref. 1). In the collision of a nucleon with a quiescent nucleus of an "air atom," the number of particles produced is greater since, according to the Landau theory,

$$N \sim E_c^{3/4} V_c^{1/4}. \tag{2}$$

where E_c is the energy of the colliding particles in their center-of-mass system and V_c is the volume of the system formed immediately after the collision.

We have assumed that the interaction occurs between a nucleon and a mass of nuclear material contained in a cylinder of radius corresponding to the radius of the nucleon $r_0 = \hbar/M_H c$ (Ref. 5). The entire calculation was carried out for a cylinder of average height $\overline{H}$, which was taken equal to the average chord of a sphere of radius $R = r_0 A^{1/3}$, where A is the atomic weight of the nucleus, i.e.,

$$\overline{H} = {}^4/_3 R = {}^4/_3 r_0 A^{1/3}. \tag{3}$$

The mass of such a cylinder is equal to

$$M_{\text{cyl}} = A^{1/3} M_H \tag{4}$$

An average value was taken for the atomic weight of the nucleus of an atom of air.

The volume formed after the collision of the system was taken equal to the volume of the cylinder of nuclear substance modified in accordance with the Lorentz contraction for the nucleon-cylinder center-of-mass system. On the basis of Eq. (2), the total number of particles in this case is equal to

$$N(E_0) = K A^{1/4}\,(E_0/2M_{H}c^2)^{1/4}, \tag{5}$$

where K has the same magnitude as in (1). Thus, taking account of a collision with a nucleus leads to an increase by a factor of $A^{1/4}$ in the number of particles given rise to.

In the calculation of the energy spectra of the particles by the Landau theory, a basic parameter is

$$L = -\ln(\Delta/a), \tag{6}$$

where Δ is the longitudinal measure of the system formed immediately after the collision and a is the transverse dimension of the same system. In a nucleon-nucleon collision

$$L = {}^1/_2 \ln(E_0/2M_{H}c^2). \tag{7}$$

We have assumed that in a nucleon-nucleus collision Δ and a correspond to the dimensions of the pre-collision cylinder in the cylinder-nucleon center-of-mass system. Then

$$L = {}^1/_2 \ln(9E_0/8AM_{H}c^2). \tag{8}$$

The energy distribution of the secondary particles in the laboratory system of coordinates is given by Landau in the parametric form

$$dN = c_1 \exp\left(\sqrt{L^2 - \lambda^2}\right) d\lambda, \tag{9}$$

$$E = B_1 M_{H} c^2 \exp\left({}^5/_6 L + \lambda + {}^1/_3 \sqrt{L^2 - \lambda^2}\right),$$

where $\lambda = -\ln \mathrm{tg}(\theta/2)$ (θ is the angle of departure of the secondary particle in the center-of-mass system). The coefficients C_1 and B_1 in Eq. (9) are found from the normalization conditions

$$\int dN = N; \int E dN = E_0. \tag{10}$$

Introducing the parameter $\nu = \lambda/L$, we obtain for C_1 and B_1 the expressions

$$C_1 = 2A^{1/4}(E_0/2M_H c^2)^{1/4} / L \int_{-1}^{0,87} e^{L\sqrt{1-\nu^2}} d\nu; \tag{11}$$

$$B_1 = E_0 \left[M_H c^2 C_1 L e^{5L/6} \right.$$

$$\left. \times \int_{-1}^{0,87} \exp L\left(\nu + \frac{4}{3}\sqrt{1-\nu^2}\right) d\nu \right]^{-1},$$

where L is to be calculated according to Eq. (7) in the case of a nucleon-nucleon collision and according to Eq. (8) in the case of a nucleon-nucleus collision.

For the solution of practical problems, it is convenient to have the energy spectrum in graphical rather than parametric form. For this purpose it is expedient to choose the representation $dN/d \ln E$, since in this case the form of the curves describing the spectrum is symmetrical, almost Gaussian. Thus, letting $y_0 = \ln E_0$ and $y = \ln E$, we obtain

$$f(y_0, y) = \frac{dN}{d \ln E} \tag{12}$$

$$= C_1 L e^{L\sqrt{1-\nu^2}} / (1 - \nu / 3\sqrt{1-\nu^2}),$$

$$y = \ln E = \ln (B_1 M_H c^2)$$

$$+ L\left({}^5/_6 + \nu + {}^1/_3 \sqrt{1-\nu^2}\right).$$

Here, as in what follows, the energy is expressed in electron bolts.

It is clear that Eq. (12) is not applicable for large values $\nu \sim 1$, since for $\nu = 0.95$, when $\nu/3\sqrt{1-\nu^2} = 1$, the function $dN/d \ln E$ breaks off, but the energy of the particles attains a maximum for this value of ν and subsequently falls off.

However, the energy spectrum of the particles calculated on the basis of the Landau theory is characterized by a slow fall-off with increase in energy in the region of applicability of Eq. (12), so that a significant portion of the energy is carried off by particles the energy of which corresponds to the region of the spectrum where $\nu \approx 0.9$, that is, near the limit of applicability of the Landau formula.

From the basic concepts of the theory there is no reason to expect that the spectrum should break off sharply at $\nu \approx 0.9$, since the singularity at $\nu = 0.95$ occurs as a result of the form in which the calculations of Landau are represented. Hence, we have carried out a smooth extrapolation into the region of energies near E_0, for which the Landau formulas are no longer applicable, of the Landau spectra which we previously calculated up to energies corresponding to $\nu = 0.9$.

If we make graphs of the energy spectra, taking $\ln f(y_0, y)$ as ordinate and $\ln E$ as abscissa, then, designating the abscissa value corresponding to the spectral maximum as $y_{\max}$, and the difference $y - y_{\max}$ as z, we may write our chosen approximating function in the form

$$\varphi(z) = A - z^2(a + bz^k)$$

for each curve with a given value of the parameter y_0. The constant A corresponds to the spectral maximum, lying at the value $y_{\max}$. The number a is found from the curvature of the Landau curves for $y = y_{\max}$, while the numbers b and k are chosen so that the approximating function coincides exactly with the Landau function for the energy corresponding to the maximum in the energy current of the secondary particles and for the energy corresponding to the upper limit of applicability of the Landau formula (near $\nu = 0.87$). The functions $\varphi(z)$ obtained for various values of E_0 correspond with great exactness to the Landau curves for the entire region $0 < \nu < 0.9$.

The extrapolation of the curves of the energy distribution of the number of particles and the corresponding curves for the energy current $Ef(y_0, y)$ beyond the point $\nu = 0.87$ essentially changes the normalization of these curves, so that the area under these curves gives the total number of secondary particles N and the total energy of the secondary particles E_0, respectively, whereas normalization in accordance with Eq. (11) takes into account only the area to the left of the break-off point.

The values of the renormalized constants CL and $BM_H c^2$ are given in Table I for certain values of the energy. Values of the parameters A, a, b, k for the function $\varphi(z)$ are given in Table II for the same values of the energy . Figure 1 gives the dependence of $f(y_0, y)$ on y, that is, the dependence of $\ln(dN/d \ln E)$ on $\ln E$ for given values of

$y_0 = \ln E_0$, obtained on the basis of the Landau theory by the method set forth above for cases of collision of a nucleon with a nucleus of an air atom for $E_0 \geq 10^{12}$ ev. The portions of the curves lying below the dashed line were obtained by extrapolation. The integral $\int_0^{y_0} f(y_0, y)dy = n_{tot}$. Values of n_{tot} are given in Table III.

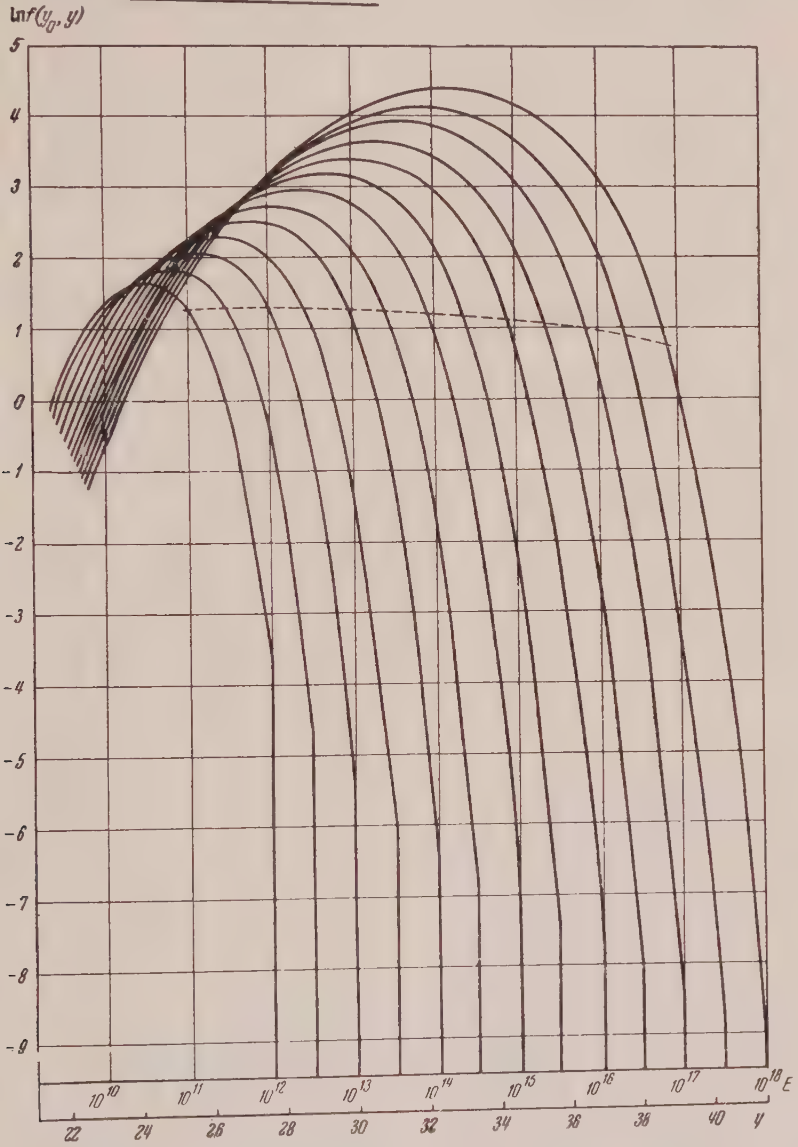

FIG. 1. Energy spectra of the secondary particles according to Landau for the case of a collision of a nucleon with the nucleus of an atom of the air. The energy of the primary particle (10^{12} ev, 3×10^{12} ev, 10^{13} ev, etc.) for each curve corresponds to the break-off of the curve at the upper limit of the spectrum.

Figure 2 gives curves showing the dependence of the current of energy carried away by the secondary particles on the $\ln E$ of these particles for the case of a collision of a nucleon with a nucleus of an air atom. The integral $\int_0^{y_0} Ef(y_0, y)\,dy = E_0$, where E_0 is the energy of the primary particle. A comparison of Figs. 1 and 2 shows that a principal part of the energy is carried away by particles with energy significantly greater than the energy possessed by particles more representative of the energy spectrum of the secondary particles.

TABLE I. Values of the finally renormalized coefficients CL and BMc^2.

Type of collision	Coeff.	E_0 (ev)			
		10^{12}	10^{14}	10^{16}	10^{18}
nucleon-nucleon	$CL \cdot 10^3$	106	23,3	6,11	1,74
	$BMc^2 \cdot 10^{-9}$	0,770	0,987	1,18	1,32
nucleon-nucleus	$CL \cdot 10^3$	551	134	33,2	9,00
	$BMc^2 \cdot 10^{-9}$	1,85	2,41	2,73	2,88

TABLE II. Values of the parameters of the function $\varphi(Z)$ approximating the curves of the energy spectrum of the secondary particles.

Type of collision	Parameter	E_0 (ev)			
		10^{12}	10^{14}	10^{16}	10^{18}
nucleon-nucleon	A	2,555	5,565	14,42	40,74
	$a \cdot 10^2$	16,14	9,32	6,53	5,02
	$b \cdot 10^4$	316,0	85,3	3,67	1,89
	k	1,358	1,577	3,062	2,873
	z_0	24,91	27,70	30,39	33,08
nucleon-nucleus	A	5,152	12,36	30,34	81,47
	$a \cdot 10^2$	22,67	11,25	7,43	5,55
	$b \cdot 10^4$	388,4	72,7	11,7	3,23
	k	1,413	2,170	2,564	2,749
	z_0	23,97	27,10	29,80	32,62

Table IV gives the share of the energy, in percent of E_0, carried away on the average by a single very fast secondary particle. It should be noted that this share contains a rather large amount of the generating particles right up to very high energies, and agrees very well with the calculations of Gerasimova and Chernavskii[8], which considered hydrodymanic problems corresponding to the collision of nucleons and took into account the presence of traveling waves. We note that the probability of emission of a particle having concentrated in itself a large portion of the energy of the primary particle which is obtained from our graphs for a collision of the nucleon-nucleon type, exceeds the estimates obtained in the work of Podgoretskii, Rosental' and Chernavskii[9].

For the calculation of energy spectra by the method of successive slopes it is necessary to calculate the number of particles of given energy, integrating the probability of their formation from primary particles with energy above the given. The representation of the function $f(y_0, y)$ in the form of a family of curves for fixed values of y_0 is inconvenient for this purpose. Hence the function $f(y_0\, y)$ in Fig. 3 is represented in the form of a family of curves for fixed y and varying y_0.

In many calculations connected with nuclear-cascade processes in the atmosphere (for example, Refs. 10-12), it is assumed that the energy of the incident particle is divided equally among the secondary particles. In this case each particle receives the average energy $\bar{E} = E_0/n_{tot}$, where n_{tot} is the total number of secondary particles occurring. But from the curves which we have obtained for the energy current of the secondary particles and the data of Table IV, it follows that the greater part of the energy is carried away by a much smaller number of particles than n_{tot}. This number of secondary particles possessing the largest energies is actually determined in the basic development of the nuclear-cascade process in the atmosphere. The effective number of such particles may be determined[6] as $n_{eff} = E_0/E_{1/2}$, where $E_{1/2}$ is the value of the energy of the secondary particles determined by the magnitude of $y_{1/2}$, from the equation

$$\int_{-\infty}^{y_{1/2}} Ef(y_0,\ y)\,dy = \int_{y_{1/2}}^{y_0} Ef(y_0,\ y)\,dy.$$

$E_{1/2}$ coincides approximately with the energy value at the maximum in the curve of the energy current.

The dependence of n_{tot}, n_{eff} and $n_{\text{tot}}/n_{\text{eff}}$ on E_0 is given in Table III for two types of collisions. According to the Landau theory $n_{\text{tot}} \sim E_0^{0.25}$. It follows from the data of Table III that, for both types of collisions, $n_{\text{eff}} \sim E_0^{0.16}$, approximately.

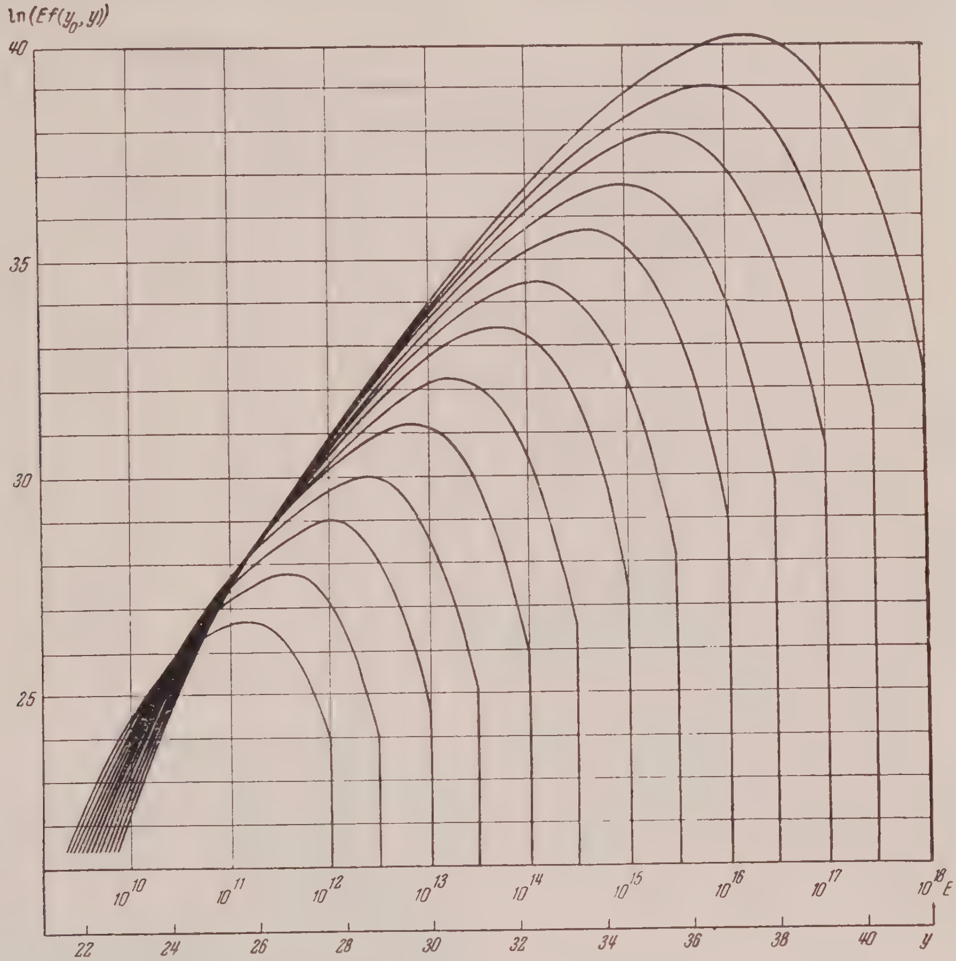

FIG. 2. Currents of energy carried away by the secondary particles, for the case of a collision of a nucleon with the nucleus of an atom of the air. E is expressed in electron volts. The energy of the primary particle for each curve corresponds to the break-off of the curve at the upper limit of the energy current.

CALCULATION OF THE ALTITUDE DEPENDENCE OF RADIOACTIVE PARTICLES OF HIGH ENERGY BY THE METHOD OF SUCCESSIVE SLOPES

In a calculation of the altitude dependence of radioactive particles in the region of high energies, for which the Landau theory is applicable ($E_0 > 10^{12}$ ev), we may neglect the ionization losses of the particles and their disintegration. In the calculations we have assumed that the result of a collision of a radioactive particle with a nucleus does not depend on the nature of the generating particle. The effective cross section for collision was assumed constant and corresponding to the free path length $\lambda_0 = 65$ g/cm^2. In this case the change in the number of radioactive particles in a given energy interval with depth x into the atmosphere may be described by the equation

$$\frac{1}{\mu_0}\frac{\partial F(y,x)}{\partial x} = -F(y,x) + \alpha\int_{y}^{\infty} F(y',x)\,f(y',y)\,dy', \tag{13}$$

where $F(y, x)dy$ is the number of radioactive particles at depth x, the energy of which lies in the interval corresponding to y, $y + dy$. The function $f(y', y)\,dy$ has the sense of the probability of formation of a secondary particle in the interval y, $y + dy$ from a primary of corresponding y'. It is represented graphically in Fig. 4. α is the fraction of radioactive particles contained in the total number of secondary particles formed in the act of collision; $\mu_0 = 1/\lambda_0$.

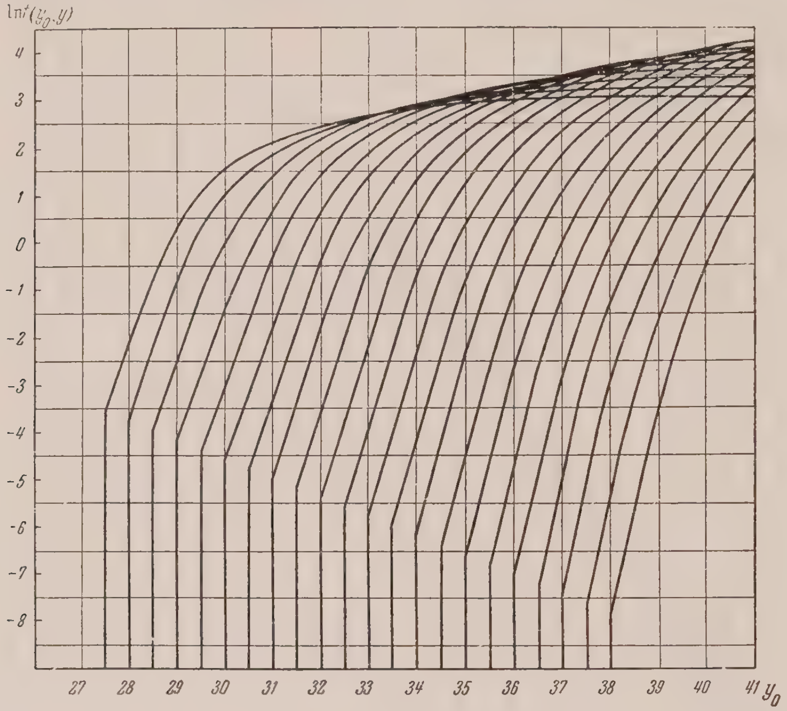

FIG. 3. Values of $\ln f(y_0, y)$ as a function of $y_0 = \ln(E/1\text{ ev})$. Each curve relates to a definite value of $\ln y$ of the secondary particle, which is equal to the value y_0 corresponding to the break-off of the curve at the upper limit.

As is well known[6,13,14], Eq. (13) is satisfied by the function $F(y, x)$ taken in the form of the series

$$F(y, x) = e^{-\mu_0 x} \sum_{i=0}^{\infty} \alpha^i \frac{(\mu_0 x)^i}{i!} F_i(y), \quad F_i(y) = \int_y^{\infty} F_{i-1}(y') f(y', y)\, dy'. \tag{14}$$

Figure 4 shows the dependence of $F_i(y)$ for $0 \leq i \leq 5$. It is not necessary to take into account the subsequent terms of the sum with $i > 5$, since they make a negligible contribution even at sea level. $F_0(y')\,dy'$ represents the differential energy spectrum of the primary particles, calculated in accordance with the integral spectrum adduced in Ref. 4.

Substituting the functions $F_i(y)$ into Eq. (14), we obtain the altitude dependence of particles of various energies, from which we may calculate the coefficient of absorption at various altitudes.

The graph of Fig. 5 gives the absorption curve for particles with $E = 10^{12}$ ev. Curves *1* and *2* represent the result of calculations wherein it is assumed that $\alpha = 2/3$ and $\alpha = 1$, respectively. Curve *3*, which was observed experimentally, represents the absorption curve of particles with $E = 10^{12}$ ev. In its construction the experimental results of Kaplon *et al.*[3] were used for the interval of depth less than 700 g/cm^2. According to these authors, the coefficient of absorption in this interval corresponds to $1/\mu = 120$ g/cm^2. Similarly, the experimental results of Ryzhkova and Sarycheva[2] were used in the interval of depth from 650 to 100 g/cm^2. These results gave $1/\mu = (112 \pm 9)$ g/cm^2 in this interval of depth. Curve *4* gives the absorption curve which would be observed if each act of collision with a nucleus led to complete absorption of the particle ($1/\mu_0 = 65$ g/cm^2).

From the results given in Fig. 5 it is clear that experiment gives a significantly smaller magnitude for the coefficient of absorption than does calculation. The coefficient of absorption of the particles may be represented in the form

$$\mu(y, x) = \mu_0 [1 - \Delta(y, x)],$$

whence, according to Eq. (14),

$$\Delta(y, x) = \int_y^\infty F(y', x) f(y', y)\, dy' / F(y, x).$$

As a consequence of the fact that $F(y, x)$ falls off quickly with increasing y ($F \sim e^{-\gamma y}$, $\gamma \approx 1.5$ to 2), the magnitude of Δ depends essentially on the value of $f(y', y)$ for $y \approx y'$, that is, on the probability of formation of a secondary particle with energy near the energy of the primary. Thus, the magnitude of Δ is extremely sensitive to the mechanism of the elementary act of the nuclear collision.

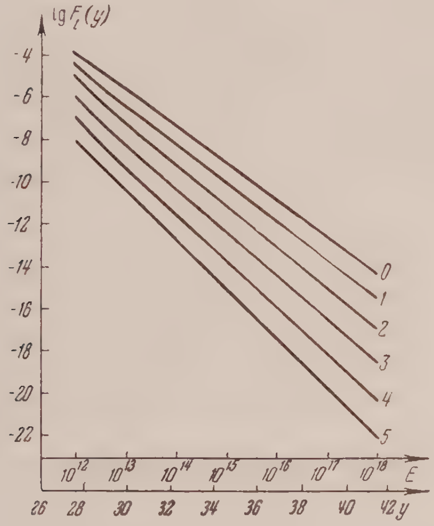

FIG. 4. Energy spectra of successive slopes of radioactive particles in the atmosphere. $F_0(y)\,dy$ represents the differential energy spectrum of the primary cosmic ray particles, expressed in units of $\mathrm{cm}^{-2}\ \mathrm{sec}^{-1}\ \mathrm{sterad}^{-1}$. The numbers on the curves indicate the value of i.

From Eq. (14) we obtain

$$\Delta(y, x) = \sum_{i=0}^{\infty} \alpha^{i+1} \frac{(\mu_0 x)^i}{i!} \times F_{i+1}(y) \Big/ \sum_{i=0}^{\infty} \alpha^i \frac{(\mu_0 x)^i}{i!} F_i(y).$$

Figure 6 shows the calculated dependence $\Delta(x)$ for particles with $E = 10^{12}$ ev. The value of $\Delta(y, x)$ in Fig. 6 does not exceed 0.25 and falls off quickly with depth into the atmosphere, while according to the experimental results $\Delta(x)$ depends weakly on the depth, remaining equal to about 0.5 or 0.4.

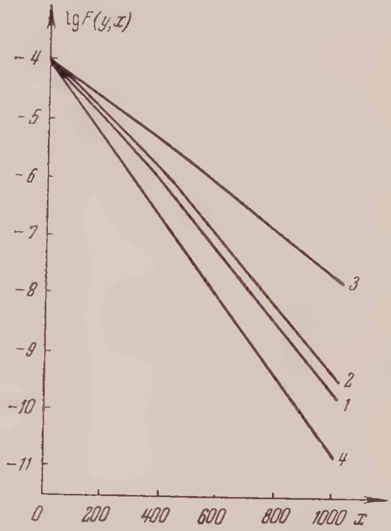

FIG. 5. Altitude dependence of the particles with energy 10^{12} ev. The atmospheric depth in $\mathrm{g/cm^2}$ is plotted as abscissa, and the common logarithm of the function $F(y, x)$ is plotted as ordinate.

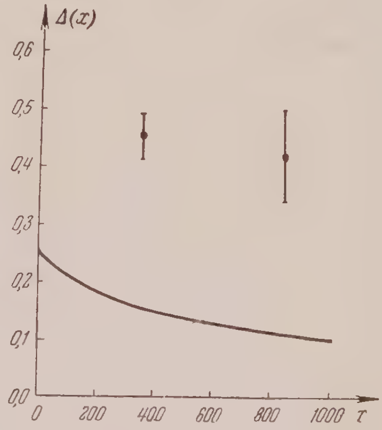

FIG. 6. Dependence of Δ on x for $E = 10^{12}$ ev. The points correspond to the experimental results given in Refs. 2 and 3. The continuous curve gives the results of calculations according to the Landau theory.

Thus the spectra of the secondary particles which we have calculated on the basis of the Landau theory do not correspond to that which actually occurs. The character of the lack of correspondence shows that for nuclear collisions of high energy the probability of having a great part of the energy ($E/E_0 > 0.5$) concentrated in a single particle is significantly greater than is obtained from the spectra of Fig. 2 (Table IV). Moreover, the small change in the experimental value of Δ with depth shows that this probability decreases more weakly with increasing energy of the generating nucleon than is called for by the Fermi-Landau theory.

TABLE III.

Type of collision	E_0 (ev)	10^{12}	10^{14}	10^{16}	10^{18}
nucleon-nucleon	n_{tot}	9,5	30,1	95,4	302,0
	n_{eff}	3,7	8,0	17,1	36,6
	$n_{\text{tot}}/n_{\text{eff}}$	2,57	3,76	5,58	8,25
nucleon-nucleus	n_{tot}	18,7	59,2	187,0	592,0
	n_{eff}	8,9	18,4	37,7	76,8
	$n_{\text{tot}}/n_{\text{eff}}$	2,10	3,22	4,96	7,72

TABLE IV. Average fraction, in percent, of the energy of the primary particle which is found in a single very fast secondary particle.

Type of collision	E_0 (ev)			
	10^{12}	10^{14}	10^{16}	10^{18}
nucleon-nucleon	48,6	35,0	24,8	17,2
nucleon-nucleus	30,0	19,8	14,3	01,5

CALCULATION OF THE NUMBER OF μ-MESONS OF HIGH ENERGY AT SEA LEVEL

The method of successive slopes allows us to write the intensity of μ-mesons at arbitrary depth in the atmosphere in the form of a series, each term of which represents the μ-mesons arising from a disintegration of π-mesons of the corresponding generation.

In calculations for the region of high energy, $E > 10^{12}$ ev, only the first term of the series, corresponding to the disintegration of $\pi^{\pm}$-mesons in the very highest layers of the atmosphere, contributes a significant amount to the energy. All the other members of the series contribute an insignificant amount, since practically no disintegration of $\pi^{\pm}$-mesons of high energy occur deep in the atmosphere. Thus for the region $E \geq 10^{12}$ ev it is sufficient to calculate only the μ-mesons arising from the disintegration of $\pi^{\pm}$-mesons originating in the first collisions of the primary protons with nuclei of atoms of the air.

In the Landau theory, it is customary to assume that all the secondary particles originating in nuclear collisions are π-mesons. Hence, in the calculation we have used the results shown in Fig. 4, assuming that $\pi^{\pm}$-mesons comprise 2/3 of the total number of particles, corresponding to curve $F_1(y)$.

The disintegration of μ-mesons during their passage through the atmosphere and their ionization losses may be neglected. Then the number of μ-mesons of given energy can be written in the form

$$F^{(\mu)}(E)\,dE = \frac{2}{3}\int\limits_{E}^{EM_\pi^2/M_\mu^2} \frac{F_1^{(\pi)}(E')\,dE'}{1+\dfrac{E_\pi}{E}}\,\frac{E_\pi}{E} \times \frac{dE'}{E'\,(1-M_\mu^2/M_\pi^2)},$$

where M_μ and M_π are the masses of the μ- and π-mesons and $F_1(\pi)(E')dE'$ is the spectrum of the first generation of π-mesons generated. The coefficient E_π/E_x characterizes the probability of disintegration of a $\pi^{\pm}$-meson with energy E in the interval of path x, $x + dx$. According to Refs. 6 and 14,

$$E_\pi / E = l_0\lambda_0 T / T_0\rho_0 (E / M_\pi c^2)\tau_0 = 1.17\times 10^{11}\ \text{ev}/E.$$

Here T is the temperature of the air (we assume it constant and equal to 225° K); ρ_0 is the density of the air in g/cm^2 at sea level and at temperature T_0; τ_0 is the average lifetime of a $\pi^{\pm}$-meson at rest.

The total number of μ-mesons with energy higher than the given is obtained as

$$\Phi^{(\mu)}(>E) = \int\limits_{E}^{\infty} F^{(\mu)}(E)\,dE.$$

We obtain as a result $\Phi^{(\mu)}(> 10^{12}\ \text{ev}) = 4.4 \times 10^{-7}$ particles cm^{-2} sec^{-1} sterad^{-1}. The calculated magnitude of the current of μ-mesons may be compared with the experimental magnitude obtained on the basis of Ref. 15, according to which $\Phi^{(\mu)}(> 10^{12}\ \text{ev}) = 1.8 \times 10^{-7}$ particles cm^{-2} sec^{-1} sterad^{-1}. We see that the calculated magnitude of the intensity of the μ-meson current exceeds the experimentally observed magnitude by approximately 2.5 times.

As a consequence of the fact that the number of μ-mesons of given energy is determined by the number of $\pi^{\pm}$-mesons of approximately the same energy , it follows that the number of μ-mesons which we have calculated exceeds by at least 2.5 times the number of π-mesons actually formed. Since the primary spectrum of the cosmic rays falls rapidly with increasing energy, a basic contribution to the number of π-mesons of given energy is made by mesons which are formed with energy near the energy of the nucleons which generate them. Thus the result which we have obtained shows that the probability of forming π-mesons with energy near the energy of the nucleon which generates them is at least 2.5 times less than that which follows from the curves of Fig. 1.

DISCUSSION OF THE RESULTS

The calculations just carried out show that the energy spectra of the secondary particles which we have obtained on the basis of the Landau energy (by use of the assumptions on the magnitude of the effective collision cross section and on the composition of the secondary particles) leads to a discrepancy with experimental results both with respect to the absorption of radioactive particles and with respect to the number of observed μ-mesons of high energy. The fact that we allowed a certain arbitrariness in the extrapolation of the energy spectra of the secondary particles into the region of energy near the energy of the generating particle does not seem essential for qualitative results, due to the character of the deviations of the experimental results from the theoretical.

Actually, to produce agreement of the theoretical and experimental results with respect to the absorption curve for radioactive particles, it would be necessary to change the energy spectra in such a way that the probability of formation of secondary particles with energy near that of the primary would be greater. On the other hand, in order to reconcile the observed number of μ-mesons with the calculated number, it is necessary to suppose that the probability of formation of $\pi^{\pm}$-mesons with theory near the the energy of the primary particles is less than that obtained from the spectra found.

Although the assumption that the effective interaction cross section of nucleons of high energy differs essentially from the geometrical cross section (being less than the geometrical by about 1.5 times) may do away with the discrepancies we have obtained, it can nevertheless not be assumed, since it is contradicted by many experimental results. Clearly, the only possible cause of the contradictions we have found is the assumption which we made, in agreement with Landau's work, that all the secondary particles are π-mesons.

The essential difference (by approximately a factor of 2) between the experimental coefficient of absorption of the radioactive particles and the reciprocal magnitude of the free path of these particles shows that after a collision with an atom of the air, a significant portion of the energy (of the order of 0.6 to 0.7) of the primary radioactive particle is concentrated on the average in a single secondary particle[6]. On the other hand, the small number of observed μ-mesons shows that these secondary particles cannot be $\pi^{\pm}$-mesons or other particles disintegrating with a lifetime less than that of $\pi^{\pm}$-mesons and giving μ-mesons as a result of their decay. Thus these secondary particles in which the larger portion of the energy is concentrated cannot be the K-mesons found in stars produced by primary particles of high energy. Hence, of all the particles known at the present time, only nucleons (and hyperons) satisfy the stipulated conditions.

The small number of μ-mesons with high energy in comparison with the number of primary cosmic ray particles with such energy shows that the energy spectra which we have obtained on the basis of the Landau theory gives too great a probability of formation of $\pi^{\pm}$-mesons with energy near the energy of the generating nucleon.

In the calculations we assumed that $\pi^{\pm}$-mesons comprise 2/3 of the total number of particles produced. Certain experimental results show that a significant portion of the particles produced are not π-mesons but K-mesons. However, taking account of these K-mesons which make up a part of the secondary particles can lead only to an increase in the observed discrepancy.

Actually, the lifetime of K-mesons is significantly smaller than that of $\pi^{\pm}$-mesons. In the region of energy $E > 10^{12}$ ev, the number of μ-mesons produced is inversely proportional to the lifetime of the particle from the disintegration of which they are produced (if this lifetime is not too small). Hence, the assumption that a portion of the secondary particles are K-mesons leads only to a still greater number of expected μ-mesons. Since on the basis of experimental results with photoemulsions we may consider that $\pi^{\pm}$-mesons and K-mesons make up the basic number of the secondary particles, the result which we have obtained shows that the energy spectrum of the mesons produced in nuclear collisions is weaker than that calculated on the basis of the Landau theory.

On the basis of the calculations which we have carried out, we may draw the following conclusions:

1. The theory of nuclear collisions of very high energy, in the form in which it is given in Landau's work[1], does not allow one to carry out a quantitative calculation of cascade processes, because of the indeterminacy of the form of the energy spectrum of the secondary particles near the upper limit;

2. Experimental results show that the energy distributions of secondary particles of various types are essentially different from each other. However, we can at least affirm that in the case of nucleons (or hyperons) emitted as a result of nuclear collisions, there is a great probability that a significant portion of the energy of the incident nucleon is concentrated in one of them. On the other hand, the probability of concentration of a significant amount of energy in individual $\pi^{\pm}$-mesons or K-mesons is small.

After the calculations reported above had been carried out, it was shown by Belen'kii[16,17] that, in spite of the opinion expressed earlier, a systematic consideration of nuclear collisions on the basis of the Landau concepts leads to a notable probability of the appearance of particles heavier than π-mesons. Belen'kii showed further that the hydrodynamic character of the expansion of the system formed after the collision of the nucleons leads to a dependence of the energy concentration on the mass of the particles considered, with the concentration increasing with increasing mass. Thus, the further development of the Landau theory carried out by Belen'kii must lead to a smaller discrepancy between the theoretical and experimental results. Detailed calculations; analogous to those carried out in the present work, are needed in order to determine how well the Landau-Belen'kii theory agrees with present results.

It seems to us, however, that even the detailed theory cannot be reconciled with experimental results, since even it must clearly lead to an essential increase in the cœfficient of absorption of radioactive particles with increasing energy of the particles and increasing depth into the atmosphere. In our opinion, consequently, serious consideration should be given to the development of a theory of nuclear collisions which will be based on new premises[18], taking account of the possible "stucturedness" of the nucleon, and which will provide for the concentration of a large portion of the energy in a single nucleon and a small concentration of energy in mesons.

---

[1] L. D. Landau, Izv. Akad. Nauk SSSR, Ser. Fiz. **17**, 51 (1953).

[3] K. P. Ryzhkova and L. I. Sarycheva, J. Exptl. Theoret. Phys. (U.S.S.R.) **28**, 618 (1955); Soviet Phys. JETP **1**, 572 (1955).

[3] Kaplon, Klose, Ritson and Walker, Phys. Rev. **91**, 1573 (1953).

[4] Barrett, Bollinger, Cocconi, Eisenberg and Greisen, Rev. Mod. Phys. **24**, 133 (1952).

[5] I. L. Rozental' and D. S. Chernavskii, Usp. Fiz. Nauk **52**, 185 (1954).

[6] G. T. Zatsepin, Dissertation, Moscow, Physical Institute, Academy of Sciences, USSR, 1954.

[7] E. Fermi, Usp. Fiz. Nauk **46**, 71 (1952).

[8] N. M. Gerasimova and D. S. Chernavskii, J. Exptl. Theoret. Phys. (U.S.S.R.) **29**, 372 (1955); Soviet Phys. JETP **2**, 344 (1956).

[9] Podgoretskii, Rozental' and Chernavskii, J. Exptl. Theoret. Phys. (U.S.S.R.) **29**, 296 (1955); Soviet Phys. JETP **2**, 211 (1956).

[10] G. T. Zatsepin, J. Exptl. Theoret. Phys. (U.S.S.R.) **19**, 1104 (1949).

[11] K. Sitte, Phys. Rev. **78**, 721 (1950).

[12] I. L. Rozental', Dokl. Akad. Nauk SSSR **80**, 731 (1951).

[13] N. L. Grigorov, Dokl. Akad. Nauk SSSR **94**, 835 (1954).

[14] G. T. Zatsepin and I. L. Rozental', Dokl. Akad. Nauk SSSR **99**, 369 (1954).

[15] E. George, *Physics of Cosmic Rays* **1**, IIL, 1954, p. 328 (Russian translation).

[16] S. Z. Belen'kii, Dokl. Akad. Nauk SSSR **99**, 523 (1954).

[17] S. Z. Belen'kii, J. Exptl. Theoret. Phys. (U.S.S.R.) **28**, 111 (1955); Soviet Phys. JETP **1**, 161 (1955).

[18] Vernov, Grigorov, Zatsepin and Chudakov, Izv. Akad. Nauk SSSR, Ser. Fiz. **19**, 493 (1955).

Translated by M. G. Gibbons
175

SOVIET PHYSICS JETP VOLUME 4, NUMBER 5 JUNE, 1957

Reflection of Waves from an Isotropic Inhomogeneous Layer

A. G. ZHARKOVSKII AND O. M. TODES

(Submitted to JETP editor August 8, 1955)
J. Exptl. Theoret. Phys. (U.S.S.R.) 31, 815-818 (November, 1956)

An approximate method is constructed for the calculation of the reflection coefficient of a plane electromagnetic wave from an isotropically inhomogeneous layer for media whose dielectric constant and conductivity depend on a single spatial coordinate. This method can be also applied to the solution of analogous acoustical problems.

FOR the solution of a series of applied problems, it is necessary to be able to calculate the reflection coefficient of waves from different types of stratified structures. An exact solution of the problem can be obtained only for certain individual regularities of the layers[1-6]. In the other cases, we have to apply various approximate methods[7,8], which have definite limits of applicability. Chief practical interest attaches to stratified media, for which the optical constants can undergo discontinuous changes inside the layer and on its boundaries. For such cases, it is appropriate to make use of the approximate method of calculation proposed in the present research.

1. METHOD OF SOLUTION

Let us consider an infinite-laminar inhomogeneous strip of thickness d, on which a plane electromagnetic wave is incident from the left at an angle θ_1 with the normal. In this case, the wave is partially transmitted through the layer and falls on the second boundary of the layer at an angle θ_2. Let us place the origin at the front boundary of the layer. We draw the OZ axis perpendicular to this boundary, to the right, inside the layer and the OX axis parallel to the boundary in the plane of incidence of the oncoming wave.

The propagation constant of the electromagnetic waves in the layer depends on the coordinate z according to the law

$$k(z) = (\omega/c)[n(z) + i\varkappa(z)] = (\omega/c)\sqrt{\varepsilon^*(z)}, \quad (1)$$

$$n(z) = \left[\frac{\varepsilon(z)}{2} + \sqrt{\frac{\varepsilon^2(z)}{4} + \frac{4\pi^2\sigma^2(z)}{\omega^2}}\right]^{1/2},$$

$$\varkappa(z) = \left[-\frac{\varepsilon(z)}{2} + \sqrt{\frac{\varepsilon^2(z)}{4} + \frac{4\pi^2\sigma^2(z)}{\omega^2}}\right]^{1/2}. \quad (2)$$

The dielectric constant $\epsilon(z)$ and the conductivity $\sigma(z)$ change along the layer according to some law. To the left of the layer is a semi-infinite homogeneous medium with a propagation constant k_1 = const, in which the incident and reflected waves are propagated. To the right of the layer is a semi-infinite homogeneous medium with propagation constant k_2 = const, in which the transmitted wave is propagated. All three media are presumed nonferromagnetic, and their magnetic permeability is taken to be unity. Computation of the reflection coefficient of the wave from the layer is carried out separately for waves polarized in the plane of incidence and perpendicular to the plane of incidence.

As a first case we consider s-waves, whose electric vapor is perpendicular to the plane of incidence. The amplitude $E = E_y$ satisfies the equation

$$(\partial^2 E_y/\partial x^2) + (\partial^2 E_y/\partial z^2) + k^2(z)E_y = 0. \quad (3)$$

The solution of Eq. (3) inside the layer is sought in the form (see Refs. 9 and 10)

$$E_y = \exp[ik(z)\sin\theta(z)x] \times \left\{E^+\exp\left[i\frac{\omega}{c}\int_0^z f_s(z)\,dz\right] + E^-\exp\left[-i\frac{\omega}{c}\int_0^z F_s(z)\,dz\right]\right\}, \quad (4)$$

where $\theta(z)$ is the angle variable, defined by the conditions

$$k(z)\sin\theta(z) = k_1\sin\theta_1 = \text{const}, \quad (5)$$

and $f_s(z)$ and $F_s(z)$ are unknown functions which satisfy conjugate equations of first order:

$$f_s^2 - \varepsilon^*\cos^2\theta - i\frac{c}{\omega}\frac{df_s}{dz} = 0, \quad (6)$$

$$F_s^2 - \varepsilon^*\cos^2\theta + i\frac{c}{\omega}\frac{dF_s}{dz} = 0.$$

Solving these equations with consideration of the boundary conditions for the incident, reflected and transmitted waves, we can then determine the reflection coefficient from the layer.

For an approximate solution of Eq. (6), we expand the functions f_s and F_s in power series. For layers whose thickness is many times greater than the wavelength ($d \gg c/\omega$), we look for the solution in the form of the series

$$f_s = \sum_{m=0}^{\infty} (c/\omega)^m f_{s,m}(z), \qquad (7)$$

$$F_s = \sum_{m=0}^{\infty} (c/\omega)^m F_{s,m}(z).$$

Substituting (7) in (6), we find the following expressions for the coefficients of the series:

$$f_{s,0} = \sqrt{\varepsilon^*(z)}\cos\theta(z) = F_{s,0}, \qquad (8)$$

$$f_{s,1} = \frac{i}{2}\,\frac{d\ln(\sqrt{\varepsilon^*}\cos\theta)}{dz} = -F_{s,1},$$

$$f_{s,2} = \frac{1}{4\sqrt{\varepsilon^*}\cos\theta}\left\{\frac{1}{2}\left[\frac{d\ln(\sqrt{\varepsilon^*}\cos\theta)}{dz}\right]^2 - \frac{d^2\ln(\sqrt{\varepsilon^*}\cos\theta)}{dz^2}\right\} = F_{s,2}$$

etc. The coefficients $f_{s,0}$ and $F_{s,0}$ correspond to the usual approximation of geometric optics.

For layers that are thin in comparison with the wavelength ($d \ll c/\omega$), the solution is sought in the form of the series

$$f_s = \sum_{m=0}^{\infty} (\omega/c)^m f_{s,m}(z), \qquad (9)$$

$$F_s = \sum_{m=0}^{\infty} (\omega/c)^m F_{s,m}(z).$$

The coefficients of these series are computed by successive integration:

$$f_{s,0} = \text{const}, \qquad F_{s,0} = \text{const}, \qquad (10)$$

$$f_{s,1} = i\int_0^z [\varepsilon^*\cos^2\theta - f_{s,0}^2]\,dz,$$

$$F_{s,1} = -i\int_0^z [\varepsilon^*\cos^2\theta - F_{s,0}]\,dz,$$

$$f_{s,2} = 2f_{s,0}\int_0^z\int_0^{z'} [\varepsilon^*\cos^2\theta - f_{s,0}^2]\,dz\,dz',$$

$$F_{s,2} = 2F_{s,0}\int_0^z\int_0^{z'} [\varepsilon^*\cos^2\theta - F_{s,0}^2]\,dz\,dz'$$

etc. Making use of Eqs. (8) and (10), we can compute the functions f_s and F_s in any approximation, after which it is easy to find the amplitude reflection coefficient.

In the second case of the p-wave, whose electric vector lies in the place of incidence, it is more appropriate to solve the equation for the magnetic vector

$$\frac{\partial^2 H_y}{\partial x^2} + \frac{d^2 H_y}{dz^2} + \frac{1}{k^2(z)}\,\frac{dk^2(z)}{dz}\,\frac{\partial H_y}{\partial z} + k^2(z)H_y = 0. \qquad (11)$$

Applying the analogous substitution

$$H_y = \exp[ik(z)\sin\theta(z)\,x] \times \left\{H^+\exp\left[i\frac{\omega}{c}\int_0^z f_p(z)\,dz\right] + H^-\exp\left[-i\frac{\omega}{c}\int_0^z F_p(z)\,dz\right]\right\} \qquad (12)$$

and expanding the functions $f_p(z)$ and $F_p(z)$ in power series in c/ω or ω/c, we get: for "thick" layers,

$$f_{p,0} = \sqrt{\varepsilon^*(z)}\cos\theta(z) = F_{p,0}, \qquad (13)$$

$$f_{p,1} = \frac{i}{2}\,\frac{d}{dz}\ln\frac{\cos\theta(z)}{\sqrt{\varepsilon^*(z)}} = -F_{p,1},$$

$$f_{p,2} = \frac{f_{p,1}}{2f_{p,0}}\left[i\frac{d}{dz}\ln\frac{f_{p,1}}{\varepsilon^*} - f_{p,1}\right];$$

$$F_{p,2} = \frac{F_{p,1}}{2F_{p,0}}\left[-i\frac{d}{dz}\ln\frac{F_{p,1}}{\varepsilon^*} - F_{p,1}\right],$$

and for "thin" layers,

$$f_{p,0} = \varepsilon^*(z) = F_{p,0}, \qquad (14)$$

$$f_{p,1} = i\varepsilon^*(z)\int_0^z [\cos^2\theta(z) - \varepsilon^*(z)]\,dz = -F_{p,1},$$

$$f_{p,2} = 2\varepsilon^*\int_0^z \varepsilon^*(z')\int_0^{z'} [\cos^2\theta(z) - \varepsilon^*(z)]\,dz\,dz' = F_{p,2}.$$

For the analogous acoustical problem, the pressure in the layer satisfies the equation

$$\frac{d^2p}{dz^2} - \frac{d\ln\rho}{dz}\frac{dp}{dz} + \frac{\omega^2}{c_3^2}n^2p = 0, \qquad (15)$$

where the density $\rho(z)$, the sound velocity $c_s(z)$, and the relative index of refraction of the medium $n(z)$ are given as functions of the coordinate z, perpendicular to the surface of the layer.

Introducing the similar substitution

$$p = p^+ \exp\left[i\frac{\omega}{c_3}\int_0^z \varphi(z)\,dz\right] \qquad (16)$$

$$+ p^- \exp\left[-i\frac{\omega}{c_3}\int_0^z \varphi(z)\,dz\right],$$

we can, in the same way as for electromagnetic waves, derive the differential equation for the function $\varphi(z)$, expand it in a power series in ω/c_s or c_s/ω, and find the reflection coefficient from the entire surface.

In practice, we can limit ourselves to 2-3 first terms of the corresponding series. In the intermediate region ($d \approx \lambda$), we can make use of interpolated expressions for R which consist of calculated limiting formulas.

2. EXAMPLE

For a layer law

$$n(z) = -2d/z \qquad (17)$$

with boundary conditions: $n = n_1 = 1$ for $z \leq -2d$, and $n = n_2$ for $z \geq -d$, the problem has an exact solution. Calculation of the energy reflection coefficient for the normally incident electromagnetic waves yields the exact expression

$$R(x) = \frac{\sin^2[\sqrt{4x^2 - {}^1/_4}\ln 2]}{16x^2 - \cos^2[\sqrt{4x^2 - {}^1/_4}\ln 2]}, \qquad (18)$$

$$x = \frac{\omega}{c}d = 2\pi\frac{d}{\lambda_0}.$$

Calculation according to our approximate formulas yields, with accuracy up to terms of second order of smallness,

$$R_0(x) = (1 - 0{,}56\,x^2)/(9 - 0.56\,x^2) \qquad (19)$$

for $x \ll 1$,

$$R_\infty(x) = \frac{\sin^2[2x\ln 2 - \ln 2/16x]}{16x^2 - \cos^2[2x\ln 2 - \ln 2/16x]} \qquad (20)$$

for $x \gg 1$.

Numerical computation according to these equations shows that over the whole range of values of $\omega d/c$, the divergence between the exact and the approximate formulas for $\sqrt{R(x)}$ lies only in the third decimal place. Moreover, both expansions (in powers of x and of $1/x$) give neighboring values even for $x \approx 1$.

In those cases when our expansion in powers of x and $1/x$ diverge strongly in the region $x \approx 1$, we must compute these series with higher order approximations for the region $x \approx 1$. We then use interpolation formulas of the type

$$R(x) \approx [R_0(x) + xR_\infty(x)]/(1 + x). \qquad (21)$$

[1] L. A. Zhekulin, J. Exptl. Theoret. Phys. (U.S.S.R.) 4, 76 (1934).

[2] L. M. Brekhovskikh, Usp. Fiz. Nauk **50**, 539 (1953).

[3] K. Försterling, Ann. Physik **11**, 1 (1931).

[4] S. M. Rytov and F. S. Iudkevich, J. Exptl. Theoret. Phys. (U.S.S.R.) **10**, 887 (1940).

[5] J. Wallot, Ann. Physik **60**, 734 (1919).

[6] G. J. Elias, Proc. Inst. Radio Engrs. **19**, 891 (1931).

[7] V. L. Ginzburg, *Theory of propagation of radio waves in the ionosphere*, GTTI, Moscow, 1949.

[8] L. M. Brehkovskikh, J. Tech. Phys. (U.S.S.R.) **19**, 1126 (1949).

[9] W. Kofink and E. Menzer, Ann. Physik **39**, 388 (1941).

[10] Hines, Quart. Appl. Math. **11**, 9 (1953).

Translated by R. T. Beyer
174

SOVIET PHYSICS JETP VOLUME 4, NUMBER 5 JUNE, 1957

Expansion of Single Particle Wave Functions in Functions of The Relative Motion of the Nucleons

A. I. BAZ'

(Submitted to JETP editor August 31, 1955)
J. Exptl. Theoret. Phys. (U.S.S.R.) 31, 831-836 (November, 1956)

For small energies of relative motion, identical nucleons interact with each other only when their relative orbital momentum is zero. Therefore, it can be expected that a nucleon in the nucleus does not interact with all of the nucleons, but only with those three which are in an *S*-state relative to it. These considerations lead to a picture which is in many respects similar to the α-particle model of the nucleus. The wave functions of the shell model are investigated from this point of view and a number of common properties of the shell and α-particle models of the nucleus are shown. Several regularities in the binding energies of light nuclei are discussed.

USUALLY the state of the nucleons in the nucleus is described by giving their angular momenta relative to the center of gravity of the nucleus (shell model). In such a case, the question of what angular momenta the nucleons in the nucleus have relative to each other is not considered. However, just this question is of particular interest for an understanding of the energetics of the nucleus and for an explanation of the structure of its state. The point is that the nucleons in the nucleus have a comparatively small kinetic energy (the mean energy is of the order 10-20 mev) and, as is known from experiments on nucleon-nucleon scattering, at these energies the nucleons interact only if they are in *S*-states relative to each other. Therefore, we can conclude that a nucleon in the nucleus does not interact with all nucleons, but only with those which are in *S*-states relative to it, and thus, for an evaluation of the energy of a given state of the nucleus and for an explanation of its structure, it is necessary to know the distribution of the angular momenta of relative motion of the nucleons.

The basic properties of the nucleus are clearly best described by the shell model, and therefore it is of interest to ask what the distribution of angular momenta of relative motion is in the shell-model wave functions. The elucidation of this question is the main aim of this article.

1. TWO NUCLEONS IN THE 1*p* SHELL

The simplest cases to study are the Li^6 and He^6 nuclei, where in addition to the full shell $(1s)^4$ there are two nucleons in states with $l = 1$ relative to the center of gravity of the nucleus. In the *LS*-coupling scheme, where the total orbital angular momentum L and spin S of the two nucleons are given, the wave functions of these nucleons break up into the product of the radial wave function $R(r_1)R(r_2)$, the angular wave function Λ, the spin function χ and isotopic spin function Ω:

$$\Psi(LST) = R(r_1)\,R(r_2)\,\Lambda(\theta_1, \varphi_1; \theta_2, \varphi_2)\,\chi(S)\,\Omega(T). \tag{1}$$

Here the angular wave function has the form

$$L = 0;\ M_L = 0; \tag{2}$$

$$\Lambda = \frac{1}{\sqrt{3}}\,[Y_{11}(\theta_1, \varphi_1)\,Y_{1-1}(\theta_2, \varphi_2) + Y_{1-1}(\theta_1, \varphi_1)\,Y_{11}(\theta_2, \varphi_2) - Y_{10}(\theta_1, \varphi_1)\,Y_{10}(\theta_2, \varphi_2)];$$

$$L = 1;\ M_L = 1;\ \Lambda = \frac{1}{\sqrt{2}}\,[Y_{11}(\theta_1, \varphi_1)\,Y_{10}(\theta_2, \varphi_2) - Y_{10}(\theta_1, \varphi_1)\,Y_{11}(\theta_2, \varphi_2)]$$

$$L = 2;\quad M^L = 2;\quad \Lambda = Y_{11}(\theta_1, \varphi_1)\,Y_{11}(\theta_2, \varphi_2),$$

where Y_{1m} is the spherical harmonic, and r_i, θ_i, φ_i are the spherical coordinates of the ith nucleon.

We introduce new coordinates: the radius vector of the center of gravity of the two nucleons $\mathbf{R} = \frac{1}{2}(\mathbf{r}_1 + \mathbf{r}_2)$ and the radius vector of the distance between the nucleons $\mathbf{r} = \frac{1}{2}(\mathbf{r}_1 - \mathbf{r}_2)$. We obtain the desired expansion of the wave function in states with given relative angular momentum of the nucleons by replacing $\mathbf{r}_1$ and $\mathbf{r}_2$ in the wave function (1) by their expression in terms of $\mathbf{R}$ and $\mathbf{r}$ and expanding the resulting expression in angular functions of Θ, Φ and ϑ, φ (spherical angles of the vectors $\mathbf{R}$ and $\mathbf{r}$, respectively). The expansion of the angular part of the wave function can be carried out at once, using the relations

$$r_1 \cos\theta_1 = R\cos\Theta + r\cos\vartheta; \qquad (3)$$

$$r_1 \sin\theta_1 e^{\pm i\varphi_1} = R\sin\Theta e^{\pm i\Phi} + r\sin\vartheta e^{\pm i\varphi},$$

$$r_2 \cos\theta_2 = R\cos\Theta - r\cos\vartheta;$$

$$r_2 \sin\theta_2 e^{\pm i\varphi_2} = R\sin\Theta e^{\pm i\Phi} - r\sin\vartheta e^{\pm i\varphi},$$

which follow from the definition of the vectors **R** and **r**.

From this it is found that the angular wave functions of the S-, P- and D-states of two nucleons are proportional to

$$\Lambda(L=0) \sim Y_{00}(\Theta,\ \Phi)\, Y_{00}(\vartheta,\ \varphi) / r_1 r_2; \qquad (4)$$

$$\Lambda(L=1,\ M_L=1) \sim [Y_{11}(\Theta,\ \Phi)\, Y_{10}(\vartheta,\ \varphi) - Y_{10}(\Theta,\ \Phi)\, Y_{11}(\vartheta,\ \varphi)] / r_1 r_2;$$

$$\Lambda(L=2,\ M_L=2) \sim [R^2 Y_{22}(\Theta,\ \Phi)\, Y_{00}(\vartheta,\ \varphi) - r^2 Y_{00}(\Theta,\ \Phi)\, Y_{22}(\vartheta,\ \varphi)] / r_1 r_2.$$

It is still necessary to find the expansion of the radial part of the wave function. It is easy to see that this expansion has the following form:

$$R(r_1)\, R(r_2) = \sum_{lm} B_l(r, R)\, Y_{lm}(\Theta, \Phi)\, Y_{l-m}(\vartheta, \varphi)\, (-)^m. \qquad (5)$$

Since the form of the function $R(r_i)$ is unknown, it is impossible to calculate the coefficients B_l. However, this is not necessary, since for any reasonable form of this function, the first term of this expansion is most important, so that approximately $R(r_1)R(r_2) \approx B_0(r, R)$, where B_0 is a function of the absolute values of the quantities **r** and **R**. The justification of this approximation is clear from the fact that r_1 and r_2, which are respectively equal to $(r^2 + R^2 \pm 2\mathbf{rR})^{1/2}$, depend strongly on the directions of the vectors **R** and **r** only when $r \approx R$ and $\mathbf{Rr} \approx rR$, which corresponds to a comparatively small region in the space of the variables r and R.

Collecting the result , we see that in states with $L = 0$ the nucleons are in S-states relative to each other and their center of gravity is in an S-state relative to the center of gravity of the nucleus; in the state with $L = 1$ the nucleons have a relative angular momentum $l = 1$ and their center of gravity moves relative to the center of gravity of the nucleus with unit angular momentum and, finally, that in a state with $L = 2$ the nucleons spend about half the time in an S-state relative to each other and about half the time in a D-state; their center of gravity also is in either an S- or a D-state relative to the center of gravity of the nucleus with approximately equal weights.

It is already possible to draw the conclusion confirmed by experiment[1] that the S-state of two nucleons ($L = 0$) is energetically most favorable, than the D-state ($L = 2$) and, finally, the state with $L = 1$ will have the highest energy. In fact, in the framework of the shell theory, the energies of these states differ only by the interaction energy of the two nucleons considered, and since the nucleons interact strongly only if they are in an S-state relative to each other, the states which are most favorable energetically will be those in which the nucleons spend the most time in S-states relative to each other.

We note one curious feature of our results. It is well known that the ground state of Li^6 is a ${}^3S_1$-state ($L = 0$, $S = 1$). As we have just seen, in this state two external nucleons in the p-shell have a relative angular momentum equal to zero and therefore, the ground state of Li^6 can be considered as a sum of an α-particle (closed shell $(1s)^4$] and a deuteron (two nucleons in the p-shell in an S-state relative to each other). It should be kept in mind, however, that this analogy is true only as long as we are concerned with the angular wave function of Li^6; the dependence of the wave function on the distance between the two external nucleons can be completely different from that in the deuteron.

2. GENERAL CASE OF n NUCLEONS IN THE SAME SHELL

In the case where more than two nucleons are outside the closed shell, the expansion is, in principle, carried out in the same way as in the case of two nucleons considered above. The calculation here, however, is extremely cumbersome; therefore, we limit ourselves to several general statements.

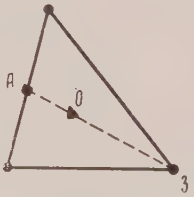

FIG. 1.

It is easy to show that the Pauli principle prohibits more than four nucleons from being in S-states relative to each other. (When we speak of several nucleons being in S-states relative to each other, we understand by that a state in which each nucleon of that group is in an S-state relative to any other nucleon of the group.) In fact, it is sufficient to note that nucleons which are in S-states relative to each other are also in S-states relative to the center of gravity*, and obviously, more than four nucleons cannot be in an S-state relative to the same point.

Thus, the maximum number of nucleons, which are at the same time in relative S-states, is equal to four. However, this number is an upper limit and cannot be attained in several states. The analysis shows that the criterion here is the scheme of Jahn of the given state.

In order to understand how this comes about, we consider a concrete example of five nucleons which are in a p-shell (this corresponds to the nuclei B^9 and Be^9). If four nucleons are in S-states relative to each other, then each of these is in an S-state relative to the general center of gravity. Consequently, in the coordinate system connected with their center of gravity, all of them are in the same spatial state and therefore, the spatial part of their wave functions in this system should be symmetrical in all four particles. But the symmetry property of wave functions does not change in the transition from one system of coordinates to another and thus we come to the conclusion that four nucleons, which are in the same shell, can be in S-states relative to each other in case the spatial part of the wave function is symmetrical in these nucleons. But the symmetry properties of the wave functions are determined by the scheme of Jahn, who shows how many particles of a given shell are in symmetrical states, or, in other words, how many particles can be simultaneously in one of the spatial states (that is, have the same value of the magnetic quantum number). Thus, for example, in the case of five particles in a p-shell, the states can be described by the following schemes of Jahn: [41], [32], [311], [221]. In states described by the scheme [41], the spatial part of the wave function is symmetrical in four nucleons and, consequently, the four nucleons can be in the same spatial state, because in these states the Pauli principle allows four nucleons to be simultaneously in the four S-states relative to each other. In those states, described by the scheme [32], the four nucleons cannot have the same values of the magnetic quantum number, and therefore they cannot be simultaneously in S-states relative to each other. As one sees from the scheme, in this case only three nucleons can be in one spatial state, and two others, in the other. Thus, the maximum number of nucleons simultaneously in S-states relative to each other is here equal to three. Here the remaining two nucleons can have the same magnetic quantum number and, consequently, be in S-states relative to each other.

Thus, we come to the following conclusion. In order for four nucleons in a given state to be simultaneously in S-states relative to each other, it is necessary that in the scheme of Jahn $[f_1, f_2, \ldots f_r]$, corresponding to this state, at least one number f_i must be equal to 4. If the Jahn scheme contains several numbers equal to 4: $f_1 = f_2 = \ldots = f_k = 4$, then in this state several groups of nucleons (four in each group) can exist in S-states relative to each other. The condition that in a given state three or two nucleons can be in relative S-states is formulated in a completely analogous fashion.

The conditions formulated above are necessary, but not sufficient. Direct calculations carried out for several states of three or four particles in the p-shell show, however, that in all those cases, when according to these conditions four or three nucleons can be simultaneously in S-states relative to each other, terms actually occur in the expansion of the wave function describing such groups of nucleons. The fact that, together with this term, the expansion gives also other terms corresponding, for example, to two nucleons in S-states and a third in a p-state relative to them, etc., is connected with the specific form of the wave functions of the shell model, which describe a system of noninteracting and, consequently, uncorrelated particles.

---

* The proof of this statement is based on the following lemma: if two nucleons are in an S-state relative to the same point, then their center of gravity is in an S-state relative to this point. This lemma is proved directly by expanding the single-particle wave functions in functions of the relative motion of the nucleons. The corresponding calculation differs from that given in Sec. 1 only in that there nucleons in a p-shell were considered, whereas it is necessary to consider two nucleons in an s-shell.

We consider the case of three nucleons (Fig. 1). Let the 1st and 2nd nucleon be in an S-state relative to the 3rd. Then, according to our lemma, the center of gravity of the 1st and 2nd nucleons A is also in an S-state relative to the 3rd nucleon and, consequently, the 3rd nucleon and the center of gravity of the 1st and 2nd nucleons is in an S-state relative to the general center of gravity of all those nucleons O. Beginning with the calculation of the 1st and 2nd nucleon, it is possible to show in the same way that they are in an S-state relative to the general center of gravity.

The generalization to the case of a larger number of particles is obvious.

3. CONCLUSIONS AND COMPARISON WITH EXPERIMENT

We enumerate the basic theses of our article:

1. Nucleons in the nucleus interact strongly only with those nucleons which are in S-states relative to them. The number of nucleons simultaneously in S-states relative to each other cannot exceed four.

2. Insofar as nucleons interact strongly only in S-states, one can expect that in the energetically most favorable states of the nucleus (the ground and first excited states) the nucleons will be strongly correlated with each other so that the largest number of nucleons can be in S-states relative to each other. Here, in analogy with the deuteron, with tritium and the α-particle, consisting respectively of two, three and four nucleons in relative S-states, one can expect the mutual binding energy of the nucleons in S-states to grow with the number of nucleons n faster than the number of bonds between nucleons $n(n-1)/2$. Therefore, the grouping of four correlated nucleons should be especially favorable energetically.

3. The existence of such groups of nucleons (four in each) in the nucleus is definitely indicated by the experimental data. We speak here of the great aggregate of data which is usually drawn upon as a basis for the α-particle model (see Ref. 1 for the literature). One should also bear in mind the following experimental facts:

a) From the analysis of the masses of light nuclei it is possible to find out at which excitation energies the first level with different isotopic spins T appears[3] in a nucleus with atomic number A. Here it turns out that there is a striking difference between the spectra of nuclei with $A = 4n$ and $A = 4n + 2$; in nuclei with $A = 4n$ the energy differences are small between first levels with $T = 1$ and $T = 2$, and between those with $T = 3$ and $T = 4$, and large between first levels with $T = 1$ and $T = 0$, and between those with $T = 2$ and $T = 3$ (Fig. 2a). In nuclei with $A = 4n + 2$ the former differences $2-1$ and $4-3$ are, on the other hand, large and the latter differences $1-0$ and $3-2$ are small (Fig. 2b). In addition, it is of interest that with nuclei of the same type ($A = 4n$ or $A = 4n + 2$) the general form of the spectrum changes only slightly in going from nucleus to nucleus and that all spectra are periodic in T with the period $\Delta T = 2$ (the differences $1-0$ or $3-2$; and $2-1$ or $4-3$ are almost the same for nuclei of the same type). The general picture of these spectra is as if the total isotopic spin of the nucleus were divided into the isotopic spins of separate groups of nucleons (with four in each group, and with nuclei of the type $A = 4n + 2$, in addition a group of two nucleons), which are successively excited with increasing energy of the nucleus;

b) If we construct a cruve of the dependence of the nucleon binding energy as a function of mass number in nuclei with a minimum neutron surplus ($N - Z$) for a given A, then we obtain a saw-toothed curve with maxima at $A = 4n$ and minima at $A = 4n + 1$ (Fig. 3). The picture is, especially for small A, very similar to that which would be obtained if separate groups (four in each) of strongly interacting nucleons existed in the nucleus, these groups weakly interacting with the other nucleons in the nucleus.

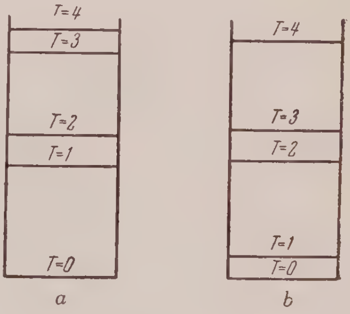

FIG. 2.

4. The shell-model wave functions contain a considerable proportion of states corresponding to the presence of one or several groups of nucleons in relative S-states. The scheme of Jahn for a given state is the criterion for how many particles in a given single-particle state are in S-states relative to each other, and for which groups they can be split up into (with two, three or four nucleons in a group). For example, in a given single-particle state described by the scheme [432] there are three groups of nucleons which are in relative S-states: groups of four, three and two particles, respectively. Similarly, in a state with the scheme [441] there exist only two groups with four nucleons in each.

Beginning from this correspondence between the Jahn scheme and the structure of the state, and remembering that the nucleons interact only in S-states, one can see why in the shell theory the states which are energetically most favorable are those states which, in the Jahn scheme, have the maximum possible number of fours, threes and twos (such states are often called states of maximum symmetry in the literature). For example, the state with the scheme [411] is energetically more favorable than the state with the scheme [321], and the latter is, in turn, more favorable than the state with the scheme [222].

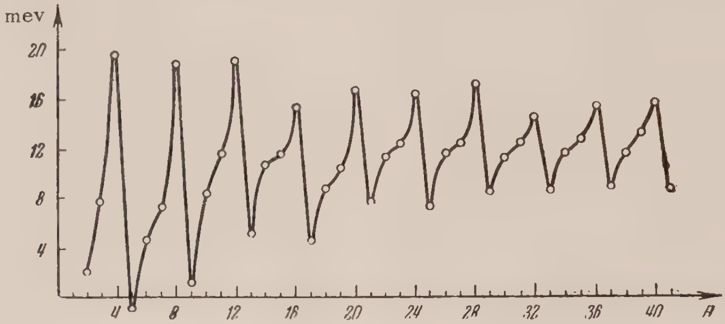

FIG. 3.

5. We note, finally, the connection between the classification outlined above of states according to the number of nucleons in S-states relative to each other, and the classification according to the seniority quantum number[2], defined as $v = n - 2x$, where n is the total number of particles in the shell and x is the number of pairs of nucleons (each nucleon is counted once) having total orbital momentum $L = 0$. As we saw from the example of the Li^6 nucleus, every such nucleon pair is in an S-state relative to the other. Therefore, the classification of states according to the value of v is a classification according to the number of pairs of nucleons (each nucleon counted only once!) which are in S-states relative to the other.

The main shortcoming of such a classification consists in the fact that each nucleon is counted only once and therefore this description of the state is not complete. In fact, if the nucleons interact only in S-states, then the total number of nucleon pairs in S-states is important for the determination of the energy of the state, and for this it may be necessary to count the same nucleon several times (if more than two nucleons are in an S-state relative to each other).

In conclusion, I would like to use the opportunity to thank Ia. A. Smorodinskii for numerous discussions and constant interest in this work.

---

[1] D. R. Inglis, Rev. Mod. Phys. 25, 390 (1953).

[2] H. A. Jahn, Proc. Roy. Soc. (London) A201, 516 (1950).

[3] A. I. Baz' and Ia. A. Smorodinskii, Usp. Fiz. Nauk 55, 215 (1955); D. C. Peaslee, Phys. Rev. 95, 717 (1954).

Translated by G. E. Brown
176

SOVIET PHYSICS JETP VOLUME 4, NUMBER 5 JUNE, 1957

Theory of Nonlocal Interaction

V. S. BARASHENKOV

(Submitted to JETP editor August 31, 1955)
J. Exptl. Theoret. Phys. (U.S.S.R.) 31, 837-841 (November, 1956)

The possibility of a Hamiltonian structure in the theory of nonlocal interaction is considered. By way of example, the one-dimensional oscillator is considered by Pauli's method. The initial integro-differential equations of motion and the canonical system of equations of motion obtained by Pauli's method are not equivalent. The procedure of Hayashi is shown to be internally inconsistent in any given order. Thus, conclusions about the essentially non-Hamiltonian character of nonlocal interactions are confirmed.

1. THE theory of nonlocal fields has been intensively discussed in recent years* in connection with the investigation of possible ways to remove the fundamental difficulties of field theory, which are reflected in the apparatus of the present theory in the presence of divergent quantities having no physical meaning, and also in the impossibility of consistently carrying through a renormalization program, and in the divergence of experimental and theoretical data in mesodynamics, etc. At present, we still know comparatively little about the laws of motion in small ($r \lesssim 10^{-13}$ cm, $\tau \lesssim 10^{-23}$ sec) space-time regions. Therefore, a theoretical study of possible deviations in small space-time regions from the requirements and principles, justified through phenomena taking place in macroscopic space-time regions, is completely in order and even unavoidable. At the present time the theory of nonlocal interactions should, in our view, be considered as a phenomenological study of the possibility of introducing signals which have velocities greater than light in small space-time regions into the framework of linear field theory, as a first rough phenomenological exploration into the region of possible structures of elementary particles.

In this connection, the investigation of problems concerning the Hamiltonian structure of theories of nonlocal interactions is important. By 1945-1948, it had been shown in the works of Blokhintsev and Markov[1, 4-7] that, in the theory with form-factors, the state of the physical system given on the hyper surface σ does not uniquely determine the state on the hyper surface $\sigma + \delta\sigma$ as a result of the presence of signals with velocity greater than light; in microscopic space-time regions; in other words, that the theory does not have a Hamiltonian structure and that it is necessary to formulate supplementary conditions** to pick out the solution with a definite physical meaning.

However, following this, work was published[5,6] in which it was asserted that a Hamiltonian formulation of the theory is possible. In addition, it was asserted that the conditions of integrability are satisfied, not only on a space-like hyper surface, but also in finite time-like regions, and that they are conserved in the limit of the transition to the theory with local interactions.

2. Pauli[5] set out to construct a theory with nonlocal interaction in Hamiltonian form, using the connection, which is well known in analytical dynamics, of the Hamiltonian system of the equations of motion with bilinear differential forms obtained from the equations of motion in the Lagrangian variables[8]. For example, for the case of the one-dimensional oscillator with nonlocal interaction, from the equation of motion

$$\ddot{q}(t) + \omega^2 \int_{-\infty}^{+\infty} K(t-t_1)\, q(t_1)\, dt_1 = 0 \qquad (1)$$

it is easy to obtain the bilinear differential form

$$I(t;\ D;\ \delta) = (Dq(t);\ \delta\dot{q}(t)) \qquad (2)$$

$$+ \frac{\omega^2}{2} \int_{-\infty}^{+\infty} \varepsilon(t-t_2)\, K(t_2-t_1)\, (Dq(t_2);$$

$$\delta q(t_1))\, dt_1 dt_2,$$

satisfying the condition

$$(d/dt)\, I(t;\ D;\ \delta) = 0. \qquad (3)$$

---

* A detailed bibliography is given in the reviews, Refs. 1 and 2, and also in Ref. 3.

** We do not consider the theory with a dynamically deformable form-factor.

Here

$$(Dq(t);\ \delta\dot{q}(t)) \equiv [Dq(t)\,\delta\dot{q}(t) - \delta q(t)\,D\dot{q}(t)];$$

$$\varepsilon(t) = \begin{cases} +1 & \text{for} \quad t > 0 \\ -1 & \text{for} \quad t < 0. \end{cases}$$

It is essential to note that in (2) the independent variations of the dynamical variables are taken at different times, which prevents the direct applications of theorems of analytical dynamics. In order to overcome this difficulty, Pauli proposed, starting from the equation of motion (1), to express $q(t_1)$ and $q(t_2)$ through the independent dynamical variables q and q, taken at time t, where

$$q(t_j) = q(t)\,Q_1(t_j - t) + \dot{q}(t)\,Q_2(t_j - t), \tag{4}$$

$$Q_1(t_j - t) = \cos k^*(t_j - t);$$

$$Q_2(t_j - t) = (1/k^*)\sin k^*(t_j - t)$$

and k^* is the root of the equation*

$$k^2 - \omega^2 \mathscr{K}(t) = 0;\ \mathscr{K}(k) = \int_{-\infty}^{+\infty} K(t)\,e^{-itk} dk. \tag{5}$$

The differential form (2), when expressed in terms of the independent variations $Dq(t)$, $\delta q(t)$ and $dq(t)$, also satisfies the condition

$$dI(t;\ D;\ \delta) + \delta I(t;\ d;\ D) + DI(t;\ \delta;\ d) = 0$$

and it can be considered as a bilinear covariant of some Pfaffian form[5], which can be reduced to canonical form by the corresponding transformation of dynamical variables[9].

The argument given above is essentially based on the possibility of solving the equation of motion (1) which, however, requires supplementary conditions to be given either in the whole interval $[-\infty;\ +\infty]$ or, in some cases, at the infinite points* $t = \pm\infty$. As a consequence, the initial equation of motion (1) and the canonical system of equations of motion found by the method of Pauli are not equivalent. In other words, the method of Pauli is equivalent to the replacement of integro-differential equations of motion by differential equations for which the problem of Cauchy can be formulated (i.e., which do not require supplementary conditions over the infinite interval) and the solutions of which coincide with those of the initial integro-differential equations of motion obtained from the variational principle.

Since the canonical system of equations of Pauli is constructed with the aid of a solution of the initial integro-differential equation (1) found previously, that system of equations is essentially superfluous and cannot give anything new over and above that given by Eq. (1).

3. In Hayashi's work[6] the method of Umezawa and Takahashi[7], which had previously been successfully applied to the theory with local interaction, was employed to write down the system of equations of motion for nonlocal interaction in Hamiltonian form.

The system of equations of motion of Bloch and Møller[11] for interaction of a scalar neutral field $A(x)$ and a scalar charged field $\psi(x)$ can be written in the form

$$\frac{\delta A_0[x;\ \sigma]}{\delta\sigma(x')} = -g\int \Delta_\mu(x - x')\,\psi^*(x_1)\,\psi(x_3)\,F(x_1x'x_3)\,d^4(x_1x_3) - \frac{\delta}{\delta\sigma(x')}\sum_{k=1}^{\infty} g^k a_k[x;\ \sigma]; \tag{6}$$

$$\frac{\delta\psi_0[x;\ \sigma]}{\delta\sigma(x')} = -g\int \Delta_m(x - x')\,A(x_2)\,\psi(x_3)\,F(x'x_2x_3)\,d^4(x_2x_3) - \frac{\delta}{\delta\sigma(x')}\sum_{k=1}^{\infty} g^k \varphi_k[x;\ \sigma], \tag{7}$$

$$A(x) = \sum_{k=0}^{\infty} g^k A_k[x;\ \sigma]; \tag{8}$$

$$\psi(x) = \sum_{k=0}^{\infty} g^k \psi_k[x;\ \sigma].$$

If the equations (6) and (7) are rewritten in the form

---

* It is assumed that the form-factor $K(t)$ is such that (5) has only two roots $k = \pm k^*$, differing by sign. Otherwise, the argument would have to be changed because in that case there will be a larger number of independent dynamical variables.

* Supplementary conditions must be given in the interval $[-\infty;\ +\infty]$ even in the simpler case of the solution of the homogeneous integral equation[10]

$$q(t) = \int_{-\infty}^{+\infty} K(t - t_1)\,q(t_1)\,dt_1.$$

$$\delta A_0[x;\ \sigma]/\delta\sigma(x') = i\,[H(x'/\sigma);\ A_0[x;\ \sigma]]; \tag{9}$$

$$\delta\psi_0[x;\ \sigma]/\delta\sigma(x') = i\,[H(x'/\sigma);\ \psi_0[x;\ \sigma]], \tag{10}$$

then, comparing the right-hand sides of Eqs. (6) and (9), (7) and (10), and choosing in a corresponding fashion expressions for the supplementary fields $a_k[x;\sigma]$ and $\varphi_k[x,\sigma]$, it is possible to find a formal expression* for the functional $H[x;\sigma]$, also in the form of a series in powers of g:

$$H[x;\ \sigma] = \sum_{k=1}^{\infty} g^k H_k[x;\ \sigma]^5. \tag{11}$$

The equations (9), (10) are integrable only if

$$\left[\frac{\delta}{\delta\sigma(x'')};\ \frac{\delta}{\delta\sigma(x')}\right] A_0[x;\ \sigma] = 0; \tag{12}$$

$$\left[\frac{\delta}{\delta\sigma(x'')};\ \frac{\delta}{\delta\sigma(x')}\right] \psi_0[x;\sigma] = 0,$$

or, taking into account the expansion, Eq. (11),

$$[\delta/\delta\sigma(x'');\ \delta/\delta\sigma(x')]\,A_0[x;\ \sigma]$$
$$= i\sum_{k=1}^{\infty} g^k\left\{\left[H_k(x'/\sigma);\ \frac{\delta A_0[x;\ \sigma]}{\delta\sigma(x'')}\right]\right.$$
$$-\left[H_k(x''/\sigma);\ \frac{\delta A_0[x;\sigma]}{\delta\sigma(x')}\right]$$
$$+\left[\frac{\partial H_k(x'/\sigma)}{\partial\sigma(x'')};\ A_0[x;\ \sigma]\right]$$
$$\left.-\left[\frac{\partial H_k(x''/\sigma)}{\partial\sigma(x')};\ A_0[x;\ \sigma]\right]\right\} \text{ etc.}$$

where the symbol $\partial/\partial\sigma(x)$ denotes differentiation on the hyper surface σ, and clearly enters into the expression for the Hamiltonian $H_k[x;\sigma]$.

Employing the expression for $H_k[x;\sigma]$ obtained by Hayashi[6], it can be shown that

$$\sum_{k=1}^{\infty} g^k\left\{\left[H_k(x'/\sigma);\ \frac{\delta A_0[x;\ \sigma]}{\delta\sigma(x'')}\right] - \left[H_k(x''/\sigma);\ \frac{\delta A_0[x;\ \sigma]}{\delta\sigma(x')}\right]\right\}$$
$$= i\,[[H_1(x'/\sigma);\ H_1(x''/\sigma)];\ A_0[x;\ \sigma]]\,g^2 + O(g^3)$$
$$= i\int F(x_1x_2x_3)\,F(x_1'x_2'x_3') \sum_{i,\,j=1}^{3} a_i a_j\,[\delta(x'-x_i)\,\delta(x''-x_j')$$
$$-\,\delta(x'-x_j')\,\delta(x''-x_i)]\ \Delta_m(x_3'-x_1)\,\psi_0^*[x_1';\ \sigma]\ \psi_0[x_3,\sigma]\{\Delta_\mu(x_2-x)\,A_0[x'_2;\sigma]$$
$$+\,\Delta_\mu(x_2'-x)\,A_0[x_2;\ \sigma]\}\,d^4(x_1\ldots x_3') + O(g^3);$$

$$\left[\frac{\partial H_2[x';\ \sigma[}{\partial\sigma(x'')};\ A_0[x;\ \sigma]\right] = -\frac{i}{2}\int F(x_1x_2x_3)\,F(x_1'x_2'x_3')$$
$$\times \sum_{i;\ j=1}^{3} a_i a_j\,\delta(x'-x_i)\,\delta(x''-x_j')\,\{\Delta_\mu(x_2-x)\,A_0[x_2';\ \sigma]$$
$$+\,\Delta_\mu(x_2'-x)\,A_0[x_2;\ \sigma]\}\,\{\Delta_m(x_1-x_1')\,\psi_0[x_3';\ \sigma]\,\psi_0[x_3;\ \sigma]$$
$$+\,\Delta_m(x_3-x_3')\,\psi_0^*[x_1;\ \sigma]\,\psi_0^*[x_1';\ \sigma]\}\,d^4(x_1\ldots x_3');$$

$$\left[\frac{\delta}{\delta\sigma(x'')};\ \frac{\delta}{\delta\sigma(x')}\right] A_0[x;\ \sigma] = -g^2\int d^4(x_1\ldots x_3')\,F(x_1x_2x_3)\,F(x_1'x_2'x_3')$$
$$\times \sum_{i;\ j=1}^{3} a_i a_j\,[\delta(x'-x_i)\,\delta(x''-x_j') - \delta(x'-x_j')\,\delta(x''-x_i)]$$
$$\times\{\Delta_\mu(x_2-x)\,A_0[x_2';\ \sigma] + \Delta_\mu(x_2'-x)\,A_0[x_2;\ \sigma]\}$$
$$\times\{\Delta_m(x_3-x_1)\,\psi_0^*[x_1';\sigma]\,\psi_0[x_3;\sigma] - {}^1\!/_2\Delta_m(x_1-x_1')\,\psi_0[x_3';\sigma]\,\psi_0[x_3;\sigma]$$
$$-\,{}^1\!/_2\Delta_m(x_3-x_3')\,\psi_0^*[x_1;\ \sigma]\,\psi_0^*[x_1';\ \sigma]\} + O(g^3).$$

An analogous expression can be obtained also for the field $\psi_0[x;\sigma]$. In the theory of nonlocal interaction these expressions do not go to zero, and consequently, the conditions (12) are not satisfied. Thus, the procedure of Hayashi is internally inconsistent in an arbitrary kth order ($k \neq \infty$), and the equations of motion do not have a Hamiltonian structure.

However, from consideration of Eqs. (6) and (7), it follows that the condition of integrability (12)

---

* In the particular case of the first approximation ($k = 1$) we obtain

$$H_1[x'\cdot\ \sigma] = -\int \psi_0^*[x_1;\ \sigma]\,A_0[x_2;\ \sigma]\,\dot{\psi}_0[x_3;\ \sigma]\,F(x_1x_2x_3)$$
$$\sum_{i=1}^{3} a_i\delta(x'-x_i), \tag{11$'$}$$

where $a_1 = a_3$; $a_1 + a_2 + a_3 = 1$. It is easy to convince oneself of the validity of this expression by the direct substitution of (11′) in the equations (9) and (10). After substitutions, these equations coincide with (6) and (7) to order g^2. The hyper surface σ clearly enters into $H_k[x;\sigma]$ in subsequent approximations ($k \geq 2$).

will be fulfilled in the limit of $k \neq \infty$, if for arbitrary* $k > 1$

$$\left[\frac{\delta}{\delta\sigma(x'')};\ \frac{\delta}{\delta\sigma(x')}\right] a_k[x;\ \sigma] = 0; \tag{13}$$

$$\left[\frac{\delta}{\delta\sigma(x'')};\ \frac{\delta}{\delta\sigma(x')}\right] \varphi_k[x;\ \sigma] = 0,$$

and the series (8) and (11) converge.

In this case the many-time equations of motion for the fields $A_0[x, \sigma]$ and $\psi_0[x; \sigma]$, and also the corresponding equation of Tomonaga-Schwinger in the interaction representation would have solutions for signals with velocity faster than light. These equations would also have single-valued solutions in finite time-like regions for transitions to the limit $\lambda \to 0$.

The investigation of the convergence of the series (8) and (11) presents considerable difficulty because of the complexity of the procedure of determining the quantities $H_k[x; \sigma]$; $a_k[x; \sigma]$ and $\varphi_k[x; \sigma]$. However, the very rapid increase in the number of terms in the expressions for $H_k[x; \sigma]$; $a_k[x; \sigma]$ and $\varphi_k[x; \sigma]$ as $k \to \infty$ gives no grounds for expecting that the series (8) and (11) will be convergent.

At this point there is an essential difference from the theory with local interaction, where--ignoring the divergence of the expansion in powers of the coupling constant g--after carrying out the procedure of renormalization, it is possible to use several of the initial terms in these expansions; this gives, in many cases, a sufficiently good asymptotic representation of the quantities considered, as is shown by comparison with experiment. In the theory with nonlocal interaction, it is impossible to stop at a finite number of terms, since the condition (12) is not fulfilled in this case.

It is also important to note that the theory of Hayashi and the method of Pauli are both essentially tially based on the possibility of solving the integro-differential equations of motion of Bloch and Møller, which is impossible without the use of supplementary conditions over the finite interval $x \epsilon [-\infty + \infty]$.

Thus, in both the Heisenberg representation and the interaction representation[3] it is not possible to construct a theory with nonlocal interaction which has a Hamiltonian structure.

In conclusion, I should like to thank D. I. Blokhintsev for interesting discussions and valuable advice, and also Prof. A. S. Davidov for discussion and helpful criticism.

---

* Since the fields $a_k[x; \sigma]$ and $\varphi_k[x; \sigma]$ in Ref. 6 can still be expanded in series in powers of the constant g, it is clear that the fulfillment of Eq. (12) to order g^{k^*} does not follow from the validity of Eq. (13) for some value of $k = k^* > 1$.

[1] M. A. Markov, Usp. Fiz. Nauk **29**, 269 (1946).

[2] M. A. Markov, Usp. Fiz. Nauk **51**, 317 (1953).

[3] V. S. Barashenkov, J. Exptl. Theoret. Phys. (U.S.S.R.) **28**, 579 (1955); Soviet Phys. JETP **1**, 467 (1955).

[4] D. I. Blokhintsev, J. Exptl. Theoret. Phys.(U.S.S.R.) **17**, 267 (1947); **18**, 566 (1948); Reports of Moscow State Univ., Fisika **3**, No. 77 (1945).

[5] W. Pauli, Nuovo Cimento **10**, 648 (1953).

[6] C. Hayashi, Progr. Theor. Phys. **10**, 533 (1953).

[7] H. Umezawa and Y. Takahashi, Progr. Theor. Phys. **9**, 501 (1953).

[8] E. T. Whittaker, *Analytical Dynamics* (Russian translation) ONTI, Moscow, 1937.

[9] P. K. Rashevskii, *Geometrical Theory of Equations with Partial Derivatives*, GTTI, Moscow, 1947.

[10] E. K. Titchmarsh, *Introduction to the Theory of Fourier Integrals* (Russian translation), State Publishing House, Moscow, 1948.

[11] P. Kristensen and C. Møller, Dan. Mat. Fys. Medd. **27**, No. 7 (1952); C. Bloch, Dan. Mat. Fys. Medd. **27**, No. 8 (1952).

Translated by G. E. Brown
177

SOVIET PHYSICS JETP VOLUME 4, NUMBER 5 JUNE, 1957

The Interaction of an Electron Hole with the Lattice Vibrations in a Homopolar Crystal

K. B. TOLPYGO AND A. M. FEDORCHENKO
Kiev State University

(Submitted to JETP editor September 24, 1955)
J. Exptl. Theoret. Phys. (U.S.S.R.) **31**, 845-853 (November, 1956)

The motion of a hole in a homopolar crystal of the diamond type is examined on the basis of the many-electron equations of Schrödinger. The presence of a hole is represented by the substitution of one paired bond by a monoelectronic one, which leads to the appearance of an additional force tending to deform the crystal. The corresponding term in the Hamiltonian is considered as the interaction of the hole with the deformations of the lattice. The meaning of the force obtained in the way for the problem of autolocalization of the hole, the scattering of current carriers by the lattice vibrations, and the theories of mobility, thermal emf and Nernst effect, is discussed.

1. INTRODUCTION

THE experimental study of the temperature dependence of the mobility, thermal emf and galvanomagnetic effects in Ge, and in particular in Si, indicates the insufficiency of the elementary theory of scattering of electron waves on the acoustic oscillations of the lattice[1], leading in particular to a temperature behavior of the mobility $u \sim T^{-3/2}$. For Ge of p-type the mobility more closely follows the formula $u \sim T^{-2.3}$ [2]. There are known to be anomalies in the dependence of the latter. The value of the effective mass of a hole in Ge is found to be different in different experiments (in particular, cyclotron resonance gives $m_{\text{eff}}/m \sim 0.04$[3]).

These anomalies are usually connected with the complex structure of the valence band at its upper edge (the triple degeneracy, whereby the surface of constant energy in k-space for small k differs from the spherical shape and the maximum energy corresponds to $\mathbf{k} \neq 0$ [4]). The corresponding calculations of the energy bands in Si, Ge and diamond[5-7], in general support this conclusion. However, in examining such detailed effects as the temperature dependence of mobility, the anisotropy of the resistivity in a magnetic field, etc., it is hardly possible completely to trust the one-electron approximation and the entire band scheme.

It is expedient to examine the motion of a hole on the basis of the many-electron problem and to find the energy of the crystal as a function of its wave vector, taking into account that the valence electrons of a homopolar crystal bring about bonding forces between the atoms therein. The formation of a hole must therefore produce the breaking of a bond and the appearance of forces tending to deform the crystal. There is no reason to expect that the corresponding potential energy will have the usual form $\mathbf{u}\nabla V$ ($\mathbf{u}$ is the displacement of a point of the crystal, V is the periodic potential). The destruction of the bond must lead to a strong interaction of the hole, particularly with the optical vibrations, which obliges us to examine the mobility anew. In the work of Kontorova[8], who studied the scattering of the conduction electrons by the acoustic vibrations of the lattice, using the dispersion law $\omega = \omega_0$ in place of the usually assumed law $\omega = ck$ (c is the velocity of sound), the mobility turned out to be proportional to $T^{-5/2}$, in better agreement with experiment than the usual theory gives[1]. In fact, the dispersion law $\omega = \omega_0$ can take place in the optical modes. However, the term $\mathbf{u}\nabla V$ assumed by all authors (among them Kontorova also) for the interaction with the vibrations cannot guarantee any strong scattering by the optical modes. Furthermore, the concept of a periodic potential V for the hole is devoid of meaning. In this case the interactions are more correctly considered as the alterations of the bonds between the atoms.

Finally, the mean free path of the current carriers is usually (except in Ge) of the order of or smaller than the de Broglie wavelength[9]. In each case the criterion for applicability of the perturbation theory, $uM/m \gg 500$ cm^2/sec/v (M is the mass of a current carrier, m is the electron mass, u is the mobility), shown by Pekar, is very seldom satisfied[10]. Therefore, the possibility is not excluded that the current carriers in a homopolar crystal, as in a polar one, are so-called "condensons" considered by Pekar and Deigen[11]. It is clear that the success of the computation of the "condensons" depends essentially on the correct choice for the forces of interaction between electron and lattice.

One of us (A.M.F.) has carried out a calculation of the wave functions and energy of the crystal with an electron missing from one of the bonds (hole)[12], taking into account a possible small deformation of the crystal. The results of this calculation and consideration of the consequences of the interaction found for a hole with the lattice vibrations are presented below.

2. THE WAVE FUNCTION AND ENERGY ON AN IDEAL CRYSTAL

We consider a diamond crystal, having in view that for Si, Ge and α-Sn, the structure of the lattice and the configurations of the valence electrons and bonds are quite similar.

In the union of C atoms into a crystal the wave functions of the valence electrons of each atom are deformed, with the formation of σ-bonds with each of the four nearest neighbors. The functions of the σ-bonds, considering the symmetry of the crystal, are approximately represented by the formula[13]

$$\psi_a(\mathbf{r}) = c_1 S(r) + 3c_2 P(r)\cos\vartheta, \tag{1}$$

where ϑ is the angle between the radius vector of the electron $\mathbf{r}$ and the radius vector of the nucleus nearest to the given electron, $S(r)$ and $P(r)$ are radial parts of the s- and p-functions, c_1, c_2 are approximation parameters.

We seek the wave-function of the crystal in the form of an antisymmetrized product of wave functions of the bonds of each pair of atoms a, b:

$$\Psi_{ab}(\mathbf{r}_1\sigma_1, \mathbf{r}_2\sigma_2) = [\alpha_a(\sigma_1)\beta_b(\sigma_2) - \alpha_a(\sigma_2)\beta_b(\sigma_1)][\psi_a(\mathbf{r}_1)\psi_b(\mathbf{r}_2) + \psi_a(\mathbf{r}_2)\psi_b(\mathbf{r}_1)], \tag{2}$$

α, β are spin functions equal to 1 or 0 for $\sigma = \pm 1/2$. In what follows we shall number the atoms with a cell-index l, the index of the atom in the cell $s = 1,2$, and we shall also introduce for each function the number of the bond $\alpha = 1, 2, 3, 4$.

Besides interchanges of the electrons inside the bond (2) we consider also interchanges between the wave functions belonging to the same atom. In Fig. 1 this corresponds to the interchange of electrons between Ψ_{ab} and Ψ_{ac} only in the terms $\psi_a(r_1)$ and $\psi_a(r_3)$. We neglect the exchange and the exchange energy of electrons found on different atoms but not on the same bond. The potential energy excludes the mutual interaction of all the valence electrons and the nuclei, screened by the internal electrons. The wave functions of the electrons on different nuclei we consider approximately orthogonal. The functions of the electrons of one atom but of different bonds are orthogonal on account of the angular parts [see Eq. (1)]. With these assumptions the energy of the system will be

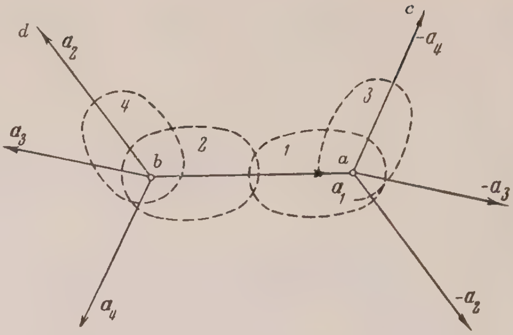

FIG. 1. Schematic representation of the bonds in a crystal of the diamond type. The dotted ovals *1, 2, 3, 4* represent the form of the ψ-cloud of electrons $\psi_a(1)$, $\psi_b(2)$, $\psi_a(3)$, $\psi_b(4)$. The vectors $\mathbf{a}_1$, $\mathbf{a}_2$, $\mathbf{a}_3$, $\mathbf{a}_4$ (or what is the same thing, a_{si}, since $a_{1i} = -a_{2i}$) represent the directions of the bonds.

$$\overline{\mathcal{H}} = \int\!\cdots\!\int \sum_P \varepsilon(P)\, P \prod_{ls\alpha} \Psi_{ls\alpha}(\mathbf{r}_{ls\alpha1}\sigma_{ls\alpha1}\mathbf{r}_{ls\alpha2}\sigma_{ls\alpha2})\, \overline{\mathcal{H}} \times \prod_{ls\alpha} \Psi_{ls\alpha}(\mathbf{r}_{ls\alpha1}\sigma_{ls\alpha1}\mathbf{r}_{ls\alpha2}\sigma_{ls\alpha2})\, d\tau; \tag{3}$$

P is the exchange operator for electrons, $\epsilon(P) = \pm 1$. In computing the average potential energy of an electron located on the bond ab of Fig. 1, atom c can be considered neutral. In the indicated approximation Eq. (3) breaks up into the sum of the average energies of the separate bonds; in this the energies of the interactions of the electrons on the bonds ab and ac are conveniently divided equally between these bonds. In atomic units,

$$\begin{aligned}\overline{\mathcal{H}} = \sum_{ls\alpha} \mathcal{H}_{ls\alpha}(\mathbf{R}_a,\ \mathbf{R}_b) = \sum_{ls\alpha} \Big\{ & 3\,(1+S^2)^{-2} \int \frac{1}{r_{13}}\,[\rho_a(1) + S\rho_{ab}(1)]\,[\rho_a(3) \\ & + S\rho_{ac}(3)]\,d\tau_1 d\tau_3 + 6\,(1+S^2)^{-2} \int \frac{1}{r_{23}}\,[\rho_b(2) + S\rho_{ba}(2)]\,[\rho_a(3) \\ & + S\rho_{ac}(3)]\,d\tau_2 d\tau_3 + \frac{Z^2}{a} - \frac{2Z}{1+S^2} \int \frac{1}{r_{a1}}\,[\rho_a(1) + \rho_b(1) + 2S\rho_{ab}(1)]\,d\tau_1 \\ & - \frac{6Z}{1+S^2} \int \frac{1}{r_{1c}}\,[\rho_a(1) + S\rho_{ab}(1)]\,d\tau_1 + (1+S^2)^{-2} \sum^{(9)} \int \frac{1}{r_{34}}\,[\rho_a(3) \\ & + S\rho_{ac}(3)]\,[\rho_b(4) + S\rho_{bd}(4)]\,d\tau_3 d\tau_4 \\ & + \frac{1}{2\,(1+S^2)} \int \frac{1}{r_{12}}\,[\psi_a(1)\,\psi_b(2) + \psi_a(2)\,\psi_b(1)]\,d\tau_1\,d\tau_2 \\ & - \frac{1}{1+S^2} \Big[\int \psi_a \Delta \psi_a d\tau + 2S \int \psi_a \Delta \psi_b d\tau \Big] \Big\}. \end{aligned} \tag{4}$$

Here the first two terms give the interaction of the electrons on bond *ab* with electrons found on the bonds of atom *a* with atoms of type *c*; the third term gives the interaction of the nuclei *a*, *b*; the fourth and fifth terms, the interaction of the electrons on bond *ab* with their own and also with neighboring nuclei; the sixth term, the interaction of electrons on bonds *bd* with electrons on the bonds *ac*. The last two terms represent the exchange and kinetic energy of the electrons of the bond *ab* (see Fig. 1).

3. THE WAVE FUNCTION AND ENERGY OF THE CRYSTAL WITH ONE ELECTRON REMOVED

In the presence of a hole it is necessary to find the wave function of the system in the form of a linear combination of functions $\Psi_{ls\alpha}$ of the type (2), in each of which one of the bond functions Ψ_{ab} is replaced with a function of one electron with indeterminate direction of spin

$$\varphi_b(r_{ls\alpha})\,[\alpha_l(\sigma_{ls\alpha}) + \beta_l(\sigma_{ls\alpha})], \tag{5}$$

that is,

$$\Psi = \sum_{ls\alpha} A_{ls\alpha} \Psi_{ls\alpha}. \tag{6}$$

If all the atoms are at rest at the lattic sites, then

$$A_{ls\alpha} = N^{-1/2} A_{s\alpha}(\mathbf{k}) \exp\,\{ik\mathbf{R}_s^l\}. \tag{7}$$

Substitution of Eqs. (5)-(7) into $\overline{\mathcal{H}}$ gives

$$\begin{aligned}\overline{\mathcal{H}}' = \sum_{s\alpha} \{ & |A_{s\alpha}|^2 \mathcal{H}_{s\alpha,\,s\alpha} + \sum_{\alpha'} \overset{*}{A}_{s\alpha} A_{s\alpha'} \mathcal{H}_{s\alpha,\,s\alpha'} \\ & + \sum_{\alpha' l} \overset{*}{A}_{s\alpha} A_{s'\alpha'} \mathcal{H}^{l-l'}_{s\alpha,\,s'\alpha'} \exp\{ik\,(\mathbf{R}^{l'}_{s'} - \mathbf{R}^{l}_{s})\}, \end{aligned} \tag{8}$$

where $\overline{\mathcal{H}}_{s\alpha,s\alpha}$ is the average value of the Hamiltonian $\overline{\mathcal{H}}$ over the functions $\Psi_{ls\alpha}$, which does not depend on the index l and which is obtained by striking out of the expression (4) the terms corresponding to the missing electron. $\overline{\mathcal{H}}_{sd,sd'}$ and $\overline{\mathcal{H}}^{l-l'}_{s\alpha,s'\alpha'}$ are matrix elements for the transition of a hole from the bond *ab* to the bond *ac* and correspongingly, from atom *a* to atom *b* on the same bond *ab*. Only these off-diagonal matrix elements are considered which correspond to the transition of an electron from one atom to the neighboring one on the same bond, or to the transition of an electron on a single atom from one bond to another.

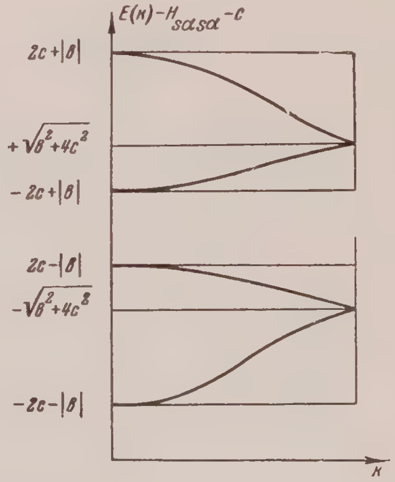

FIG. 2. Relative locations of the hole bands in the crystal of the diamond type. The energy levels (9)-(10) coincide, respectively, with the lower edge of the first and the upper edge of the second band.

Figure 1 gives the notation for the vectors $\mathbf{a}_1$, $\mathbf{a}_2$, $\mathbf{a}_3$, $\mathbf{a}_4$ characterizing the directions of the bonds 1, 2, 3, 4. The coefficient A_{12} designates that the hole is found on atom 1 and bond 2, etc.

Applying a variational principle, we obtain a system of linear equations for the eight coefficients $A_{s\alpha}$; setting the determinant of this system equal to zero, we obtain the eigenvalues of the energy:

$$E = \mathcal{H}_{s\alpha,\, s\alpha} + c \pm [b^2 + 4c^2 \pm 2bc\sqrt{\varphi(\mathbf{k})}]^{1/2}, \tag{9}$$

$$E = \mathcal{H}_{s\alpha,\, s\alpha} \pm b - c, \tag{10}$$

$$\varphi(\mathbf{k}) = 1 + \cos(k_x d/2)\cos(k_y d/2) + \cos(k_x d/2)\cos(k_z d/2) + \cos(k_y d/2)\cos(k_z d/2) \tag{11}$$

$$a = \mathcal{H}_{s\alpha,s\alpha} - E;\ c = \mathcal{H}_{s\alpha,s\alpha'};\ b = \mathcal{H}^{l-l'}_{s\alpha,s'\alpha'}$$

(d is the edge of the lattice cube); the roots (10) are double-valued. In analogy with the results of calculations for molecules, one can expect that $c > 0$ and $b < 0$ [13].

Figure 2 shows the arrangement of the bands. For hole conduction only the lowest band (signs –, +) is significant. The states in this band are nondegenerate and the energy for small k can be written as

$$E - \mathcal{H}_{s\alpha,s\alpha} - c = -2c - |b| + (\hbar^2/2\mu)k^2; \tag{12}$$

$$\hbar^2/2\mu = (d^2/16)|b|c/(2|c| + |b|).$$

In this way in our approximation it is impossible to explain the peculiarities observed in hole Ge (the presence of two effective masses, the selective infra-red absorption, the anisotropy of magnetoresistivity, etc.). Obviously, for this it is necessary to keep the exchange integrals for more weakly overlapping wave functions, which leads to a splitting of the levels (10) into four bands.

4. INVESTIGATION OF LOCAL HOLE COMPOUNDS OF LARGE RADIUS

If the atoms of the crystal are deformed, the coefficients $\mathcal{H}_{s\alpha,s\alpha}$, etc. depend on the coordinates of all the atoms, and the solution (7) will not obtain. However, it is possible to use the more general formula (6) with arbitrary constants $A_{ls\alpha}$, or their Fourier expansions:

$$A_{sl\alpha} = \frac{1}{N^{1/2}}\int A(\beta, \mathbf{k})\, A_{s\alpha}(\mathbf{k}) \exp\{i\mathbf{k}\,\mathbf{R}^l_s\}\, d\mathbf{k}. \tag{13}$$

The $A(\beta, \mathbf{k})$ are functions of $\mathbf{k}$ to be determined; they contain certain approximation parameters β. We assume that the "radius of the state" of our hole is large enough and that in the expansion (14) there enter only values of $\mathbf{k}$ small compared with the inverse lattice constant. Then it is possible to use Eq. (12) for the energy and assume approximately $A_{s\alpha}(k) \approx A_{s\alpha}(0)$. For the lowest bands:

$$A_{11} = A_{21} = A_{12} = A_{22} = 1/\sqrt{8};$$

$$A_{13} = A_{23} = A_{14} = A_{24} = -1/\sqrt{8}.$$

The average value of the Hamiltonian over the functions (6) will be :

$$\overline{\mathcal{H}}' = \frac{\hbar^2}{2\mu}\int A^*(\beta, \mathbf{k})\, \mathbf{k}^2 A(\beta, \mathbf{k})\, d\mathbf{k} + \iint A^*(\beta, \mathbf{k}')\, W[u^l_s]_{\mathbf{k}'\mathbf{k}}\, A(\beta, \mathbf{k})\, d\mathbf{k}\, d\mathbf{k}'; \tag{14}$$

$$W[\mathbf{u}^l_s]_{\mathbf{k}\mathbf{k}'} = \frac{1}{N}\sum_{\substack{sl\alpha\\ s'l'\alpha'}} A_{s\alpha} A_{s'\alpha'} \exp\{-i\mathbf{k}\mathbf{R}^{l'}_{s'} + i\mathbf{k}'\,\mathbf{R}^l_s\}\int \Psi_{l's'\alpha'}\, \hat{\mathcal{H}}\, \Psi_{ls\alpha}\, d\tau. \tag{15}$$

On account of the axial symmetry of the wave functions with $\mathbf{R}^l_s \neq \mathbf{R}^{l'}_{s'}$ the basic dependence of the integral (15) will be a dependence on the distances of the atoms occurring in the bond ll', ss'; $\mathbf{a}_{si} = \mathbf{R}^l_s - \mathbf{R}^{l'}_{s'}$. But if $\mathbf{R}^l_s = \mathbf{R}^{l'}_{s'}$, then the principal role in the dependence of the deformation will be played by the term for the interaction of an atom lacking an electron with the neighboring atom. We designate the corresponding terms

$$\mathcal{H}^{l-l'}_{s\alpha,s'\alpha'} + F_2(\mathbf{u}^l_s - \mathbf{u}^{l'}_{s'})\,\mathbf{a}_{si}/|\mathbf{a}_{si}| \text{ and } \mathcal{H}_{s\alpha,s\alpha} + F_1(\mathbf{u}^l_s - \mathbf{u}^{l'}_{s'})\,\mathbf{a}_{si}/|\mathbf{a}_{si}|. \tag{16}$$

The first components in (16) [after the summation in (15) over l and l'] are retained only for $\mathbf{k}' = \mathbf{k}$, and will give a constant contribution to $\overline{\mathcal{H}}$. In summing the second components, we shall change from the deformations $\mathbf{u}^l_s$ to the normal coordinates of the crystal $q_{\mathbf{f}\gamma}$ by the formula:

$$\mathbf{u}^l_s = \sum_{\mathbf{f}\gamma} \mathbf{u}^\gamma_s(\mathbf{f}) \exp\{i\mathbf{f}\mathbf{R}^l_s\}\, q_{\mathbf{f}\gamma}; \tag{17}$$

f is the wave vector, $\mathbf{u}_s^\gamma$ and γ are the amplitude and branch number of the eigenfrequencies. Substitution of (16) and (17) into (15) gives

$$W[\mathbf{u}_s^l]_{\mathbf{kk}'} = \sum_{\mathbf{f}\gamma}(\mathbf{u}_s^\gamma - \mathbf{u}_{s'}^\gamma e^{i\mathbf{fa}_{si}})\, q_{\mathbf{f}\gamma} \tag{18}$$

$$\times\left[F_1\mathbf{a}_{si} + \frac{1}{2}(e^{i\mathbf{ka}_{si}} + e^{-i(\mathbf{k}+\mathbf{f})\mathbf{a}_{si}})F_2\mathbf{a}_{si}\right]$$

$$\times\,\delta_{\mathbf{k}+\mathbf{f},\,\mathbf{k}'}/|\mathbf{a}_{si}|.$$

The local states of the hole will be stable if $\mathcal{H}' + U^0$ has a minimum and lies lower than the bottom of the band. Here U^0 is the work of deformation of the crystal, equal to

$$U^0 = {}^1\!/_2 N \sum \omega_{\mathbf{f}\gamma}^2 q_{\mathbf{f}\gamma}^* q_{\mathbf{f}\gamma}. \tag{19}$$

Adding (14) and (19) and minimizing the sum over $q_{\mathbf{f}\gamma}$ we find the equilibrium deformations of the atoms of the crystal, $\bar{q}_{\mathbf{f}\gamma}$. We take as an approximation

$$A(\beta, k) = (2\pi\beta^2)^{-3/4} e^{-k^2/4\beta^2} \tag{20}$$

and limit ourselves to only the interactions with the longitudinal vibrations of the lattice, whereby the optical and acoustic frequencies are $\omega_{\text{opt}} = \omega_0$, $\omega_{\text{ac}} = cf$. As the result of a moderatley long computation[12] we obtain:

$$\overline{\mathcal{H}} + U^0(\bar{q}_{\mathbf{f}\gamma}) \tag{21}$$

$$= (4F_1^2/3(2\pi)^{3/2}\omega_0^2|a_{si}|^2)[(B\hbar^2x^2/2\mu) - J(x)],$$

$$B = 9\rho(a_{si}(2\pi)^{3/2}\omega_0^2/4F_1^2, \quad x = \beta|\mathbf{a}_{si}|;$$

$$J(x) = x^3\Big\{1 - e^{-8x^2/3} + e^{-4x^2} \tag{22}$$

$$+ e^{-4x^2/3} + 4\frac{F_2}{F_1}e^{-x^2/2}(e^{-x^2/4} - e^{-19x^2/12}$$

$$+ e^{-9x^2/4} - e^{-11x^2/12})$$

$$+ 4\frac{F_2^2}{F_1^2}e^{-x^2}(1 - e^{2x^2/3} + e^{-x^2} + e^{-x^2/3})\Big\}$$

$$+ \frac{\sqrt{\pi}|a_{si}|^2\omega_0^2}{4c^2}\Big\{\frac{2}{\sqrt{\pi}}x - \sqrt{\frac{3}{8}}\,\Phi\Big(\sqrt{\frac{8}{3}}x\Big)$$

$$-\frac{1}{2}\Phi(2x) + \sqrt{\frac{3}{4}}\,\Phi\Big(\sqrt{\frac{4}{3}}x\Big)$$

$$+\frac{4F_2}{F_1}\Big[2\Phi\Big(\frac{x}{2}\Big) - \sqrt{\frac{12}{19}}\,\Phi\Big(\sqrt{\frac{19}{12}}x\Big)$$

$$-\frac{2}{3}\Phi\Big(\frac{3}{2}x\Big) + \sqrt{\frac{22}{11}}\,\Phi\Big(\sqrt{\frac{11}{12}}x\Big)\Big]$$

$$+4\frac{F_2^2}{F_1^2}e^{-x^2}\Big[\frac{2}{\sqrt{\pi}}x - \sqrt{\frac{3}{2}}\,\Phi\Big(\sqrt{\frac{2}{3}}x\Big)$$

$$-\Phi(x) + \sqrt{3}\,\Phi\Big(\frac{x}{\sqrt{3}}\Big)\Big]\Big\},$$

$$\Phi(x) = \frac{2}{\sqrt{\pi}}\int_0^x e^{-x^2}dx.$$

The quantity $J(x)$ for $x \ll 1$ behaves like

$$(a_{si}^2\omega_0^2/c^2)x^3({}^{11}\!/_9 + 13F_2/36F_1 + 7F_2^2/9F_1^2),$$

and for $x \gg 1$ like

$$(a_{si}^2\omega_0^2x/2c^2) + x^3.$$

The true order of magnitude of B can be obtained by considering that $F_1 \sim e^2/a_{si}^2$. Then $B\hbar^2/\mu \sim 50$. Consequently, the minimum of Eq. (21) is attained for $x \sim 30$, i.e., for very small radii of the state, when the effective-mass approximation is insufficient. Thus the existence in a homopolar crystal of states of large radius, similar to those in a polar crystal, appears hardly likely.

5. INVESTIGATION OF LOCAL HOLE STATES OF SMALL RADIUS

For local states of small radius it is convenient to use an expansion of the form (6), into which will enter only a small number of terms. From the form of the symmetries one can expect that the lowest local states of the hole will be of two types:

a) Coefficients $A_{ls\alpha}$ for a certain central atom are all equal to A, but on the four nearest neighbors to it only those $A_{ls\alpha}$ which refer to the bonds of these atoms with the central one are equal to $B \neq 0$;

b) The coefficients $A_{ls\alpha}$ for two neighboring atoms are equal to A, if α is their common bond, and to B if α denotes their bonds with neighbors. The normalization conditions will be

$$\text{a) } 4(A^2 + B^2) = 1, \quad \text{b) } 2A^2 + 6B^2 = 1. \tag{23}$$

The average value of the Hamiltonian $\mathcal{H}$ over the functions (5) is equal to

$$\text{a) } \overline{\mathcal{H}}' = 6A^2c + 4ABb + 4(A^2 + B^2)\mathcal{H}_{s\alpha,s\alpha}, \tag{24}$$

b)

$$\overline{\mathscr{H}}' = A^2b + 6ABc + 6B^2c + (2A^2 + 6B^2)\,\mathscr{H}_{s\alpha,s\alpha}. \qquad (25)'$$

Finding the minimum $\overline{\mathscr{H}}'$ and the coefficients A and B in both cases, we obtain

$$\text{a)}\ E = \mathscr{H}_{s\alpha,s\alpha} + {}^3/_4\, c \pm {}^1/_4 \sqrt{9c^2 + 4b^2}; \qquad (26)$$

$$B/A = -4b/[-6c \mp \sqrt{36c^2 + 16b^2}],$$

$$\text{b)}\ E = \mathscr{H}_{s\alpha,s\alpha} + {}^1/_2 c + {}^1/_4 b \pm {}^1/_4 \sqrt{(4c - b)^2 + 4bc}; \qquad (27)$$

$$B/A = -c/[c - {}^1/_2 b \mp {}^1/_2 \sqrt{(4c - b)^2 + 4bc}].$$

Comparison with Eqs. (12) shows that the autolocalization of the holes is energetically disadvantageous with respect to the bottom of the lowest hole band. It is easy to imagine that a calucation of the deformation of the lattice leads to a small change in the coefficients b and c and cannot change these results significantly. It is possible to interpret them thus: local states are not satisfactory since the short-range forces and the interactions of the holes with the deformations of a small number of atoms cannot compenstae for the increase of kinetic energy occurring upon localization of a hole.

6. INVESTIGATION OF THE INTERACTION OF A HOLE WITH THE LATTICE BY THE PERTURBATION METHOD

For the deformed crystal the wave function in the general case can be represented in the form (13), but the equations for the coefficients $A(\beta, k)$ are found from the variational principle by minimizing $\overline{\mathscr{H}}'$ (14). The average Hamiltonian of the crystal will be

$$\overline{\mathscr{H}}' = \int A(\mathbf{k}) \frac{\hbar^2 k^2}{2\mu} A(\mathbf{k})\, d\mathbf{k} \qquad (28)$$

$$+ \iint A(\mathbf{k})\, A(\mathbf{k}') \sum_{\mathbf{f}\gamma s i} (\mathbf{u}^{\gamma}_{s\mathbf{f}} - \mathbf{u}^{\gamma}_{s'\mathbf{f}} e^{i\mathbf{f}\mathbf{a}_{si}})$$

$$\times \left[F_1 \mathbf{a}_{si} + \frac{1}{2}(e^{i\mathbf{k}\mathbf{a}_{si}} + e^{-i(\mathbf{k}+\mathbf{f})\mathbf{a}_{si}})\, F_2 \mathbf{a}_{si}\right]$$

$$\times \frac{\delta_{\mathbf{k}+\mathbf{f},\,\mathbf{k}'}}{|a_{si}|}\, d_{\mathbf{k}} d_{\mathbf{k}'} + \frac{N}{2} \sum \omega^2_{\mathbf{f}\gamma} q^*_{\mathbf{f}\gamma} q_{\mathbf{f}\gamma}.$$

We consider the second term in Eq. (28) a small perturbation and determine the scattering of holes by the vibrations by the methods of perturbation theory. In the zero-order approximation the wave function and the energy of the system are equal to

$$A(\mathbf{k}_1)\, \delta(\mathbf{k} - \mathbf{k}_1)\, \Phi_{\ldots n_{\mathbf{f}\gamma}\ldots}(\ldots q_{\mathbf{f}\gamma}\ldots); \qquad (29)$$

$$E = (\hbar^2 k^2 / 2\mu) + \sum \hbar\omega_{\mathbf{f}\gamma} (n_{\mathbf{f}\gamma} + {}^1/_2).$$

Φ is an oscillator wave function, $n_{\mathbf{f}\gamma}$ the quantum numbers of the oscillators. We find the mixed matrix elements:

$$(\ldots n'_{\mathbf{f}\gamma\ldots}\, \mathbf{k}' \,|\, W \,|\, \mathbf{k} \ldots n_{\mathbf{f}\gamma\ldots}) \qquad (30)$$

$$= \sum_{si} (\mathbf{u}^{\gamma}_{s,\,\mathbf{k}'-\mathbf{k}} - \mathbf{u}^{\gamma}_{s',\,\mathbf{k}'-\mathbf{k}} e^{i(\mathbf{k}'-\mathbf{k})\mathbf{a}_{si}})$$

$$\times \left[F_1 \mathbf{a}_{si} + \frac{1}{2}(e^{i\mathbf{k}\mathbf{a}_{si}} + e^{-i\mathbf{k}'\mathbf{a}_{si}})\, F_2 \mathbf{a}_{si}\right]$$

$$\times \frac{1}{|\mathbf{a}_{si}|} \left\{ \begin{matrix} \sqrt{(\hbar / 2N\omega_{\mathbf{f}\gamma})\,(n_{\mathbf{k}'-\mathbf{k},\,\gamma} + 1)} \\ \sqrt{(\hbar / 2N\omega_{\mathbf{f}\gamma})\, n_{\mathbf{k}'-\mathbf{k},\,\gamma}} \end{matrix} \right\},$$

where all numbers $n_{\mathbf{f}\gamma}$ on the right and left are assumed equal, except for that one $n_{\mathbf{f}\gamma}$ for which $\mathbf{f} = \mathbf{k}' - \mathbf{k}$.

The probability of scattering of a wave with vector $\mathbf{k}$ into the solid angle $d\Omega$ is

$$W_{\mathbf{k}\mathbf{k}'} = (2\pi / \hbar)\,|(\ldots n_{\mathbf{f}\gamma} \qquad (31)$$

$$\mp 1 \ldots \mathbf{k} \pm \mathbf{f} \,|\, W \,|\, \mathbf{k} \ldots n_{\mathbf{f}\gamma\ldots})|^2 (V / 8\pi^3)(\mu k' / \hbar^2)\, d\Omega$$

in applying the conservation conditions

$$\mathbf{k}' = \mathbf{k} \pm \mathbf{f}; \quad (\hbar^2 / 2\mu)(k'^2 - k^2) = \pm \hbar\omega_{\mathbf{f}\gamma}. \qquad (32)$$

For the thermal electrons k is much smaller than a vector of the reciprocal lattice; therefore, there will be emitted and absorbed only phonons with $f \sim k$, but for them it is possible to take $|\mathbf{f}\mathbf{a}_{si}| \ll 1$ and expand the matrix element (30) into powers of $\mathbf{f}\mathbf{a}_{si}$:

$$(\ldots n_{\mathbf{f}\gamma} \mp 1 \ldots \mathbf{k} \pm \mathbf{f} \,|\, W \,|\, \mathbf{k} \ldots n_{\mathbf{f}\gamma} \ldots) \qquad (33)$$

$$= \sqrt{\frac{\hbar}{2N\omega_{\mathbf{f}\gamma}}} \Big\{ \sum_{si} \pm i\,(\mathbf{f}\mathbf{a}_{si})(\mathbf{a}_{si}\, \mathbf{u}^{\gamma}_{s'\mathbf{f}})(F_1 + F_2)$$

$$\mp i\,(\mathbf{f}\mathbf{a}_{si})\, \mathbf{a}_{si}\, (\mathbf{u}^{\gamma}_{sf} - \mathbf{u}^{\gamma}_{s'f})\, F_2 \Big\} \frac{1}{|\mathbf{a}_{si}|} \left\{ \begin{matrix} \sqrt{n_{\mathbf{f}\gamma} + 1} \\ \sqrt{n_{\mathbf{f}\gamma}} \end{matrix} \right\}.$$

As a simplification we assume that for the limit of long waves, for the longitudinal acoustic vibrations, $\mathbf{u}^{\gamma}_{s\mathbf{f}} \parallel \mathbf{f}$ and it does not depend on the index s, but $\omega_{\mathbf{f}\gamma} = cf$; for the optical vibrations $\mathbf{u}^{\gamma}_{1f} = -\mathbf{u}^{\gamma}_{2\mathbf{f}} \parallel \mathbf{f}$, and $\omega_{\mathbf{f}\gamma} = \text{const}$. We neglect the interaction with the transverse vibrations. Then

$$\sum_i (\mathbf{f}\mathbf{a}_{si})(\mathbf{u}^{\gamma}_{s\mathbf{f}}\,\mathbf{a}_{si})$$

$$=(2M)^{-1/2} f a_{si}^2 \sum_{i=1}^{4} \cos^2(\widehat{\mathbf{f}\mathbf{a}_{si}}) = 4a_{si}^2 f / 3\sqrt{2M}$$

and our matrix element is equal for the acoustic vibrations to

$$\pm\sqrt{\frac{\hbar}{2Nfc}}\,\frac{4f\,|\mathbf{a}_{si}|}{3\sqrt{2M}}\,(F_1+F_2)\cdot\left\{\begin{matrix}\sqrt{n_{\mathbf{f}\gamma}+1}\\ \sqrt{n_{\mathbf{f}\gamma}}\end{matrix}\right\}, \quad (34a)$$

and for the optical ones to

$$\pm\sqrt{\frac{\hbar}{2N\omega_{\gamma}}}\,\frac{4f\,|\mathbf{a}_{si}|}{3\sqrt{2M}}\,(F_1+3F_2)\left\{\begin{matrix}\sqrt{n_{\mathbf{f}\gamma}+1}\\ \sqrt{n_{\mathbf{f}\gamma}}\end{matrix}\right\}. \quad (34b)$$

Thus for the probability of scattering by the acoustic and optical vibrations we find, respectively,

$$W_{\mathbf{k}\mathbf{k}'} = \frac{\mu k'\,\Delta a_{si}^2\, f\,(F_1+F_2)^2}{9\pi^2 Mc\hbar^2}\left\{\begin{matrix}n_{\mathbf{f}\gamma}+1\\ n_{\mathbf{f}\gamma}\end{matrix}\right\}, \quad (35a)$$

$$W_{\mathbf{k}\mathbf{k}'} = \frac{\mu k'\Delta\,|a_{si}|^2 f^2 (F_1+3F_2)^2}{9\pi^2 M\omega_{\gamma}\hbar^2}\left\{\begin{matrix}n_{\mathbf{f}\gamma}+1\\ n_{\mathbf{f}\gamma}\end{matrix}\right\}, \quad (35b)$$

$\Delta = V/N$ is the volume of an elementary cell.

In calculating the mobility we assume that (1) the velocity of sound c is much smaller than the velocity of an electron, and the change of its energy in emitting or absorbing a phonon can be neglected; $k' \approx k$, $f = 2k \sin(\theta/2)$, θ is the scattering angle; (2) the temperature is not too low and for acoustic phonons $\hbar\omega \ll \varkappa T$ ($\varkappa$ = Boltzmann's constant). For the change of the energy-distribution functions as a result of collisions Eq. (35a) gives the usual quantity $(v/l)\chi\mathbf{v}$, where $\chi\mathbf{v}$ is the nonsymmetrical part of the distribution and l is the mean free path:

$$l = 9\pi Mc^2\hbar^4 / 8\mu^2\Delta\,|a_{si}|^2 (F_1+F_2)^2 \varkappa T. \quad (36)$$

This gives the usual dependence of mobility with temperature: $u \sim T^{-3/2}$. The interaction of a hole with the optical vibrations of the lattice is conveniently considered in two limiting cases: $\hbar\omega_{\text{opt}} \gg \varkappa T$ and $\hbar\omega_{\text{opt}} \ll \varkappa T$. In the former case only transitions with absorption are possible, and $k'^2 = 2\mu\omega_{\gamma}/\hbar \approx f^2$. Then the change of the distribution functions on account of scattering of the type (35b) gives the quantity $\chi\mathbf{v}/\tau$, where

$$\tau = 9\pi M\hbar^3\omega_{\gamma}\,(e^{\hbar\omega_{\gamma}/\varkappa T} - 1)/\mu\,(2\mu\omega_{\gamma}/\hbar)^{1/2} \quad (37)$$

$$\times\,\Delta\,|a_{si}|^2\, 2\mu\omega_{\gamma}\,(F_1+3F_2)^2.$$

The time of free path does not depend on the velocity of the hole. This gives a mobility proportional to $e^{\hbar\omega_{\gamma}/\varkappa T} - 1$.

For high temperatures, computation with Eq. (35b) leads to the approximations $k' = k$, $f = 2k\sin(\theta/2)$; $\overline{2n+1} = 2\varkappa T/\hbar\omega_{\gamma}$. This leads to the formula $(v/l)\chi\mathbf{v}$, with

$$l = 27\pi M\hbar^4\omega_{\gamma}^2 / 64\mu^2\Delta\,|a_{si}|^2 (F_1+3F_2)^2 \varkappa T k^2. \quad (38)$$

The free path length is inversely proportional to the square of the velocity and to the temperature. This gives a dependence of mobility on temperature of the form $u \sim T^{-5/2}$. If the exchange forces are more sensitive to the distance, then $|F_2| \gg |F_1|$ and the numerical factor of the probability of scattering by optical vibrations differs by a factor $9fc/\omega_{\gamma}$ from the probability of scattering by the acoustic vibrations.

Therefore, at high temperatures, the scattering by optical vibrations can prove to be dominating. This also leads to a different temperature dependence of the mobility: $u \sim T^{-5/2}$. At low temperatures, $\bar{n}_{\text{ac}} \gg \bar{n}_{\text{opt}}$ and $fc \ll \omega_{\gamma}$, and one must obtain the previous formula $u \sim T^{-3/2}$.

It is of interest to examine the thermo- and galvanoelectrical and magnetic effects, the coefficients of which are determined from the dependence of the free-path length on the velocity. In the case of a power-law $l \sim v^n$ the corresponding formulas were obtained in the work of one of the authors[14]. As is obvious from Eqs. (36)-(38), essentially new results can be obtained only at high temperatures: $\varkappa T \gg \hbar\omega_{\gamma}$, if the scattering by optical vibrations dominates. Thus, in the formula for the thermal emf

$$\alpha = \frac{\varkappa}{e}\left\{\frac{n}{2} + 2 + \ln\frac{2\,(2\pi\mu\varkappa T)^{3/2}}{h^3}\right\}$$

the constant component is equal here to 1 instead of 3, according to the theory of Davydov and Shmushkevich. Since at low temperatures the results coincide, the temperature dependence of α must also change correspondingly.

For the transverse Nernst-Ettingshausen effect:

$$\text{emf} = {}^1/_2 (n - 1)(\varkappa T/e) R\sigma H dT/dx$$

(H is the magnetic field, R is the Hall constant, σ is the electrical conductivity) one must expect an increase of the coefficient ($n - 1$) by a factor of three.

---

[1] B. I. Davydov and I. M. Shmushkevich, Usp. Fiz. Nauk **24**, 19 (1940).

[2] W. C. Dunlap, Phys. Rev. **79**, 286 (1950).

[3] Dresselhaus, Kip and Kittel, Phys. Rev. **92**, 827 (1953).

[4] F. G. Morin, Phys. Rev. **93**, 62 (1954).

[5] F. Herman, Phys. Rev. **88**, 1210 (1952).

[6] D. K. Holmes, Phys. Rev. **87**, 782 (1952).

[7] F. Herman and J. Callaway, Phys. Rev. **89**, 518 (1953).

[8] T. A. Kontorova, J. Tech. Phys. (U.S.S.R.) **24**, 2217 (1955).

[9] K. B. Tolpygo, J. Exptl. Theoret. Phys. (U.S.S.R.) **22**, 378 (1952).

[10] S. I. Pekar, J. Tech. Phys. (U.S.S.R.) **25**, 2030 (1955).

[11] S. I. Pekar and M. F. Deigen, J. Exptl. Theoret. Phys. (U.S.S.R.) **18**, 481 (1948).

[12] A, M. Fedorchenko, Thesis, Kiev State University, 1954.

[13] G. Gell-Mann, *Quantum Chemistry*, ONTI, Moscow-Leningrad, 1937.

[14] K. B. Tolpygo, Trudy Inst. Fiz., Akad. Nauk SSSR **3**, 52 (1952).

Translated by C. W. Helstrom
179

SOVIET PHYSICS JETP VOLUME 4, NUMBER 5 JUNE, 1957

On the Theory of the Stability of a Layer Located at a Superadiabatic Temperature Gradient in a Gravitational Field

V. N. GRIBOV AND L. E. GUREVICH
Leningrad Physico-Technical Institute, Academy of Sciences, USSR

(Submitted to JETP editor October 8, 1955)
J. Exptl. Theoret. Phys. (U.S.S.R.) 31, 854-864 (November, 1956)

The stability of a layer of liquid or gas in the presence of a superadiabatic temperature gradient is investigated for cases in which the upper and lower boundaries of the layer are not fixed, and convection arising in it may spread into stable regions bordering it.

1. INTRODUCTION

IT is known that the equilibrium of a layer located in a gravitational field is stable if its entropy S increases with ehight[1]. A series of authors[2-4] have investigated the stability of a layer bounded by horizontal planes on which the temperature is given and the vertical component of the velocity $v_z = 0$. However, in a whole series of cases, the layer in which instability arises, causing an increase of convection, is bordered on one or both sides by stable layers in which the temperature gradient is less than adiabatic, but in which the motion is propagated, occupying a region considerably exceeding the region of instability. The propagation of convection beyond the limits of the unstable layer may be understood in the following way.

With a random rise of a separate convective element, a lifting force is developed proportional to the difference between the temperature ϑ of this element and that of the surrounding medium, and increases monotonically up to the upper boundary of the unstable layer. Therefore, the convective element arrives at the upper boundary with maximum acceleration. Above the boundary, the temperature difference, and consequently the acceleration, start to decrease, becoming zero at some height, at which the rising velocity is maximum. Only then does the element begin to slow down, coming to rest at a still greater height.

Similar effects also result when a convective element sinks below the boundary of the unstable region. Thus, for example, the height of the troposphere, i.e., the region of convective mixing, reaches 15 km, i.e., exceeds by a factor of three the height of the layer where the temperature gradient is superadiabatic. Such propagation of convection beyond the limits of a region of instability may occur under the most diverse circumstances, from the mixing of molten metal, or oil in a well[5], to the effects of convective mixing in the atmospheres of stars[6] and their central regions[7], and also in interstellar matter.

Up to the present time, however, this possibility has not been taken into account in spite of the fact that is consideration may substantially change a series of conclusions.

We consider two cases: 1) convection may propagate only upwards; on the lower boundary the temperature is everywhere the same, and friction is negligible, and 2) convection may propagate both upwards and downwards from the unstable layer.

We shall assume that the vertical dimensions of all regions of mixing are sufficiently small so that a) throughout its extent the relative change of temperature $\Delta T/T$, and consequently the relative changes of all other essential quantities (density, viscosity, thermal conductivity, etc.) are negligibly small, and b) the density in the absence of convection may be considered independent of height.

2. CASE OF UPWARD PROPAGATION OF CONVECTION

The system of equations of stationary convection in a linear approximation has the form[1]

$$\nabla P = -\rho\beta g\vartheta + \eta\nabla^2\mathbf{v}, \quad \operatorname{div}\mathbf{v} = 0,$$
$$\rho T(\mathbf{v}\nabla S) = \varkappa\nabla^2\vartheta,$$

which is easily reduced to one equation

$$\Delta^3 v_z = \frac{\rho^2\beta g T(\partial S/\partial z)}{\varkappa\eta}\left(\frac{\partial^2}{\partial x^2} + \frac{\partial^2}{\partial y^2}\right)v_z. \qquad (1)$$

If the height h of the unstable layer is introduced as the unit of length, and if we assume that all variables, including v_z, are proportional to $\exp\{i(p_x x + p_y y)\}$, then Eq. (1) takes the form

$$(\partial^2/\partial z^2 - p^2)^3 v_z = -p^2 C v_z \quad 0 < z < 1, \qquad (2)$$

$$(\partial^2/\partial z^2 - p^2)^3 v_z = p^2 C_1 v_z \quad z > 1, \qquad (3)$$

where

$$C = \rho\beta g T\,|\partial S/\partial z|\,h^4/\varkappa\eta, \qquad (4)$$

and in C_1 we replace $|\partial S/\partial z|$ by the corresponding value $|\partial S_1/\partial z|$ above the unstable layer. We assume that $|\partial S_1/\partial z|$ is independent of z. The difference in sign occurs since $\partial S/\partial z < 0$, and $\partial S_1/\partial z > 0$.

On the lower boundary of the unstable layer $z = 0$, neglecting friction, we have[3]

$$v_z = 0, \quad \partial^2 v_z/\partial z^2 = 0, \quad \partial^4 v_z/\partial z^4 = 0, \qquad (5)$$

and on its upper boundary v_z and its derivatives up to fifth order inclusive must be continuous. At $z = \infty$,

$$v_z = 0. \qquad (6)$$

The solution of Eq. (2), satisfying conditions (5) on the lower boundary of the unstable layer, has the form

$$v_z = \sum_{k=1}^{3} A_k \operatorname{sh}\mu_k z, \qquad (7)$$

where A_k are arbitrary coefficients, and

$$\mu_k^2 = p^2 - (p^2 C)^{1/3} e^{2\pi i(k-1)/3}. \qquad (8)$$

Similarly, the solution of Eq. (3) satisfying boundary condition (6) at infinity has the form

$$v_z = \sum_{k=1}^{3} B_k e^{\nu_k z}, \qquad (9)$$

$$\nu_k^2 = p^2 + (p^2 C_1)^{1/3} e^{2\pi i(k-1)/3}, \quad \operatorname{Re}\nu_k < 0. \qquad (10)$$

The continuity conditions on the upper boundary of the unstable layer yield six equations. The condition that these equations have a solution is

$$\begin{Vmatrix} \sinh\mu_1 & \sinh\mu_2 & \sinh\mu_3 & 1 & 1 & 1 \\ \mu_1\cosh\mu_1 & \mu_2\cosh\mu_2 & \mu_3\cosh\mu_3 & \nu_1 & \nu_2 & \nu_3 \\ \mu_1^2\sinh\mu_1 & \mu_2^2\sinh\mu_2 & \mu_3^2\sinh\mu_3 & \nu_1^2 & \nu_2^2 & \nu_3^2 \\ \mu_1^3\cosh\mu_1 & \mu_2^3\cosh\mu_2 & \mu_3^3\cosh\mu_3 & \nu_1^3 & \nu_2^3 & \nu_3^3 \\ \mu_1^4\sinh\mu_1 & \mu_2^4\sinh\mu_2 & \mu_3^4\sinh\mu_3 & \nu_1^4 & \nu_2^4 & \nu_3^4 \\ \mu_1^5\cosh\mu_1 & \mu_2^5\cosh\mu_2 & \mu_3^5\cosh\mu_3 & \nu_1^5 & \nu_2^5 & \nu_3^5 \end{Vmatrix} = 0 \qquad (11)$$

This is the equation from which, with a fixed value of the parameter C_1 determining the degree of stability of the region lying above the unstable layer, we can determine the parameter C (i.e., the entropy gradient necessary for the realization of stationary convection) as a function of the parameter p, determining the horizontal dimensions of the convective cells. Basically, our problem consists of the determination of the minimum possible value of C, and the value of p corresponding to it.

We denote the columns of this determinant by Roman numerals and replace IV, V and VI, respectively, by the combinations

$$\mathrm{VI}' = \frac{1}{\nu_3 - \nu_2}\left[\frac{\mathrm{VI} - \mathrm{IV}}{\nu_3 - \nu_1} - \frac{\mathrm{V} - \mathrm{IV}}{\nu_2 - \nu_1}\right],$$

$$\mathrm{V}' = \frac{\mathrm{V} - \mathrm{IV}}{\nu_2 - \nu_1} - (\nu_1 + \nu_2)\,\mathrm{VI}',$$

$$\mathrm{IV}' = \mathrm{IV} - \nu_1\mathrm{V}' - \nu_1^2\,\mathrm{VI}'.$$

These transformations do not change the roots of the equations having physical significance. Here the equation takes the form of a determinant (11) equal to zero, in which the three right-hand columns are replaced by the following:

$$\begin{matrix} 1 & 0 & 0 \\ 0 & 1 & 0 \\ 0 & 0 & 1 \\ \gamma & \beta & \alpha \\ \alpha\gamma & \alpha\beta + \gamma & \alpha^2 + \beta \\ (\alpha^2 + \beta)\gamma & \alpha\gamma + \alpha^2\beta + \beta^2 & \alpha^3 + 2\alpha\beta + \gamma, \end{matrix} \qquad (12)$$

where

$$\alpha = \nu_1 + \nu_2 + \nu_3, \qquad (13)$$

$$\beta = -(\nu_1\nu_2 + \nu_1\nu_3 + \nu_2\nu_3), \quad \gamma = \nu_1\nu_2\nu_3.$$

a) *The case* $C_1 \ll 1$ (*the above-lying region near the stability limit*).

In this case, evidently the convective region will considerably exceed the dimensions of the unstable layer. On the other hand, the minimum of the parameter C must correspond to the possibility of comparable vertical and horizontal dimensions of the convective cells, and therefore it may be expected that in this case $p \ll 1$. The complete calculation shows that for minimum C, $p \sim \mu_k \sim C_1^{1/4}$.

We expand μ_k and $\cosh\mu_k$ in Eq. (11) in a series of powers of μ_k and limit ourselves to two terms of these series. If we then perform a transformation on the first three columns, completely similar to that described in the preceding section for the second three columns, and note that in view of Eq. (8), $(\mu_k^2 - p^2)^3 = -p^2C$, then the three left-hand columns of (11) take the form

$$\begin{matrix} 1 & 1/6 & 0 \\ 1 & 1/2 & 0 \\ 0 & 1 & 1/6 \\ 0 & 1 & 1/2 \\ {}^1/_6\,(p^6 - p^2C) & -{}^1/_2\,p^4 & 1 + {}^1/_2\,p^2 \\ {}^1/_2\,(p^6 - p^2C) & -{}^3/_2\,p^4 & 1 + {}^3/_2\,p^2. \end{matrix}$$

For future transformations we note that $\alpha \sim p$, $\beta \sim p^2$, $\gamma \sim p^3$ and we will subsequently neglect terms of order p with respect to unity.

We denote by Roman numerals I, II, ..., VI the rows of the determinant obtained, and perform two successive transformations without changing the magnitude of the determinant:

$$\mathrm{VI}' = \mathrm{VI} - \alpha\mathrm{V} - \beta\mathrm{IV}, \qquad (a)$$

$$\mathrm{V}' = \mathrm{V} - \alpha\mathrm{IV}, \quad \mathrm{IV}' - \mathrm{IV};$$

$$\mathrm{IV}'' = \mathrm{IV}' - \gamma\mathrm{I} - \beta\mathrm{II} - \alpha\mathrm{III}, \qquad \text{(b)}$$

$$\mathrm{V}'' = \mathrm{V}' - \gamma\mathrm{II} - \beta\,\mathrm{III}, \quad \mathrm{VI}'' = \mathrm{VI}' - \gamma\,\mathrm{III}.$$

The right lower quadrant of the determinant is transformed into a null matrix. Therefore, the equation is reduced to a determinant of the third rank, equated to zero. Expanding this determinant, we obtain in the indicated approximation

$${}^{1}/_{3}\, p^2 C = \alpha\beta + \gamma. \qquad (14)$$

Introducing $\xi = p/(p^2C_1)^{1/6}$, we have, in view of Eqs. (10) and (13),

$$\begin{gathered}\alpha = -(p^2C_1)^{1/3}\{\sqrt{\xi^2+1} + \sqrt{2(\xi^4-\xi^2+1)^{1/2}+2\xi^2-1}\}, \\ \beta = -(p^2C_1)^{2/3}\{\sqrt{\xi^2+1}\sqrt{2(\xi^4-\xi^2+1)^{1/2}+2\xi^2-1} + \sqrt{\xi^4-\xi^2+1}\}, \\ \gamma = -(p^2C_1)\sqrt{1+\xi^6}.\end{gathered} \qquad (15)$$

According to Eqs. (14) and (15),

$$\begin{gathered}C = C_1^{1/4} F(\xi), \\ F(\xi) = 3\xi^{-3/2}\{4\sqrt{1+\xi^6} + (2\xi^2-1)\sqrt{1+\xi^2} \\ + (1+\xi^2+\sqrt{\xi^4-\xi^2+1})\sqrt{2(\xi^4-\xi^2+1)^{1/2}+2\xi^2-1}\}.\end{gathered} \qquad (16)$$

The function $F(\xi)$ tends toward infinity for $\xi = 0$ and $\xi = \infty$, has a lower bound, and attains its minimum value $F_{\min} \approx 35$ at $\xi \approx 0.7$. Therefore,

$$C_{\min} \approx 35 C_1^{1/4}, \quad p_{\min} \approx 0.6\, C_1^{1/4}. \qquad (17)$$

These expressions justify the assumption used in calculating the determinant that for $C_1 \ll 1$, $\mu_k \ll 1$.

We call the total height h^* of the convective region the distance from the lower boundary of the unstable region to the point in the stable region at which the velocity v_z is $1/e$ times ths value at the lower boundary of this region, i.e.,

$$(h^* - h)/h \approx [\mathrm{Re}(-\nu_{1,2})]^{-1}, \qquad (18)$$

since ν_1 and $\mathrm{Re}\,\nu_2$ are approximately equal near $p \approx p_{\min}$. Keeping in mind that $C_1^{1/4} \ll 1$, we obtain from Eqs. (10) and (17)

$$h^* = C_1^{-1/4} h, \quad C_{\min} \approx 35\, h/h^*. \qquad (19)$$

b) *The case* $C_1 \gg 1$ (*the above-lying region possesses considerable stability*).

We show that in this case $p_{\min} \sim 1$, where $p_{\min}$ is the value of p corresponding to the minimum of criterion C. Therefore, $|\alpha| = |\nu_1 + \nu_2 + \nu_3| \gg 1$, $\beta \sim \alpha^2$, $\gamma \sim \alpha^3$. We will limit ourselves to the term in the determinant (11) containing α to the highest degree.

It is easily shown that the determinant A, consisting of the right lower quadrant of (11) is $\sim \alpha^9$, and all other minors have an order not exceeding α^8. Therefore, if terms of the order $1/\alpha$ are neglected, determinant (11) is reduced to the product of determinant A and an additional minor B, consisting of the elements of the upper left quadrant. Since $A \neq 0$, Eq. (11) reduces to $B = 0$. Expanding the determinant of the third rank, we obtain

$$\begin{gathered}\mu_1 \operatorname{cth}\mu_1(\mu_2^2 - \mu_3^2) + \mu_2 \operatorname{cth}\mu_2(\mu_3^2 - \mu_1^2) \\ + \mu_3 \operatorname{cth}\mu_3(\mu_1^2 - \mu_2^2) = 0.\end{gathered} \qquad (20)$$

Let us write $\mu_1 = iz$, $\mu_2 = \mu_3^* = x - iy$, where

$$\begin{gathered}x = {}^{1}/_{2}[2[p^4 + p^2(p^2C)^{1/3} \\ + (p^2C)^{2/3}]^{1/2} + 2p^2 + (p^2C)^{1/3}]^{1/2}, \\ y = {}^{1}/_{2}[2[p^4 + p^2(p^2C)^{1/3} \\ + (p^2C)^{2/3}]^{1/2} - 2p^2 - (p^2C)^{1/3}]^{1/2}, \\ z = [(p^2C)^{1/3} - p^2]^{1/2};\end{gathered} \qquad (21)$$

we agree to take the root with the positive sign. Then Eq. (20) takes the form

$$\begin{gathered}-z\cot z = [(x + \sqrt{3}\,y)\sinh 2x \\ + (\sqrt{3}\,x - y)\sin 2y]/(\cosh 2x - \cos 2y).\end{gathered} \qquad (22)$$

Since $x > 0$, $y > 0$ and, according to Eq. (21) $x > y$, the right-hand side of Eq. (22) is greater than zero. Hence, it follows that z is real, since if $\mu_1 = iz$ is real, then

$$-z\cot z = -\mu_1 \coth \mu_1 < 0.$$

Furthermore, it follows that $z > \pi/2$. But since [in view of Eq. (21)] $x > z$, we may neglect e^{-2x} compared with unity in the right-hand side of Eq. (22). Under these conditions, we obtain

$$-z\cot z = x + \sqrt{3}y. \tag{23}$$

Substituting $(p^2C)^{1/3} = z^2 + p^2$ on the right, and solving for p^2, we find

$$p^2 = {}^1/_2 z^2 [3^{-1/2}(\cot^4 z - 2\cot^2 z)^{1/2} - 1]. \tag{24}$$

This equation, together with the relation $z^2 = (p^2C)^{1/3} - p^2$, determines z and p as functions of the parameter C. We are interested in the minimum value of C at which these equations are joined, and the corresponding value of p. This means that in the (p^2, z^2) plane we must construct the curve determined by Eq. (24), and curves of $z^2 = (p^2C)^{1/3} - p^2$, and find the minimum value of C at which they intersect. This construction yields the values:

$$C_{\min} \approx 370, \quad z_{\min} \approx 2{,}7, \tag{25}$$

$$p_{\min} \approx 1.9, \quad x_{\min} \approx 3.4.$$

Let us note that in the usual statement of the problem, in which convection does not go beyond the limits of the unstable region, and $v_z = v_z^{\mathrm{II}} = v_z^{\mathrm{IV}} = 0$ at both boundaries,

$$C_{\min} \approx {}^{27}/_4\,\pi^4 \approx 665, \tag{26}$$

$$z_{\min} \approx \pi, \quad p_{\min} \approx \pi/\sqrt{2}.$$

In order to determine the total height of the region of mixing from Eq. (18), we take into account that [by Eq. (10)] with

$$(p^2C_1)^{1/3} \gg p^2, \quad \mathrm{Re}\,(-\nu_2) \approx {}^1/_2 (p^2C_1)^{1/6},$$

$$-\nu_1 \approx (p^2C_1)^{1/6},$$

the total height is determined by the least of these expressions, i.e.,

$$(h^* - h)/h = 2(p^2C_1)^{-1/6} \approx 1.6\, C_1^{-1/6}. \tag{27}$$

Thus, for $C_1^{1/6} \gg 1$, mixing occurs practically only in the unstable region. We must keep in mind that in all calculations for the case just considered we have neglected the quantity $1/\alpha \sim C_1^{-1/6}$, and consequently, the calculations are valid for $C_1^{1/6} \gg 1$.

3. CASE OF UPWARD AND DOWNWARD PROPAGATION OF CONVECTION

If convection is propagated both above and below the unstable layer, then we must add to Eqs. (2) and (3) a similar equation for $z < 0$, containing a parameter C_2 analogous to C_1. Also, the boundary conditions (5) are replaced by the condition $v_z = 0$ for $z \to -\infty$. The usual solution of this problem has the form:

$$v_z = \sum_{k=1}^{6} A_k e^{\mu_k z}, \quad 0 < z < 1, \tag{28}$$

$$v_z = \sum_{k=1}^{3} B_k^j e^{\nu_{kj} z}, \quad j = 1$$

$$\text{for} \quad z > 1, \quad j = 2 \quad \text{for} \quad z < 0;$$

$$\mu_k^2 = p^2 - (p^2C)^{1/3} e^{2\pi i(k-1)/3}, \tag{29}$$

$$\nu_{kj}^2 = p^2 + (p^2C_j)^{1/3} e^{2\pi i(k-1)/3},$$

$$\mathrm{Re}\,\nu_{k1} < 0, \quad \mathrm{Re}\,\nu_{k2} > 0.$$

The condition of continuity is equivalent to the condition that the following determinant be equal to zero:

$$\left\| \begin{array}{cccccccccccc} e^{\mu_1} & e^{\mu_2} & e^{\mu_3} & e^{\mu_4} & e^{\mu_5} & e^{\mu_6} & 1 & 1 & 1 & 0 & 0 & 0 \\ \mu_1 e^{\mu_1} & \cdot & \cdot & \cdot & \cdot & \mu_6 e^{\mu_6} & \nu_{11} & \nu_{21} & \nu_{31} & 0 & \cdot & \cdot \\ \mu_1^2 e^{\mu_1} & \cdot & \cdot & \cdot & \cdot & \mu_6^2 e^{\mu_6} & \nu_{11}^2 & \cdot & \nu_{31}^2 & 0 & \cdot & \cdot \\ \mu_1^3 e^{\mu_1} & \cdot & \cdot & \cdot & \cdot & \mu_6^3 e^{\mu_6} & \nu_{11}^3 & \cdot & \nu_{31}^3 & 0 & \cdot & \cdot \\ \mu_1^4 e^{\mu_1} & \cdot & \cdot & \cdot & \cdot & \mu_6^4 e^{\mu_6} & \nu_{11}^4 & \cdot & \nu_{31}^4 & 0 & \cdot & \cdot \\ \mu_1^5 e^{\mu_1} & \cdot & \cdot & \cdot & \cdot & \mu_6^5 e^{\mu_6} & \nu_{11}^5 & \cdot & \nu_{31}^5 & 0 & \cdot & \cdot \\ 1 & 1 & 1 & 1 & 1 & 1 & 0 & 0 & 0 & 1 & 1 & 1 \\ \mu_1 & \cdot & \cdot & \cdot & \cdot & \mu_6 & 0 & \cdot & \cdot & \nu_{12} & \nu_{22} & \nu_{23} \\ \mu_1^2 & \cdot & \cdot & \cdot & \cdot & \mu_6^2 & 0 & \cdot & \cdot & \nu_{12}^2 & \cdot & \nu_{23}^2 \\ \mu_1^3 & \cdot & \cdot & \cdot & \cdot & \mu_6^3 & 0 & \cdot & \cdot & \nu_{12}^3 & \cdot & \nu_{23}^3 \\ \mu_1^4 & \cdot & \cdot & \cdot & \cdot & \mu_6^4 & 0 & \cdot & \cdot & \nu_{12}^4 & \cdot & \nu_{23}^4 \\ \mu_1^5 & \cdot & \cdot & \cdot & \cdot & \mu_6^5 & 0 & \cdot & \cdot & \nu_{12}^5 & \cdot & \nu_{23}^5 \end{array} \right\| \tag{30}$$

We break this determinant into four parts of six rows and columns each, and denote them by

$$\left\| \begin{array}{cc} A & B \\ C & D \end{array} \right\|. \tag{31}$$

For the investigation of limiting cases which will be of interest to us in the future, it is convenient to subject this determinant to a transformation which results in C taking the form of a unit matrix. Determinant C is the Vandermond determinant, and can without difficulty be reduced to such a form by the use of combinations of only one of the columns. This transformation is broken into two parts:

a) We replace column II by the combination $(\mathrm{II} - \mathrm{I})/(\mu_2 - \mu_1) = \mathrm{II}_1$. Then we replace III by column III_1 which is obtained by subtracting column I from III, dividing by $\mu_3 - \mu_1$, subtracting II_1 from the new expression, and then dividing by $\mu_3 - \mu_2$. Similarly, we subtract successively from each column up to the sixth inclusive, all the preceding columns already changed by the corresponding transformations, each time dividing the difference by the corresponding difference of the form $\mu_i - \mu_k$.

b) From each (ith) column, beginning with the fifth, we subtract a linear combination of the succeeding columns, formed in the following way: the $(i+1)$th column is multiplied by $\mu_1 + \mu_2 + \ldots + \mu_i$, the $(i+2)$th column is multiplied by $\sum\limits_{j \le k \le i} \mu_j \mu_k$, the $(i+3)$th column by $\sum\limits_{j \le k \le l \le i} \times \mu_j \mu_k \mu_l$, etc. Here, a column already transformed by similar preceding operations, is subtracted each time.

The elements a_{ik} of determinant A then take the form:

$$a_{k1} = {}^1/_6\, (p^2C)^{-1/_3}\, (p^2 - p^2C) \sum_{n=1}^{6} e^{\mu_n} \mu_n^{k-3}\, e^{-4\pi i(n-1)/3},$$

$$a_{k2} = {}^1/_6\, (p^2C)^{-1/_3} \sum_{n=1}^{6} e^{\mu_n} \mu_n^{k-2}\, (\mu_4^4 - 3p^2\mu_n^2 + 3p^4)\, e^{-4\pi i(n-1)/3},$$

$$a_{k3} = {}^1/_6\, (p^2C)^{-1/_3} \sum_{n=1}^{6} e^{\mu_n} \mu_n^{k-1}\, (\mu_n^2 - 3p^2)\, e^{-4\pi i(n-1)/3},$$

$$a_{k4} = {}^1/_6\, (p^2C)^{-1/_3} \sum_{n=1}^{6} e^{\mu_n} \mu_n^{k-2}\, (\mu_n^2 - 3p^2) e^{-4\pi i(n-1)/3},$$

$$a_{k5} = {}^1/_6\, (p^2\ )^{-1/_3} \sum_{n=1}^{6} e^{\mu_n} \mu_n^{k-1}\, e^{-4\pi i(n-1)/3},$$

$$a_{k6} = {}^1/_6\, (p^2C)^{-1/_3} \sum_{n=1}^{6} e^{\mu_n} \mu_n^{k-2}\, e^{-4\pi i(n-1)/3}. \tag{32}$$

Expression (29) for μ_k was used to obtain Eq. (32).

The first three columns of determinant B and the second three columns of determinant D are transformed similarly to the transformation applied to the second three columns of determinant (11). As a result, these columns coincide with Eq. (12), except that instead of α, β, γ, we have, respectively, α_1, β_1, γ_1, α_2, β_2, γ_2, determined by the equations

$$\alpha_j = \nu_{1j} + \nu_{2j} + \nu_{3j}, \qquad (33)$$

$$\beta_j = -(\nu_{1j}\nu_{2j} + \nu_{1j}\nu_{3j} + \nu_{2j}\nu_{3j}),$$

$$\gamma_j = \nu_{1j}\nu_{2j}\nu_{3j}.$$

a) *The case in which the regions above and below the unstable layer are near the stability limit.*

As in Sec. 2a, under these conditions the μ_k corresponding to the minimum C are small, and therefore in the expression for a_{ki} we can expand e^{μ_k} in a series and limit ourselves to terms up to the second order, inclusively. Here, the expansions for all of the elements a_{ki} begin with terms of the order μ_n^4. Having performed these expansions, we apply transformations to the rows of determinants AB and C, identical to transformations a) and b) of determinant (11). After these transformations, the initial determinant is easily reduced to a determinant of the 6th order. Since under the conditions of interest to us $p \ll 1$, we neglect terms $\sim p$ with respect to unity. We take into account that $|\alpha| \sim p$, $|\beta| \sim p^2$, $|\gamma| \sim p^3$. Then the determinant of the 6th order takes the form

$$\begin{Vmatrix} \gamma_1 & \beta_1 & \alpha_1 & -1 & -1 & -1/2 \\ 1/2\,(p^2C - p^6) & \gamma_1 & \beta_1 & \alpha_1 & -1 & -1 \\ (p^2C - p^6) & -p^6 & \gamma_1 & \beta_1 & \alpha_1 & -1 \\ \gamma_2 & \beta_2 & \alpha_2 & -1 & 0 & 0 \\ 0 & \gamma_2 & \beta_2 & \alpha_2 & -1 & 0 \\ 0 & 0 & \gamma_2 & \beta_2 & \alpha_2 & -1 \end{Vmatrix}$$

Hence, we obtain, to the assumed approximation,

$$p^2C = F_1/F_2; \; F_2 = \beta^2 - \alpha\gamma + \alpha(\alpha_1\beta_2 - \alpha_2\beta_1), \qquad (34)$$

$$F_1 = \gamma^3 + \alpha(\gamma_1\alpha_2 - \gamma_2\alpha_1)$$

$$+ (\gamma_1\beta_2 - \gamma_2\beta_1)[\beta^2 - 2\alpha\gamma + \alpha(\alpha_1\beta_2 - \alpha_2\beta_1)]$$

$$+ \gamma\beta(\gamma_2\alpha_1 - \gamma_1\alpha_2),$$

where

$$\alpha = \alpha_2 - \alpha_1, \quad \beta = \beta_2 - \beta_1, \quad \gamma = \gamma_2 - \gamma_1.$$

From the explicit expressions for α_j, β_j, γ_j (33), and from Eq. (34), it follows that F_1 is a homogeneous function of the 9th degree of the quantities p, $(p^2C_1)^{1/6}$, $(p^2C_2)^{1/6}$, and F_2 is a homogeneous function of the 4th degree of the same quantities. Moreover, both functions are symmetric with respect to the parameters C_1 and C_2. We take the factor $(p^2C_2)^{9/6}$ outside the brackets in the numerator, and the factor $(p^2C_2)^{4/6}$ outside the brackets in the denominator, and introduce the symbol $\xi = p/(p^2C_2)^{1/6}$. Equation (34) then takes the form:

$$C = C_2^{3/4}\,\xi^{-1/2} J_1(\xi, C_1/C_2)/J_2(\xi, C_1/C_2). \qquad (35)$$

With a given value of the ratio C_1/C_2 and with $\xi \to \infty$

$$J_1(\xi, C_1/C_2) \sim \xi^9, \quad J_2(\xi, C_1/C_2) \sim \xi^4.$$

For $\xi \to 0$, both functions have finite positive values. Consequently, $C \to \infty$ when $\xi \to \infty \to 0$, and has a minimum at a finite ξ.

In view of the unwieldiness of the expressions for J_1 and J_2, we shall consider the case $C_1/C_2 \to 0$ and neglect $(C_1/C_2)^3$ with respect to ξ^2. This neglect will be justified by the calculations which show that C is a minimum when ξ is comparable with 1. Then

$$J_1 = (1+\xi^2)^{1/2}[67\xi^8 - 40\xi^6 + 40\xi^4 \qquad (36)$$

$$+ 27\xi^2 + 2\xi - 1] + 3\rho(1 + 8\xi^6)$$

$$+ \eta\xi^2[27\xi^6 + 8\xi^5 + 8\xi^4$$

$$+ 27] + (1+\xi^6)^{1/2}[64\xi^6 + 9\xi^3 - 1]$$

$$+ 3(1+\xi^2)^{1/2}\eta\xi(1 + 8\xi^6)$$

$$+ 8\rho\eta\xi^4[6\xi^2 + 5] + 3\xi^6 + 40\xi^9;$$

$$J_2 = (1+\xi^6)^{1/2}[(1+\xi^2)^{1/2} \qquad (37)$$

$$+ \eta + 6\xi] + (1+\xi^2)^{1/2}\xi(14\xi^2 - 3)$$

$$\eta\xi(3 + 3\rho + 11\xi^2) + 9\xi^2[\rho + (1+\xi^2)^{1/2}\eta] + 18\xi^4;$$

$$\rho = (\xi^4 - \xi^2 + 1)^{1/2}, \quad \eta = (2\rho + 2\xi^2 - 1)^{1/2}.$$

The minimum C occurs at $\xi \approx 0.4$, which corresponds to $p^2_{\min} \approx 0.06\, C_2^{1/2}$. Here,

$$C_{\min} \approx 1.5 \times C_2^{3/4}. \qquad (38)$$

Replacing C_2 by C_1 in this expression, we obtain the solution of the opposite limiting case $C_2 \ll C_1$.

A solution is also easily obtained for $C_1 = C_2$. In this case, $\alpha_1 = -\alpha_2, \beta_1 = \beta_2, \gamma_1 = -\gamma_2$. Then Eq. (34) takes the form:

$$C = \gamma_2 (\gamma_2^2 + 9p^6 + 6\alpha_2\gamma_2 p^2 - 3p^4\beta_2) / 3p^4 (3p^2 - \beta_2) \tag{39}$$

or, in the previous notation,

$$C = C_2^{3/4} \xi^{-5/2} J_1' (\xi) / J_2' (\xi). \tag{40}$$

C is a minimum at $\xi \approx 0.7$, and has the value

$$C \approx 7.3\ C_2^{3/4}. \tag{41}$$

Let us now turn to physical deductions from these calculations. Together with the minimum value of the criterion C, determined in the two cases considered by Eqs. (38) and (41), and the corresponding horizontal dimensions $\sim 1/p$, we are interested in the total height of the region of mixing

$$h^* = \{1 + 1 / (\mathrm{Re}\,(-\nu_{k1}))_{\min} + 1 / (\mathrm{Re}\,\nu_{k2})_{\min}\}\, h. \tag{42}$$

For $C_1 \ll C_2$:

$$\mathrm{Re}\,(-\nu_{k1}) = p,\ \ (\mathrm{Re}\,\nu_{k2})_{\min}$$

$$= {}^1/_2\, p\, [2 (\sqrt{\xi^4 - \xi^2 + 1} + \xi^2) - 1]^{1/2},$$

using the explicit expressions (29) for ν_{kj}, and the definition $\xi = p/(p^2 C_2)^{1/6}$.

Hence, remembering that in this case $p \ll 1$, we have

$$h^* / h \approx 3/p \approx 12\, C_2^{-1/4}, \tag{43}$$

whence

$$C \approx 2.5 \times 10^3 (h / h^*)^3. \tag{44}$$

For $C_1 = C_2$,

$$h^* / h \approx 2.4 / p \approx 4 C_2^{-1/4}, \tag{45}$$

whence

$$C \approx 470\, (h / h^*)^3. \tag{46}$$

Consideration of these limiting cases indicates that in the general case also, the dependence $C \sim (h/h^*)^3$ must be approximately conserved.

This result differs from the result of Sec. 2a obtained in the same approximation, but for the case in which mixing propagates only into the region lying above the unstable layer. There we found that $C \approx 35\, h/h^*$. A second essential difference is that in case (1) the total height of the region increased without limit when the stable region approached the stability limit, i.e., for $C_1 \to 0$. But in the case considered now, $h^* \to \infty$ only when $C_1 \to 0$ and $C_2 \to 0$ simultaneously. If either one of these stability criteria is finite, then h^* is also finite and is determined by this criterion.

b) *The case in which the regions lying above and below the unstable layer possess considerable stability* ($C_1 \gg 1$, $C_2 \gg 1$).

In this case $\alpha_1, \alpha_2, \beta_1, \beta_2, \gamma_1, \gamma_2$ cannot be small, since we would obtain formally the results of the preceding paragraph, from which it would follow that at $C = C_{\min}$, $p \sim C_{1,2}^{1/4}$, which would give large values of α, β, γ. Therefore, we will assume, and will confirm in the following calculation, that α, β and $\gamma \gg 1$.

We limit ourselves to the principal term of determinant (9), which as is easily shown, has the form:

$$\begin{Vmatrix} \gamma_1 & \beta_1 & \alpha_1 \\ \alpha_1\gamma_1 & \alpha_1\beta_1+\gamma_1 & \alpha_1^2+\beta_1 \\ (\alpha^2+\beta_1)\gamma_1 & \alpha_1\gamma_1+\alpha_1^2\beta_1+\beta_1^2 & \alpha_1^3+2\alpha_1\beta_1+\gamma_1 \end{Vmatrix} \cdot \tag{47}$$

$$\begin{Vmatrix} \gamma_2 & \beta_2 & \alpha_2 \\ \alpha_2\gamma_2 & \alpha_2\beta_2+\gamma_2 & \alpha_2^2+\beta_2 \\ (\alpha_2^2+\beta_2)\gamma_2 & \alpha_2\gamma_2+\alpha_2^2\beta_2+\beta_2^2 & \alpha_2^3+2\alpha_2\beta_2+\gamma_2 \end{Vmatrix} \cdot \begin{Vmatrix} a_{14} & a_{15} & a_{16} \\ a_{24} & a_{25} & a_{26} \\ a_{34} & a_{35} & a_{36} \end{Vmatrix}.$$

Since the first two factors in Eq. (47) are not equal to zero, omitting them and calculating the third determinant, we obtain:

$$\begin{gathered} 2\sinh\mu_1/\mu_1 - \sinh\mu_2/\mu_2 - \sinh\mu_3/\mu_3 + i\sqrt{3}\,(\sinh\mu_3/\mu_3 - \sinh\mu_2/\mu_2) \\ + 3(p^2C)^{1/3}\sinh\mu_1\sinh\mu_2\sinh\mu_3/\mu_1\mu_2\mu_3 - 2\sinh\mu_1\cosh\mu_1\cosh\mu_2/\mu_1 + \cosh\mu_1\,(\cosh\mu_2\sinh\mu_3/\mu_3 \\ + \sinh\mu_2\cosh\mu_3/\mu_2) + i\sqrt{3}\,(\sinh\mu_2\cosh\mu_3/\mu_2 - \cosh\mu_2\sinh\mu_3/\mu_3)\cosh\mu_1 = 0. \end{gathered} \tag{48}$$

Let

$$\mu_2 = x - iy, \quad \mu_3 = x + iy, \tag{49}$$

$$\begin{gathered} x = {}^1/_2\,\{2\,[p^4 + p^2(p^2C)^{1/3} + (p^2C)^{2/3}]^{1/2} + 2p^2 + (p^2C)^{1/3}\}, \\ y = {}^1/_2\,\{2\,[p^4 + p^2(p^2C)^{1/3} + (p^2C)^{2/3}]^{1/2} - 2p^2 - (p^2C)^{1/3}\}. \end{gathered} \tag{50}$$

When $p \gtrsim 1$, $x > 1$ and therefore as a first approximation we can neglect the first three terms in Eq. (48) compared with the remaining ones. This means neglecting the quantity e^{-x} with respect to unity. Then we obtain the equation

$$\coth\mu_1 = [2\mu_2\mu_3 - 3\,(p^2C)^{1/3}]\,/\,2\mu_1(x - \sqrt{3}y). \tag{51}$$

We consider the domain of values of p in which $p^2 < (p^2C)^{1/3}$. We let $\mu_1 = iz$, replace $(p^2C)^{1/3}$ by $z^2 + p^2$ in the right-hand side, and introduce $\eta^2 = z^2/p^2$. Then Eq. (5 1) takes the form:

$$\cot z = \frac{2\sqrt{\eta^4+3\eta^2+3} - 3\,(\eta^2+1)}{\sqrt{2\,(\eta^4+3\eta^2+3)^{1/2}+\eta^2+3} - \sqrt{3}\sqrt{2\,(\eta^4+3\eta^2+3)^{1/2}-\eta^2-3}} = f\,(\eta^2). \tag{52}$$

Hence

$$z = \operatorname{arc\,cot} f\,(\eta^2). \tag{53}$$

On the other hand, from the definitions of η^2 and z,

$$z = C^{1/4}\eta\,/\,(1+\eta^2)^{3/4}. \tag{54}$$

The minimum value of C for which the curves (53) and (54) in the (z, η) plane intersect, and the corresponding values of z, p and x, are

$$C_{\min} \approx 106, \quad p_{\min} \approx 2{,}6, \tag{55}$$
$$z \approx 1.2, \quad x \approx 3.4.$$

We turn now to the domain of values of p, $p^2 > (p^2C)^{1/3}$, for which μ_1 is real. A numerical solution of Eq. (61) shows that for $(p^2C)^{1/3}p^2 = \eta^2 > 0.8$, the criterion C is greater than $C_{\min} = 106$, and therefore this region does not interest us. On the other hand, for $\eta^2 \ll 1$, the right-hand side of (51) tends rapidly towards 1 with decreasing η^2. At $\eta^2 \approx 0.8$, the right-hand side of (51) differs from 1 by less than 0.06, and can be calculated by the series

$$1 + (17\,/\,128)\,\eta^8 + \cdots$$

For $\eta^2 < 0.8$, it may appear that $C < C_{\min}$, but here, according to Eq. (51), $\coth\mu_1 \to 1$ and differs from 1 by the quantity $e^{-2\mu_1}$. But since $\mu_1 = \sqrt{1-\eta^2 p}$, then for $\eta^2 < 0.8$, $\mu_1 \gtrsim p/2$, and therefore $e^{-2\mu_1} \sim e^{-p}$, i.e., is a magnitude which we neglected in deducing (51) from (48). This means that for $\eta^2 < 0.8$ we must set $\coth\mu_1 = 1$ in Eq. (51), but then it will have only the trivial solution $C = 0$. Therefore, we must return to Eq. (48) and investigate its behavior in this case.

For large p, $\mathrm{Re}\,\mu_2 = \mathrm{Re}\,\mu_3 = x$ is large, but $\mu_1 = p\sqrt{1-\eta^2}$ may be small when $\eta^2 \to 1$. Therefore, for $\eta^2 > 0.8$ we could also consider Eq. (28), but in the case $\eta^2 < 0.8$, we must return to Eq. (25) and consider both x and μ_1 large.

After straightforward transformations, Eq. (48) can be written in the form

$$\begin{aligned} -\alpha\sinh\mu_1\cosh 2x &+ 2\mu_2\mu_3[\sinh(2x-\mu_1) - \sinh\mu_1\cos 2y + 2\sinh\mu_1 - 2\sinh x\cos y] \\ &- 3(p^2C)^{1/3}[\sinh(2x-\mu_1) + \sinh\mu_1\cos 2y - 2\sinh x\cos y] \\ &- 2\mu_1(\sqrt{3}x+y)[2\sinh x\sin y - \cosh\mu_1\sin 2y] - \alpha\sinh(2x-\mu_1) \\ &+ 2\alpha\sinh x\cos y = 0, \end{aligned} \tag{56}$$

where

$$\alpha = 2\mu_2\mu_3 - 3(p^2C)^{1/3} \tag{57}$$

$$-2\mu_1(x-\sqrt{3}y) = (17/128)\,\eta^8 + \cdots$$

Clearly, the first term in Eq. (56) is dominant. If we limit ourselves only to this principal term, the equation will have a solution only for $C = 0$.

The whole of Eq. (56) will have only this solution for large p if for all the remaining terms, $C = 0$ is a root of multiplicity not less than that of the first term. Expansion in a series of powers of η^2 and $p\eta^2$ shows that $C = 0$ is a root of the same multiplicity for all the terms of the equation. We are therefore led to the conclusion that the solution (55) is unique.

Solution (55) shows that in the case considered, in which convection is propagated into the regions lying above and below the unstable layer, the minimum value of C is 2.5 times smaller than the value obtained in case 1, and is 6.5 times smaller than the value obtained in the usual case.

The total height of the region of mixing [determined by Eq. (42)] in this case is equal to

$$h^* = h[1 + 2/(p^2C_1)^{1/6} + 2/(p^2C_2)^{1/6}]. \tag{58}$$

The calculations of this section are valid under the conditions $C_1^{-1/6} \ll 1$, $C_2^{-1/6} \ll 1$.

---

[1] L. Landau and E. Lifshitz, *Mechanics of Continuous Media*, Sec. 4, GTTI, Moscow, 1953.

[2] Rayleigh, Phil. Mag. 32, 529 (1916).

[3] A. Pellew and R. V. Southwell, Proc. Roy. Soc. (London) **176A**, 312 (1940).

[4] S. Chandrasekhar, Proc. Roy.Soc. (London) **217A**, 306 (1953).

[5] G. A. Ostroumov, *Free Convection Under the Conditions of the Interior Problem*, GTTI, Moscow, 1952.

[6] A. Unsold, *Physics of Stellar Atmospheres*, 1949 (Russian translation).

[7] S. Chandrasekhar, *Intorduction to the Study of Stellar Structure*, 1939 (Russian translation).

Translated by D. Lieberman
180

SOVIET PHYSICS JETP VOLUME 4, NUMBER 5 JUNE, 1957

The Establishment of Thermal Equilibrium between Quanta and Electrons*

A. S. KOMPANEETS
Institute of Chemical Physics, Academy of Sciences, USSR

(Submitted to JETP editor October 15, 1955)
J. Exptl. Theoret. Phys. (U.S.S.R.) 31, 876-885 (November, 1956)

The role of the Compton effect in the establishment of equilibrium between quanta and electrons is considered in the nonrelativistic approximation.

1. INTRODUCTION

In order that radiation be considered as a closed system, it is appropriate to assume that it is contained in a vessel with perfectly reflecting walls. By itself, radiation in such a vessel cannot achieve thermodynamic equilibrium: the equations of electrodynamics are strictly linear and the exchange of energy between vibrations of different frequency, direction of propagation and polarization does not occur. Therefore, we must consider that there is in the container, besides the radiation, a suitably small "carbon particle" which does not appreciably disturb the field at any given moment, but which is capable of absorption and radiation of energy of all frequencies. Over a sufficiently long time, the absorption and emission of quanta by the "particle" leads to the establishment of thermodynamic equilibrium.

What will happen if we put a free electron in place of the material particle in the container? The container is taken to be large enough that we can neglect the quantization of the energy of the electron. The free electron does not absorb and emit, but only scatters quanta; therefore, the total number of quanta in the vessel does not change. What sort of equilibrium is established? If the occupation numbers n of the individual states are small in comparison with unity, then we can neglect induced transitions and assume that the probability of scattering a quantum in a certain state does not depend on the number of quanta occupying this state. In other words, we replace the factor $1 + n$ in the transition probability by 1. Then the same distribution will be set up among the quanta as in an ideal gas with a constant number of particles; i.e., we obtain a distribution of the form $n = e^{-h\omega/kT}$ (Wien's law). In this case the mean energy of the quantum is $3kT$. Planck's distribution is established only much later, since it exists as the result of induced emission.

The physical conditions under which Wien's distribution can exist can be represented in the following way. Let the matter be momentarily in a state with very high temperature, so that all the atoms are completely ionized, but assume radiation has not yet been produced. Then the absorption and emission of quanta will occur at the expense of a "free-free" mechanism. The corresponding emission process is nothing else than the bremsstrahlung of the electrons. This process is the more probable the lower the frequency of the emitted quantum. The same applies to the probability of the reverse process, the "free-free" absorption; therefore, for sufficiently low frequencies, thermal equilibrium will be established by means of the absorption and emission of quanta. For high frequencies, the probability of Compton scattering exceeds the absorption probability. Since the quanta are scattered by the moving electrons, their frequency can also be increased in the scattering. Initially, the number of quanta is not large: they will all tend toward thermal equilibrium independently of each other (i.e., induced processes will not constitute any significant part of all the scattering processes). The Wien distribution, with mean energy $3kT$, is established among such quanta.

For this reason, the transition of energy from matter to radiation will be much more rapid than if it took place at the expense of bremsstrahlung of the electrons. The bremsstrahlung quanta which have frequencies ω greater than a certain definite frequency ω_0, will quickly and irreversibly increase their energy by a Compton mechanism, tending to go to the maximum energy $3kT$.

In the Sections below, the distribution function will be found for quanta which undergo the Compton process. In the Appendix we shall consider what energy the quanta extract from the electrons in a body of finite dimensions.

---

* This research was completed in 1950 at the Institute of Chemical Physics, Academy of Sciences, USSR, Report No. 336.

2. THE KINETIC EQUATION

Let us write down the kinetic equation for the distribution function n of the quanta in an unbounded medium for the case of a single scattering. For generality, we shall at first not neglect induced processes. The equation has the following form:

$$\left(\frac{\partial n}{\partial t}\right)_C = -\int d\tau \int [n(1+n')\,N(\varepsilon) \qquad (1)$$

$$- n'(1+n)\,N(\varepsilon + h\omega - h\omega')]\,dW.$$

Here N is the distribution function for the free electrons, $d\tau$ is the element of phase space of the electrons, dQ is the differential probability of transition from a given state into another, compatible with the laws of conservation of energy and momentum. The index C on dn/dt denotes that only Compton processes are considered in the equation. Statistical equilibrium among the electrons in the plasma is established very quickly, independently of the radiation; therefore, we can consider the distribution function $N(\epsilon)$ to be Maxwellian. Then, if we replace n in Eq. (1) by the Planck distribution $n = (e^{h\omega/kT} - 1)^{-1}$, then the right and the left parts vanish, as they must.

We shall consider that the energy of the electrons is nonrelativistic; i.e., we assume that the inequality $kT \ll mc^2$ holds. Then the energy transferred in each separate act is small in comparison with the energy quantum $h\omega$: $\omega' - \omega \equiv \Delta \ll \omega$.

Making use of this inequality, we expand the integrand of Eq. (1) in a power series in Δ up to terms of the second order, inclusively. We set $h\omega/kT \equiv x$:

$$\left(\frac{\partial n}{\partial t}\right)_C = \left[\frac{\partial n}{\partial x} + n(1+n)\right]\frac{h}{kT}\int d\tau \int dW\,N(\varepsilon)\,\Delta \qquad (2)$$

$$+ \left[\frac{\partial^2 n}{\partial x^2} + 2(1+n)\frac{\partial n}{\partial x} + n(1+n)\right]$$

$$\times \frac{1}{2}\left(\frac{h}{kT}\right)^2 \int d\tau \int dW\,N(\varepsilon)\,\Delta^2.$$

The second integral on the right side of Eq. (2) is much easier to compute than the first ; but it suffices to compute only one of the two integrals. The other is determined from the condition that the equation ought to guarantee conservation of the total number of quanta in the scattering.

The laws of energy and momentum conservation in the nonrelativistic approximation are written in the form:

$$(h\omega/c)\,\mathbf{n} + \mathbf{p} = (h\omega'/c)\,\mathbf{n}' + \mathbf{p}', \qquad (3)$$

$$h\omega + p^2/2m = h\omega' + p'^2/2m.$$

Here $p^2/2m = \epsilon$, $\mathbf{p}$ and $\mathbf{p}'$ are the momenta of the electron before and after the collision, $\mathbf{n}$ and $\mathbf{n}'$ are the directions of propagation of the quantum. Eliminating p' from these equations, we obtain an equation which determines ω' as a function of ω, $\mathbf{p}$ and the angles of scattering. In this equation, we set $\omega = \omega' + \Delta$ and limit ourselves to terms that are linear in Δ, at least while we determine the integral which contains Δ^2. After simple transformations, we get

$$h\Delta = -\frac{hc\omega\,(\mathbf{p}, \mathbf{n} - \mathbf{n}') + (h\omega)^2\,(1 - \mathbf{n}\mathbf{n}')}{mc^2\,[1 + (h\omega/mc^2)\,(1 + \mathbf{n}\mathbf{n}') - \mathbf{p}\mathbf{n}/mc]}. \qquad (4)$$

It is valid to replace the brackets in the denominator of Eq. (4) with unity for the case of interest to us. The first term in the numerator has the order of magnitude $(kT/mc^2)^{3/2}$ and the second term the order $(kT/mc^2)^2$. But we shall determine the integral of Δ^2; therefore, the contribution of the first term in the averaging over the angles does not vanish. Consequently, upon substitution in Eq. (2), we must compute the following integral:

$$I = (h\omega/mc)^2 \int d\tau \int dW\,(\mathbf{p}, \mathbf{n} - \mathbf{n}')^2\,N(\varepsilon). \quad (5)$$

After averaging over all directions of $\mathbf{p}$ we get

$$I = {}^1\!/_3\,(h\omega/mc)^2 \int p^2 N(\varepsilon)\,d\tau \int |\mathbf{n} - \mathbf{n}'|^2\,dW. \quad (6)$$

The first integral is equal to $2m(3kT/2) = 3mkT$. In the second integral, we replace the Compton cross section in the nonrelativsitic approximation by the Thomson cross section, which is symmetric relative to scattering over the angles θ amd $(\pi - \theta)$, so that $\int \mathbf{n}\,\mathbf{n}'\,dW = 0$. The Thomson cross section does not depend on the energy of the quantum; consequently,

$$I = (h\omega)^2\,(kT/mc^2)\,c/l, \qquad (7)$$

where l is the Compton range, which is determined by the total cross section $(8\pi/3)(e^2/mc^2)$.

In order that Eq. (2) guarantee the conservation of the total number of quanta, we must set

$$\int d\tau \int dWN(\varepsilon)\,\Delta = (kT/mc^2)(c/l)\,h\omega\,(4 - h\omega/kT). \tag{8}$$

Equation (8) can be obtained in the following way. The kinetic equation for the quanta must look like a sort of conservation law

$$(\partial n/\partial t)_{\mathrm{C}} = -x^{-2}\,\partial(x^2 j)/\partial x, \tag{9}$$

where j is the "flow" of quanta in frequency space. Since Eq. (2) is of second order relative to x and contains the second derivative d^2n/dx^2 linearly, without a coefficient depending on n, the current must have the form of the sum of the first derivative $\partial n/\partial x$ and a certain function depending on n. But in the state of total equilibrium, when $n = (e^x - 1)^{-1}$, the flow vanishes. In this case, $\partial n/\partial x = -n(1+n)$. It therefore follows that

$$j = g(x)\,[\partial n/\partial x + n(1+n)], \tag{10}$$

where the function $g(x)$ must be determined. Substituting (10) in Eq. (9), and comparing with (2), we find that $g = -x^2$, and the unknown function $\Delta = x(4 - x)$, which is equivalent to (8). Equation (8) is in qualitative agreement with Wien's law: the energy of the quantum increases so long as $h\omega < 4kT$.

We now introduce the dimensionless time y by the expression

$$t = (mc^2/kT)(l/c) = y. \tag{11}$$

In these units, the kinetic equation is written in the following form:

$$\left(\frac{\partial n}{n y}\right)_{\mathrm{C}} = \frac{1}{x^2}\frac{\partial}{\partial x}\,x^4\left(\frac{\partial n}{\partial x} + n + n^2\right). \tag{12}$$

If $n \ll 1$, then this equation transforms into the linear relation

$$\left(\frac{\partial n}{\partial y}\right)_{\mathrm{C}} = \frac{1}{x^2}\frac{\partial}{\partial x}\,x^4\left(\frac{\partial n}{\partial x} + n\right). \tag{13}$$

This equation will also be solved. According to Eq. (13), it is easy to compute the time in which the energy of the quantum increases by a factor e as a result of the Compton effect. Multiplying both sides of Eq. (13) by x^3 and integrating, we get

$$\frac{d}{dy}\int_0^\infty nx^3\,dx = 4\int_0^\infty nx^3\,dx - \int_0^\infty nx^4\,dx. \tag{14}$$

While $h\omega$ is still small in comparison with kT, we can neglect the second integral on the right in (14). Here $x = x_{\mathrm{init}}e^{4y}$. This means that the time for the energy to increase by a factor e is equal to

$$\tau_{\mathrm{C}} = (mc^2/4kT)\,l/c. \tag{15}$$

3, BREMSSTRAHLUNG SPECTRUM

The bremsstrahlung spectrum in the general case appears rather complicated. We assume that such conditions are satisfied in which the Born approximation is applicable for the determination of the spectrum. These conditions are satisfied in the light elements for sufficiently high temperature (from several tens of kilovolts and higher). At the same time, it is taken into account that the inequality $kT \ll mc^2$ is satisfied. We shall not take into account the scattering of electrons on electrons, with emission of quanta, since such a process makes a significant contribution only in very light materials and in each case it does not exceed the bremsstrahlung emission on nuclei, always remaining smaller than it.

In the Born approximation, and in the nonrelativistic case, the bremsstrahlung cross section is [Ref. 1, p. 183, Eq. (18)]:

$$d\sigma = \frac{3}{8}\frac{Z^2e^6}{mhc^3}\frac{1}{\varepsilon}\ln\frac{(\sqrt{\varepsilon} + \sqrt{\varepsilon - h\omega})^2}{h\omega}\cdot\frac{d\omega}{\omega}. \tag{16}$$

In order to go over to the total number of quanta of a given frequency that are emitted per second, we need to multiply the cross section by $LN(\epsilon)\,v\,d\tau$ (L is the number of nuclei per unit volume, v is the velocity of the electron), integrate over all states of the electron and refer to the number of states of a quantum of given frequency per unit volume. Thus we obtain the equation

$$\frac{1}{\tau_{\mathrm{B}^0}} = 3\sqrt{\frac{\pi^3}{8m^3kT}}\,\frac{Z^3L^2e^6}{h\omega^3}\,e^{-h\omega/2kT}K_0\left(\frac{h\omega}{2kT}\right) \equiv B\,\frac{e^{-x/2}K_0(x/2)}{h\omega^3}. \tag{17}$$

Here K_0 is the Macdonald function (Ref. 2, p. 206), τ_{B}^0 is the magnitude of the time interval which characterizes the bremsstrahlung. If we take into consideration the inverse absorption of quanta and their induced emission, then we obtain the rate of change of the quanta as a result of bremsstrahlung and free-free absorption:

$$(\partial n / \partial t)_{\mathrm{B}} = (1 / \tau_{\mathrm{B}}^{0}) \left[(1 + n) - n e^{h\omega / kT} \right]. \tag{18}$$

The derivative vanishes if we put the Planck distribution in place of n

Digressing from the Compton process, and assumign that the total change dn/dt appears on the left side of Eq. (18), we can integrate (18). If $n(0) = 0$, then we get

$$n = \frac{1}{e^{h\omega / kT} - 1} \left(1 - \exp\left\{ - \frac{t}{\tau_{\mathrm{B}}^{0}} \left(e^{h\omega/kT} - 1 \right) \right\} \right). \tag{19}$$

It then follows that the relaxation time for thermal equilibrium of the quanta, for a pure bremsstrahlung mechanism, is equal to

$$\tau_{\mathrm{B}} = \tau_{\mathrm{B}}^{0} / (e^{h\omega / kT} - 1). \tag{20}$$

The total kinetic equation, which takes into account the Compton and bremsstrahlung processes, is now written

$$\left(\frac{\partial n}{\partial t}\right)_{\mathrm{C}} + \left(\frac{\partial n}{\partial t}\right)_{\mathrm{B}} = \frac{\partial n}{\partial t} = \frac{kT}{mc^2} \frac{c}{l} \frac{1}{x^2} \frac{\partial}{\partial x} x^4 \left(\frac{\partial n}{\partial x} + n + n^2 \right) + \frac{1}{\tau_{\mathrm{B}}^{0}} \left[(1 + n) - n e^{x} \right]. \tag{21}$$

Going over again to the dimensionless time y, we get

$$\frac{\partial n}{\partial y} = \frac{1}{x^2} \frac{\partial}{\partial x} x^4 \left(\frac{\partial n}{\partial x} + n + n^2 \right) + \frac{4\tau_{\mathrm{C}}}{\tau_{\mathrm{B}}^{0}} \left[(1 + n) - n e^{x} \right]. \tag{22}$$

The braking time τ_{B} decreases with decrease in the frequency, for example, as ω^2; therefore, the quanta for sufficiently low frequencies will always undergo transition to statistical equilibirum in processes of emission and absorption. The quanta of high frequencies will be taken up by the Compton process and thus increase their frequency, approaching the Wien distribution. It should not be thought that frequency of the quantum increases monotonically; Eq. (12) is of second order, of the diffusion type. The approximation of quanta to incomplete equilibrium (with respect to energy but not with respect to number) is in the fashion of Brownian motion. The limit of the frequency, for which the Compton process takes up the quanta more rapidly than it succeeds in being absorbed, is determined by the following estimate: $\tau_{\mathrm{C}}/\tau_{\mathrm{B}} \sim 1$. Substituting τ_{C} and τ_{B} in it, we get

$$(9\sqrt{\pi} / 64\sqrt{2}) L Z^2 m^{1/2} c^5 h^2 e^2 \times (kT)^{-9/2} e^{-x_0 / 2} x_0^{-3} K_0(x_0 / 2)(e^{x_0} - 1) \sim 1. \tag{23}$$

The entire process considered (i.e., the establishment of equilibrium by the Compton effect) presents interest only in the case in which $h\omega_0 \ll kT$, since only then is there a frequency interval, $\omega \gg \omega_0$, in which the Compton effect plays an essential role. For small x_0, the function K_0 can be replaced by an expansion in x_0 (Ref. 2, p. 96): $K_0(x_0/2) = \ln(4/\gamma x_0)$, where $\ln \gamma = 0.577$. Thus x_0 is determined by the equation

$$A x_0^{-2} \ln(2.35 / x_0) \sim 1. \tag{24}$$

This equation has meaning only if A is a small number.

We now compare the transfer of energy from the electrons to the quanta by pure bremsstrahlung and by the Compton mechanism*.

The total energy of the quanta emitted by the electrons per unit volume is

$$\left(\frac{dE}{dt}\right)_{\mathrm{B}} = \int \frac{1}{\tau_B} h\omega \frac{\omega^2 \, d\omega}{\pi^2 c^3} = \frac{BkT}{\pi^2 c^3 h} \int_0^\infty dx \, e^{-x/2} K_0\left(\frac{x}{2}\right) = \frac{2BkT}{\pi^2 c^3 h} \tag{25}$$

(Ref. 2, p. 424). All quanta whose frequencies are greater than ω_0 transfer energy to the electrons by the Compton mechanism; on the average the energy of the quanta approaches $3kT$. Therefore, the energy transferred per unit time is

$$(dE / dt)_{\mathrm{C}} = 3kT \int_{\omega_0}^{\infty} \tau_{\mathrm{B}}^{-1} \omega^2 \, d\omega / \pi^2 c^3. \tag{26}$$

The principal contribution to the integral is provided by the low frequencies. Therefore, we can replace the function K_0 under the integral by its approximate value; to avoid divergence at the upper limit, we do not integrate to infinity, but to $\omega = kT/h$. We get

---

* This comparison was pointed out to us by L. D. Landau.

$$\left(\frac{dE}{dt}\right)_{\mathrm{C}} = 3kT\,\frac{B}{\pi^2 c^3 h}\int\limits_{\omega_0}^{kT}\frac{d\omega}{\omega}\ln\frac{4kT}{\gamma h\omega} \tag{27}$$

$$\sim \frac{3}{2}\,\frac{BkT}{\pi^2 c^3 h}\ln^2\frac{4kT}{\gamma h\omega_0}\,.$$

If we do not make use of the approximate expression for K_0, then there will still stand a numerical component in front of the logarithm in Eq. (27). That is, in place of $\ln^2(4/\gamma x_0)$, the integral gives $\ln^2(4/\gamma x) - 0.27$. But we can hardly consider this to be accurate, since the frequency ω_0 is found by an estimation method.

The ratio of the energy transferred by the Compton mechanism to the energy transferred to the quanta upon emission is equal to

$$\left(\frac{dE}{dt}\right)_{\mathrm{C}} : \left(\frac{dE}{dt}\right)_{\mathrm{B}} = \frac{3}{4}\ln^2\frac{4kT}{h\gamma\omega_0}\,, \tag{28}$$

which can reach a few score.

If we assume that quanta with frequency less than ω_0 do not undergo Compton scattering at all, we commit a certain error. There is another, and somewhat more accurate, method of computing dE/dt. For sufficiently low frequencies, the state of the quanta is stationary, and for $x \to 0$, it tends toward $1/x$, i.e., toward the limiting form of Planck's formula. Therefore, n satisfies the ordinary differential equation which is obtained from (22) if we discard $\partial n/\partial y$ in it. Moreover, we should also discard n in comparison with n^2, and consequently regard x as a small quantity in the second component of the right side. This gives

$$\frac{d}{dx}x^3\left(\frac{dn}{dx} + n^2\right) + \frac{4A}{x}(1 - nx)\ln\frac{2.35}{x} = 0.^{*} \tag{29}$$

We now set $n = z'/z$, $z = x + \psi$, $\psi \ll x$. Then we get the equation

$$\frac{d}{dx}x^3\psi'' - \frac{4A}{x}\psi'\ln\frac{2.35}{x} = 0 \tag{30}$$

for ψ'.

This can be integrated approximately (by the WKB method) if we consider the coefficient for ψ' to be a large number. With this accuracy,

$$\psi' = C\exp\left\{-\frac{2\sqrt{A}}{x}\sqrt{\ln\frac{2.35}{x}}\right\}. \tag{31}$$

Such a solution is valid, strictly speaking, only when the exponent is large in comparison with unity. But if we choose $C = -1$, then we get an interpolation formula for the distribution function, which possesses the necessary properties and for $x \gg x_0$:

$$n = \frac{1}{x}\left(1 - \exp\left\{-\frac{2\sqrt{A}}{x}\sqrt{\ln\frac{2.35}{x}}\right\}\right). \tag{32}$$

For large x/x_0, the number of quanta is much less than the equilibrium number. Adding the factor $(1 - nx)$ under the integral (27), a factor which takes into account induced emission and absorption of quanta, we get a converging expression which can be integrated from $\omega = 0$:

$$\left(\frac{dE}{dt}\right)_{\mathrm{C}} = 3kT\,\frac{B}{\pi^2 c^3 h}\int\limits_0^\infty \frac{1}{\tau}\,\omega^2\,d\omega \tag{33}$$

$$\times \exp\left\{-\frac{2kT\sqrt{A}}{h\omega}\sqrt{\ln\frac{2.35\,kT}{h\omega}}\right\}.$$

The function under the integral vanishes for sufficiently small ω. The effective limit of integration lies at about $\omega \sim \omega_0$.

4. GENERAL FORMULAS FOR THE AVERAGE FREQUENCY IN THE COMPTON PROCESS

If the photon gas is still far from statistical equilibrium with the electrons, then the number of photons with frequency $\omega > \omega_0$ is small in comparison with unity. In this phase of the process, we can write down the following linearized kinetic equation for quanta with frequency $\omega > \omega_0$:

$$\frac{\partial n}{\partial y} - \frac{1}{x^2}\frac{\partial}{\partial x}x^4\left(\frac{\partial n}{\partial x} + n\right) = 4\tau_{\mathrm{C}}/\tau_{\mathrm{B}}^0. \tag{34}$$

Let us first consider the corresponding homogeneous equation. For this we introduce a new unknown function by the formula

$$n = e^{-x/2}\varphi(x)/x. \tag{35}$$

φ satisfies the equation (we are considering the homogeneous equation)

$$\frac{\partial\varphi}{\partial y} = x\frac{\partial^2}{\partial x^2}x\varphi + \left(-\frac{x}{2} + 2 - \frac{2}{x}\right)x\varphi \equiv \hat{A}(x)\,\varphi. \tag{36}$$

---

* It is further assumed that $\ln(2.35/x) \gg 1$.

Here $\hat{A}(x)$ is an operator on the right-hand side. Some simplifications of the calculations arise because of the fact that $\hat{A}(x)$ is a Hermitian operator*.

Let us assume that the initial photon distribution is given in the form of some function $n_0(x)$; then the distribution at any later moment is written symbolically as

$$\varphi(x, y) = e^{\hat{A}(x)y} x e^{x/2} n_0(x); \tag{37}$$

$$n = \frac{e^{-x/2}}{x} e^{\hat{A}(x)y} x e^{x/2} n_0(x).$$

We assume that a quantum with frequency ω_1 is emitted at the initial moment. Then $n_0(x) = \delta(x - x_1)/x_1^2$. We also compute (in dimensionless form) the mean frequency which this quantum will have over some time interval as a result of the quantum process:

$$\begin{aligned} \bar{x} &= \int_0^\infty x n x^2 \, dx = \int_0^\infty x^2 e^{-x/2} e^{\hat{A}(x)\, y} e^{x/2} \frac{\delta(x - x_1)}{x_1^2} \, dx \\ &= \int_0^\infty e^{x/2} \frac{\delta(x - x_1)}{x_1} e^{\hat{A} y} x^2 e^{-x/2} dx \\ &= \frac{1}{x_1} e^{x_1/2} e^{\hat{A}(x_1) y} x_1{}^2 e^{-x_1/2} \equiv \frac{1}{x_1} e^{x_1/2} \chi(x_1). \end{aligned} \tag{38}$$

Here we have made use of the fact that a function of a Hermitian operator is also a Hermitian operator. In Eq. (38), there enters the function $\chi(x_1)$, which clearly satisfies, relative to x_1, the same equation (36) as $\varphi(x)$ relative to x. In contrast to φ, the function χ is subject to a different initial condition:

$$\chi(y = 0) = x_1^2 e^{-x_1/2}. \tag{39}$$

In what follows, the index 1 will be omitted from x_1, because the "current frequency" x enters no further.

Thus, in order to find the mean frequency of the quantum, which is emitted with an initial frequency x, we must solve Eq. (36) with the initial condition (39). For this purpose, we must first determine the spectrum of the Hermitian operator $\hat{A}(x)$. We set

$$z = \ln x, \ \chi = e^{-z/2} f_\mu(z) e^{-(\mu^2 - {}^9/_4)y}. \tag{40}$$

The function $f_\mu(z)$ satisfies an ordinary differential equation of the same form as the Schrödinger equation for the vibration levels of the diatomic molecules, if the potential function of the nuclei is taken in the form of a Morse potential:

$$-d^2 f_\mu/dz^2 + (-2e^z + {}^1/_4 e^{2z}) f_\mu = \mu^2 f_\mu. \tag{41}$$

Equation (41) is integrated with the help of the degenerate hypergeometric functions, which we denote by the variable x:

$$\chi = C x^{-1} W_{2, i\mu}(x) \tag{42}$$

(Ref. 3, Sec. 16). Here $W_{2,i\mu}(x)$ is the Whittaker function, which is a combination of two ordinary degenerate hypergeometric functions:

$$\begin{aligned} W_{2,i\mu}(x) = {} & \frac{\Gamma(-2i\mu)}{\Gamma(-{}^3/_2 - i\mu)} M_{2,i\mu}(x) \\ & + \frac{\Gamma(2i\mu)}{\Gamma(-{}^3/_2 + i\mu)} M_{2,-i\mu}(x). \end{aligned} \tag{43}$$

Here $M_{2,i\mu}(x)$ is determined by the well-known series

$$\begin{aligned} M_{2,i\mu}(x) = {} & x^{1/2 + i\mu} e^{-x/2} \left(1 + \frac{(-{}^3/_2 + i\mu) x}{1!\,(2i\mu + 1)} \right. \\ & \left. + \frac{(-{}^3/_2 + i\mu)(-{}^1/_2 + i\mu) x^2}{2!\,(2i\mu + 1)(2i\mu + 2)} \right). \end{aligned} \tag{44}$$

The function W falls off at infinity as e^{-x}, while M does not possess this property. Therefore, χ is also expressed by W.

We now find the function for the discrete spectrum, analogous to the vibrational states of the diatomic molecule (functions of the continuous spectrum correspond to a dissociating molecule). The discrete spectrum is possible for negative μ^2 [see Eq. (41)] or for purely imaginary μ. The corresponding eigenfunctions should be quadratically integrable. According to Eqs. (42)-(44), the functions W, for small x and purely imaginary μ, consist of two components of the form $x^{-1/2 + |\mu|}$. However, we cannot integrate the square of the function for this upper sign. Consequently, the eigenvalues are numbers for which W consists only of functions with an integrable square. Here the numbers are $|\mu| = 3/2$ and $|\mu| = 1/2$, since the first component of Eq. (43) vanishes [$\Gamma(-2) = \infty$, $\Gamma(-3) = \infty$].

---

* We have introduced the operator $\hat{A}(x)$ and found its spectrum by making use of the results of I. M. Gel'fand.

The series for the functions $M_{2,\frac{1}{2}}(x)$ and $M_{2,\frac{3}{2}}(x)$ are broken off. Elementary functions are obtained which we at once write with normalized coefficients

$$\chi_{1/2}(x) = \sqrt{2}\,(1 - x/2)\,e^{-x/2}, \quad \chi_{3/2} = 2^{-1/2} x e^{-x/2}. \tag{45}$$

The functions for the continuous spectrum are normalized by transition to their normalized asymptotic expansion in a way entirely analogous to that used in the problem of the hydrogen atom. The expansions are referred, not to large but to small x, because for large x the function W decays exponentially. It is seen from Eq. (41) that for $z \to -\infty$, i.e., for small x, the function f_μ is proportional to $\cos(\mu z + \lambda)$. The normalized factor of the cosine is $\sqrt{2/\pi}$. Expressing W in terms of $\cos(\mu z + \beta) = \cos(\mu \ln x + \lambda)$, we get the normalized functions of the continuous spectrum

$$\chi_\mu = \frac{1}{\sqrt{2\pi}} \left| \frac{\Gamma(-{}^3/_2 + i\mu)}{\Gamma(2i\mu)} \right| \frac{W_{2,i\mu}(x)}{x}. \tag{46}$$

It is now easy to write down the general formula for $\bar{x}$ (x on the right-hand side gives the initial frequency of the quantum, previously called x_1)

$$\bar{x} = \frac{1}{x} e^{x/2} \left[e^{-9y/4} \int_0^\infty e^{-\mu^2 y} \zeta_\mu \chi_\mu \, d\mu + e^{-2y} \zeta_{1/2} \chi_{1/2} + \zeta_{3/2} \chi_{3/2} \right], \tag{47}$$

where ζ_μ, $\zeta_{\frac{1}{2}}$ and $\zeta_{3/2}$ are the expansion coefficients of the function $x^2 e^{-x/2}$ [see Eq. (38)] in the orthogonal set of functions χ_μ; $\zeta_{\frac{1}{2}}$ and $\zeta_{3/2}$ are found in elementary fashion. For the determination of ζ_μ we make use of the integral representation of the function $W_{2,i\mu}(x)$ (Ref. 3, p. 345):

$$W_{2,i\mu}(x) = \frac{x^2 e^{-x/2}}{2\pi i} \times \int_{-i\infty}^{i\infty} \frac{\Gamma(\sigma)\,\Gamma(-\sigma - i\mu - {}^3/_2)\,\Gamma(-\sigma + i\mu - {}^3/_2)\,x^6}{\Gamma(-i\mu - {}^3/_2)\,\Gamma(i\mu - {}^3/_2)} \, d\sigma.$$

With the aid of Eq. (46), we find

$$\zeta_\mu = \frac{1}{\sqrt{2\pi}} \left| \frac{\Gamma(-{}^3/_2 + i\mu)}{\Gamma(2i\mu)} \right| \frac{1}{2\pi i} \times \int_{-i\infty}^{i\infty} \frac{\Gamma(\sigma)\,\Gamma(\sigma + 4)\,\Gamma(-\sigma - i\mu - {}^3/_2)\,\Gamma(-\sigma + i\mu - {}^3/_2)}{\Gamma(-i\mu - {}^3/_2)\,\Gamma(i\mu - {}^3/_2)} \, d\sigma$$

$$= \frac{1}{\sqrt{2\pi}} \left| \frac{\Gamma(-{}^3/_2 + i\mu)}{\Gamma(2\mu)} \right| \Gamma({}^5/_2 + i\mu)\,\Gamma({}^5/_2 - i\mu),$$

where the complex integral is taken according to Barnes' formula[3]. Substituting this in Eq. (47), making use of the equation $\Gamma(u)\Gamma(1-u) = \pi \csc \pi u$, and the fact that $W_{2,i\mu}(x)$ is an even function of μ, we get the expression for $\bar{x}$ in the form of a complex integral

$$\bar{x} = \frac{i}{x^2} e^{-x/2} e^{-9y/4} \int_{-i\infty}^{i\infty} e^{s^2 y} W_{2,-s}(x) \,\mathrm{tg}\, \pi s \times s\,ds - 2\left(\frac{1}{x} - \frac{1}{2}\right) e^{-2y} + 3. \tag{48}$$

It is therefore evident that, as a result of the Compton process, the mean frequency of any quantum tends toward $3kT/h$, independently of its initial frequency. Application of Eq. (48) will be given in the Appendix.

In conclusion, I wish to express my sincere gratitude to Ia. B. Zel'dovich who set up the present problem and displayed a constant interest in it, and also to L. D. Landau and I. M. Gel'fand who made a series of important suggestions. Much of the results of Sec. 3 were obtained with the participation of the late S. P. D'iakov.

APPENDIX

THE COMPTON PROCESS IN A BODY OF FINITE DIMENSIONS

We can compute the average frequency which is possessed by quanta in a body of finite dimensions as a result of the Compton process. Since the Thomson cross section does not depend on the energy, the diffusion coefficient of the quantum is a constant. Here the probability of emission of a quantum at the instant of time y depends exponentially on the time only if the initial distribution corresponds to one of the eigenfunctions of the diffusion problem. It is natural to take a distribution which corresponds to the ground state eigenvalue since only it of all the functions is constant in sign. In dimensionless units, the probability of emission of a quantum from the system is given by

$$dw(y) = \beta e^{-\beta y} dy. \qquad \text{(I)}$$

The mean frequency of the emitted quantum in this case is less than $3kT/h$. It can be determined if we multiply (I) by $\overline{x}$ and integrate over y:

$$\overline{\overline{x}} = \int \overline{x}\, dw(y) = \frac{i\beta e^{x/2}}{x^2} \int_{-i\infty}^{i\infty} \operatorname{tg} \pi s W_{2,-s}(x) \times \frac{s\,ds}{{}^9/_4 + \beta - s^2} - \frac{2\beta(1/x - {}^1/_2)}{\beta + 2} + 3. \qquad \text{(II)}$$

The energy transferred to the quanta from the electrons under these conditions is equal to the integral (II), taken over the bremsstrahlung spectrum. We introduce the notation

$$H(x_0, s) = \int_{x_0}^{\infty} M_{2,-s}(x) K_0\left(\frac{x}{2}\right) \frac{dx}{x^3}. \qquad \text{(III)}$$

We then have

$$\overline{\overline{\overline{x}}} = \int \overline{\overline{x}} e^{-x/2} K_0\left(\frac{x}{2}\right) \frac{dx}{x} \qquad \text{(IV)}$$

$$= i\beta \int_{-i\infty}^{i\infty} \operatorname{tg} \pi s \left\{ \frac{\Gamma(2s)}{\Gamma(-{}^3/_2 + s)} H(x_0 s) + \frac{\Gamma(-2s)}{\Gamma(-{}^3/_2 + s)} H(x_0, -s) \right\} \frac{s\,ds}{\beta + {}^9/_4 - s^2}$$

$$- 2\beta \int_{x_0}^{\infty} \frac{(1/x - {}^1/_2)}{\beta + 2} e^{-x/2} K_0 \frac{x}{2} \frac{dx}{x}$$

$$+ 3 \int_{x_0}^{\infty} e^{-x/2} K_0\left(\frac{x}{2}\right) \frac{dx}{x}.$$

The complex integral of the first component is completed by the integral over an infinite semicircle in the left half-plane. Then the entire integral is expressed in the form of the sum of the residues of the expression under the integral from poles located to the left of the imaginary axis. These poles are located at the points $s = -1/2, -3/2, -5/2$ and, furthermore, at the point $s = \sqrt{\beta + 9/4}$. The residues at the first two points are reduced with the last two integrals in Eq. (IV). The residues at the points $s = -5/2, -7/2, -9/2$ remain finite even for $x_0 = 0$. Therefore, we can replace x_0 in them by 0. All these residues give only a small contribution to the integral. The principal contribution is made by the residue for $s = -\sqrt{9/4 + \beta} = -(3/2 + u)$. (If the body has dimensions that are not too small, then u is a small number.) For $\overline{\overline{x}}$, we get the expression

$$\overline{\overline{\overline{x}}} = -2\pi\beta \operatorname{tg} \pi \sqrt{\beta + {}^9/_4}\, \frac{\Gamma(-2\sqrt{\beta + 9/4})}{\Gamma(-3/2 - \sqrt{\beta + 9/4})} \times H(x_0, -\sqrt{\beta + 9/4}) \qquad \text{(V)}$$

$$+ \sum_{k=2}^{\infty} \frac{(-)^k (k+2)!}{(2k+1)!} \frac{\beta}{\beta + {}^9/_4 - (2k+1)^2/4} \times H\left(0, -\frac{2k+1}{2}\right).$$

The quantities $H(0, -(2k+1)/2)$ are decomposed into the converging numerical series $H(0, -5/2) = 2.27$, $H(0, -7/2) = 2.31$; the remaining expressions of this type are multiplied by small coefficients. We put $H(x_0, -\sqrt{\beta + 9/4})$ in the form of the difference between two integrals

$$H(x_0, -\sqrt{\beta + 9/4}) = \int_0^{\infty} M_{2,-({}^3/_2+u)}(x) K_0\left(\frac{x}{2}\right) \frac{dx}{x^3} - \int_0^{x_0} M_{2,-({}^3/_2+n)}(x) K_0\left(\frac{x}{2}\right) \frac{dx}{x^3}. \qquad \text{(VI)}$$

The first integral [we call it $F(u)$] is computed by expansion of M in a power series, The numerical values of $F(u)$ are the following:

u =	0.01	0.03	0.1	0.2	
$F(u)$=	10080	1137	107	28.8	
u =	0.3	0.4	0.5	0.75	1.0
$F(u)$=	13.7	8.2	5.7	3.3	2.2

In the second integral in (VI), we must use the expressions M and K_0 for small x. This gives

$$\int_0^{x_0} x^{u-1} \ln\left(\frac{x\gamma}{4}\right) dx = \frac{x_0^u}{u}\left(-\ln\frac{4}{\gamma u} - \frac{1}{u}\right).$$

As u tends to zero, we obtain the results for an unbounded medium that we already know.

---

[1] W. Heitler, *Quantum theory of radiation.*

[2] G. N. Watson, *Theory of Bessel functions.*

[3] E. T. Whittaker and G. N. Watson, *Modern Analysis*, 4th ed.

Translated by R. T. Beyer
182

SOVIET PHYSICS JETP VOLUME 4, NUMBER 5 JUNE, 1957

Polarization of Relativistic Protons in Coulomb Scattering

M. G. URIN AND V. N. MOKHOV
Moscow Institute of Engineering Physics

(Submitted to JETP editor September 15, 1955)
J. Exptl. Theoret. Phys. (U.S.S.R.) 31, 842-844 (November, 1956)

Perturbation theory was used to determine the polarization of relativistic protons which experience Coulomb scattering.

WHEN we limit ourselves to weak and almost constant electromagnetic fields the equation which describes a particle with spin 1/2 and magnetic moment $\mathfrak{M}_p = \alpha e\hbar/2mc$ (m is the proton mass and $\alpha = 2.79$) for $v \ll c$ is as follows[1]

$$\{i\gamma_k(p_k - eA_k) + {}^1/_2 i\mathfrak{M}'\gamma_k\gamma_l F_{kl} + m\}\Psi = 0,$$

where A_k is the four-dimensional potential, F_{kl} is the electromagnetic field tensor and $\mathfrak{M}' = \mathfrak{M}_p - e/2m$ (here and in the following $\hbar = c = 1$). For stationary states we have $\mathscr{H}\psi = \varepsilon\psi$.

In a Coulomb field ($\mathbf{A} = 0$; $A_4 = i\varphi = iZe/r$):

$$\mathscr{H} = i\beta\gamma\mathbf{p} + \beta m + e\varphi + \mathfrak{M}'\gamma\nabla\varphi.$$

Since the vectors in the problem can be used to form a unique pseudovector, that is, $[\mathbf{p}_0\mathbf{p}_1]$ (where $\mathbf{p}_0$ and $\mathbf{p}_1$ are the proton momentum before and after scattering) polarization in the scattering plane is zero; therefore, we naturally analyze the spin perpendicular to that plane (in the z direction). We assume elestic scattering, i.e., $p_1 = p_0 = p$.

Whenever the external field can be regarded as a perturbation the following formula holds true in first approximation:

$$d\sigma_{\mu_0\mu_1} = (2\pi/v)\left|\int \psi_1^* V\psi_0 d\mathbf{r}\right|^2 \delta(\varepsilon_1 - \varepsilon_0)d\mathbf{p}_1/(2\pi)^3$$

$$= [\varepsilon^2/(2\pi)^2]\,|V_{0\mu_0}^{1\mu_1}|^2\, d\Omega_{\mathbf{p}_1},$$

where $d\sigma_{\mu_0\mu_1}$ is the differential scattering cross section; v is the velocity of the proton; $\psi_0 = u_{\mu_0\lambda_0}e^{i\mathbf{p}_0\mathbf{r}}$ and $\psi_1 = u_{\mu_1\lambda_1}e^{i\mathbf{p}_1\mathbf{r}}$ are the free wave functions of the proton before and after scattering; $u_{\mu_0\lambda_0}$, $u_{\mu_1\lambda_1}$ are the unit bispinors which characterize states with certain polarization in the z direction); $V = e\varphi + \mathfrak{M}'\gamma\nabla\varphi$ is the perturbation; $d\Omega_{\mathbf{p}_1}$ is the element of solid angle in the direction of the scattered proton momentum;

$$V_{0\mu_0}^{1\mu_1} = u_{\mu_1\lambda_1}^* \int e^{i\mathbf{q}_{01}\mathbf{r}}(e\varphi + \mathfrak{M}'\gamma\nabla\varphi)\,d\mathbf{r}\, u_{\mu_0\lambda_0}$$

$$= (4\pi Ze^2/q_{01}^2)\,u_{\mu_1\lambda_1}^*[1 - (\mathfrak{M}'/e)\,i\gamma\mathbf{q}_{01}]\,u_{\mu_0\lambda_0},$$

where $\mathbf{q}_{01} = \mathbf{p}_0 - \mathbf{p}_1$.

For an unpolarized primary proton beam

$$d\sigma_{\mu_1} = {}^1/_2\sum_{\mu_0}[\varepsilon^2/(2\pi)^2]\,|V_{0\mu_0}^{1\mu_1}|^2\, d\Omega_{\mathbf{p}_1}, \tag{1}$$

where $\sum_{\mu_0}$ denotes summation over initial polarizations. Since $u_{\mu\lambda}$ is the eigenfunction of the operator $1/2\,\Sigma_z\beta$, $u_{\mu_1\lambda_1}$ can be replaced by

$$\left[\mu_1 + {}^1/_2\,\Sigma_z\beta\right]u_{\mu\lambda_1}/2\mu_1 = \delta_{\mu\mu_1}u_{\mu\lambda_1},$$

which enables us to sum over μ_1 in (1). Then, using Casimir's operator[2] $(H_j + \lambda_j)/2\lambda_j$, where $H_j = \beta(i\gamma\mathbf{p}_j + m)$ in order to sum over λ_0, λ_1, we obtain

$$d\sigma_{\mu_1} = {}^1/_2(Ze^2/q_{01}^2)^2\,\mathrm{Sp}\,\{[1 - (\mathfrak{M}'/e)\,i\gamma\mathbf{q}_{01}]\,(H_0 + \varepsilon)$$
$$\times[1 + (\mathfrak{M}'/e)\,i\gamma\mathbf{q}_{01}]\,(H_1 + \varepsilon)\left[\mu_1 + {}^1/_2\,\Sigma_z\beta\right]/2\mu_1\}\,d\Omega_{\mathbf{p}_1}.$$

Then the total differential scattering cross section is

$$d\sigma_{1/2} + d\sigma_{-1/2}$$
$$= {}^1/_2(Ze^2/q_{01}^2)^2\,\mathrm{Sp}\,\{[1 - (\mathfrak{M}'/e)\,i\gamma\mathbf{q}_{01}]\,(H_0 + \varepsilon)$$
$$\times[1 + (\mathfrak{M}'/e)\,i\gamma\mathbf{q}_{01}]\,(H_1 + \varepsilon)\}\,d\Omega_{\mathbf{p}_1}$$
$$= \frac{(Ze^2/2pv)^2}{\sin^4(\theta/2)}\,[1 - 2v^2L\sin^2(\theta/2)]\,d\Omega_{\mathbf{p}_1},$$

$L = [(\alpha - 1/2) - 1/2\,\alpha^2 v^2]/(1 - v^2)$; θ is the angle between $\mathbf{p}_0$ and $\mathbf{p}_1$.

In this approximation we have for the polarization

$$d\sigma_{1/2}-d\sigma_{-1/2}$$
$$=1/2\,(Ze^2/2pv)^2\,\mathrm{Sp}\,\{[1-(\mathfrak{M}'/e)\,i\gamma\mathbf{q}_{01}]\,(H_0+\varepsilon)$$
$$\times\,[1+(\mathfrak{M}'/e)\,i\gamma\mathbf{q}_{01}]\,(H_1+\varepsilon)\,\Sigma_z\beta\}\,d\Omega_{\mathbf{p}_1}=0.$$

We therefore consider the scattering cross section in the second perturbation approximation:

$$d\sigma_{\mu_1}=\frac{1}{2}\sum_{\mu_0}\frac{\varepsilon^2}{(2\pi)^2}\left|V_{0\mu_0}^{1\mu_1}\right.$$
$$\left.+\int\sum_{\mu_i\lambda_i}\frac{V_{i\mu_i}^{1\mu_1}V_{0\mu_0}^{i\mu_i}}{\varepsilon-\lambda_i}\frac{d\mathbf{p}_i}{(2\pi)^3}\right|^2 d\Omega_{\mathbf{p}_1},$$

where the integral with respect to p_i is taken along the real axis encircling the point $p_i=p$ from below[3].

Retaining the first nonvanishing terms in the expression for the polarization we obtain

$$d\sigma_{1/2}-d\sigma_{-1/2}$$
$$=\sum_{\mu_0}\frac{\varepsilon^2}{(2\pi)^2}\mathrm{Re}\Big[(V_{0\mu_0}^{1\,1/2})^*\int\sum_{\mu_i\lambda_i}\frac{V_{i\mu_i}^{1\,1/2}V_{0\mu_0}^{i\mu_i}}{\varepsilon-\lambda_i}\frac{d\mathbf{p}_i}{(2\pi)^3}$$
$$-(V_{0\mu_0}^{1\,-1/2})^*\int\sum_{\mu_i\lambda_i}\frac{V_{i\mu_i}^{1\,-1/2}V_{0\mu_0}^{i\mu_i}}{\varepsilon-\lambda_i}\frac{d\mathbf{p}_i}{(2\pi)^3}\Big]\,d\Omega_{\mathbf{p}_1}.$$

We must here sum over μ_i, λ_i, μ_0, and just as was done above we introduce the summations over λ_0, λ_1, μ_1:

$$d\sigma_{1/2}-d\sigma_{-1/2}=[(Ze^2)^i/(2\pi)^2q_{01}^2]$$
$$\mathrm{Re}\Big[\int\mathrm{Sp}\,F\,d\mathbf{p}_i/iq_{01}^2q_{i1}^2\,(\varepsilon^2-\varepsilon_i^2)\Big]\,d\Omega_{\mathbf{p}_1},$$
$$F=\beta\,[1-(\mathfrak{M}'/e)\,i\gamma\mathbf{q}_{i1}]\,(H\ +\varepsilon)$$
$$\times\,[1-(\mathfrak{M}'/e)^3\,\gamma\mathbf{q}_{0i}]\,(H_0+\varepsilon)$$
$$\times\,[1+(\mathfrak{M}'/e)\,i\gamma\mathbf{q}_{01}]\,(H_1+\varepsilon)\,\gamma_1\gamma_2.$$

Here use has been made of $\Sigma_z=\gamma_1\gamma_2/i$. It is easily seen that

$$\int d\Omega_{\mathbf{p}_i}\int p_i^2dp_i\,\mathrm{Sp}\,F/iq_{0i}^2q_{i1}^2\,(\varepsilon^2-\varepsilon_i^2)$$
$$=-\pi\int[p_i\varepsilon_i\,\mathrm{Sp}\,F/q_{0i}^2q_{i1}^2\,(\varepsilon+\varepsilon_i)]_{p_i=p}\,d\Omega_{\mathbf{p}_i}$$
$$-\int d\Omega_{\mathbf{p}_i}-\!\!\!\!\!\!\int p_i^2dp_i\,\mathrm{Sp}\,F/iq_{0i}^2q_{i1}^2\,(\varepsilon^2-\varepsilon_i^2).$$

The second integral with respect to dp_i is taken along the real axis in the sense of the principal value.

Since the imaginary part of F is the sum of products of an odd number of γ matrices, Sp F is a real quantity and, consequently,

$$\mathrm{Re}\int d\Omega_{\mathbf{p}i}-\!\!\!\!\!\!\int p_i^2dp_i\,\mathrm{Sp}\,F/iq_{0i}^2q_{i1}^2\,(\varepsilon^2-\varepsilon_i^2)=0.$$

Then

$$d\sigma_{1/2}-d\sigma_{-1/2}$$
$$=-\Big[p\,(Ze^2)^3/8\pi q_{01}^2\Big]\,d\Omega_{\mathbf{p}_l}\int d\Omega_{\mathbf{p}_i}\,[\mathrm{Sp}\,F/q_{0i}^2q_{i1}^2]_{p_i=p}$$
$$=\{mpL\,|\,[\mathbf{p}_0\mathbf{p}_1]\,|\,(Ze^2)^3/\pi q_{01}^2\}$$
$$\times\,[1-2\,(\mathfrak{M}'/me)\,p^2]\,d\Omega_{\mathbf{p}_i}$$
$$\times\int\left[\frac{1-\mathbf{p}_i\,(\mathbf{p}_0+\mathbf{p}_1)/(p^2+\mathbf{p}_0\mathbf{p}_1)}{q_{0i}^2q_{i1}^2}\right]_{p_i=p}d\Omega_{\mathbf{p}_i}.$$

Integrating over the angles of $\mathbf{p}_i$ and converting to ordinary units we obtain

$$d\sigma_{1/2}-d\sigma_{-1/2}=\left(\frac{Z}{137}\right)^3\frac{\hbar^2mc}{p^3}\frac{KL}{\sin\theta}\ln\frac{1}{\sin(\theta/2)}\,d\Omega_{\mathbf{p}_1},$$
$$K=1-\frac{\alpha\beta^2}{1-\beta^2},\quad\beta=\frac{v}{c}.$$

The integral cross section is

$$\sigma_{1/2}-\sigma_{-1/2}=2\pi^2\ln 2\,(Z/137)^3\,(\hbar^2mc/p^3)\,KL.$$

It can be seen that for $\beta=0.6$ and 0.77 the polarization vanishes.

The relative polarization is

$$\frac{d\sigma_{1/2}-d\sigma_{-1/2}}{d\sigma_{1/2}+d\sigma_{-1/2}}$$
$$=\frac{(Z/137)\,4\beta\sqrt{1-\beta^2}KL}{1-2\beta^2L\sin^2(\theta/2)}\frac{\sin^3(\theta/2)}{\cos(\theta/2)}\ln\frac{1}{\sin(\theta/2)}.$$

When $v\ll c$ we arrive at the previously known result[4]:

$$\frac{d\sigma_{1/2}-d\sigma_{-1/2}}{d\sigma_{1/2}+d\sigma_{-1/2}}$$
$$=4\left(\alpha-\frac{1}{2}\right)\frac{v}{c}\frac{Z}{137}\frac{\sin^3(\theta/2)}{\cos(\theta/2)}\ln\frac{1}{\sin(\theta/2)}.$$

The problem has been solved by perturbation theory. Since $|e\varphi|>|\mathfrak{M}'\gamma\nabla\varphi|$ the criterion for applying perturbation theory to the present case will be the inequality $Ze^2/\hbar v\ll 1$. For relativistic protons this is equivalent to $Z/137\ll 1$.

The formulas which have been obtained are applicable to the angular range

$$\hbar/pR_{\mathrm{nuc}}<\theta<Ze^2/\varepsilon R_{\mathrm{nuc}}$$

For angles greater than $Ze^2/\epsilon R_{\mathrm{nuc}}$ nuclear scattering is important. Small angles may also be excluded because the Coulomb field of the nucleus is screened by atomic electrons.

These results can also be used as a correction to polarization in nuclear scattering. In this case

$$d\sigma_{1/2} - d\sigma_{-1/2} \sim |A_{\text{nuc}\,1/2} + A_{q\,1/2}|^2 - |A_{\text{яд}\,-1/2} + A_{q\,-1/2}|^2,$$

where A_{nuc} and A_q are the nuclear and Coulomb scattering amplitudes, respectively. In the interference term it is sufficient to take A_q in the first order perturbation approximation.

The authors are deeply grateful to Prof. A. B. Migdal for his direction of this work.

---

[1] L. L. Foldy, Phys. Rev. 87, 688 (1952).

[2] W. Heitler, *Quantum Theory of Radiation* (Russian translation) GTTI, Moscow, 1940.

[3] L. Landau and E. Lifshitz, *Quantum Mechanics*, GTTI, Moscow, 1948.

[4] Iu. A. Zaveniagin, thesis, Moscow Institute of Engineering Physics, 1952.

Translated by I. Emin
178

SOVIET PHYSICS JETP VOLUME 4, NUMBER 5 JUNE, 1957

Isotopic Invariance and the Creation of Particles

L. I. Lapidus
Institute for Nuclear Problems
Academy of Sciences, USSR

(Submitted to JETP editor October 13, 1955)

The consequences of conservation of isotopic spin are investigated. Relations between different cross sections are found which are valid if in the meson nucleon interaction a state with a particular value of isotopic spin predominates. The relations of Smorodinskii and Jacobson for elastic nucleon-nucleon cross sections are generalized for the case of meson and nucleon–antinucleon pair production. Furthermore, the consequences of isotopic spin conservation are given for the following cases: meson production on nuclei, creation of heavy meson pairs and nucleon antinucleon pairs in π–nucleon collisions, and for some processes of nucleon annihilation in collisions with deuterons.

1. IN connection with the increase in the number of possible high energy experiments on nucleons and mesons it is interesting to investigate the consequences of the so called hypothesis of charge independence or isotopic invariance.

The meson creation processes should allow the most direct experimental verification of the conservation of isotopic spin. Besides the relation given by Yang[1]

$$d\sigma(p + p \rightarrow \pi^+ + d) = 2d\sigma(n + p \rightarrow \pi^0 + d),$$

one can show,[2,3] using just one condition derived from isotopic invariance, that the following relation also holds

$$d\sigma(p + d \rightarrow \mathrm{H}^3 + \pi^+) = 2d\sigma(p + d \rightarrow \mathrm{He}^3 + \pi^0).$$

Several reactions are forbidden by isotopic invariance. Among them is the following curious case: in d–d collisions leaving the deuterons intact, only even numbers of mesons can be created. The forbidden character of the reactions

$$d + d \rightarrow d + d + \pi^0; \quad d + d \rightarrow \mathrm{He}^4 + \pi^0$$

is clear. The case of three π^0–mesons can be proven as follows. Calling Ψ_{T,T_z} a function with definite T^2 and T_z, one has for the wave function of two π^0–mesons

$$(\pi^0\pi^0) = \{\sqrt{2}\psi_{2,0} - \psi_{0,0}\} / \sqrt{3},$$

which does not contain $T = 1$ components. Therefore a system of three π^0–mesons cannot have a part with $T = 0$. This shows that three π^0–mesons cannot be created since the nuclear system has $T = 0$ before and after the collision.

2. The investigation of the consequences of isotopic spin conservation furthermore allows one to obtain information on the meson–nucleon and nucleon–nucleon interaction in states of definite isotopic spin. For example, as is well known, the elastic and the charge exchange scattering cross section of mesons is given in terms of the amplitudes of the states with $T = 3/2$ and $T = 1/2$, a_3

and a_1, respectively, in the following way:

$$d\sigma(\pi^+p \rightarrow \pi^+) = |a_3|^2, \quad d\sigma(\pi^-p \rightarrow \pi^-) = {}^1/_9\,|a_3 + 2a_1|^2, \quad d\sigma(\pi^-p \rightarrow \pi^0) = {}^2/_9\,|a_3 - a_1|^2. \tag{1}$$

One sees from (1) that the elastic cross sections in the $T = 3/2$ and $T = 1/2$ states are given by

$$d\sigma_{3/2} = d\sigma(\pi^+p \rightarrow \pi^+),$$
$$d\sigma_{1/2} = {}^1/_2\{3[d\sigma(\pi^-p \rightarrow \pi^-) + d\sigma(\pi^-p \rightarrow \pi^0)] - d\sigma(\pi^+p \rightarrow \pi^+)\},$$

which yield for the total cross sections

$$\sigma_{3/2} = \sigma(\pi^+p \rightarrow \pi^+) = \sigma^+, \quad \sigma_{1/2} = {}^3/_2\{[\sigma(\pi^-p \rightarrow \pi^-) + \sigma(\pi^-p \rightarrow \pi^0)] - \sigma^+\} = {}^1/_2(3\sigma^- - \sigma^+). \tag{2}$$

For meson production in π–N collisions, one can obtain

$$d\sigma_{3/2}(\pi N \rightarrow N\pi\pi) = d\sigma(\pi^+p \rightarrow \pi^+\pi^+) + d\sigma_+(\pi^+p \rightarrow \pi^+\pi^0),$$
$$d\sigma_{1/2}(\pi N \rightarrow N\pi\pi) = {}^1/_2\{3[d\sigma(\pi^-p \rightarrow \pi^0\pi^0) + d\sigma_+(\pi^-p \rightarrow \pi^-\pi^0) + d\sigma_+(\pi^-p \rightarrow \pi^+\pi^-)] - d\sigma_{3/2}(\pi N \rightarrow N\pi\pi)\}, \tag{3}$$

where, for example

$$d\sigma_+(\pi^-p \rightarrow \pi^+\pi^-) = d\sigma(\pi^-p \rightarrow n\pi^+\pi^-) + d\sigma(\pi^-p \rightarrow n\pi^-\pi^+),$$

The yield for the total cross sections

$$\sigma_{3/2}(\pi N \rightarrow N\pi\pi) = \sigma(\pi^+p \rightarrow \pi\pi),$$
$$\sigma_{1/2}(\pi N \rightarrow N\pi\pi) = {}^1/_2\{3\sigma(\pi^-p \rightarrow \pi\pi) - \sigma(\pi^+p \rightarrow \pi\pi)\}. \tag{4}$$

Let σ^+, σ°, and σ^- be the cross section for multiple production of mesons by positive, uncharged and negative meson respectively. Then it can be shown that expressions of the form (2) are valid for any number of produced mesons; therefore, they remain valid for the total meson–nucleon interaction cross section. The validity of these relations is connected with the fact that the isotopic spin of the meson system can be only 0, 1, or 2 if the total isotopic spin of the meson–nucleon system is $T = 1/2$ or $T = 3/2$.

If the elastic cross section predominates, one obtains for a state with $T_{\pi T} = 3/2$ (as is well known)

$$d\sigma(\pi^+p \rightarrow \pi^+) : d\sigma(\pi^-p \rightarrow \pi^0) : d\sigma(\pi^-p \rightarrow \pi^-) = 9 : 2 : 1.$$

In order to obtain the quantitative consequences of the predominance of the $T = 3/2$ state in the meson–nucleon interaction in meson production, one has to expand the final system into subsystems. In the analysis of meson production processes by nucleons, the final state of the system is usually classified in the way that the isotopic spin is a sum of the isotopic spin of the nucleons and of the meson.[4,5] This way one can follow through transitions taking place in the nucleon system.[6] However, expanding into meson–nucleon subsystems, one can explore the transitions undergone by subsystems with different $T_{\pi N}$ and as a result establish relations between different cross sections which are due to the predominance of certain values of $T_{\pi N}$ in the meson nucleon interaction.

If isotopic spin is conserved, one can express the cross section of single meson production in N–N collisions in terms of three independent matrix elements. Two of them correspond to transitions with $T = 1$, and one with $T = 0$. Usually the two $T = 1$ states of the final system are classified according to their symmetry with respect to nucleon exhange. In the scheme adopted in the present paper, the total isotopic spin $T = 1$ is obtained by combining the spin of the nucleon $T_N = 1/2$ with the πN subsystem in either the $T_{\pi N} = 1/2$ or the $T_{\pi N} = 3/2$ state.

Denoting the transition amplitudes into the T=1 state with A_{13} and A_{11}, and into the $T = 0$ state with A_{01} the cross sections for the different processes of single meson production can be expressed as follows:

$$M(pp \rightarrow \pi^+pn) = 3^{1/2}2^{-1}A_{13},$$
$$M(pp \rightarrow \pi^+np) = -12^{-1/2}A_{13} + 2^{1/2}3^{-1/2}A_{11},$$
$$M(pp \rightarrow \pi^0pp) = -6^{-1/2}A_{13} - 3^{-1/2}A_{11},$$
$$M(np \rightarrow \pi^+nn) = 2^{-1/2}\{6^{-1/2}A_{13} + 3^{-1/2}A_{11} + 3^{-1/2}A_{01}\},$$
$$M(np \rightarrow \pi^-pp) = -2^{-1/2}\{6^{-1/2}A_{13} + 3^{-1/2}A_{11} - 3^{-1/2}A_{01}\},$$
$$M(np \rightarrow \pi^0pn) = 2^{-1/2}\{3^{-1/2}A_{13} - 6^{-1/2}A_{11} - 6^{-1/2}A_{01}\}, \tag{5}$$
$$M(np \rightarrow \pi^0np) = -2^{-1/2}\{3^{-1/2}A_{13} - 6^{-1/2}A_{11} + 6^{-1/2}A_{01}\}.$$

The two nucleon–meson states ($\pi\, pn$) and (πnp) are obtained from each other by exchanging the nucleons. Writing $d\sigma_+ (pp \to \pi^+) = d\sigma\, (pp \to \pi^+ np) + d\sigma\, (pp \to \pi^+ pn)\, l + c$ we obtain immediately

$$d\sigma_+ (pp \to \pi^+) + d\sigma\, (np \to \pi^+) + d\sigma\, (np \to \pi^-) = 2\, [d\sigma\, (pp \to \pi^0) + d\sigma_+ (np \to \pi^0)]. \tag{6}$$

Furthermore, one can obtain relations from (5) between cross sections for different processes if the meson nucleon interaction of one $T_{\pi N}$ predominates. Thus, if π meson–nucleon interaction occurs only in the $T_{\pi N} = 3/2$ state, then the following relation obtains

$$d\sigma\, (pp \to \pi^+) = 5 d\sigma\, (pp \to \pi^0) = 2{,}5\, d\sigma\, (np \to \pi^0) = 10\, d\sigma\, (np \to \pi^-) = 10\, d\sigma\, (np \to \pi^+). \tag{7}$$

In the complementary case where only the $T_{\pi N} = 1/2$ state contributes, (7) changes into

$$d\sigma_+ (pp \to \pi^+) = 2 d\sigma\, (pp \to \pi^0), \tag{8}$$

$$d\sigma_+ (np \to \pi^-) + d\sigma\, (np + \pi^+) = 2 d\sigma_+ (np \to \pi^0). \tag{9}$$

The relations (6) to (9) are true for certain parts of the meson spectrum. These relations can only be approximately true for the total cross sections even if the main part of the spectrum consists of meson energies where the interaction in a particular $T_{\pi N}$ state predominates.

It is known from experimental results on the meson-nucleon interaction that for meson energies of 150 to 200 mev, the interaction in the $T_{\pi N} = 3/2$ state predominates. The experimental total cross sections for single meson production at a nuclear energy of ≈ 650 mev, where the center of mass of the spectrum of outgoing mesons lies at 150 to 200 mev, do not contradict Eq. (7).[7,8,9]

From (5) one can express A_{13}, A_{11}, and A_{01} in terms of cross sections. Thus, $d\sigma_0 = |A_{01}|^2$, the cross section for meson production in the $T = 0$ state takes the form

$$d\sigma_0\, (NN \to \pi) = 3\, \{d\sigma\, (np \to \pi^+) + d\sigma\, (np \to \pi^-) - d\sigma\, (pp \to \pi^0)\}. \tag{10}$$

Close to the meson production threshold, all quantities on the right hand side of (10) are small in comparison to $\sigma\, (pp \to \pi^+)$. This leads to the well known predominance of the $T_{NN} = 1$ state for meson creation.[10] In the range of large energies, where the meson–nucleon interaction occurs in the $T_{NN} = 3/2$ state, the expression (10) due to (7) also tends to zero.

From the experimental data on the nucleon–nucleon interaction one can obtain information on the interaction in states of definite isotopic spin in a fashion analogous to the way in which Eqs. (2) gave similar information on the meson–nucleon interaction.

Let $\sigma^y_{np}(\theta)$, $\sigma^y_{pp}(\theta) = \sigma^y_1(\theta)$ and $\sigma^y_0(\theta)$ be the differential nucleon scattering cross sections. Then, as shown by Smorodinskii[11] and Jacobson[12] holds

$$d\sigma^y_0(\theta) = 2\, [d\sigma^y_{np}(\theta) + d\sigma^y_{np}(\pi - \theta)] - d\sigma^y_{pp}(\theta),$$

For the total cross sections, this becomes

$$\sigma^y_0 = 2\sigma^y_{np} - \sigma^y_{pp}. \tag{11}$$

Using (10) one can obtain another expression from (5) for single meson production in the $T = 0$ state:

$$\sigma_0\, (NN \to \pi) = \sigma_0 = 2\sigma\, (np \to \pi) - \sigma\, (pp \to \pi) = 2\sigma_{np} - \sigma_{pp}, \tag{12}$$

Here $\sigma\, (np \to \pi)$ is the total single meson production cross section in n–p collisions and $\sigma(pp \to \pi) = \sigma_1$ is the total single meson production cross section in p–p collisions. The relation (6) appears as the result of the existence of two expressions, (9) and (12) for σ_0. From the last two relations it follows that (12) holds for the total cross sections of nucleon interactions, including both elastic scattering and meson production. It remains valid even in presence of multiple meson production if the contribution from the latter processes is subtracted.

3. In the analysis of meson creation in π–N collisions[2,5] the final state was expressed such that the total isotopic spin was given as the sum of the nucleon isotopic spin and the isotopic spin of the meson system. Thereby the possibility arose to investigate the transitions into states of different meson exchange symmetries. When dividing the system into meson–nucleon subsystems the remarkable fact emerged that the meson–nucleon subsystem of the final state can have $T_{\pi N} = 3/2$ or $1/2$ even if the total system had the same T respectively.

In the case where both $T = 3/2$ and $T_{\pi N} = 3/2$

the cross sections of the different processes obey the relations

$$d\sigma_{+}(\pi^{+}p\to\pi^{+}\pi^{0}) \tag{13}$$
$$=\frac{13}{2}d\sigma(\pi^{+}p\to\pi^{+}\pi^{+})=\frac{117}{2}d\sigma(\pi^{-}p\to\pi^{0}\pi^{0})$$
$$=\frac{117}{17}d\sigma_{+}(\pi^{-}p\to\pi^{-}\pi^{0})=\frac{117}{10}d\sigma(\pi^{-}p\to\pi^{-}\pi^{+}),$$

Clearly the first of these processes predominates over all meson–proton processes.

For $T=3/2$ and the isotopic spin for the subsystem $T_{\pi N}=1/2$, one obtains, instead of (13),

$$d\sigma(\pi^{+}p\to\pi^{+}\pi^{+}) \tag{14}$$
$$=2d\sigma_{+}(\pi^{+}p\to\pi^{+}\pi^{0})=9d\sigma(\pi^{-}p\to\pi^{0}\pi^{0})$$
$$={}^{18}/_{5}\,d\sigma_{+}(\pi^{-}p\to\pi^{0}\pi^{-})=9d\sigma_{+}(\pi^{-}p\to\pi^{-}\pi^{+}).$$

In both these expressions, i.e., if the total isotopic spin is $T=3/2$ with arbitrary isotopic spin of the subsystems, the following relations hold:

$$d\sigma(\pi^{+}p\to\pi^{+}\pi^{+}):d\sigma(\pi^{0}p\to\pi^{0}\pi^{0}):d\sigma(\pi^{-}p\to\pi^{0}\pi^{0})$$
$$=9:2:1, \tag{15}$$
$$2\,[d\sigma(\pi^{+}p\to\pi^{+}\pi^{+})$$
$$+d\sigma_{+}(\pi^{+}p\to\pi^{+}\pi^{0})]=3\,[d\sigma(\pi^{0}p\to\pi^{0}\pi^{0})$$
$$+d\sigma_{+}(\pi^{0}p\to\pi^{+}\pi^{-})+d\sigma_{+}(\pi^{0}p\to\pi^{+}\pi^{0})],$$
$$2d\sigma_{+}(\pi^{-}p\to\pi^{-}\pi^{0})$$
$$=d\sigma_{+}(\pi^{-}p\to\pi^{-}\pi^{+})+4d\sigma(\pi^{-}p\to\pi^{0}\pi^{0}).$$

In the case when the interaction predominates for $T=1/2$ of the total system, nothing happens for incoming positive mesons. Besides the known expressions

$$4d\sigma(\pi^{-}p\to\pi^{0}\pi^{0})$$
$$+d\sigma_{+}(\pi^{-}p\to\pi^{-}\pi^{0})=2d\sigma_{+}(\pi^{-}p\to\pi^{+}\pi^{-}), \tag{16}$$
$$d\sigma(\pi^{-}p\to\pi^{0}\pi^{0})=2d\sigma(\pi^{0}p\to\pi^{0}\pi^{0}),$$
$$d\sigma_{+}(\pi^{-}p\to\pi^{+}\pi^{-})=2d\sigma_{+}(\pi^{0}p\to\pi^{+}\pi^{0})$$

there exist still further relations when $T_{\pi N}$ is specified. For $T_{\pi N}=3/2$ ($T=1/2$), one obtains, instead of (12), the relation

$$d\sigma_{+}(\pi^{-}p\to\pi^{-}\pi^{+})=2{,}5\,d\sigma_{+}(\pi^{-}p\to\pi^{-}\pi^{0})$$
$$=2{,}5\,d\sigma(\pi^{-}p\to\pi^{0}\pi^{0}), \tag{17}$$

and for $T_{\pi N}=1/2$),

$$d\sigma_{+}(\pi^{-}p\to\pi^{-}\pi^{+}) \tag{18}$$
$$=d\sigma_{+}(\pi^{-}p\to\pi^{0}\pi^{-})=4d\sigma(\pi^{-}p\to\pi^{0}\pi^{0}).$$

In the energy range where the interaction of the mesons with the nucleon in the final state occurs only in the $T_{\pi N}=3/2$ state, but where the total isotopic spin is both 3/2 and 1/2, the expressions (13) change only for interactions involving negative mesons and protons since $T=1/2$ states do not participate in the ($\pi^{+}p$) system. Denoting the total cross section of the change of a positive meson into two mesons by $d\sigma(\pi^{+}p\to\pi\pi)$, we obtain the relation in the form

$$65d\sigma(\pi^{-}p\to\pi^{0}\pi^{0})+6d\sigma(\pi^{+}p\to\pi\pi)$$
$$=40d\sigma_{+}(\pi^{-}p\to\pi^{-}\pi^{0}) \tag{19}$$
$$+10d\sigma_{+}(\pi^{-}p\to\pi^{-}\pi^{+}).$$

4. In analyzing the nonproduction of mesons from the point of view of isotopic spin invariance[13,14] one has to consider (in addition to the operator S which transforms like a scalar) an operator which transforms like the third component V_z of a vector in isotopic spin space. The only nonvanishing matrix elements of such an operator are (see for Example Ref. 15).

$$(V_z)^{nTT_z}_{n'TT_z}=V^{nT}_{n'T}T_z, \tag{20}$$

$$(V_z)^{nT-1\,T_z}_{n'TT_z}=(V_z)^{nTT_z}_{n'T-1\,T_z}=V^{nT}_{n'T-1}(T^2-T_z^2)^{1/2}. \tag{21}$$

Here n and n' are all other indices specifying the state of the system.

We shall now investigate the process of single meson photoproduction on deuterium and look for relations between different cross sections, considering the meson–nucleon system to be in definite $T_{\pi N}$ states. Because of (20), $(V_Z)^{nT0}_{nT_0}=0$; hence the different matrix elements of the photoprocess have the form

$$\begin{aligned}
M(\gamma d\to\pi^{+}nn)&=3^{-1/2}S_0+6^{-1/2}V_{13}+3^{-1/2}V_{11},\\
M(\gamma d\to\pi^{-}pp)&=3^{-1/2}S_0-6^{-1/2}V_{13}-3^{-1/2}V_{11},\\
M(\gamma d\to\pi^{0}pn)&=-6^{-1/2}S_0+3^{-1/2}V_{13}-6^{-1/2}V_{11},\\
M(\gamma d\to\pi^{0}np)&=-6^{-1/2}S_0-3^{-1/2}V_{13}+6^{-1/2}V_{11},
\end{aligned} \tag{22}$$

Here S_0 is the transition amplitude connected with the operator S, and V_{11} and V_{13} are the corresponding quantities for V_z; V_{13} is the amplitude connected with transitions into states with $T_{\pi N}=3/2$ and V_{11} into states with $T_{\pi N}=1/2$, when the isotopic spin of the total system equals one.

In the energy range where the $T_{\pi N}=3/2$ state predominates in the meson–nucleon interaction the processes involving V_{13} will also predominate. Then the following relations will hold between the cross sections:

$$d\sigma(\gamma d \to \pi^+) = d\sigma(\gamma d \to \pi^-) = {}^1/_4\, d\sigma(\gamma d \to \pi^0). \tag{23}$$

In the energy range when the interaction in the $T_{\pi N} = 1/2$ state predominates one obtains from (22)

$$d\sigma(\gamma d \to \pi^+) + d\sigma(\gamma d \to \pi^-) = 2d\sigma(\gamma d \to \pi^0). \tag{24}$$

In the analysis of meson photoprocesses the smallness of S as compared with V_z is sometimes taken as a starting point.[16] This is based on the smallness of S_0 as compared with V_{13}. However, the smallness of the matrix element S_0 may be due to the predominance of the meson–nucleon interaction in the $T_{\pi N} = 3/2$ state. The rather large cross section for the "elastic" π° photoproduction[17,18] also may be due solely to the above mentioned characteristics of the meson-nucleon interaction (the quantity S_0 does not make any contribution to the $\gamma d \to d + \pi^\circ$ process).

As shown above in many examples, the predominance of the nucleon–meson interaction in states of definite T can result in relations between the cross sections of different but related meson production processes. The derivation of these relations did not involve any details of the meson–nucleon interaction besides the assumption of conservation of isotopic spin. These relations must therefore also follow from the more detailed models if they include the strong interaction in the $T = 3/2$ state, independently of the other aspects of the model. Relations of the type (7) must also appear in the different "isobaric models".[19] However in the same way as the experimental verification of the 9:2:1 ratios in meson scattering did not decide the question of the resonance character of the state, the experimental verification of relation of the type (7) does not confirm the "isobaric model" but only points up the significantly larger importance of the $T_{\pi N} = 3/2$ state as compared to the doublet state. This clearly holds for all processes of real meson production.

5. The majority of the published relations between cross sections for scattering or production of π-mesons concern interactions with nucleons or deuterons. However, there exist similar relations even for nuclei, if they are in a definite isotopic spin state. Such nuclei are the light nuclei, as is well known. We shall now investigate the consequences of isotopic invariance for meson production in nucleon–nucleus collisions. We shall consider specifically nuclei with a difference between neutron and proton numbers of one and two. The relations which we will thus obtain are useful for checking the hypothesis of isotopic invariance, or for obtaining information on the purity of the isotopic spin in the states of the nuclei, and also for obtaining information regarding difficult reactions.

As is well known, the cross sections for production of positive (σ^+), negative (σ^-), and neutral (σ°) mesons in nucleon–deuteron collisions in case of isotopic invariance have to obey the relation

$$\sigma^+ + \sigma^- = 2\sigma^0. \tag{25}$$

The same relation clearly holds for all nuclei with $T = 0$.

We shall now investigate the production of mesons by nucleon collision with mirror nuclei like H^3, He^3, and Li^7, Be^7. They have all isotopic spin $T = 1/2$. The total isotopic spin of nucleus plus nucleon therefore can be 0 or 1. The final state consists of an even number of nucleons and a single meson. The case $T = 0$ of the total system requires a nucleon isotopic spin $T_N = 1$ because of $T_\pi = 1$. The case $T = 1$ can be obtained with $T_N = 2, 1$ or 0. Since no states with $T_N > 2$ can participate, it is clear that the results obtained for He^3 and H^3 hold for all similar pairs of mirror nuclei. On the other hand, one sees immediately that the results of the present section have to go over into the case of meson production in nucleon–nucleon collisions when taking into account that there the state with $T_N = 2$ is absent.

As a result of the usual considerations, one obtains the following relations

$$\begin{aligned}&[\sigma_{T_z=-1/2}(n, \pi^-) + \sigma_{T_z=-1/2}(p, \pi^-)]\\ &\quad + [\sigma_{T_z=-1/2}(n, \pi^+) + \sigma_{T_z=-1/2}(p, \pi^+)]\\ &\quad\quad = 2[\sigma_{T_z=-1/2}(p, \pi^0) + \sigma_{T_z=-1/2}(n, \pi^0)],\end{aligned} \tag{26}$$

Here, for example, $\sigma_{T_z=-1-2}(p, \pi^+)$ denotes the cross section for π^+–meson production by protons summed over all nucleons of a $T_z = -1/2$ nucleus like H^3 or $3e^9$.

Because of charge symmetry,

$$\sigma_{T_z=-1/2}(n, \pi^\pm) = \sigma_{T_z=+1/2}(p, \pi^\mp), \tag{27}$$

$$\sigma_{T_z=-1/2}(n, \pi^0) = \sigma_{T_z=+1/2}(p, \pi^0), \tag{28}$$

One therefore can transform (26) into

$$[\sigma_{T_z=-1/2}(p,\pi^+)+\sigma_{T_z=+1/2}(p,\pi^+)] \qquad (29)$$
$$+[\sigma_{T_z=-1/2}(p,\pi^-)+\sigma_{T_z=+1/2}(p,\pi^-)]$$
$$=2\,[\sigma_{T_z=-1/2}(p,\pi^0)+\sigma_{T_z=+1/2}(p,\pi^0)].$$

One can easily check that for the case of the simplest mirror "nuclei," the proton and the neutron, (29) changes into the well known formula

$$1/2\,\sigma(pp\to\pi^+)=\sigma(np\to\pi^0)$$
$$+\sigma(pp\to\pi^0)-\sigma(np\to\pi^+),$$

if we note that

$$\sigma_{T_z=+1/2}(p,\pi^-)=\sigma(pp\to\pi^-)=0,$$
$$\sigma(np\to\pi^+)=\sigma(np\to\pi^-).$$

In addition to Eq. (29), it is possible to establish several inequalities, as, for example,

$$\sigma_{T_z=+1/2}(p,\pi^0)\geqslant 1/2\,\sigma_{T_z=+1/2}(p,\pi^-), \qquad (30)$$
$$\sigma_{T_z=+1/2}(p,\pi^+)\geqslant 1/6\,\sigma_{T_z=+1/2}(p,\pi^-),$$
$$1/3\,\sigma_{T_z=+1/2}(p,\pi^-)+\sigma_{T_z=+1/2}(p,\pi^+)$$
$$\geqslant\sigma_{T_z=+1/2}(p,\pi^0)\geqslant 1/3\,\sigma_{T_z=+1/2}(p,\pi^-).$$

One can apply a similar analysis to nuclei with $T_N = 1$ forming an isobaric triplet. The result is

$$[\sigma_{T_z=+1}(p,\pi^+)+\sigma_{T_z=0}(p,\pi^+) \qquad (31)$$
$$+\sigma_{T_z=-1}(p,\pi^+)]+[\sigma_{T_z=+1}(p,\pi\ )$$
$$+\sigma_{T_z=0}(p,\pi^-)+\sigma_{T_z=-1}(p,\pi^-)]$$
$$=2\,[\sigma_{T_z=+1}(p,\pi^0)+\sigma_{T_z=0}(p,\pi^0)$$
$$+\sigma_{T_z=-1}(p,\pi^0)].$$

Similarly one can obtain inequalities such as

$$\sigma_{T_z=+1}(p,\pi^+)\geqslant 1/10\,\sigma_{T_z=+1}(p,\pi^-); \qquad (32)$$
$$\sigma_{T_z=+1}(p,\pi^+)\geqslant 1/4\,\sigma_{T_z=+1}(p,\pi^0);$$
$$\sigma_{T_z=+1}(p,\pi^+)+\sigma_{T_z=-1}(p,\pi^-)\geqslant 2/3\,\sigma_{T_z=+1}(p,\pi^0)$$

and a number of others.

6. We shall now illustrate the characteristic peculiarities of the relation between the meson-creation cross sections in case of predominance of certain $T_{\pi N}$ in the meson–nucleon interactions, and choose as an example, a very simple nucleus, the deuteron. The final state in the case of meson production in a d–p collision can be split into subsystems considering the meson and nucleon as one, and the remaining two nucleons as the other, subsystem. The matrix elements for the production of mesons of different charge, M^+, M^-, and M^0, can be expressed in terms of three quantities R_t, N_t and N_s, which characterize the transitions in the different possible isotopic spin states of the subsystems. Here $R_t = 3\sqrt{2}\,r_t$ corresponds to transitions with $T_{\pi N} = 3/2$, $T_{NN} = 1$; for $T_{\pi N} = 1/2$, $N_t = 3\,n_t$ corresponds to transitions with $T_{NN} = 1$ and $N_s = \sqrt{3}\,n_s$ to transitions with $T_{NN} = 0$. The different matrix elements then are given by

$$M(pd\to\pi^-ppp)=r_t+2n_t, \qquad (33)$$
$$M(pd\to\pi^+nnp)=-r_t+n_t+n_s,$$
$$M(pd\to\pi^+npn)=-r_t+n_t-n_s,$$
$$M(pd\to\pi^+pnn)=3r_t.$$

In the energy range where n_s and n_t are negligible with respect to r_t, the $T_{\pi N} = 3/2$ state predominates in the π–nucleon interaction. The large π^+– π^--production branching ratio then follows from Eq. (33):

$$d\sigma^+ : d\sigma^- = 11:1. \qquad (34)$$

For the neutral mesons one then obtains [from (25)]:

$$d\sigma^0 = {}^6/_{11}\,d\sigma^+, \qquad (34')$$

This can also be obtained from expressions of the type (34) which have not been written down here.

The case of heavier nuclei with $T = 0$ is considerably more involved. Even for He^4 it is not possible to obtain equations of type (34); the complications arise from states with $T_{NN} = 2$.

It should be mentioned that relations of the type (34) have been derived earlier[19] under the assumption that the meson is created in collisions of the incoming particle with individual nucleons of the target nucleus. In that approximation, (34) is valid for all $T = 0$ nuclei.

The strong predominance of the $T_{\pi N} = 3/2$ state in the energy region 150 to 200 mev also shows up strongly in the interaction of mesons with nuclei such as the deuteron. Considerations of similar nature to the foregoing show that the following relation holds between the charge exchange and non—charge exchange scattering cross sections:

$$2d\sigma(\pi^- d \to \pi^-) = 5d\sigma(\pi^- d \to \pi^0). \qquad (35)$$

The probability for charge exchange scattering is therefore much smaller than the probability for straight scattering, in marked contrast to π-nucleon scattering in the same energy region.

7. It has been deduced from experimental evidence on hyperons and K-particles[20, 21, 22] that the isotopic spin of the different particles is $T_\lambda = 1/2$; $T_\lambda = 0$; $T_\vartheta = 1/2$; $T_\tau = 1/2$. With this assignment it is possible to understand many properties of the "strange" particles. The large value of the K^- / K^+ ratio in K-production with nuclei can be explained in this way. Furthermore, the scheme of associated production of K and Y particles in nucleon—nucleon collisions removes the difficulty of the long half—life of the particles as compared with the rather high production probability, etc.

The reactions of creation of new particles in π-nucleon collisions have several peculiarities as compared with creation in nucleon—nucleon collisions. In particular, it is possible to create a pair of K-particles without creating a hyperon ($\pi + N \to N + K + K$). This reaction will occur at a kinetic energy of the meson greater than

$$W = (2m_K - m_\pi)c^2[1 + (2m_K + m_\pi)/2M_p] \cong 1400 \text{ mev}$$

($\widetilde{K}$ denotes the antiparticle of K ; for example if $T_z^{\vartheta t} = 1/2$ $T_z^{\vartheta 0} = -1/2$, then $T_z^{\vartheta -} = -1/2$, and $\widetilde{T}_z^{\vartheta 0} = 1/2$).

The conservation laws of charge and projection of the isotopic spin allow just the following reactions

$$\pi^+ + p \to p + K^+ + \widetilde{K}^0, \quad \pi^- + p \to n + K^+ + K^-, \quad \pi^- + p \to p + K^0 + K^-. \qquad (36)$$

No production of $\widetilde{K}^\circ$ particles is possible in π^-—p collisions since in a reaction like $\pi^- + p \to p + K^- + \widetilde{K}^0$, allowed by conservation of charge, T_z is not conserved. The cross sections of the allowed reactions can be expressed in the form

$$\begin{aligned} \sigma(\pi^+ p \to pK^+\widetilde{K}^0) &= |\alpha_3|^2 = \sigma_{3/2}(\pi N \to NK\widetilde{K}), \\ \sigma_+(\pi^- p \to nK^+K^-) &= {}^1/_3\{{}^2/_3|\alpha_3 - \alpha_1|^2 + 2|\beta_1|^2\}, \\ \sigma_+(\pi^- p \to pK^0K^-) &= {}^1/_9|\alpha_3 + 2\alpha_1|^2, \end{aligned} \qquad (37)$$

Here α_1 and β_1 correspond to transitions with $T = 3/2$. The cross sections $\sigma_{1/2}$ for K-pair production in the $T = 1/2$ state are given by

$$\begin{aligned} \sigma_{1/2}(\pi N \to NK\widetilde{K}) &= {}^1/_2\{3[\sigma_+(\pi^- p \to K^+K^-) \\ &\quad + \sigma_+(\pi^- p \to K^0K^-)] \\ &\quad - \sigma_{3/2}(\pi N \to NK\widetilde{K})\} \\ &= {}^1/_2\{3\sigma(\pi^- p \to K\widetilde{K}) - \sigma(\pi^+ p \to K\widetilde{K})\}, \end{aligned} \qquad (38)$$

which has the same form as (4).

One sees from (37) that the probabilities of K^+ and K^- production have comparable magnitude. The direct dependence of the relations between the different cross sections on the isotopic spin also follows immediately from (37). If one considers, in addition to the reactions (36), K-pair creation induced by π° —mesons, one can easily derive relations between the different crosssections analogous to Heitler's relations for π—meson scattering.

8. In connection with the possibility of experiments in the bev range, it is of interest to consider the creation and the interactions of antinucleons. One of the rather low threshold processes is the nucleon pair creation in π— N collisions, i.e., the reaction $\pi + N \to N + N' + \widetilde{N}'$. Its threshold lies at a meson kinetic energy of

$$W = 4Mc^2\left(1 - \frac{m_\pi}{2M}\right)\left(1 + \frac{m_\pi}{4M}\right) \cong 3760 \text{ mev}.$$

Nucleon pairs can be produced in the following meson—proton collisions:

$$\begin{gathered} \pi^+ + p \to p + p + \widetilde{n}; \\ \pi^- + p \to n + \underset{\sim}{p} + \widetilde{\widetilde{p}}; \quad \pi^- + p \to n + n + \widetilde{n}; \\ \pi^0 + p \to p + p + \widetilde{p}; \quad \pi^\circ + p \to p + n + \widetilde{n}. \end{gathered}$$

Introducing crosssections for $\widetilde{n}$ and $\widetilde{p}$ creation, summed over nucleons, i.e., denoting

$$\sigma(\pi^- \widetilde{p} \to \widetilde{p}) = \sigma(\pi^- p \to np\widetilde{p}) + \sigma(\pi^- p \to pn\widetilde{p})$$

etc., one can write for the relation between the crosssections

$$\sigma(\pi^-p\to\widetilde{n})+\sigma(\pi^-p\to\widetilde{p})+\sigma(\pi^+p\to\widetilde{n})$$
$$=2[\sigma(\pi^0p\to\widetilde{p})+\sigma(\pi^0p\to\widetilde{n})], \quad (39)$$

This equation allows one to obtain the cross section of antinucleon creation by neutral mesons from experimentally determined cross sections of antinucleon creation by charged mesons.

Similarly we have

$$\sigma_{1/2}(\pi N\to\widetilde{N})=\tfrac{1}{2}\{3[\sigma(\pi^-p\to\widetilde{p}) \quad (40)$$
$$+\sigma(\pi^-p\to\widetilde{n})]-\sigma(\pi^+p\to\widetilde{n})\}$$
$$=\tfrac{1}{2}\{3\sigma(\pi^-p\to\widetilde{N})-\sigma(\pi^+p\to\widetilde{N})\}.$$

If the $T=3/2$ state predominates in the π–N interaction, one obtains

$$\sigma(\pi^+p\to\widetilde{n}):\sigma(\pi^-p\to\widetilde{p}):\sigma(\pi^-p\to\widetilde{n})=9:2:1.$$

On the other hand, if the $T=1/2$ is the important one, we have

$$\sigma(\pi^-p\to\widetilde{n})+\sigma(\pi^-p\to\widetilde{p}) \quad (41)$$
$$=2[\sigma(\pi^0p\to\widetilde{n})+\sigma(\pi^0p\to\widetilde{p})].$$

From (40) and (41) it follows immediately that

$$d\sigma(\pi^-p\to d+\widetilde{p}) \quad (42)$$
$$=2d\sigma(\pi^0p\to d+\widetilde{n})=2d\sigma(\pi^0n\to d+\widetilde{p})$$

in processes where the final state contains a deuteron, or also in the inverse process of the annihilation of antinucleons on deuterium in the emission of a single meson.

Relations between antinucleon–nucleon annihilation cross sections in the emission of two and three π–mesons have been derived earlier by Kobzarev and Shmushkevich.[23,24] For two–meson antiproton annihilation processes on deuterium one can obtain

$$2[\sigma(\widetilde{p}d\to n\pi^+\pi^-) \quad (43)$$
$$+\sigma(\widetilde{p}d\to n\pi^-\pi^+)]=4\sigma(\widetilde{p}d\to n\pi^0\pi^0)$$
$$+\sigma(\widetilde{p}d\to p\pi^-\pi^0)+\sigma(\widetilde{p}d\to p\pi^0\pi^-),$$

which for the total cross sections go over into

$$2\sigma(\widetilde{p}d\to\pi^+\pi^-) \quad (43')$$
$$=4\sigma(\widetilde{p}d\to\pi^0\pi^0)+\sigma(\widetilde{p}d\to\pi^0\pi^-)$$

which coincide with the expressions for antinucleon–nucleon annihilation obtained by Kobzarev and Shmushkevich. For three-meson antiproton annihilation on deuterium one obtains

$$\sigma_+(\widetilde{p}d\to\pi^+\pi^-\pi^-) \quad (44)$$
$$=2\sigma(\widetilde{p}d\to\pi^0\pi^0\pi^0)+\sigma_+(\widetilde{p}d\to\pi^0\pi^0\pi^-),$$

and for the total cross sections we do get Shmushkevichs expressions for three-meson nucleon–antinucleon annihilation. For annihilation cross sections involving π^+, π^-, π^0 –mesons, which do not appear in (44), one obtains the inequality

$$\sigma_+(\widetilde{p}d\to\pi^+\pi^-\pi^0)\geqslant\sigma_+(\widetilde{p}d\to\pi^0\pi^0\pi^-). \quad (45)$$

The cross sections of (44) and (45) are summed over π-mesons, for example

$$\sigma_+(\pi^+\pi^-\pi^-)=\sigma(\pi^+\pi^-\pi^-)+\sigma(\pi^-\pi^+\pi^-)+\sigma(\pi^-\pi^-\pi^+).$$

The requirement of isotopic invariance yields a number of inequalities for nucleon pair creation in N–N collisions, such as

$$3\sigma_+(pp\to\widetilde{n})\geqslant\sigma(pp\to\widetilde{p}),$$
$$2[\sigma(np\to\widetilde{p}) \quad (46)$$
$$+\sigma(np\to\widetilde{n})]\geqslant\sigma(pp\to\widetilde{p})+\sigma(pp\to\widetilde{n}),$$

The cross sections σ_1 and σ_0 of pair creation in states of definite isotopic spin of the N–N system are given by

$$\sigma_1(NN\to\widetilde{N})=\sigma(pp\to\widetilde{p})+\sigma(pp\to\widetilde{n}), \quad (47)$$
$$\sigma_0(NN\to\widetilde{N})=2[\sigma(np\to\widetilde{n})$$
$$+\sigma(np\to\widetilde{p})]-\sigma_1(NN\to\widetilde{N})$$

in complete analogy with relation (12).

The author is very grateful to I. Ia. Pomeranchuk and to Ia. A. Smorodinskii for their keen interest in this work and their valuable comments.

---

[1] C. N. Yang, as quoted by R. L. Garwin, Phys. Rev. 85, 1045 (1952).

[2] I. I. Lapidus, Inst. Nucl. Problems, Acad. of Sciences, USSR, Report 1952; Thesis, Inst. Nucl. Problems, Acad. of Sciences, USSR, 1953.

[3] J. M. Luttinger, Phys. Rev. 86, 571 (1952).

[4] A. M. I. Messiah, Phys. Rev. 86, 430 (1952).

[5] Van Hove, Marshak and Pais, Phys. Rev. 88, 1211 (1952).

[6] A. H. Rosenfeld, Phys. Rev. 96, 139 (1954).

[7] M. G. Meshcheriakov and B. S. Neganob, Dokl. Akad. Nauk SSSR 100, 677 (1955).

[8] Tiapkin, Kozodaev, and Prokoshkin, Dokl. Akad. Nauk SSSR 100, 689 (1955).

[9] M. G. Meshcheriakov, Proceedings of the Conference of Peaceful Uses of Atomic Energy at the Academy of Sciences USSR 1955, p. 32.

[10] B. M. Pontecorvo and G. I. Selivanov, Dokl. Akad. Nauk SSSR 102, 495 (1955).

[11] Ia. A. Smorodinskii, Problems Soviem. Fiz. 7, 7 (1954).

[12] B. A. Jacobsohn, Phys. Rev. 89, 881 (1953).

Translated by M. Danos
181

Letters to the Editor

Temperature Dependence of Viscosity of Liquid Argon

N. F. ZHDANOVA
Khar'kov State University

(Submitted to JETP editor July 10, 1956)
J. Exptl. Theoret. Phys. (U.S.S.R.) 31, 724-725
(October, 1956)

THIS work continues the investigation of the temperature dependence of the viscosity of elementary liquids at constant density[1,2]. The object of our investigation is liquid argon. The method and apparatus to measure the viscosity coefficient at constant density were described previously[2].

The measured temperature dependence of the viscosity of liquid argon at constant density (in the range from 90 to 270°K) is shown graphically in Fig. 1, in which the ordinate represents the fluidity in cgs units, and the abscissa the absolute temperature. Curve *a-a* shows the temperature dependence of the fluidity of argon in equilibrium with its vapor pressure. The Table lists the experimental data corresponding to curve *a-a*. The family of curves $\varphi(T)$ at ρ = const, obtained for argon, is very similar to an analogous family of curves previously obtained for nitrogen[2].

Two types of curves are obtained, depending on how the viscosity (fluidity) varies with temperature at constant density. At high densities the fluidity of argon increases with temperature; at low temperatures, to the contrary, the fluidity of argon diminishes with increasing temperature. It should be noted that in both argon and nitrogen the character of the temperature dependence of viscosity changes at approximately the same value of relative liquid density ($\rho / \rho_k \approx 2$). One can assume that the character of the temperature dependence of the viscosity of nitrogen and argon (and perhaps also of other elementary liquids) changes at a density close to $2\rho_k$ because of the change in the mechanism of viscosity. The liquid mechanism of viscosity predominates at $\rho > 2\rho_k$, while the gas mechanism predominates at $\rho < 2\rho_k$.

Figure 2 shows a family of isothermal viscosity curves for argon obtained by calculation from the data of Fig. 1. The abscissa represents the density of the substance in g/cm³, the ordinate the viscosity ($\times 10^6$) in cgs units. It is evident from Fig. 2 that argon viscosity depends monotonically on its density. The isothermal curves for argon intersect each other and intersect the equilibrium curve in approximately one point, at a liquid density nearly equal to $2\rho_k$.

Results of an investigation of the viscous properties of strongly compressed argon at a temperature above 0° have recently been published[3]. In

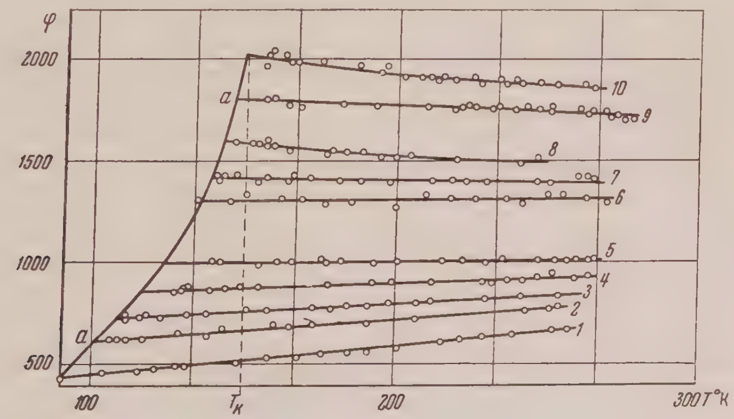

FIG. 1. Temperature dependence of fluidity of liquid argon in equilibrium with its vapor pressure; *1* – ρ = 1.37 g/cm³; *2* – 1.31 g/cm³; *3* – 1.22 g/cm³; *4* – 1.16 g/cm³; *5* – 1/10 g/cm³; *6* – 1.02 g/cm³; *7* – 0.95 g/cm³; *8* – 0.88 g/cm³; *9* – 0.78 g/cm³; *10* – 0.70 g/cm³.

TABLE

T°K	η, g/cm^{-1} sec^{-1}	φ, g^{-1}/cm/sec
84.25	0.00282*	355*
86.25	0.00262*	382*
86.90	0.00256*	391*
87.30	0.00252*	397*
90.0	0.00232	432
99.5	0.00162	618
111.0	0.00137	750
120	0.00116	862
127	0.00100	1000
133.5	0.00077	1300
138.7	0.00070	1430
143	0.00063	1590
147	0.00056	1790
149	0.00050	2000

* Values cited from work of N. S. Rudenko[4].

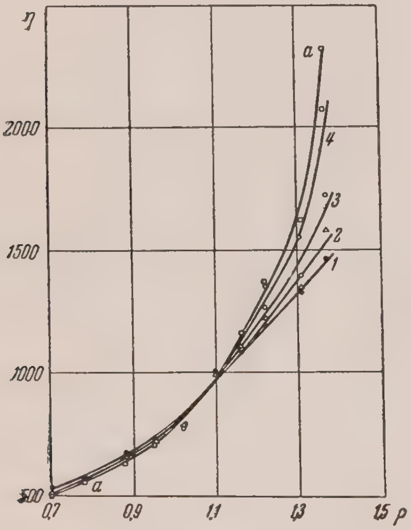

FIG. 2. Isothermal plots of argon viscosity vs. density. 1 – 260° K; 2 – 230° K; 3 – 200° K; 4 – 125° K.

our investigation, the viscosity coefficient of argon was measured at temperatures below +18° C, and the results can therefore be compared only for a narrow temperature interval. Our results are nevertheless in good agreement with those of Ref. 3; the maximum discrepancy does not exceed 10%.

The temperature dependence of the viscosity of liquid argon at constant density in excess of $2\rho_k$ can be quite satisfactorily represented by an equation of the type $\eta = Ae^{U/T}$, where A and U are constants. A similar temperature dependence of viscosity was formerly obtained for nitrogen[2].

In conclusion, I must thank B. I. Berkin and N. S. Rudenko for supervising this work.

---

[1] B. I. Berkin and N. S. Rudenko, J. Exptl. Theoret. Phys. (U.S.S.R.) 20, 523 (1950).

[2] F. Zhdanova, J. Exptl. Theoret. Phys. (U.S.S.R.) 31, 14 (1956); Soviet Phys. JETP 4, 19 (1957).

[3] Michels, Botzen and Schurman, Physica 20, 1141 (1954).

[4] N. S. Rudenko, J. Techn. Phys. (U.S.S.R.) 18, 1123 (1948).

Translated by J. G. Adashko
156

The HDSe Microwave Spectrum

V. G. VESELAGO AND A. M. PROKHOROV
P. N. Lebedev Physical Institute
Academy of Sciences, USSR

(Submitted to JETP editor July 13, 1956)
J. Exptl. Theoret. Phys. (U.S.S.R.) 31, 731
(October, 1956)

THE HDSe microwave spectrum was investigated with a radio spectroscope with electric molecular modulation.

Preliminary calculations called for two transitions to exist in the 9000 mc region: $2_{20}-2_{21}$ and $4_{31}-4_{32}$. An investigation of the spectrum in the 8400-9300 mc range disclosed two groups of six lines each, one for each of the selenium isotopes.

Study of the Stark effect of the observed lines disclosed that one group of lines corresponds to the $2_{20}-2_{21}$ transition, the other to the $4_{31}-4_{32}$ transition. The frequencies of the observed lines are given in the Table.

The frequencies were measured with the aid of a quartz multiplier. The measurement accuracy was ±0.1 mc. The frequencies of the Se^{74} lines were not measured, for this isotope occurs infrequently and its lines are of low intensity. In addition to observing the HDSe lines, we also observed two previously known[1] HDO lines, at 8577.7 and 8836.95 mc.

The intensity of the HDSe line reaches values of the order of 10^{-6} cm^{-1}. The HDO line at 8836.95 mc [2] was used to calibrate the spectroscope sensitivity.

The observed lines were used to calculate the frequencies of other possible transitions. Calculations called for a $9_{54}-9_{55}$ transition to exist in the vicinity of 14,000 mc. The lines corresponding to this transition were found, but a discrepancy on the order of 60 mc was found between

TABLE

Transition	Selenium Isotope	Frequency, mc
4_{31}—4_{32}	82	8756.7
	80	8771.05
	78	8786.05
	77	8793.95
	76	8801.85
2_{20}—2_{21}	82	9127.75
	80	9138.55
	78	9149.65
	77	9155.85
	76	9161.50
9_{54}—9_{55}	82	13827.7
	80	13862.65
	78	13899.3
	77	13918.3
	76	13937.8

the calculated and the experimental data. This is attributed to the failure to allow in the calculations for the centrifugal perturbation, which is large for this molecule. To find the constants of the centrifugal perturbation, it is necessary to measure the frequencies of a few more transitions; this will be done in the future.

In conclusion, the authors thank G. Ia. Vzenkova for preparing the HDSe compound.

---

[1] D. W. Poesener and M. W. P. Strandberg, Phys. Rev. 95, 374 (1954).

[2] D. W. Posener, J. Chem. Phys. 23, 1728 (1955).

Translated by J. G. Adashko
161

"Seniority" Quantum Number Selection Rules in Nuclear Reactions

V. G. NEUDACHIN

(Submitted to JETP editor May 30, 1956)
J. Exptl. Theoret. Phys. (U.S.S.R.) 31, 891
(November, 1956)

A "SENIORITY" quantum number appears in the theory of atomic and nuclear shells[1-4]. Let us denote this by v. At the present time, the degree of accuracy of this quantum number has not been established. The question of the correctness of v is closely related to the question of the accuracy of jj coupling, although it does not entirely coincide with the latter. For the purpose of obtaining the required experimental information, it is necessary to investigate the satisfying of the selection rules for v in nuclear reactions. These rules can be derived in a very simple way on the basis of the results given in the articles referred to above.

1. In a reaction involving the capture or emission of a j nucleon (initial configuration j^n, final configuration j^{n+1}, or vice versa) $\Delta v = \pm 1$.

In particular, stripping in even-even nculei, for example, with an $f_{7/2}$ shell, should not lead to the formation of a resultant nucleus in the excited state $J = 7/2-$, $T = T_{gr}$ with $v = 3$ (the ground state of the initial nucleus has $v = 0$ and $J = 0$; the ground state of the final nucleus, with the exception of Ti^{49}_{22} and V^{49}_{23}, has $v = 1$ and $J = 7/2-$). However, such excited states of nuclei with $f_{7/2}$ shells have not yet been observed experimentally.

2. For $M1$ or $M3$ transitions in nuclei where there are only neutrons outside of the filled shells (for example, Ca^{43}_{20}), or only protons (for example, V^{51}_{23}), which are characterized by the configuration j^n, $\Delta v = 0$.

Thus the selection rules in Ca^{43} and V^{51} for v forbid an $M1$ transition from any level of the $(f_{7/2})^n$ configuration to the ground level of this configuration with $v = 1$, $J = j = 7/2-$, which is ground level for these nuclei.

3. For $M1$ or $M3$ γ-transitions in the case of a j^n configuration formed by neutrons and protons ($|M_T| < n/2$): $\Delta v = 0, \pm 2$, $\Delta T = \pm 1.0$; when the isobaric spin T of the initial and final states is zero, $\Delta v = 0$.

For $E2$ radiation the selection rules for v will be $\Delta v = 0, \pm 2$. These have no practical value.

Selection rules 1 are intuitively clear and require no explanation. Selection rules 2 and 3 can also be derived by a very clear method. We shall now discuss selection rules 2.

The wave function of a state of configuration j^n with seniority v can be written as:

$$\Psi^J_M(n, v) = \sum_P (-1)^P P\Psi^0_0(1, 2)$$

$$\ldots \Psi^0_0(n - v - 1, n - v)\ \Psi^J_M(v, v);$$

where the P are permutation operators of n numbers: $(-1)^P = +1$ when P is even and -1 when P is odd. It is important to note that even in other cases where such a wave function of the j^n configuration is broken up into factors, none of the factors can be a symmetric function (antisymmetrization of a function which is symmetric with respect to even two particles gives a vanishing result). Thus no factor can be $\Psi^{J'}_{M'}(1, 2)$, where J' is odd (j is a half integer).

The operator of a $M1$ transition is a pseudovector operator; therefore, the matrix element vanishes for a transition between a state with the wave function $\Psi^0_0\,(1,2)$ and a state with the wave function $\Psi^{J'}_{M'}(1, 2)$, where J', as we have seen, can only be even. This simply denotes that transitions with $\Delta v \neq 0$ are forbidden.

It is expedient in practice to investigate experimentally the satisfaction of the selection rules for v only for nuclei which are heavier than Ca^{40}_{20}, since nuclei between O^{16}_8 and Ca^{40}_{20} evidently do not possess a shell structure, $1d$ and $2s$ configurations are highly mixed.

In particular, for nuclei with a $1f_{7/2}$ shell these experiments can determine whether jj or intermediate coupling takes place[5] and whether collective interactions are significant. v will be a good quantum number only when j— is a good quantum number and collective effects are unimportant. Experimental investigations of the accuracy of v are naturally performed through experimental investigations of the accuracy of j [6].

---

[1] G. Racah, Phys. Rev. **63**, 367 (1943).

[2] A. Edmonds and B. Flowers, Proc. Roy. Soc. (London) **214A** 515 (1952).

[3] C. Schwartz and A. de-Shalit, Phys. Rev. **94**, 1257 (1954).

[4] M. Umesawa, Progr. Theor. Phys. **8**, 509 (1952).

[5] D. R. Inglis, Rev. Mod. Phys. **25**, 390 (1953).

[6] J. B. French and B. J. Raz, Phys. Rev. **98**, 1523 (1955).

Translated by I. Emin
186

Gamma Quanta Emitted by I, Rh and Co Nuclei in Thermal Neutron Capture

I. V. ESTULIN, L. F. KALINKIN AND
A. S. MELIORANSKII
Moscow State University

(Submitted to JETP editor April 22, 1956)
J. Exptl. Theoret. Phys. (U.S.S.R.) **31**, 886-887
(November, 1956)

THE most reliable data on the energy and the absolute yield of γ-quanta emitted by nuclei upon thermal neutron capture have been obtained by Kinsey's group[1] and by the Soviet scientists Groshev, Ad'iasevich and Demidov[2,3]. In Kinsey's work[1], only γ-rays with energies greater than 3 mev were detected while in the work of Ref. 2, the spectrum of γ-quanta with energies greater than 0.3 mev was investigated. Meanwhile, measurements carried out with the help of scintillation spectrometers[4,5] proved the presence of discrete lines in the low energy part of the spectra. The authors working with scintillation spectrometers were not able to determine the absolute intensities of the observed lines.

In the present work, the energies and absolute intensities of γ-quanta with energies of 50 to 600 kev emitted by I, Rh and Co nuclei during thermal neutron capture were determined. In the work, a scintillation spectrometer was used with a NaI (Tl) crystal of cylindrical shape (height 9 mm, diameter, 28 mm). The resolving power of the spectrometer, η, depends on the energy of the γ-quanta (E_γ) according to the law

$$\eta = 186\, E_\gamma^{-1/2} + 2.5, \qquad (1)$$

where E_γ is expressed in kev and η in percent. In experiments carried out with radioactive emitters having monoenergetic γ-ray spectra, the efficiency of the spectrometer ϵ_Φ, was determined, enabling one to convert the area of the photo peak to the number of γ-quanta falling on the NaI (Tl) crystal.

A heavy water physics research reactor[6] was used in this work as a source of thermal neutrons. A well-collimated beam of neutrons came out of a horizontal channel in the reactor shielding. A target of the material being investigated was located in the center of the beam. A NaI (Tl) crystal and a photomultiplier tube were placed under the target, and were carefully shielded with lead and with boron carbide . A channel of 10 or 15 mm diameter, used as a collimator for γ-rays coming from the target to the NaI (Tl) crystal, was located in the spectrometer shielding. The aperture of the γ-ray collimator was covered with boron carbide of 0.3 gm/cm^2 thickness, blocking the passage of thermal neutrons scattered in the target.

In the measurement of γ-rays from the capture of neutrons, measurements were made with an open beam of thermal neutrons, N_0, and with a beam of neutrons filtered at the exit of the neutron collimator by a B_4C shield (N_1). The effect of thermal neutrons in the target N is equal to the difference between these two values:

$$N = N_0 - N_1.$$

The photopeaks of soft γ-rays in the spectra of the targets investigated that are emitted by nuclei as a result of thermal neutron capture are seen on a background of impulses from harder γ-quanta. The presence of this "base" limits the accuracy of the determination of the areas of the photopeaks. In order to lower the background due to hard γ-quanta, the study of the low energy part of the γ-ray spectra included measurements of the absorption of the γ-quanta in lead. In such a way, the γ-ray spectra absorbed in thin lead filters were measured. In these spectra, it is possible to isolate the desired photopeak area with certainty; this area is directly related to the intensities of the measured γ-rays.

In order to determine the number of γ-quanta of a given energy resulting from the capture of one neutron, it is necessary to know the neutron current falling on the target as well as the solid angle subtended by the target relative to the NaI(Tl) crystal. With the goal of measuring these quantities experimentally, we replaced in the neutron beam the target being investigated with a B_4C target, similar in shape to the target of the material being investigated. The B_4C target completely absorbed the thermal neutrons falling on it. Comparison of the area of the photopeak from 482 kev γ-quanta, emitted by a B_4C target, with the area of the photopeak arising from the target of the material being investigated permitted determination of the emission of γ-quanta during capture of a single neutron. Here use was made of the absorption cross section for thermal neutrons[7] and the experimentally determined efficiency of the scintillation spectrometer. The results of measurements on I, Rh and Co are presented below.

During the measurement of thermal neutron capture, γ-rays from I nuclei, γ-quanta with energy $E = 135 \pm 4$ kev, not apparent earlier in the work of other authors[4,5], were observed. The results of one of the experiments with an I target are presented in the Figure. The photopeak of γ-rays with 135 kev energy is clearly seen. The intensity of these γ-quanta per 100 captures of thermal neutrons was $n = 30$. The accuracy in the determination of the absolute yield is 15%. On the Figure, to the left of the principal photopeak, there are seen two small instrumental peaks. In addition, a photopeak from γ-quanta of energy 510 kev is noticed in the spectrum of the γ-radiation from an I target. It is possible, however, that these quanta have a secondary origin. Gamma-quanta with an energy of 255 kev, observed in Ref. 5 on the reaction I(n,γ), did not appear in our measurements.

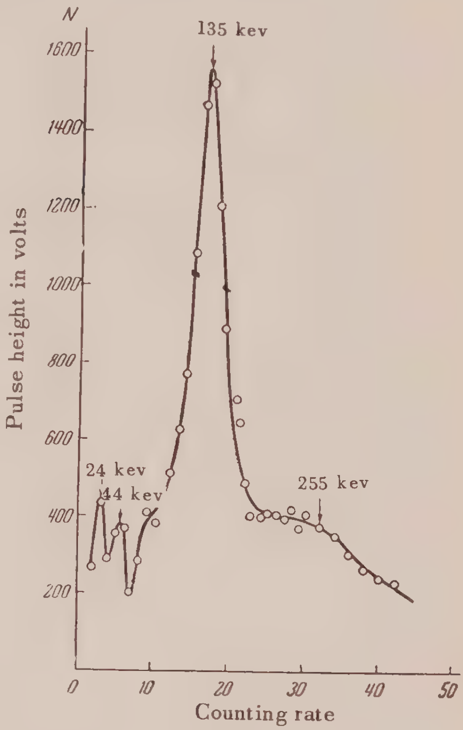

FIG. The γ-ray spectrum from Iodine.

Four discrete lines, with energies $E_1 = 217 \pm 4$; $E_2 = 176 \pm 4$; $E_3 = 133 \pm 4$; $E_4 = 96 \pm 4$ kev, and with intensities (for 100 captures of thermal neutrons) respectively equal to $n_1 = 9.3$, $n_2 = 18$, $n_3 = 8$ and $n_4 = 16$, have been observed as the result of the measurement of the γ-ray spectra emitted by Rh nuclei upon thermal neutron capture. The ratio n_1/n_4 is determined with an accuracy of 15-20%. The lines found cannot be connected with the activation of the target, since they differ in energies from the γ-quanta from the isomer Rh^{104} [8]. In the work of Hamermesh and Hummel[4], γ-quanta of energies 80 and 160 kev found in the γ-radiation from radiative capture of neutrons by Rh nuclei, were assigned in error to target activation. In this work, it is probable that the most intense of the γ-rays registered by us were detected. In the work of Kinsey and Bartholomew[9], the energies and intensities of the hardest γ-quanta emitted upon slow neutron capture were measured. On the basis of these data, it is possible to establish the energies of the low-lying levels of the Rh^{104} nucleus. The γ-lines found by us correspond to transitions between these levels.

Gamma-quanta with energies $E_1 = 276$ and $E_2 = 226$ kev and approximately equal intensities of about 20 γ-quanta per 100 neutron capture have been observed in the measurement of the spectra of the γ-rays from the radiative capture of thermal neutrons by Co nuclei. The energies of the γ-quanta E_1 and E_2 are in agreement with the data from the work of Reier and Shamos[5].

In conclusion, the authors thank A. M. Safronov and the association of co-workers operating the physics reactor for their help in the work.

---

[1] B. B. Kinsey and G. A. Bartholomew, Canad. J. Phys. 31, 537 (1953).

[2] Groshev, Ad'iasevich and Demidov, Papers at the International Conference on the peaceful applications of atomic energy, Geneva, 1955; Physics Research, p. 252, Acad. of Sci., USSR, Moscow, 1955.

[3] Ad'iasevich, Groshev and Demidov, Session of the Acad. of Sci., USSR, on the peaceful applications of atomic energy, July 1-5, 1955; Meeting of the division of physical-mathematicl sciences, publication of the Acad. Sci., USSR, Moscow, 1955.

[4] B. Hamermesh and V. Hummel, Phys. Rev. **88**, 916 (1952).

[5] M. Reier and M. H. Shamos, Phys. Rev. **95**, 636 (1954).

[6] Alikhanov, Vladimirskii, Nikitin, Galanin, Gavrilov and Burgov, Papers at the International Conference on the peaceful applications of atomic energy, Geneva, 1955; Reactor construction and the theory of reactors, p. 105, Acad. of Sci., USSR, Moscow, 1955.

[7] D. J. Hughes, *Pile Neutron Research*, IIL, Moscow, 1954.(originally published in the United States by Addison-Wesley).

[8] Jordan, Cork and Burson, Phys. Rev. **90**, 463 (1953).

[9] B. B. Kinsey and G. A. Bartholomew, Canad. J. Phys. **31**, 1025 (1953).

Translated by F. Ajzenberg-Selove
183

Concerning a Certain Possibility in Quantum Field Theory

IU. M. LOMSADZE
Moscow State University

(Submitted to JETP editor February 28, 1955)
J. Exptl. Theoret. Phys. (U.S.S.R.) 31, 887-889
(November, 1956)

THE author has attempted to overcome the well-known difficulties of contemporary relativistic quantum field theory which result, first, from the appearance of irremovable infinities in many "unrenormalizable" variants of the theory (among which are evidently all variants with an interaction Hamiltonian which either consists of the product of more than three field operators or contains the derivatives of these operators) and, secondly, from the divergence of series that are obtained after the elimination of all infinities in the "renormalizable" variants (particularly in electrodynamics).

It would seem that the explanation of these difficulties must be sought not in a deficiency of the theory itself but in a short-coming of the method that is used to solve the equations of the theory (the Lomonoga-Schwinger equations), namely, the perturbation method (the decomposition of the desired solution in a MacLaurin series of powers of the field binding constant g). In other words, the series which is obtained formally in the course of the solution, because of the illegitimacy of this very expansion within the framework of ordinary mathematical analysis, does not provide the desired solution in the usual sense of a sum (the limit of the sum of n terms as $n \to \infty$)*.

It can reasonably be asked, however, whether it is possible in some manner to derive from the formally obtained series the solution which was improperly expanded in this very series. In other words, what mathematical operation should be understood by the "sum" of the series so that this "sum" would give the solution formally expanded in the series even when the ordinary concept of a sum leads to an obviously incorrect result ($\equiv \infty$). If the S matrix $S(g, p)$ of a process is selected as the solution of the quantum equations (where p denotes the set of momenta of "real" particles), then, assuming that this S matrix is an analytic function of p, our question can be answered by introducing the following generalizations of the usual concept of the sum of an infinite series, which satisfy general axiomatic requirements (see, for example, Ref. 1).

If the series $\sum_i U_i(\xi)$ converges in some interval of ξ to the analytic function $S(\xi)$, then by the generalized sum $\sum_{i\xi}$ (with respect to ξ) of this series (in the intervals where it diverges) we shall understand the analytic continuation of $S(\xi)$ in these intervals. Given a series of the form $\sum_i \int_{(l)} U_i(l, \xi)$, where each of the l-integrals can diverge**, then by the l-sum $\sum_i{}^l_\xi$ (for ξ) of this series, if it exists, we shall understand the l-integral of the generalized sum with respect to l and ξ of the integrands:

$$\sum_{i}{}^{l}_{\xi} \int_{(l)} U_i(l, \xi) = \int_{(l)} \sum_{i}{}_{l,\xi} U_i(l, \xi).$$

The proposed method is applicable to the pair theory of interactions of spinor fields and of a spinor and pseudoscalar field. The entire infinite set of series terms, each of which corresponds to a Feynman diagram, is divided in a definite manner into (infinite) subsets and the l-summation of the terms in each subset is performed (this l-summation can be accomplished in closed form). It results (as can be shown by the inductive method which the author used previously to solve another problem[2]) that the modified series which results from this operation, consisting of subsets summed in the l sense is not only renormalizable, but (after renormalization) converges in the usual sense and converges absolutely in each case for large momenta of "real" particles. Each term of the renormalized modified series is a complicated function of g which cannot be reduced to an integral power; for small g the series decomposes the S matrix in increasing powers of $g \ln g$, which reveals the origin of the irremovable infinities in the original perturbation series.

A natural result is that the modified series is equivalent to the original series in the following sense. If in the original series the l-integration is limited by some $l_{\max}$, then such a "cutoff" series A can be compared with another series A' such that the formal expansion of each term A' in a Maclaurin series with respect to g (which converges to give the expanded term only for small values of $l_{\max}$) leads to series A. For small g and large $l_{\max}$, series A' gives an expansion in increasing powers of $g \ln (g + c/l_{\max}^2)$. In the limit $l_{\max} \to \infty$, A' coincides with our modified series, which we obtained without this intervening "cutting-off" procedure. This fact is extremely important for an understanding of the relationship between modified and ordinary series, since it emphasizes the difference in principle between the proposed method and the usual methods such as the introduction of cut-off factors, for which such equivalence obviously does not exist.

One of the peculiarities of the foregoing modification is the fact that now the interaction potential of two spinor particles in any approximation of pair theory has a singularity at the origin which is not stronger than $1/r \ln r$ (compare the results in Ref. 3), which makes it possible to use pair theory for the solution of problems concerning nuclear forces. An analysis of the potential of the first nonvanishing approximation in one of the variants of pair theory shows that attraction at large distances which decreases exponentially as $r \to \infty$, becomes repulsion at small distances (with a $1/r$ singularity at the origin. This is the result required by experiment.

It should be noted, in conclusion, that the proposed method can be used in electrodynamics and in the variants of the theory containing derivatives, although the latter possibility is obviously associated with certain difficulties.

The author takes this opportunity to thank D. D. Ivanenko for valuable discussions.

---

* The origin of the difficulty resulting from "irremovable" infinities can be illustrated by the formal expansion of the function $\ln g$ in a Maclaurin series; the difficulty resulting from series divergence can be illustrated by expansion of the function $(1 - g^2)^{-1}$ for $g^2 \geq 1$.

** Keeping in mind that l can mean any set of virtual momenta and ξ another set of both virtual and real momenta.

[1] G. H. Hardy, *Divergent Series*, IIL, 1951 (Russian translation).

[2] Iu. M. Lomsadze, J. Exptl. Theoret. Phys. (U.S.S.R.) **30**, 707 (1956); Soviet Phys. JETP **3**, 556 (1956).

[3] Iu. M. Lomsadze, Dokl. Akad. Nauk SSSR **110**, 545 (1956).

Translated by I. Emin
184

Accuracy of Isobaric Spin for the $1f_{7/2}$ Shell

V. G. NEUDACHIN

(Submitted to JETP editor June 18, 1956)
J. Exptl. Theoret. Phys. (U.S.S.R.) 31, 892-893
(November, 1956)

RADICATY[1] has calculated the accuracy of the isobaric spin T for the lightest nuclei on the assumption that the inaccuracy of T is caused by Coulomb forces alone. We have carried through analogous calculations for nuclei with $1d$ and $1f_{7/2}$ shells. These calculations, which followed the method of Racah[2,3], are characterized as follows:

1. The matrix elements of the Coulomb interaction can be of several kinds.

a) $\langle j^n T(\sigma) JM_T | G^c | j^n T'(\sigma') JM_T \rangle$,

$$G^c = \sum_{i>j}^{n} g_{ij}^c, \quad g_{ij}^c = \frac{(1/2 - \tau_i)(1/2 - \tau_j)}{|\mathbf{r}_i - \mathbf{r}_j|} e^2,$$

τ_i is the operator of the z component of the isobaric spin; (σ) is the symbol of the irreducible representation of the symplectic group[3]; $M_T = 1/2 \times (N - Z) = 1/2(A - 2Z)$; j^n is the nucleonic configuration of the unfilled outer shell. The inaccuracy of the isobaric spin of the lowest nuclear states which is associated with matrix elements of this form is $10^{-4} - 10^{-6}$ (squares of the amplitudes of the additional terms) and is relatively independent of configurations and types of coupling (LS or jj coupling).

b) Proton density of distribution in a closed spherically symmetrical shell. $P(r)$ denotes the combined density of protons in all closed shells. Neglecting exchange interaction[4], we can represent the Coulomb interaction operator of nucleons in the outer unfilled shell with the filled shells as

$$\sum_i f_i (1/2 - \tau_i), \quad f_i = e^2 \int \frac{P(r)\, d\tau}{|\mathbf{r} - \mathbf{r}_i|}.$$

A matrix element which is nondiagonal with respect to T:

$$\langle j^n T(\sigma) JM_T | \Sigma_i f_i (1/2 - \tau_i) | j^n T'(\sigma') JM_T \rangle$$

vanishes because of the well-known orthogonality of the genealogical coefficients[2,3]. This conclusion is not changed when the exchange interaction is taken into account and the matrix element is written in rigorous form, using the formulas given by Elliott and by Janagawa[5].

c) $\langle (N_j)^n T(\sigma) JM_T |$

$$\times \sum_i (1/2 - \tau_i) f_i \, | (N_j)^{n-1} (N'_j) T'(\sigma') JM_T \rangle$$

N and N' ard nonidentical principal quantum numbers of the states of individual nucleons. These matrix elements are the most important.

2. The calculations were carried through with oscillator wave functions, whose parameters were determined mainly by the differences in the binding energies of mirror nuclei, assuming charge independence of nuclear forces. The values of the parameters were obtained analogously in Ref. 6. In particular, we used for Sc_{21}^{42}: $\nu^{-1/2} = 2.0 \times 10^{-13}$ cm, for F_9^{18}: $\nu^{-1/2} = 1.7 \times 10^{-13}$ cm, for Li_3^6: $\nu^{-1/2} = 1.4 \times 10^{-13}$ cm, where ν is a parameter in the wave function; for example, for the $1s$ state: $\psi = \mathrm{const}\, e^{-\nu r^2/2}$.

Calculation of matrix elements (c) gives the following values of the square of the amplitude of the added term for the ground states:

Nucleus	Li_3^6	F_9^{18}	Sc_{21}^{42}
$\alpha_{TT'}^2 =$	$5 \cdot 10^{-5}$	$4 \cdot 10^{-4}$	$1 \cdot 10^{-2}$

$T = 0, \quad T' = 1.$

These values are typical for nuclei of the corresponding shells.

Extensive experimental data are available for the lightest nuclei[7-9]. For nuclei with a $1f_{7/2}$ shell there are almost no data. Some conclusions, however, can be drawn from the following fact. The resolved β-transitions in odd nuclei with a $1f_{7/2}$ shell between the states $J_{\mathrm{in}} = J_{\mathrm{fin}} = j = 7/2$ are divided into two distinct groups: for non-mirror transitions ($T_{\mathrm{in}} = T_{\mathrm{fin}} \pm 1$): $\lg ft = 5 - 6$, and for mirror transitions ($T_{\mathrm{in}} = T_{\mathrm{fin}}$): $\lg ft \approx 3.5$. Examples are:

$$\mathrm{Ti}_{22}^{43}(\beta^+)\,\mathrm{Sc}_{21}^{43}: \ \lg ft = 3{,}4; \qquad \mathrm{Ca}_{20}^{45}(\beta^-)\,\mathrm{Sc}_{21}^{45}: \ \lg ft = 5.9.$$

Without attempting to explain this fact, whose causes are still unknown[8], we shall note that the existence of such a clear difference between the values of ft for mirror and non-morror transitions enables us to say that the squares of the amplitudes of the added terms for the isobaric spins does not exceed a few percent; otherwise, the difference in *ft* for the two groups mentioned would be smaller.

A direct experimental check of the accuracy of T for nuclei with a $1f_{7/2}$ shell is difficult since nuclei with $N = Z$ or $N = Z \pm 1$ are unstable. For this purpose it will probably be useful to study the reactions (γ, n) and (γ, p)[9].

Our examination shows that whenever the outer neutrons and protons are to be found in the same shell in a stable nucleus, T is a good quantum number.

When we pass from nuclei with a $1f_{7/2}$ shell to heavier nuclei, we find that the outer nuetrons and protons in stable nuclei are contained in different shells. For such cases the proton and neutron shells are considered separately and the isobaric spin is not used as a quantum number. This is easily understood, since one cannot speak of the "accuracy" of T for these nuclei.

The fact that T is still a good quantum number for nuclei which contain a large amount of Coulomb energy is associated with the character of the coulomb forces: these are long-range forces, so that the nondiagonal matrix elements are smaller by one order of magnitude than those matrix elements which are diagonal with respect to T. In the limiting case of an infinite range for the forces the nondiagonal elements (in T) would vanish because the Hamiltonian would be symmetrical with respect to permutations of the particles.

---

[1] L. Radicaty, Proc. Phys. Soc. (London) **66A**, 139 (1953); **67A**, 27 (1954).

[2] G. Racah, Phys. Rev. **63**, 367 (1943).

[3] Edmonds and Flowers, Proc. Roy. Soc. (London) **A214**, 515 (1952).

[4] E. U. Condon and G. H. Shortley, *Theory of Atomic Spectra*, 1948 (Russian translation); Sack, Biedenharn and Breit, Phys. Rev. **93**, 321 (1954).

[5] J. Elliott, Proc. Roy. Soc. (London) **A218**, 345 (1953); S. Janawaga, J. Phys. Soc. Japan **8**, 302 (1953).

[6] B. C. Carlson and I. Talmi, Phys. Rev. **96**, 436 (1954); W. Swiatecki, Proc. Roy. Soc. (London) **A205**, 238 (1952).

[7] A. I. Baz' and Ia. A. Smorodinskii, Usp. Fiz. Nauk **55**, 215 (1955).

[8] I. Talmi, Phys. Rev. **91**, 122 (1935); A. Bohr and B. Mottelson, Dan. Mat. Fys. Medd. **27**, No. 16 (1953).

[9] H. Morinaga, Phys. Rev. **97**, 444 (1955).

Translated by I. Emin
187

The Theory of Slowing Down of Neutrons

A. IA. TEMKIN
Institute for Geophysical Methods of Prospecting, Petroleum Ministry of the USSR

(Submitted to JETP editor June 5, 1956)
J. Exptl. Theoret. Phys. (U.S.S.R.) **31**, 893-895 (November, 1956)

THE integral of the collisions of neutrons with the nuclei of a moderator[1] can be written as

$$\sum_\alpha \int_0^u du' \int_{-1}^{1} d\mu' \int_0^{2\pi} d\beta' f_{\alpha 0}(u-u') \frac{\lambda(u')}{\lambda_\alpha(u')} \times \delta(\mu_0 - \gamma_\alpha)\, \psi(\mathbf{r}, u', \mu', \beta') = \sum_\alpha \hat{K}_\alpha \hat{B}_\alpha \psi, \tag{1}$$

$$\hat{K}_\alpha \equiv \int_0^u du' f_{\alpha 0}(u-u') \frac{\lambda(u')}{\lambda_\alpha(u')} \times \int_{-1}^{1} d\mu' K_\alpha(\mu, \mu', u-u'), \tag{2}$$

$$K_\alpha \equiv (1 - \mu^2 - \mu'^2 - \gamma_\alpha^2 - 2\gamma_\alpha \mu\mu')^{-1/2}, \tag{3}$$

$$\hat{B}_\alpha \equiv \int_0^{2\pi} \delta(\beta' - \overline{\beta})\, d\beta', \tag{4}$$

where ψ is the distribution function for collisions between neutrons and moderator nuclei (see, for example, Refs. 1 and 2), α is an index which designates individual elements with mass number M_α contained in the moderator, ϑ and β are the spherical angles of the vector $\boldsymbol{\omega} = \mathbf{p}/p$ (where $\mathbf{p}$ is the neutron momentum and $\mathbf{r}$ is its radius vector), $u = \ln(2mE_0/p^2)$ with E_0 as the initial neutron energy and m as the neutron mass, λ_α is the partial neutron mean free path allowing for inelastic collisions with nuclei of mass M_α, and λ is the total neutron mean free path in the medium,

$$\gamma_\alpha(u) \equiv [(M_\alpha + m)\, e^{-u/2} - (M_\alpha - m)\, e^{u/2}] / 2m, \tag{5}$$

$$f_{\alpha_0}(u) \equiv \begin{cases} [(M_\alpha + m)^2 / 4mM_\alpha]\, e^{-u} & \text{for} \quad u \leqslant q_\alpha, \\ 0 & \text{for} \quad u > q_\alpha, \end{cases} \tag{6}$$

$$q_\alpha = 2\ln[(M_\alpha + m)/(M_\alpha - m)], \tag{7}$$

$$\mu_0 = \omega\omega' = \mu\mu' + \sqrt{1-\mu^2}\sqrt{1-\mu'^2}\cos(\beta' - \beta), \tag{8}$$

$\bar\beta$ $(0 < \bar\beta < 2\pi)$ is the root of the equation

$$\mu\mu' + \sqrt{1-\mu^2}\sqrt{1-\mu'^2}\cos(\bar\beta - \beta) - \gamma_\alpha = 0. \tag{9}$$

We note that in the one-dimensional problem which was considered in Refs. 3-6, the function ψ is independent of β, so that $B_\alpha\psi = \psi$. In this case it is easy to derive an equation for K_α in the form of a series of Legendre polynomials:

$$K_\alpha = \pi\sum_{l=0}^{\infty}(2l+1)P_l(\gamma_\alpha)P_l(\mu)P_l(\mu'). \tag{10}$$

$K_\alpha(\mu, \mu', u)$ is the angular distribution (with respect to angle ϑ) of neutrons scattered by a nucleus in the laboratory system. It is well known that its strongest dependence on μ and μ' occurs for the scattering of neutrons by hydrogen. We shall now show that even in this case the principal part is played in (10) by the sum of a few $(n_0 + 1)$ first terms of the series which we shall denote by K^0_α. If we now express K_α according to Eq. (3) the remainder of series (10) $\tilde{K}_\alpha = K_\alpha - K^0_\alpha$ can be written as a finite expression. In (2) we now replace $\hat{K}_\alpha$ by K^0_α or $\tilde{K}_\alpha$ and obtain the operators $\hat{K}^0_\alpha$ and $\hat{K}_\alpha$.

Regarding all functions of u and μ as points in in the metric space L_2, defining the norm of $V(u,\mu)$ as

$$\|V\| = \int_0^u due^{-u/2}\int_{-1}^{1} d\mu V^2(u, \mu) \tag{11}$$

and denoting $\epsilon = \|\tilde{K}_\alpha\|^{1/2}/\|K^0_\alpha\|^{1/2}$, we obtain $\epsilon = 0.33 < 1$ from (10) with $M = m$ and $n_0 = 1$.

Let n be chosen so that $\epsilon < 1$. Instead of the exact kinetic equation[1]

$$\hat{L}\psi = \sum_\alpha \hat{K}_\alpha\hat{B}_\alpha\psi + S \tag{12}$$

we shall consider the equation

$$\hat{L}\psi^0 = \sum_\alpha \hat{K}^0_\alpha\hat{B}_\alpha\psi^{(0)} + S, \tag{13}$$

where S is the density of neutron sources and $\hat{L}_r(u, \mu, \beta) \equiv \lambda(u)\,\omega\,\mathrm{grad} + 1$.

Comparing (12) and (13), we find by using Schwarz' inequality that $(\|\psi - \psi^{(0)}\|^{1/2}/\|\psi^{(0)}\|^{1/2}) \leq \epsilon$.

The effect of $\hat{K}_\alpha$ can be regarded as a small perturbation. For this purpose we write

$$\psi - \psi^{(0)} = \psi^{(1)} + \psi^{(2)} + \ldots + \psi^{(n)} + \ldots. \tag{14}$$

Substituting this series in (1), breaking it off for successive values of $n = 1, 2, \ldots$, taking (13) into account and each time dropping a term of the form

$$S^{(n)} = \sum_\alpha \hat{\tilde{K}}_\alpha\hat{B}_\alpha\psi^{(n)}, \tag{15}$$

we arrive at an equation for the determination of the nth correction which differs from (13) only in that S is replaced by $S^{(n-1)}$.

The solutions of these equations can be written with the aid of their Green's functions G in the form

$$\psi^{(n)}(\mathbf{r}, u, \mu, \beta) = \int S^{(n-1)}(\mathbf{r}_1, u_1, \mu_1, \beta_1) \times G(\mathbf{r}, \mathbf{r}_1, u, u_1, \mu, \mu_1, \beta, \beta_1)\,d\mathbf{r}_1\,du_1\,d\mu_1\,d\beta_1, \tag{16}$$

setting $S^{(-1)} = S$.

Recalling how the equations for $\psi^{(n)}$ were derived by the use of (13) and (16), we find that $(\|\psi^{(n)}\|^{1/2}/\|\psi^{(0)}\|^{1/2}) \leq \epsilon^n$,

$$\left(\left\|\psi - \psi^{(0)} - \sum_{i=1}^{n}\psi^{(i)}\right\|^{1/2} \Big/ \left\|\psi^{(0)}\right\|^{1/2}\right) \leqslant \varepsilon^{n+1}, \tag{17}$$

that is, the series (14) converges to $\psi - \psi^{(0)}$ with the error defined by (17). We note that the convergence of a point sequence in space L_2, which we have used, corresponds, as is well known, to the convergence in the mean of a sequence of functions.

The Green's function G satisfies (13) when we set $S = \delta(\mathbf{r} - \mathbf{r}_1) \times \delta(u - u_1)\delta(\mu - \mu_1)\delta(\beta - \beta_1)$.

Multiplying this equation on the left by the operator L^{-1} and using g to denote the Green's function of the operator L which satisfies the boundary conditions of the problem, we put it into the form

$$G = \sum_\alpha \int d\mathbf{r}'\hat{K}^0_\alpha\hat{B}_\alpha g(\mathbf{r}, \mathbf{r}', \mu, \beta) \times G(\mathbf{r}', \mathbf{r}_1, u', u_1, \mu', \mu_1, \beta', \beta_1) + g(\mathbf{r}, \mathbf{r}_1, u, \mu, \beta)\,\delta(u - u_1)\,\delta(\mu - \mu_1)\,\delta(\beta - \beta_1). \tag{18}$$

The right-hand side of (18) actually contains G^0, the sum of the first $\sum\limits_{n=0}^{n_0}(2n+1)$ (in the one-dimensional case n_0+1)] spherical harmonics of the Green's functions. Therefore, the obtaining of G is reduced to the obtaining of G^0 by the method of spherical harmonics, that is, to the solution of a small set of integral equations which can be solved with consideration of the dependence of λ and λ_∞ on u. The Green's function G and the functions $\psi^{(0)}$ and $\psi^{(n)}$ are then determined according to (18) and (16) in finite form.

This is especially important for calculating neutron distributions in media which contain hydrogen (water, petroleum, etc.) since the usual expansion of the distribution in spherical functions[1-6] converges poorly in this case.

In conclusion, I wish to express my sincere thanks to S. A. Kantor for his assistance.

---

[1] A. I. Akhiezer and I. Ia. Pomeranchuk, *Some Problems of Nuclear Theory*, GITTL, Moscow-Leningrad, 1950.

[2] R. E. Marshak, Rev. Mod. Phys. **19**, 185 (1947).

[3] Marshak, Brooks and Hurwitz, Nucleonics **4**, 5, 6 (1949); **5**, 1, 2 (1949).

[4] M. Verde and G. C. Wick, Phys. Rev. **71**, 852 (1947).

[5] G. C. Wick, Phys. Rev. **75**, 738 (1949).

[6] G. Holte, Ark. f. Fysik **2**, 523 (1951); **3**, 209 (1951); **6**, 243 (1953); **8**, 165 (1954).

Translated by I. Emin
188

The Effect of Finiteness of Target-Nucleus Mass on Angular Distribution in (*d*, *p*) and (*d*, *n*) Reactions

D. P. GRECHUKHIN

(Submitted to JETP editor June 12, 1956)
J. Exptl. Theoret. Phys. (U.S.S.R.) 31, 895-897
(November, 1956)

IN analyzing the angular distribution of the products of (*d*, *p*) and (*d*, *n*) reactions, it is customary to use the formulas derived by Butler[1] for an infinitely heavy target-nucleus. We have calculated the angular distribution with allowance for the finiteness of the nuclear mass by the same method of smooth connection of functions and subject to the same assumptions as in Ref. 1 without considering the question of the legitimacy of these assumptions. The results of the calculation are given below.

The angular distribution is given by the following formula:

$$S(\theta)=|(Z_1^2+\alpha^2)^{-1}-(Z_1^2+(\alpha+\beta)^2)^{-1}|^2 \tag{1}$$

$$\times\sum_l N^J_{l\,k_n^s}\left|\left(\sum_{q=0}^{l}\frac{(l+q)!}{(l-q)!\,q!\,(2k_n^sR_0)^q}\right.\right.$$

$$\left.\times\,[l+q+k_n^sR_0]\right)f_l(Z_2R_0)$$

$$\left.-\left(\sum_{q=0}^{l}\frac{(l+q)!}{(l-q)!\,q!\,(2k_n^sR_0)^q}\right)(Z_2R_0)\,f_{l+1}(Z_2R_0)\right|^2,$$

where l is the orbital angular momentum of a nucleon captured in an orbit of the ultimare nucleus; k_n^s is the wave number of this nucleon in the final state. The values of N are the same as in Ref. 1. R_0 is the "reaction radius" and is obtained by setting in agreement the theoretical and experimental curves for the angular distribution of the products of stripping. The wave numbers α and β which describe the state of the deuteron, are taken to be $\alpha = 0.23\times10^{13}$ cm^{-1} and $\beta = 1.4\times10^{13}$ cm^{-1}; $f_l(x)$ are spherical Bessel functions: $f_l(x) = \sqrt{\pi/2x}\,J_{l+1/2}(x)$. This formula differs from that of Butler only in that K is replaced by Z_1, Z by Z_2 (and r_0 by R_0). Here Z_1 and Z_2 are given by

$$Z_1=\frac{1}{\hbar}\left|\left(\frac{M_a}{M}\right)^{1/2}\left(\frac{M_b}{M_b+M_c}\right)\sqrt{2(M_b+M_c)W_1}\,\mathrm{n}_1\right. \tag{2}$$

$$\left.-\left(\frac{M_a+M_c}{M}\right)^{1/2}\sqrt{2M_bW_2}\,\mathrm{n}_2\right|,$$

$$Z_2=\frac{1}{\hbar}\left|\left(\frac{M_a}{M}\right)^{1/2}\sqrt{2(M_b+M_c)W_1}\,\mathrm{n}_1\right.$$

$$\left.-\left(\frac{M_a^2}{M(M_a+M_c)}\right)^{1/2}\sqrt{2M_bW_2}\,\mathrm{n}_2\right|,$$

where $(\mathrm{n}_1, \mathrm{n}_2) = \cos\theta$, θ is the angle between the directions of the escaping nucleon and the incident deuteron in the center-of-mass system, W_1 and W_2 are the kinetic energy of the deuteron and nucleon with respect to the initial and final nucleus; M_a, M_b and M_c are the masses of the target-nucleus, the

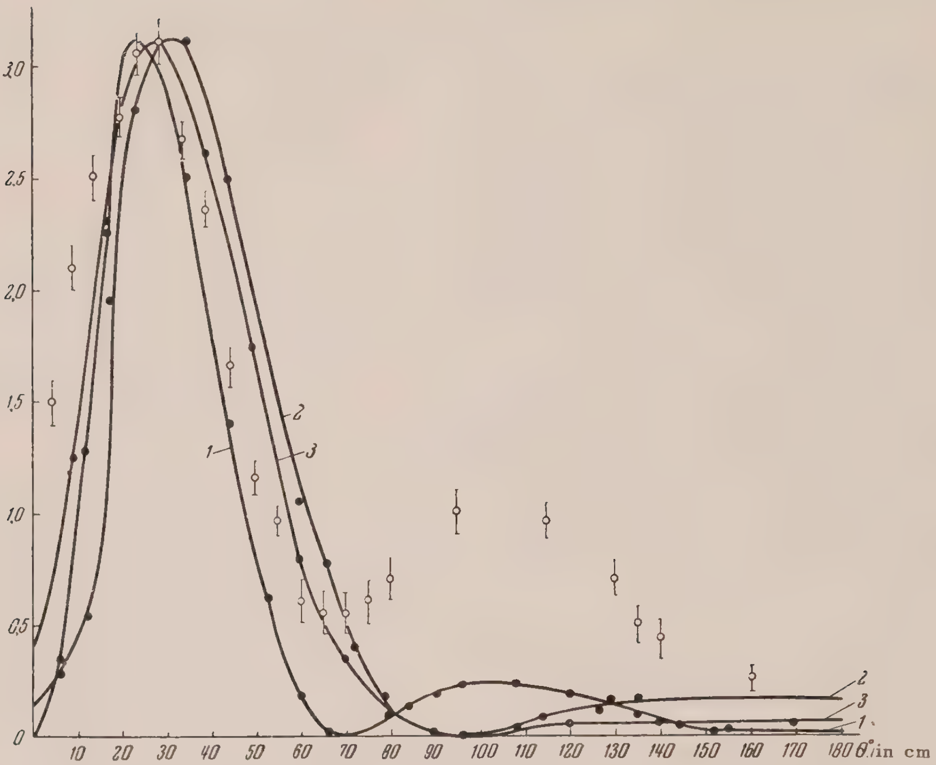

1 and *2* are the angular distributions derived theoretically for finite mass of Be_4^9 with $R_0 = 6.1 \times 10^{-13}$ cm and $R_0 = 4.5 \times 10^{-13}$ cm, respectively; *3* is the proton distribution according to Butler's theory with $r_0 = 4.5 \times 10^{-13}$ cm [2].

emitted nucleon and the captured nucleon. Obviously, $W_1 = E_d M_a / M$; $W_2 = W_1 + Q$. Here E_d is the deuteron energy in the laboratory system and Q is the reaction energy. When $M_a \to \infty$ the formula is reduced to that of Butler.

Allowance for the finiteness of the nuclear mass M_a leads to a change in magnitude of the reaction radius R_0 (which is always an increase). The angular distribution of the reaction products is also somewhat deformed (especially at angles $\theta > 50°$).

We give as an illustration the angular distribution of the group of protons resulting from the $Be_4^9(d, p)Be_4^{10}$ reaction at $E_d = 3.6$ mev with neutron capture in the ground state of Be_4^{10}; $l_n = 1$, $Q = 4.59$ mev (see the Figure); the experimental data are taken from Ref. 2. Allowance for the finiteness of M_a leads to larger values of R_0. Moreover, when R_0 is determined from agreement of the first maximum (or first minimum) the positions of the secondary maxima and minima of the distribution curve also agree with experiment.

This is not a unique example. Thus, in the $He_2^3(d, p)He_2^4$ reaction at $E_d = 10.2$ mev[3] [or $H_1^3(d,n)He_2^4$] an analogous calculation gives $R_0 = 5.3 \times 10^{-13}$ cm instead of $r_0 = 4.3 \times 10^{-13}$ cm. As in the preceding instance, agreement of the theoretical and experimental first minima leads directly to agreement of the succeeding maxima and minima. It should be noted that with increasing deuteron energy, the correction for finiteness of the mass M_a becomes more important. Therefore, the decrease of the radius r_0 which was noted by Gordon[4] probably resulted in part from the fact that he did not make allowance for the finiteness of M_a.

In conclusion I wish to thank A. Z. Dolginov for suggesting the problem and for his continued interest.

---

[1] S. T. Butler, Proc. Roy. Soc. (London) **A208**, 559 (1951).

[2] Fulbright, Bruner, Bromley and Goldman, Phys. Rev. 88, 700 (1952).

[3] S. T. Butler and J. L. Symonds, Phys. Rev. **83**, 858

(1951).

[4] M. M. Gordon, Phys. Rev. 99, 1625A (1955).

Translated by I. Emin
189

On the Mechanism of Initiation of Boiling of Liquid Metastable Systems by Ionizing Radiation

G. A. ASKAR'IAN
P. N. Lebedev Physical Institute
Academy of Sciences, USSR

(Submitted to JETP editor July 3, 1956)
J. Exptl. Theoret. Phys. (U.S.S.R.) 31, 897-899
(November, 1956)

A CERTAIN concentration of like-charged ions undoubtedly gives rise to an embryonic microburst of a liquid in which an essential role of the electropoles of the ions appears not only in the repulsion of the ions but also in the realization of binding of ions to molecules. In the calcuation of the number of bubbles which are formed as a result of the aggregation of ions in a liquid supersaturated with vapor[1] or gas[2,3], we shall assume as sufficient for the induced creation of a bubble that there originate in a region whose dimensions do not exceed the "interval of localizations" $\lambda(\xi)$ (ξ are parameters which characterize the degree of supersaturation) $\nu(\xi)$ positively charged ions, the electrons of which acquired an energy $\epsilon > \epsilon'_{\text{imp}}(\xi)$ upon ionization. (We shall call such ions noncompensated). The parameter ϵ'_{imp} characterizes the conditions of separation (averaged over all possible configurational dispositions of ν ions) for which the effect of oppositely charged centers becomes unimportant, at least in the time of formation of the embryonic cavity.

The probability $w(\epsilon_0)$ of creation of conditions adequate for the formation of an embryonic cavity somewhere along the track of a δ-electron, which has an initial energy ϵ_0, depends on the complex spatial distribution on noncompensated ions. We can, however, with sufficient confidence, assume that the most numerous δ-electrons with low energies give the chief contribution to the creation of the fluctuations which interest us. This circumstance facilitates the modeling of a distribution of noncompensated ions. Thus, for example, we can hypothesize that a large part of the noncompensated ions is formed near the tracks of low energy δ-electrons and the distributions of such ions is approximated closely by a Poisson distribution, in which the mean specific number of these noncompensated ions is related to the specific energy loss of an electron $\eta \approx (1/\epsilon_{\text{imp}})(d\epsilon/dx) \approx a/\epsilon_{\text{imp}}\epsilon$, where by ($\epsilon_{\text{imp}}$ should be understood the energy loss which occurs (on the average) per noncompensated ion formed near the track ($\epsilon_{\text{imp}} \gtrsim \epsilon'_{\text{imp}}$). Then the probability of creation of the required groups per element of length dx averaged over the track of a δ-electron is

$$dw \approx \eta \frac{(\lambda\eta)^{\nu-1}}{(\nu-1)!} dx \quad \text{for} \quad \lambda\eta \ll 1;$$

$$\text{and} \, w(\varepsilon_0) \approx \int_{\nu\varepsilon_{\text{imp}}}^{\varepsilon_0} dw(\varepsilon) + w_1(\varepsilon_0);$$

where $w_1(\epsilon_0)$ is the additional probability of a sought fluctuation at the origin of the track of a δ-electron. Integrating over the spectrum of the δ-electrons, we obtain the specific number of bubbles:

$$n_{\text{elect}} \approx \int_{\nu\varepsilon_{\text{imp}}}^{\varepsilon_{\max}} w(\varepsilon_0) \frac{KZ^2}{\beta^2} \frac{d\varepsilon_0}{\varepsilon^2_0}$$

$$\approx \frac{KZ^2}{\beta^2} \frac{(a\lambda)^{\nu-1}}{(\nu-1)!\,(\nu\varepsilon_{\text{imp}})^{\nu-1}\,\varepsilon^{\nu}_{\text{imp}}} \left(\frac{1}{\nu-1} + \frac{1}{\nu^2}\right) \approx \frac{Z^2}{\beta^2} \psi_\nu(\xi),$$

on disregarding the relativistic corrections and the weak dependence on the upper limit (Z and β are the charge and speed of an ionizing particle).

A characteristic of the process of ionic initiation in certain liquids should be noted. Thus, for example, in pure liquids of inert elements in which formation of negative molecular ions does not occur, the energy necessary for sufficient removal of electrons from ionized molecules, which take part in the formation of cavities, must be anomalously large to avoid recombination of ions with high mobility electrons before completion of formation of a cavity. Therefore, the intensity of a track in bubble chambers with inert liquids must increase with addition of certain substances which form negative ions.

In a series of events, a certain apparently relatively small number of bubbles can be formed as a result of thermal spikes generated by nuclear collisions. In calculation of the number of such bubbles we must have in mind that under the moderate supersaturation conditions prevailing, single stage nuclear collisions of ionizing particles with nuclei of atoms of the molecules of the liquid play the chief role in the creation of the necessary localization of kinetic energies of molecules. The mean energy of initiation, apparently, will not depend noticeably on the type of nucleus which has received the impulse in the collision, since this energy is further distributed among the neighboring molecules. A correct theoretical estimate of the energy necessary for "microburst" creation of embryonic voids does not appear possible, although there is some basis for thinking that it is rather large at moderate operating supersaturations in view of the dynamic resistances which arise. Assuming that the energy of initiation $\epsilon_{\text{init}}(\xi)$ exceeds the binding energy of atoms in the molecule, we obtain for the number of acts of transfer to nuclei of energy which exceeds ϵ_{init}

$$n_{\text{therm}} \approx \frac{\pi N_e}{\varepsilon_{\text{init}} M_p c^2} \left(\frac{Ze^2}{\beta}\right)^2 \approx \frac{Z^2}{\beta^2} \psi(\xi),$$

where N_e is the number of electrons per cubic centimeter of liquid and M_p is the mass of the proton. An estimate of the threshold energy for thermal initiation of boiling of some liquids for various supersaturations could be obtained by studying boiling of these liquids under the action of monochromatic neutrons, the energy of which can be varied over the range ~ 1-100 ev.

On increasing the degree of instability of the state, the initiation energy decreases and various microprocesses gradually come into effect, which guarantee a localization of thermal energy: multiple collisions, transformation of energy of excited molecules into kinetic energy of surrounding molecules, etc. The high transfer efficiency of electronic excitation energy to energy of motion of the nuclei of polyatomic molecules which is distributed in collisions with neighboring molecules can make the indicated process important in a series of concrete cases of formation of thermal spikes.

It would be natural to try to use the energy retained in the created ions for the purpose of developing a track after the passage of a particle, through some interval of time (~ 1 millisecond) sufficient for a pressure burst, i.e., for the creation of an automatically operating bubble chamber. The supersaturation necessary for retarded development of tracks must be such that the kinetic energy given off on neutralization of ionized polyatomic molecules exceeds the energy for initiation of boiling. (Various mechanisms of transformation of the energy liberated during neutralization into kinetic energy of molecules--the scattering of molecules which have been mutually neutralized, dissociation of a molecule excited during neutralization, collisions of the second kind, of surrounding molecules with a molecule excited on neutralization, etc.--give a kinetic energy which does not exceed a few electron volts.) For clear development of a track, it is necessary that a sufficient number of the ions which have remained recombine in the course of a short time interval. High specific ionization produced by the charged particles in the liquid, low coefficients of diffusion and of mobility of the ions, and the possibility of utilization of electropoles for variation of the dynamics of the recombination process of ions all create favorable conditions and allow confidence in the expediencey of attempts to set up automatic recording by going over to very high momentum-initiated superheats or supersaturations of operating liquids which contain polyatomic molecules.

According to the thermal model of electric breakdown of liquids proposed by Guntherschultz (see, for example, Ref. 4), one should also expect a manifestation of thermal spikes and vapor-gas nuclei upon "punctuated" energy loss by ions drifting in the electric field, even at pre-breakdown voltages. Therefore, use of a sufficiently strong electric field ("waiting" or switched on immediately after passage of a particle) can apparently either develop the track upon a "waiting" small superheat, or conserve the centers of development of the track until the creation of adequate supersaturation.

As another example of possible broadening of the range of varities of bubble chambers, one can cite the possibility of using the slow growth of bubbles and small background in a gas bubble chamber to demonstrate the recording of tracks of long range particles in opaque, physically-interesting, gassed liquids through bubbles which emerge on the free surface of the liquid (along the "torpedo-like" trail of the particle). In this case, some information on the spatial arrangement of a track can be estimated from the relative sizes of the bubbles along the track, as the size depends on the time needed to reach the surface.

---

[1] D. A. Glaser, Nuovo Cimento (Suppl.) **11**, Ser. 9, 2, 361 (1954); D. A. Glaser and D. C. Rahn, Phys. Rev. **97**, 474 (1955).

[2] G. Askar'ian, J. Exptl. Theoret. Phys. (U.S.S.R.) 28, 636 (1955); Soviet Phys. JETP 1, 571 (1955).

[3] P. Argan and A. Gigli, Nuovo Cimento 8, 5 1171 (1956).

[4] F. F. Wolkenstein, *Breakdown of Liquid Dielectrics*, ONTI, Moscow, 1934.

Translated by R. L. Eisner
190

Consequences of Renormalizability of Pseudoscalar Meson Theory with Two Interaction Constants

V. V. SUDAKOV AND K. A. TER-MARTIROSIAN

(Submitted to JETP editor July 14, 1956)
J. Exptl. Theoret. Phys. (U.S.S.R.) 31, 899-901
(November, 1956)

THE consequences of renormalizability of the pseudoscalar meson theory with two interaction constants obtained by Shirkov[1] are conveniently formulated as in Ref. 2.

The starting equations are again

$$\alpha(g_0^2, \lambda_0, \xi - L) = \alpha_c(g_c^2, \lambda_c, \xi) / \alpha_c(g_c^2, \lambda_c, L), \quad (1)$$

$$\beta(g_0^2, \lambda_0, \xi - L) = \beta_c(g_c^2, \lambda_c, \xi) / \beta_c(g_c^2, \lambda_c, L),$$

$$d(g_0^2, \lambda_0, \xi - L) = d_c(g_c^2, \lambda_c, \xi) / d_c(g_c^2, \lambda_c, L),$$

$$\mathcal{P}(g_0^2, \lambda_0, \xi - L) = \mathcal{P}_c(g_c^2, \lambda_c, \xi) / \mathcal{P}_c(g_c^2, \lambda_c, L).$$

One then introduces two effective charges $g(\xi)$ and $\lambda(\xi)$:

$$g^2(\xi) = g_0^2\alpha^2(g_0^2, \lambda_0, \xi - L) \quad (2)$$

$$\times\ \beta^2(g_0^2, \lambda_0, \xi - L)\, d(g_0^2, \lambda_0, \xi - L)$$

$$= g_c^2\alpha_c^2(g_c^2, \lambda_c, \xi)\, \beta_c^2(g_c^2, \lambda_c, \xi)\, d_c(g_c^2, \lambda_c, \xi),$$

$$\lambda(\xi) = \lambda_0 d^2(g_0^2, \lambda_0, \xi - L)\, \mathcal{P}(g_0^2, \lambda_0, \xi - L)$$

$$= \lambda_c d_c^2(g_c^2, \lambda_c, \xi)\, \mathcal{P}_c(g_c^2, \lambda_c, \xi).$$

The notation is the same as in Ref. 2. $\mathcal{P}$ is a quantity whose dependence on the meson-meson scattering amplitude P is given by[3]:

$$\mathcal{P} = (g_0^2 / 4\pi\lambda_0)\, P, \qquad \mathcal{P}_c = (g_c^2 / 4\pi\lambda_c)\, P_c,$$

λ_0 is a constant which appears in front of the Hamiltonian interaction terms*

$$(\lambda_0/4!)\,(\delta_{\tau_1\tau_2}\delta_{\tau_3\tau_4} + \delta_{\tau_1\tau_3}\delta_{\tau_2\tau_4} + \delta_{\tau_1\tau_4}\delta_{\tau_2\tau_3})\, \varphi_{\tau_1}\varphi_{\tau_2}\varphi_{\tau_3}\varphi_{\tau_4}.$$

The equivalence of the determination of the effective charges from either nonrenormalized or renormalized quantities follows from Eq. (1) and from the relations which exist between renormalized and nonrenormalized constants

$$g_0^2 = g_c^2\alpha_c^2(g_c^2, \lambda_c, L)\, \beta_c^2(g_c^2, \lambda_c, L)\, d_c(g_c^2, \lambda_c, L), \quad (3)$$

$$\lambda_0 = \lambda_c d_c^2(g_c^2, \lambda_c, L)\, \mathcal{P}_c(g_c^2, \lambda_c, L).$$

This is fundamentally confirmed by the fact that the logarithmic derivatives of α, β, d and $\mathcal{P}$ with respect to ξ are found to be solely dependent on the effective charges** g^2 and λ

$$(4)$$

$$\alpha'/\alpha = \alpha_c'/\alpha_c = F_1(g^2, \lambda), \quad \beta'/\beta = \beta_c'/\beta_c = F_2(g^2, \lambda),$$

$$d'/d = d_c'/d_c = F_3(g^2, \lambda), \quad \mathcal{P}'/\mathcal{P} = \mathcal{P}_c'/\mathcal{P}_c = F_4(g^2, \lambda).$$

Let us derive, for example, the last of Eqs. (4). The quantities g_c^2 and λ_c which appear in $\mathcal{P}_c'$ and $\mathcal{P}_c$ can be expressed in terms of g^2, λ and ξ by means of Eq. (2). Carrying this out, one obtains

$$\mathcal{P}'(g_0^2, \lambda_0, \xi - L) / \mathcal{P}(g_0^2, \lambda_0, \xi - L)$$

$$= F_4[g^2(g_0^2, \lambda_0, \xi - L), \lambda(g_0^2, \lambda_0, \xi - L), \xi].$$

This equation can only be satisfied if F_4 is not an explicit function of ξ; otherwise, if g_0^2 and λ_0 were kept constant, and ξ and L were varied, keeping their difference fixed, then ξ would be the sole variable appearing explicitly in F_4 only.

According to Eqs. (2) and (4), the logarithmic derivatives of the effective charges become

$$(g^2)'/g^2 = 2F_1(g^2, \lambda) + 2F_2(g^2, \lambda) \quad (5)$$

$$+ F_3(g^2, \lambda), \qquad \lambda'/\lambda = F_4(g^2, \lambda) + 2F_3(g^2, \lambda).$$

If the functions F are known, then Eqs. (5) define a system of differential equations which, together with the boundary conditions $g^2(L) = g_0^2$, $\lambda(L) = \lambda_0$, fully determine the effective charges $g^2(\xi)$ and $\lambda(\xi)$.

The functions F may be obtained from perturbation theory which applies if g_0^2, $\lambda_0 \ll 1$ and ξ is close to L, so that $g_0^2(L - \xi)$ and $\lambda_0(L - \xi)$ are small with respect to unity. We shall consider the most general case, when λ_0 and g_0^2 are of the same order of magnitude. The solution obtained in this case is also valid when one of these quantities is small with respect to the other ($g_0^2 \ll \lambda_0$ or $\lambda_0 \ll g_0^2$), since one may then simply neglect the small quantity with respect to the large one. We shall limit ourselves to the asymptotic solutions in the zero approximation, i.e., we shall consider all quantities as functions of only $g_0^2(\xi - L)$ and $\lambda_0(\xi - L)$ or, what amounts to the same thing, $g_0^2 \times (\xi - L)$ and g_0^2/λ_0. Perturbation theory calculations indicate that α, β, and d do not contain any terms in $\lambda_0(\xi - L)$, and we can therefore apply the results of Ref. 2 which give F_1, F_2, F_3 and the asymptotic forms of α, β and d, and the effective charge $g^2(\xi)$. Perturbation theory yields for $\lambda_0\mathcal{P}$:

$$\lambda_0\mathcal{P} = \lambda_0 - (g_0^4/\pi^2)(\xi - L) + {}^{11}/_{2}\lambda_0^2(\xi - L).$$

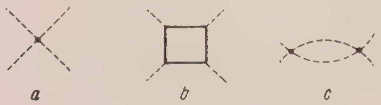

The three terms of this formula correspond to the diagrams *a*, *b*, *c*. In order to obtain the function F_4 it is necessary to compute $\mathcal{P}'/\mathcal{P}|_{\xi\to L}$ in the last formula and in the resulting expression substitute g_0^2 for g^2 and λ_0 for λ; this yields

$$F_4 = 11\lambda/2 - g^2/\pi^2\lambda. \tag{4$'$}$$

Applying Eq. (4′) and Eqs. (3′) and (4) of Ref. 2 to Eq. (5) one finds

$$\frac{\lambda'}{\lambda} = \frac{11}{2}\lambda - \frac{g_0^4}{\pi^2\lambda Q^2} + \frac{2g_0^2}{\pi Q}, \qquad Q = 1 + \frac{5g_0^2}{4\pi}(L - \xi). \tag{6}$$

Carrying out the substitution

$$\lambda(\xi) = (g_0^2/4\pi)\,\mathcal{P}(x)\,d^2(x), \quad x = Q^{3/5}, \tag{7}$$

we obtain the equation for the meson-meson scattering amplitude P.

$$dP/dx = {}^{16}/_{3} - {}^{11}/_{6}(P/x)^2$$

with the boundary condition $P(1) = 4\pi\lambda_0 g_0^2$. The solution of Eq. (7) is

$$P = \frac{16}{11}x\frac{B - x^{-19/3}}{B + (8/11)\,x^{-19/3}}; \tag{8}$$

$$B = \left(1 + \frac{1}{2}\frac{4\pi\lambda_0}{g_0^2}\right) \Big/ \left(1 - \frac{11}{16}\frac{4\pi\lambda_0}{g_0^2}\right),$$

which coincides with the results obtained in Ref. 3 for $\lambda_0 = 0$ ($B = 1$).

The present investigation may be used to compute asymptotic solutions to any order in g^2, λ from perturbation theory results to the same order.

In conclusion, the author would like to thank I. Ia. Pomeranchuk and V. B. Berestetskii.

---

*The symmetric theory is considered here.

**The expressions for the logarithmic derivatives of renormalized quantities are obtained from Eq. (1).

[1] D. V. Shirkov, Dokl. Akad. Nauk SSSR **105**, 972(1955).

[2] V. V. Sudakov, J. Exptl. Theoret. Phys. (U.S.S.R.) **31**, 729 (1956).

[3] I. T. Diatlov and K. A. Ter-Martirosian, J. Exptl. Theoret. Phys. (U.S.S.R.) **30**, 416 (1956); Soviet Phys. JETP **3**, 454 (1956).

Translated by M. A. Melkanoff
191

Excitation of Nuclear Vibrational Levels by Scattering of Fast Neutrons

E. V. Inopin
Physico-Technical Institute
Academy of Sciences, Ukrainian SSR

(Submitted to JETP editor July 15, 1956)
J. Exptl. Theoret. Phys. (U.S.S.R.) **31**, 901-902
(November, 1956)

IT is shown in Ref. 1 that there exists a large group of even-even nuclei in the interval $36 \leq N \leq 88$, whose first two excited levels apparently have vibrational character; this group property may be explained by the theory of A. Bohr[2] for the case of weak or intermediate coupling between the nuclear surface and the motion of individual nucleons. We shall consider here the excitation of the first vibrational level as it occurs during scattering of fast neutrons by a black nucleus and we shall limit ourselves to the zero coupling case.

The nuclear surface is characterized by the equation

$$r(\vartheta, \varphi) = R\left[1 + \sum_{\mu}\alpha_\mu Y_{2\mu}(\vartheta, \varphi)\right], \tag{1}$$

the coordinates A_μ are correlated with creation and annihilation operators β_μ^* and β_μ: $\alpha_\mu = \sqrt{\hbar/2B\omega} \times [\beta_\mu + (-1)^\mu \beta_{-\mu}^*]$. The wave functions for the ground and first excited states are given by χ_{00}^0 (no phonons) and $\chi_{2\mu}^1$ (one phonon with angular momentum 2 and z-component μ.) The matrix elements for the operators β_μ and β_μ^* are

$$(2\mu \,|\, \beta_{\mu'}^* \,|\, 00) = \delta_{\mu\mu'}, \qquad (2\mu \,|\, \beta_{\mu'} \,|\, 00) = 0. \tag{2}$$

The energy of the surface vibration is given by the expression $\epsilon_n = \hbar\omega(5/2 + n)$, where n is the number of phonons. The energy of the first excited level, $\epsilon_1 = \hbar\omega$, is limited to the interval $0.3 \leq \epsilon_1 \leq 2.0$ mev for the nuclei in question.

In the ground state, the nucleus performs zero order vibration of frequency ω. For sufficiently fast neutrons, the problem may be solved in the adiabatic approximation by computing the scattering of neutrons by a fixed surface nucleus. In this case, it is necessary that the period of zero order vibration, $T \approx 2\pi/\omega$, be much longer than the collision time, $\tau \approx R/v$, where R is the nuclear radius and v the neutron velocity. This leads to the condition $(\epsilon_1/4\pi E)kR \ll 1$, which is quite well satisfied for $\epsilon_1 \approx 1$ mev and for a neutron energy of several tens mev.

The amplitude for scattering by a black nucleus is obtained from the well-known formula

$$f(\theta, \alpha_\mu) = (ik/2\pi) \int e^{-i\mathbf{k}'\rho} dS, \tag{3}$$

where $\mathbf{k}$ and $\mathbf{k}'$ are the wave vectors of the incident and scattered neutrons, and the integration is to be carried out over a projected area of the nucleus whose surface is defined by the parameters α_μ, the projection being taken on a plane perpendicular to the incident vector $\mathbf{k}$. The scattering cross section in the θ direction for an excited state where there is one phonon with angular momentum 2 and component μ, is computed from the formula (see Ref. 3)

$$\sigma_\mu(\theta) = |(2\mu \,|\, f(\theta, \alpha_\mu) \,|\, 00)|^2. \tag{4}$$

Integral (3) may be calculated after carrying out a transformation of the variables which changes the surface of an ellipsoid into the surface of a sphere; the region of integration becomes a circle instead of an ellipse, the projection of an ellipsoid. Carrying out the computation, one obtains the following expression for the scattering amplitude (accurate to within terms linear in α_μ):

$$f(\theta, \alpha_\mu) = ikR^2 \left[\left(1 - \sqrt{\frac{5}{4\pi}}\alpha_0\right)\frac{J_1(kR\theta)}{kR\theta} - \frac{3}{4}\sqrt{\frac{5}{6\pi}}\left(\alpha_2 + \alpha_{-2} - \sqrt{\frac{2}{3}}\alpha_0\right) J_2(kR\theta)\right]. \tag{5}$$

The α_μ's are now replaced by the operators β_μ and β_μ^*, and the application of the expression for the matrix elements of these operators leads to the required cross section

$$\sigma_0(\theta) = pR^2[(J_1(kR\theta)/\theta) - {}^1\!/_2\, kRJ_2(kR\theta)]^2, \quad \sigma_{\pm 1}(\theta) = 0,$$
$$\sigma_{\pm 2}(\theta) = {}^3\!/_8\; p(kR)^2 R^2 J_2^2(kR\theta), \tag{6}$$

where $p = (5/8\pi)\hbar/B\omega$. The ratio of the inelastic to the elastic scattering cross section depends mainly on the quantity p. Hydrodynamical calculations give $B = (3/8\pi)MR^2$, where M is the mass of the nucleus; it is shown in Ref. 4, however, that in order to bring about agreement with experiment, this value must be multiplied by a factor of approximately five. Choosing such a value of B, the quantity p is of the order of 10^{-2}, i.e., the cross section for the process under consideration is two orders of magnitude lower than the cross section for elastic scattering.

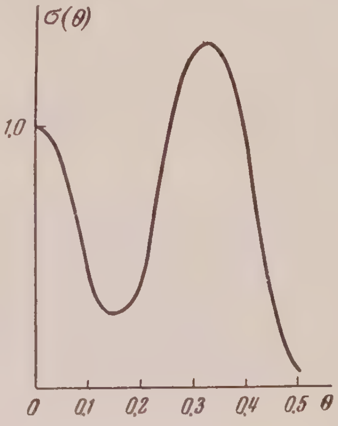

FIG. 1.

Comparison with experiment can be carried out first of all by measuring the angular distribution of inelastically scattered neutrons and comparing it with the angular distribution predicted by Eq. (6) summed over μ, i.e., with $\sigma(\theta) = \sigma_0(\theta) + 2\sigma_2(\theta)$. Fig. 1 shows $\sigma(\theta)$(in units of $pk^2R^4/4$) when $kR = 10$. Comparison with experiment can also be achieved by measuring the angular correlation between inelastically scattered neutrons and γ-rays produced during nuclear transitions to the ground state. The photons here carry two units of angular momentum; applying the well-known formula for the angular distribution of photons, one obtains the following exrpession for the transition cross section, wherein the neutrons are inelastically scattered at an angle θ and the photon makes an angle ϑ with the direction k

$$\sigma(\theta, \vartheta)\, d\Omega_n d\Omega_\gamma \tag{7}$$

$$= \frac{5}{8\pi}\left[3\left(x^2 - x^4\right)\sigma_0(\theta) + \left(1 - x^4\right)\sigma_2(\theta)\right] d\Omega_n d\Omega_\gamma,$$

where $x = \cos\vartheta$.

The author wishes to thank D. V. Volkov and L. N. Rozentsveig for valuable advice.

---

[1] G. Scharff-Goldhaber and J. Weneser, Phys. Rev. **98**, 212 (1955).

[2] A. Bohr, Dan. Mat. Fys. Medd. **26**, 14 (1952).

[3] S. I. Drozdov, J. Exptl. Theoret. Phys. (U.S.S.R.) **28**, 734 (1955); Soviet Phys. JETP **1**, 591 (1955).

[4] A. I. Akhiezer and V. B. Berestetskii, *Quantum Electrodynamics*, GITTL, Moscow, 1953.

Translated by M. A. Melkanoff
192

Density of the Normal Component for Solutions of the Isotopes of Helium

N. G. Bereznaik and B. N. Esel'son
Physico-Technical Institute
Academy of Sciences, Ukrainian SSR

(Submitted to JETP editor June 31, 1956)
J. Exptl. Theoret. Phys. (U.S.S.R.) **31**, 902-903
(November, 1956)

In accordance with current ideas[1] there are to be associated with atoms of He^3 in solution He II elementary excitations characterized by the following dependence of energy upon momentum:

$$E = E_0 + (p - p_0)^2 / 2\mu, \tag{1}$$

where μ is the effective mass of the impurity atom. The minimum of the energy corresponds either to $p_0 = 0$ or to $p_0 \neq 0$. The contribution of the impurity to the density of the normal component of the He II depends critically upon the form of the energy spectrum, and can be written in the following manner[2]:

$$\rho_n = \rho_{n0} + (\rho/m)\,\mu x \quad \text{for} \quad \rho_0 = 0, \tag{2}$$

$$\rho_n = \rho_{n0} + (\rho/m)\left(p_0^2 / 3kT\right) x \quad \text{for} \quad p_0 \neq 0, \tag{3}$$

where x is the molar concentration of the He^3 in the solution. From this it is immediately evident that an experimental determination of the temperature dependence of the normal component density for solutions of He^3 and He^4 will make it possible to establish the form of the energy spectrum.

For this purpose an experiment was performed to determine ρ_n for solutions of the helium isotopes by means of the customary method, i.e., the measurement of the period of oscillation Θ of a stack of discs immersed in the solution[3,4]. From this the ratio of ρ_n to the density ρ_λ of the solution for the corresponding λ-point was computed. The results thus obtained* are presented in Fig. 1.

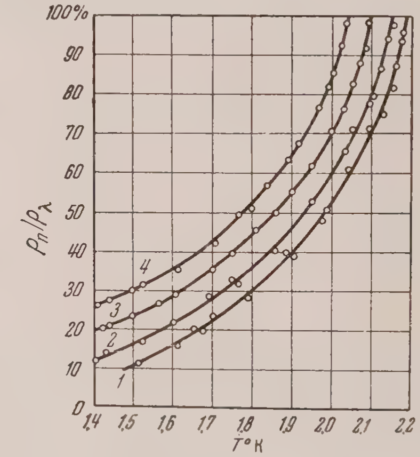

FIG. 1. Dependence of ρ_n / ρ_λ upon temperature: *1*—pure He^4 ; *2*—3.0% He^3 ; *3*—5.6% He^3 ; *4*—8.2% He^3

Using the indicated values of ρ_n / ρ_λ, and determining ρ_λ from the known densities of He^4 and He^3 [6-7], assuming them to be additive, it is possible to derive the dependence of ρ_n upon x for various temperatures, as shown in Fig. 2.

It is clearly evident that this dependence is linear down to a temperature of 1.8° K, the isotherms thus obtained being parallel to one another. A relation of this sort among ρ_n, T and x, in accordance with Eq. (2), testifies to the fact that the energy spectrum for the solution is characterized by the value $p_0 = 0$; the effective mass of the He^3 in solution can be determined from the slope of these lines. The calculations lead to the value $\mu = 3.0\, m_3$, the effective mass depending upon neither temperature nor concentration. These results fully confirm the conclusions previously reached[8]; the value for μ given here, however, is somewhat more exact, insofar as it has been determined by averaging the data obtained for several solutions having different concentrations of He^3.

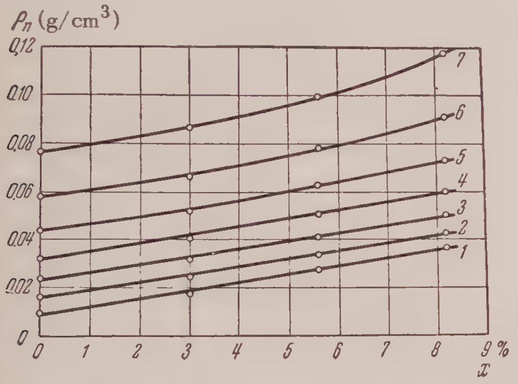

FIG. 2. Dependence of the normal component density ρ_n for solutions upon the concentration x for various temperatures: *1*–1.4; *2*– 1.5; *3*–1.6; *4*–1.7; *5*–1.8; *6*–1.9; *7*–2.0° K.

It should be mentioned that the sharp break of the $\Theta - T$ curve at the λ-point may serve to locate the latter; the values for T_λ thus obtained agree well with other data reported recently[9].

We take this opportunity to thank Prof. B. G. Lazarev for his consideration of these results.

---

* In the present experiment the temperature was determined from the He^4 vapor pressure, with the aid of the 1949 tables[5].

[1] L. Landau and I. Pomeranchuk, Dokl. Akad. Nauk SSSR **59**, 669 (1948).

[2] I, Pomeranchuk, J. Exptl. Theoret. Phys. (U.S.S.R.) **19**, 42 (1949).

[3] E. L. Andronikashvili, J. Exptl. Theoret. Phys. (U.S.S.R.) **18**, 424 (1948).

[4] A. C. Hollis-Hallet, Proc. Roy. Soc. (London) **A210**, 404 (1952).

[5] H. van Dijk and D. Shoenberg, Nature **164**, 151 (1949).

[6] H. Kammerlingh Onnes and J.D.A. Boks, Leid . Comm. **170b**.

[7] Eugene C. Kerr, Phys. Rev. **96**, 551 (1954).

[8] N. G. Berezniak and B. N. Esel'son, Dokl. Akad. Nauk SSSR **111**, 2 (1956).

[9] Esel'son, Berezniak and Kaganov, Dokl. Akad. Nauk SSSR **111**, 3 (1956).

Translated by S. D. Elliott
193

On the Total Energy of the β-Transition RaC – RaC′

A. V. KOGAN AND I. A. SOKOLOV
Leningrad Physical-Technical Institute
Academy of Sciences, USSR

(Submitted to JETP editor July 19, 1956)
J. Exptl. Theoret. Phys. (U.S.S.R.) **31**, 904
(November, 1956)

THERE exist a large number of works devoted to the study of the β-spectrum of RaC and the γ-spectrum of the excited RaC′ nucleus. Owing to the great complexity of these spectra, for a long time the diverse data obtained could not be made to conform, and to yield a perfectly definite scheme of the energy states of the RaC′ nucleus. Some authors[1,2] assume that the β-tansition with the highest limiting energy of 3.17 mev proceeds not to the ground level of the RaC′ nucleus but to an excited level with an excitation energy of 609 kev, which corresponds to a total β-transition energy of 3.78 mev.

In 1955, data obtained by studying the γ-ray spectrum of RaC′ by means of measurements of γ-γ and β-γ coincidences[3,4] were published. The absence of β–γ coincidences for the β-spectrum with the highest limiting energy furnished the basis for proposing the scheme according to which the β-transition with limiting energy 3.17 mev proceeds to the ground level[4]. It should be noted that the data of works published up to now do not exclude the possibility that the transition we are studying proceeds entirely to a metastable level rather than to the ground level.

During recent years, transitions of the type *E* 3 or *M* 3 were observed for some nuclei with half-lives of the order of a few hundred microseconds[5,6]. That an isomeric state with such a half-life also occurs in the case of RaC′(Po^{214}) is not excluded.

One can detect a metastable state by measurements of "delayed" $\beta-\gamma$ and $\beta-\alpha$ coincidences. The usual method for such measurements was employed. The impulses of a β-counter were fed to the coincidence circuit with a time delay t_d which could be adjusted from zero to a few thousand microseconds. Recording of "delayed" $\beta-\gamma$ coincidences were carried out without a selection in energies of the β- and γ-radiation. In these measurements, no metastable state was detected with half-life within the range 0.5 to 400 μ secs.

In registering "delayed" $\beta-\alpha$ coincidences, an aluminum filter was placed between the source and the β-counters. The thickness of the filter corresponded to the absorption of all the β-particles which give coincidences with γ-quanta, i.e., β-particles pertaining to the highest energy β-transition were registered. An exponential dependence of the number of $\beta-\alpha$ coincidences on t_d was obtained, corresponding to the α-decay of RaC′. It is obvious that this result excludes the possibility of the existence of a metastable state with long lifetime, preceding the α-decay.

Thus, comparison of the results from measurement of "delayed" β-γ and $\beta-\alpha$ coincidences allows one to assume that the β-transition with limiting energy 3.17 mev does not proceed to an isomeric level. The data obtained are in agreement with the decay scheme proposed by Johanson[4] and confirms that the total energy of the β-transition equals 3.17 mev.

The authors thank Prof. L. I. Rusinov for his attention and assistance in the completion of the current work.

[1] C. D. Ellis, Proc. Roy. Soc. (London) **143A**, 350 (1934).

[2] J. Surugue, J. Phys. Radium **7**, 145 (1946).

[3] R. E. Rowland, Phys. Rev. **99**, 757 (1955).

[4] S.A.E. Johansson, Arkiv f. Fysik **9**, 561 (1955).

[5] D. E. Alburger and M.H.L. Pryce, Phys. Rev. **92**, 514 (1953).

[6] S. H. Vegors and P. Axel, Phys. Rev. **101**, 1067 (1956).

Translated by R. L. Eisner
194

Decay of a τ'-Meson

V. V. ALPERS* AND A. P. MISHAKOVA

(Submitted to JETP editor July 20, 1956)
J. Exptl. Theoret. Phys. (U.S.S.R.) 31, 904-905
(November, 1956)

UPON further examination of a photographic emulsion[1] exposed in the stratosphere in May 1955, a particle was found to have stopped in the emulsion, decaying into a single positive pion which exhibited a typical picture of $\pi \to \mu \to e$-decay. The range of the μ-meson is 550μ. The track of the primary particle is inclined at a large angle to the emulsion, and that of the secondary particle (the pion) is parallel to the emulsion. This complicates an interpretation of the event which might still be considered as the scattering of a pion. Measurements were carried out on the grain density of several pion tracks inclined at the same angle and going in the same direction as the primary particle. Comparison of the grain densities of these tracks with the density of the track under consideration indicated that the scattering of a pion is definitely excluded. This must therefore be a particle decay event.

The path of the pion measures 600μ and its energy is $E = 4.6$ mev; this excludes the decay of a K-particle according to the scheme $K \to \pi + \pi^0 + Q$. The event may therefore be interpreted as the decay of a τ-meson according to an alternative decay scheme into one positive and two neutral π-meson ($\tau' \to \pi^+ + 2\pi^0$)[2-4]. Upon retracting the τ-meson trajectory, it was found that the meson had entered the emulsion having been created outside, and covered a distance of 3.76 cm in the emulsion. It is difficult to determine the τ'-meson mass exactly because its track makes a large angle with the plane of the emulsion.

Grain density measurements were carried out for the given track and for the tracks of pions and protons lying at the same angle. Results of ionization measurements indicate that the ma the particle in question is smaller than the m of a proton but greater than that of a pion.

One may therefore conclude on the basis ionization measurements that the particle mig a K-meson.

In conclusion, we should like to thank Prof. I. I. Gurevich for his expression of interest i work.

---

* Deceased.

[1] V. V. Alpers, I. I. Gurevich and A. P. Mishakova, Dokl. Akad. Nauk SSSR 108, 207 (1956).

[2] R. Dalitz, Proc. Phys. Soc. (London) A66, 710 (1953); A. Pais, Phys. Rev. 86, 663 (1953).

[3] Crussard, Kaplon, Klarmann and Noon, Phys. Rev. 93, 253 (1954).

[4] G. Stack, Collab., Nuovo Cimento 2, 1063 (1955).

Translated by M. A. Melkanoff
195

Inelastic Scattering Cross Sections of Nuclei for 2.5 MEV Neutrons

V. I. Strizhak
Institute of Physics
Academy of Sciences, Ukrainian SSR

(Submitted to JETP editor July 23, 1956)
J. Exptl. Theoret. Phys. (U.S.S.R.) 31, 907-908
(November, 1956)

In this communication we present briefly the results of measurements of inelastic cross sections for 2.5 mev neutrons. These measurements were carried out in the Institute of Physics of the Academy of Sciences, Ukrainian SSR during 1951-1952.

Inelastic scattering cross sections for neutrons can be measured rather easily by attenuation methods, using radioactive threshold detectors. In such experiments, the shapes of the scatterer and detector must be chosen in such a way as to eliminate the effect of elastic scattering or else make possible the evaluation of this effect. The threshold of the detector should be high enough so that the inelastically scattered neutrons cannot activate it. These problems were solved in two ways. In one method, a spherical scatterer was surrounded by a thin wrapper of the detector such that all neutrons elastically scattered by the scatterer had a chance to pass through the detector and activate it. Since inelastically scattered neutrons lose a significant fraction of their energy and do not activate the detector the experiment gives the attenuation of the neutron beam as a result of inelastic scattering.

In the second method, the spherical threshold detector was surrounded by a wrapping of scatterer. Here the neutrons scattered elastically by the part of the scatterer between the source of neutrons and the detector and not impinging on the detector will be compensated (completely or partly) by neutrons elastically scattered into the detector by other parts of the scatterer. It follows that in this way also the decrease in activation of the detector due to inelastic scattering can be determined after establishing the amount of cancellation.

A detailed analysis showed that both methods of measurement are valid under the experimental conditions used.

The reaction $P^{31}(n, p)Si^{31}$ was used as a threshold detector. The effective threshold here is equal to ~2 mev; the half-life is about 170 min. The neutrons were obtained from the $D(d, n)He$ reaction. A thick, heavy ice target was bombarded with 190 kev deuterons obtained from a low voltage accelerator constructed for this purpose.

The measurements were carried out in the following fashion. A detector with scatterer and a detector without a scatterer were placed symmetrically with respect to the target at an angle of 90° relative to the deuteron beam. The irradiations of the two detectors were carried out simultaneously. After the end of the irradiation the activity of the detectors was measured using counters.

TABLE. Inelastic Scattering Cross Sections for 2.5 mev Neutrons.

Scatterer	Cross section for inelastic scattering, in barns	Scatterer	Cross section for inelastic scattering, in barns
Na	0,53±0.26	Zn	1.88±0,15
Mg	0,77±0,25	Se	1.88±0,17
Al	0,96±0,17	Mo	1,9±0.3
P	0,7±0,2	Ag	2.1±0,2
S	0,54±0,21	Cd	2.2±0.2
Cl	0,6±0,3	Sn	2,2±0.2
Ca	0.4±0.2	Sb	1,9±0.2
Cr	1.4±0.3	Te	2.0±0,35
Fe	1.16±0.12	J	1,96±0.25
Co	1.40±0.11	Ba	1.6±1.0
Ni	0,83±0.12	W	2,6±0.25
Cu	1.58±0.15	Hg	2,6±0.3
		Pb	1.7±0.3
		Bi	0.7±0.3

The cross sections for chlorine and barium were calculated from measurements of the inelastic cross sections of NaCl, BaS, Na and S and the assumption of the additivity of cross sections.

The results of the measurements are shown in the Table. They make possible the following conclusions: (1) the inelastic cross sections for 2.5 mev neutrons for most nuclei increase smoothly with a mass number; (2) nuclei having a magic number of nucleons have inelastic scattering cross sections that are significantly smaller than neighboring nuclei. It may be that this is the result of the presence of particularly stable nuclear clouds, whose influence is felt even at neutron energies of 2.5 mev.

In conclusion, I take the opportunity to acknowledge the direction of A. I. Leypounskii in this work and the valuable advice and interest of M.V. Pasechnik.

Translated by A. Turkevich
199

Level Shifts in μ-Mesic Hydrogen and the Structure of the Proton

L. M. AFRIKIAN
P. N. Lebedev Physical Institute
Academy of Sciences, USSR

(Submitted to JETP editor July 27, 1956)
J. Exptl. Theoret. Phys. (U.S.S.R.) 31, 908-909
(November, 1956)

THE work of Wheeler[1] showed that a study of μ-mesic atoms can serve to give information on the internal structure of the nucleus and to determine some of its properties. The purpose of this note is to call attention to the possibility of using data on the fine structure of the μ-mesic hydrogen system to give information concerning the internal structure of the proton and the limits of the applicability of quantum electrodynamics.

The energy of the stationary state of μ-mesic hydrogen to an accuracy including order $\alpha^3 \times$ $(\alpha = e^2/\hbar c)$ can be written in the form

$$E = E_0 + \alpha E_1 + \alpha^2 E_2 + \alpha^3 E_3. \qquad (1)$$

In this equation the main term, E_0, is the energy of the μ^--meson in a Coulomb field of a point proton including the correction for retarded interaction. The correction proportional to α is due to the polarization of the electron vacuum in the neighborhood of the μ-mesic atom and was first pointed out in the work of Galanin and Pomeranchuk[2] (see also Ref. 3). The term proportional to α^2 contains the correction to the "ordinary" fine structure of the level determined by spin orbit interaction and the relativistic dependence of mass on energy, and also the second approximation to the polarization of the electron vacuum. There is also included in the approximation the so-called hyperfine structure of the level determined by the interaction of the magnetic moments of the proton and μ-meson. In the given situation this is comparable to the fine structure. Finally, the term involving α^3 includes the interaction of the μ^--meson with the zero point vibrations of the electromagnetic field, the effect of the polarization of the μ-mesic vacuum and third order corrections to the electron vacuum polarization. It should be emphasized that in all these terms, it is necessary to take into account electromagnetic corrections arising from the finite mass of the proton and retarded potentials.

It is not hard to see, however, that in addition to the electromagnetic terms included above, the terms of order α^2 and α^3 should also contain effects of nonelectromagnetic origin. The term of order α^2 should be strongly affected by the interaction of the proton with the zero point vibration of the π-mesic vacuum. The existence of this interaction should lead to a smearing of the proton charge over a distance of the order of the Compton wavelength of the π-meson. This will result in a deviation of the electric field from the Coulombic in the indicated regions. We will examine some of the effects arising from the existence of the proton in a dissociated state (neutron + π-meson) during a time interval τ. Corresponding to this effect, there exists a correction to the basic energy level of the μ-mesic hydrogen of the order of the quantity

$$\Delta E \sim \tau (\mu / m)^2 \alpha^2 n^{-3} \mathrm{Ry}' (1 + \mu / M)^{-3}, \qquad (2)$$

where m, μ and M correspond to the masses of the π, μ-meson and of the proton; $Ry' = \mu e^4 / 2k^2$. Since the quantity $(\mu/m)^2$ in Eq. (2) is of the order of unity, this effect introduces a significant contribution to the relativistic fine structure of the level of the μ-mesic hydrogen ($\sim \alpha^2$). For ordinary hydrogen, because of the smallness of the quantity $(m_e/m)^2 = (1/273)^2$, the dissociation of the proton has an effect only of the order of electromagnetic corrections proportional to α^4. This is at the borderline of present-day experimental errors. Nonelectromagnetic effects should likewise contribute significantly to corrections to the (ordinary) fine structure of μ-mesic hydrogen (α^3 approximation).

Let us examine, for example, the polarization of the vacuum in μ-mesic hydrogen. Generalizing the results of Vehling[4] for polarization corrections to arbitrary atomic and vacuum particles having masses m_0 and m_V in the case where m_0/m_V is much less than $1/\alpha$, we have:

$$\Delta E = -\frac{8}{15\,\pi}\left(\frac{m_0}{m_v}\right)^2 \frac{\mathrm{Ry}',\,\alpha^3}{n^3}\left(1+\frac{m_0}{M}\right)^{-3} G. \qquad (3)$$

The factor G in Eq. (3) is determined by the spins of the particles examined and their interaction with the vacuum fields. It follows from Eq. (3) that the polarization of the π-mesic vacuum introduces into μ-mesic atoms terms of the same order as arise from the polarization of the μ-mesic vacuum. For ordinary hydrogen the polarization of the π-mesic vacuum introduces terms of the same order as electromagnetic corrections of order α^5. These are beyond present-day experimental techniques.

At the same time, because the polarization of the π-mesic vacuum by the external electromagnetic field is seriously affected by the strong interaction of virtual π-mesic and nucleon pairs, the nonelectromagnetic additions to the fine structure of the μ-mesic hydrogen have a first order effect. The isolation of these effects might serve to establish the limits of applicability of pure electrodynamics and possibly lead to some tests of present-day ideas of the interactions of nucleons with π-mesons.

In conclusion, I thank Prof. V. L. Ginzburg for discussions of this note and for a series of critical comments.

---

[1] J. A. Wheeler, Rev. Mod. Phys. **21**, 133 (1949); Phys. Rev. **92**, 813 (1953).

[2] A. D. Galanin and I. Ia. Pomeranchuk, Dokl. Akad. Nauk SSSR **86**, 251 (1952).

[3] A. I. Akhiezer and V. B. Berestetskii, *Quantum Electrodynamics*, Moscow, 1953.

[4] E. A. Vehling, Phys. Rev. **48**, 55 (1935).

Translated by A. Turkevich
198

The Photoproduction Cross Section for Positronium in an External Field Taking into Account Radiative Corrections

A. I. Alekseev
Moscow Technical Physics Institute

(Submitted to JETP editor July 28, 1956)
J. Exptl. Theoret. Phys. (U.S.S.R.) 31, 909-910
(November, 1956)

THE differential cross section $d\sigma$ for the photoproduction of positronoum in an external field, taking into account radiative corrections of any order, is connected with the differential cross section $d\sigma_f$ for the photoproduction of the free products with zero relative velocity by the following relation:[1]

$$d\sigma = [(\bar{\psi}(0)\,\psi(0)) / (\bar{\psi}_f'(0)\,\psi_f(0))]\, d\sigma_f\,. \qquad (1)$$

where $\psi(x)$ is a wave function (in relative coordinates) of the ground state of positronium (with energy E), satisfying a Bethe-Salpeter equation which takes into account the possibility of annihilation[1,2], $\psi_f(x)$ is a wave function of the free particles and is a proper function of the same complete set (but with an energy $E_f = E + \epsilon$, where $\epsilon > 0$ is the binding energy), as is $\psi(x)$. In Eq. (1) it is necessary to evaluate $(\bar{\psi}(0)\psi(0)) = \mathrm{Sp}[\bar{\psi}(0)\psi(0)]$ with the same accuracy as is taken in the calculation of $d\sigma_f$.

If only the first radiative corrections are examined, the multiplier $(\bar{\psi}(0)\psi(0)]$ must be replaced by its nonrelativistic value, since the next correction to $|\psi_{\text{nonrel}}(0)|^2$ is of the order of $(e^2/\hbar c)^2$ [3]. In addition, when positronium is produced in a ground state, the factor $(\bar{\psi}_f(0) \times \psi_f(0))$ can be taken equal to one[3]. Thus, the calculation of the photoproduction cross section of positronium in an external field, taking into account first order radiative corrections, is reduced to the problem of finding the cross sections of either the photoproduction of the free particles or of bremsstrahlung in an external field. This latter has been investigated by Myamlin.[4] However, from his results we cannot immediately write down the cross section $d\sigma_f$, since the author's purpose was to find the radiative corrections to bremsstrahlung, and so he did not examine three diagrams corresponding to radiation with double scattering of the electron in an external field (higher Born approximation).

In view of the tedious character of the evaluation $d\sigma_f$ (taking into account the first radiative corrections), we have confined ourselves in what follows to evaluating the order of magnitude of the cross section for small velocities v of positronium, large enough, however, so that the Born approximation is still justified ($Ze^2/\hbar c \ll v/c \ll 1$). Calculations lead to the following result for the photoproduction cross section of positronium in the ground state:

$$d\sigma = Z^2 r_0^2 \alpha^4 [\Phi + \alpha (v/c)^2 (\Phi_1 + Z\Phi_2)]\, d\Omega, \qquad (2)$$

where $\alpha = e^2/\hbar c$, $r_0 = e^2/mc^2$, Ze is the charge of the external field, and the element of the solid angle $d\Omega$ indicates the direction of the total momentum $\mathbf{P}$ of the positronium. Φ_1 and Φ_2 are dimensionless functions of $\mathbf{P}$ and the photon momentum $\mathbf{k}$, having magnitudes of order of unity. Further, $Z^2 f_0^2 \alpha^4 \Phi\, d\Omega \equiv d\sigma_0$ is the cross section in the first nonvanishing approximation having the form

$$d\sigma_0 = 4Z^2 r_0^2 \alpha^4 [(mc)^3 P [\mathbf{kP}]^2 / k^2 (\mathbf{P} - \mathbf{k})^4 (\mathbf{kP} - k^2)]\, d\Omega. \qquad (3)$$

It is interesting to notice that, in contrast to Eq. (2), the first radiative corrections to the photoproduction cross section of positronium with two quanta* do not contain the multiplier $(v/c)^2$ at low velocities v.

At high velocities, the Feynman diagrams with Z^2, corresponding to a higher Born approximation, do not contribute to $d\sigma_f$ [6] and the photoproduction cross section of positronium $d\sigma$ is determined by the formula

$$d\sigma = |\psi_{\text{nonrel}}(0)|^2 [d\sigma_f^r (\mathbf{p}, \mathbf{P}) / d^3p\, (2\pi\hbar)^{-3}]_{\mathbf{p} = 0}, \qquad (4)$$

where $\mathbf{p}$ is a relative momentum, and the cross section $d\sigma_f^r(\mathbf{p}, \mathbf{P})$ is the photoproduction cross section for free particles, taking into account the radiative corrections calculated by Myamlin[4].

The infrared divergences in the radiative corrections [not only in first order (Eqs. (2) and (4)), but in any order in $e^2/\hbar c$] cancel each other in the photoproduction of positronium. This is seen as follows. The amplitude of the photoproduction of positronium, taking into account radiative corrections of any order, is the same even to the multiplier with the amplitude for the photoproduction of free particles with zero relative velocity[1]. However, in the case of free particles, the radiative corrections to the process of order $(e^2/\hbar c)^n$, which bring in the infrared divergence, can be written as (see Ref. 7): $2(\rho_1 + \rho_2)M$ where M is the amplitude of the given process to order $(e^2/\hbar c)^n$, and ρ_1 and ρ_2 are numerical coefficients proportional to $e^2/\hbar c$ and having the form**

$$\rho_1 = -\frac{e^2}{\hbar c} \frac{i}{(2\pi)^4} \int \frac{(p_i p_f)}{(p_i k)(p_f k)} \frac{d^4k}{k^2}, \qquad (5)$$

$$\rho_2 = \frac{e^2}{\hbar c} \frac{1}{(2\pi)^2} \int \frac{dk_0}{k_0},$$

where p_i and p_f are momenta corresponding to the initial and final states of the electron. Since in the case of photoproduction, $p_i = -p_2$ (p_2 is the momentum of the positron), $p_f = p_1$ (p_1 is the electron momentum), and $p_1 = p_2$, then $\rho_1 + \rho_2 = 0$; therefore, the terms with the infrared divergence in the radiative correction to the photoproduction of positronium vanish. [In an analogous fashion it can be shown (see Ref. 1 and 3) that the infrared divergences in the radiative corrections to the annihilation of positronium likewise cancel to any order of $e^2/\hbar c$.]

At high energies, the more probable process is not the formation of positronium, but the formation of interacting particles. In fact, on one hand, at high energies of the γ-quanta, the angle θ between the particles formed is small: $\theta \sim mc^2/\omega$ [8] (ω being the energy of the quantum). On the other hand, the angle θ is of the order v_{rel}/v, where v_{rel} is the relative velocity of the particles and v is the velocity of their center of mass ($v \approx c$). It follows that the particles formed go off with low relative velocity $v_{\text{rel}}/c \sim mc^2/\omega \ll 1$. In this case, taking into account the interaction between the two particles according to a formula analogous to Eq. (1) (see Ref. 1), leads to a significant increase in the differential cross section [relative to Eq. (4)] due to the factor $(\bar{\psi}(0)\psi(0))$ which, in first approximation, is equal to

$$(\bar{\psi}(0)\psi(0)) = (2\pi e^2/\hbar v_{\text{rel}})(1 - \exp\{-2\pi e^2/\hbar v_{\text{rel}}\})^{-1}. \qquad (6)$$

In conclusion, I would like to thank A. D. Galanin for discussions of the results of this work.

---

* This cross section is evaluated (see Ref. 1) by a formula analogous to Eq. (1), where the cross section $d\sigma_f$ for the photoproduction of the free particles by two quanta is calculated, together with the first radiative corrections, by Brown and Feynman[5].

** The following summation rule has been used:

$$(ab) = a_0b_0 - a_1b_1 - a_2b_2 - a_3b_3.$$

[1] A. I. Alekseev, J. Exptl. Theoret. Phys. (U.S.S.R.) (in press).

[2] R. Karplus and A. Klein, Phys. Rev. **87**, 848 (1952).

[3] A. I. Alekseev, J. Exptl. Theoret. Phys. (U.S.S.R.) **31**, 164 (1956); Soviet Phys. JETP **4**, 261 (1957).

[4] V. A. Myamlin, Thesis, M. M. I., 1953.

[5] L. Brown and R. Feynman, Phys. Rev. **85**, 231 (1952).

[6] B. Sredniawa, Acta Phys. Polon. **11**, 331 (1953).

[7] Jauch and F. Rohrlich, Helv. Phys. Acta **27**, 613 (1954).

[8] A. Borsellino, Phys. Rev. **89**, 1023 (1953); H. Bethe and W. Heitler, Proc. Roy. Soc. (London) **146A**, 83 (1934).

Translated by A. Turkevich
199

A Bubble Chamber for the Study of Cosmic Rays

E. V. KUZNETSOV, M. F. LOMANOV, G. A. BLINOV
AND CHUAN CHEN-NIANG (KHUAN SHEN-NIAN')

(Submitted to JETP editor July 30, 1956)
J. Exptl. Theoret. Phys. (U.S.S.R.) 31, 911
(November, 1956)

UP until now bubble chambers have not been used for the study of cosmic rays. The reason for this lies in the lack of control of such chambers, since the life–time of the embryonic bubbles formed by ionizing particles in going through the chamber is significantly less than the time in which decompression occurs. However, as will be seen in this work, bubble chambers can be used to study cosmic rays. This can be accomplished by increasing the efficiency of the chamber, that is, by increasing the fraction of the time in which the chamber is sensitive. The efficiency is determined by the sensitive time in each cycle as well as by the length of each cycle. By shortening the cycling time and taking certain other precautions, we have increased the efficiency of the chamber so that it has become practical to work with cosmic rays.

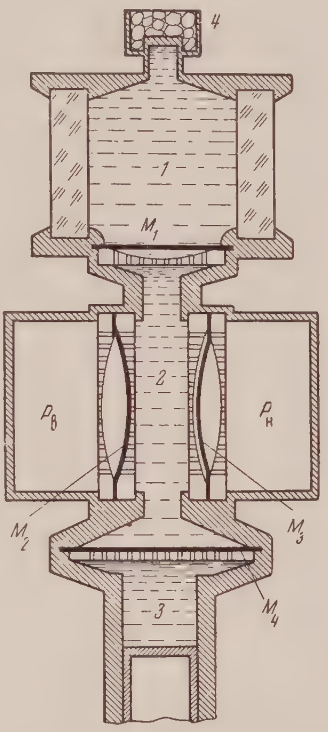

A schematic plan of the set–up is given in the Figure. It consists of the chamber *1*, a limiter *2*, and compressor *3*. The chamber *1* has a cylindrical form and is filled with freon–13 ($CClF_3$). The volume of the chamber is 1 liter. The viewing windows are discs of organic glass mounted without gaskets. The membrane M_1 is constructed out of rubber made from domestic synthetic nayrite.

The compressor *3* is made like the air-compressor type KVD and produces a periodic compression and decompression of the chamber at a rate of 10 cycles/sec. The horespower used in such a compression process is not large since the energy expended by the rotor during the compression part of the cycle is returned upon decompression. In this way, the method described is advantageously different from one using a gas. The cylinder of the compressor is filled with oil. The pressure exerted on it by the plunger is transmitted to water occupying the central volume of the limiter and through it to the working fluid in the chamber *1*.

The limiter *2* determines the limits in which the pressure in the chamber can vary. It gives the pressure curve the shape of a square wave. The upper limit is determined by the pressure p_u of the gas in the left part of the limiter; the lower limit is determined by the pressure p_1 in the right part. P_u is 1.5–2 times higher than the vapor pressure of the working liquid; P_1 is of the order of 10 atms. less than the vapor pressure of the liquid. When the plunger is in the lower part of the cylinder, as indicated in the drawing, the membrane M_2 is pressed against the right screen, the membrane M_3 is found in some middle position and the pressure in a system is equal to P_1. When, however, the plunger is in the upper position, the membrane M_3 is pressed to the right screen and the membrane M_2 is in a neutral position. The pressure in the system now is equal to P_u. The relation between the time of compression and the time of decompression can be changed by changing the amount of working liquid in the chamber or the amount of water in the limiter. The pressure curve taken using a condenser manometer has been observed on an oscillograph.

Bubbles which do not collapse during the compression, rise to the trap 4 which is cooled with dry ice; there they collapse.

The adjustment of the chamber was made using a cobalt 60 γ-ray source and cosmic rays. Figure 2 shows one of the first photographs taken of such tracks with the flash initiated by a counter telescope.

The chamber, in the basement of a two-story building, registers on the average 5 cosmic ray particles each minute. A rough efficiency calculation gives the value 0.1.

A more detailed description of the construction of the apparatus will be published later.

We are grateful to Academician A. I. Alikhanov for support of the idea of a high efficiency bubble chamber and to A. G. Meshkovskii for interest in the work. Likewise we thank Iu. V. Bardiukov who carried out most of the technical work and who contributed many valuable improvements to the construction of the chamber.

Translated by A. Turkevich
200

Some Properties of Rotating He II

B. N. Esel'son, B. G. Lazarev,
K. D. Sinel'nikov and A. D. Shvets
Physico-Technical Institute
Academy of Sciences, Ukrainian SSR

(Submitted to JETP editor July 31, 1956)
J. Exptl. Theoret. Phys. (U.S.S.R.) 31, 912
(November, 1956)

As is well known, it has been established experimentally that for oscillatory motion of a stack of discs in He II[1] only the normal component is entrained, while for rapid uniform rotation of a vessel containing He II[2] the liquid rotates as a whole. The results of these experiments have been explained in papers by Landau and Lifshitz[3] and by Feynman[4], according to which the condition of thermodynamic equilibrium for a rotating vessel filled with He II corresponds to entrainment, not only of the normal component, but of the superfluid as well; in addition, He II must have a moment of inertia which varies with the velocity of rotation from a value corresponding to entrainment of the normal component alone to a value corresponding to rotation of the liquid as a whole[5]. However, as follows from the papers cited above[4], entrainment of the superfluid component must occur at velocities smaller than those encountered in the experiments with stacks of discs, and the fact that this effect has not been observed might be explainable on the basis of an appreciable relaxation time. It would therefore be most desirable to verify experimentally the dependence of the moment of inertia of rotating He II upon the angular velocity, and to attempt to determine the relaxation time.

To resolve this question, the rotational damping of a vessel filled with He II was investigated under conditions approximating as closely as possible continuous equilibrium between the normal and superfluid components. Since the relaxation time was unknown, it was necessary for the rotating system to suffer as little damping as possible. To insure this, the method of suspending a plexiglass beaker of He II in a magnetic field was used, permitting the beaker to rotate for several hours after receiving an initial angular velocity of a few revolutions per second. The beaker (R = 1.5 cm) contained approximately 300 light aluminum discs separated by distances smaller than the penetration depth for the viscous wave. The angular velocity of the beaker of He II was raised in a few seconds to the desired value by means of a rotating magnetic field, which was then turned off. Initially, under these conditions, only the normal component of the He II should be drawn along by the discs, while after the relaxation time had elapsed the superfluid component would be entrained as well. If the relaxation time exceeds the time required to set the vessel into rotation, then, depending on the degree of entrainment of the superfluid component, an appreciable change in the moment of inertia of the beaker of helium (roughly 25%) would be expected, leading to a change in the velocity of rotation. A study of the rotational damping of the beaker of He II, however, demonstrates the absence of any significant change in velocity; this is illustrated in the Figure, in which the variation of the angular velocity of the beaker with time is shown for $T = 1.5°$ K and for starting times of 10 sec (lower curve) and 2 sec (upper curve). From this it may be concluded that the relaxation time must be less than 2 sec. These same experiments permit determination of the variation in the moment of inertia of He II with rotational velocity. It is found that for velocities greater than 0.5 rev/sec there is no such variation. This latter result is in excellent agreement with the results obtained in the experiments with a stack of discs oscillating at large amplitudes[6].

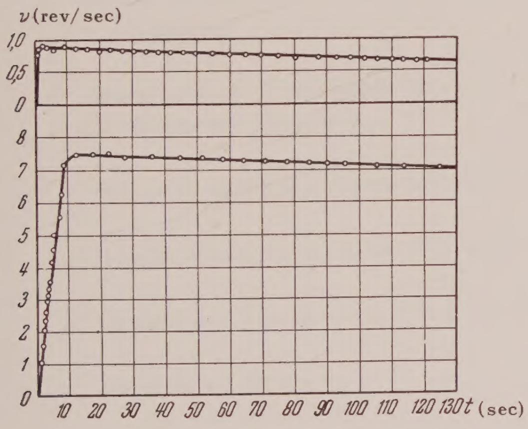

Thus, the absence of entrainment of the superfluid component in the experiments, using an oscillating stack of discs with small amplitudes cannot be explained on the basis of a long relaxation time. The question of the possibility of a velocity-dependent relaxation times, which was brought to our attention by L. D. Landau, as yet remains open.

---

[1] E. L. Andronikashvili, J. Exptl. Theoret. Phys. (U.S.S.R.) **16**, 780 (1946).

[2] D. V. Osborne, Proc. Phys. Soc. (London) **A63**, 909 (1950).

[3] L. D. Landau and E. M. Lifshitz, Dokl. Akad. Nauk SSSR **100**, 669 (1955).

[4] R. P. Feynman, Prog. in Low Temp. Phys. **1**, 17 (1955).

[5] I. M. Lifshitz and M. I. Kaganov, J. Exptl. Theoret. Phys. (U.S.S.R.) **29**, 257 (1955); Soviet Phys. JETP **2**, 172 (1956).

[6] A. C. Hollis-Hallett, Proc. Roy. Soc. (London) **A210**, 404 (1952).

Translated byS. D. Elliott
201

CONTENTS— *continued*

Letters to the Editor:

Temperature Dependence of Viscosity of Liquid Argon . . . . . . N. F. Zhdanova 749 31, 724
The HDSe Microwave Spectrum . . . . . . V. G. Veselago and A. M. Prokhorov 750 31, 731
"Seniority" Quantum Number Selection Rules in Nuclear Reactions . . . . . . V. G. Neudachin 751 31, 891
Gamma Quanta Emitted by I, Rh and Co Nuclei in Thermal Neutron Capture . . . . . . I. V. Estulin, I. F. Kalinkin and A. S. Melioranskii 752 31, 886
Concerning a Certain Possibility in Quantum Field Theory . . . . . . Iu. M. Lomsadze 754 31, 887
Accuracy of Isobaric Spin for the $1f_{7/2}$ Shell . . . . . . V. G. Neudachin 756 31, 892
The Theory on Slowing Down of Neutrons . . . . . . A. Ia. Temkin 757 31, 892
The Effect of Finiteness of Target-Nucleus Mass in Angular Distribution in (d,p) and (d,n) Reactions . . . . . . D. P. Grechukhin 759 31, 895
On the Mechanism of Initiation of Boiling of Liquid Metastable Systems by Ionizing Radiation . . . . . . G. A. Askar'ian 761 31, 897
Consequences of Renormalizability of Pseudoscalar Meson Theory with Two Interaction Constants . . . . . . V. V. Sudakov and K. A. Ter-Martirosian 763 31, 899
Excitation of Nuclear Vibrational Levels by Scattering of Fast Neutrons . . . . . . E. V. Inopin 764 31, 901
Density of the Normal Component for Solutions of the Isotopes of Helium . . . . . . N. G. Berezniak and B. N. Esel'son 766 31, 902
On the Total Energy of the β-Transition RaC-RaC$'$ . . . . . . A. V. Kogan and I. A. Sokolov 767 31, 904
Decay of a τ-Meson . . . . . . V. V. Alpers and A. P. Mishakova 768 31, 904
Inelastic Scattering Cross Sections of Nuclei for 2.5 mev Neutrons . . . . . . V. I. Strizhak 769 31, 907
Level Shifts in μ-Mesic Hydrogen and the Structure of the Proton . . . . . . L. M. Afrikian 770 31, 908
The Photoproduction Cross Section for Positronium in an External Field Taking into Account Radiative Corrections . . . . . . A. I. Alekseev 771 31, 909
A Bubble Chamber for the Study of Cosmic Rays . . . . . . E. V Kuznetsov, M. F. Lomanov, G. A. Blinov and Chuan Chen-Niang 773 31, 911
Some Properties of Rotating He II . . . . . . B. N. Esel'son, B. G. Lazarev, K. D. Sinel'nikov and A. D. Shvets 774 31, 912

SOVIET PHYSICS JETP VOLUME 4, NUMBER 5 JUNE, 1957

CONTENTS

Russian Reference

Oscillographic Determination of Energy of Electric Explosion of Wires . . . . . .
. . . . I. F. Kvartskhava, V. V. Bondarenko, A. A. Pliutto and A. A. Chernov 623 31, 745

The Ionization Spectrum of Cosmic Rays 3250 m Above Sea Level . . . .
. . . . A. G. Meshkovskii and L. I. Sokolov 629 31, 752

Investigation of σ-Stars Induced by Negative π-Mesons . . . .
S. A. Azimov, U. G. Guliamov, E. A. Zamchalova, M. Nizametolinova, M. I. Podgoretskii and A. Iuldashev 632 31, 756

Electrical Explosion of Wires in Vacuum . . . .
. . . . I. F. Kvartskhava, V. V. Bondarenko, R. D. Meladze and K. V. Suladze 637 31, 737

Alpha Decay of Pu^{240} . . . .
. . . . . . L. N. Kondrat'ev, G. I. Novikov, Iu. P. Sobolev and L. L. Gol'din 645 31, 771

Three Body Problem for Short Range Forces. I. Scattering of Low Energy Neutrons by Deuterons . . . .
. . . . G. V. Skorniakov and K. A. Ter-Martirosian 648 31, 775

Measurement of the Ionizing Power of Particles in a Bubble Chamber . . . .
. . . . G. A. Blinov, Iu. S. Krestnikov and M. F. Lomanov 661 31, 762

On the Construction of the Scattering Matrix. I. . . Integral Causality Condition in Bogoliubov's Method . . . . B. V. Medvedev 671 31, 791

Synchrotron Oscillations in Strong Focusing Accelerators I. Linear Theory . . . .
. . . . L. L. Gol'din and D. G. Koshkarev 681 31, 803

A Comparison of the Fermi-Landau Theory with Some Experimental Data on Cosmic Rays . . . .
. . . . O. A. Guzhavina, V. V. Guzhavin and G. T. Zatsepin 690 31, 819

Reflection of Waves from an Isotropic Inhomogeneous Layer . . . .
. . . . A. G. Zharkovskii and P. M. Todes 701 31, 815

Expansion of Single Particle Wave Functions in Functions of the Relative Motion of the Nucleons . . . .
. . . . A. I. Baz' 704 31, 831

Theory of Nonlocal Interaction . . . .
. . . . V. S. Barashenkov 709 31, 837

The Interaction of an Electron Hole with the Lattice Vibrations in a Homopolar . . Crystal . . . .
. . . . K. B. Tolpygo and A. M. Fedorchenko 713 31, 845

On the Theory of the Stability of a Layer Located at a Superadiabatic Temperature Gradient in a Gravitational Field . . . .
. . . . V. N. Gribov and L. E. Gurevich 720 31, 854

The Establishment of Thermal Equilibrium between Quanta and Electrons . . . . .
. . . . A. S. Kompaneets 730 31, 876

Polarization of Relativistic Protons in Coulomb Scattering . . . .
. . . . M. G. Urin and V. N. Mokov 738 31, 842

Isotopic Invariance and the Creation of Particles . . . .
. . . . L. I Lapidus 740 31, 865

(Contents continued on inside back cover)